UNIVERSITÀ DEGLI STUDI DI MILANO
DIPARTIMENTO DI CHIMICA
Doctorate School of Chemical Sciences and Technologies
PhD Course in Chemistry, XXX Cycle

Iron and Ruthenium Catalysts for the Reduction of C=O and C=N bonds

Mattia Cettolin
R10894
CHIM/06 Organic Chemistry

Tutor: Prof. Dr. Cesare Gennari
Co-tutor: Dr. Luca Pignataro

Coordinator: Prof. Dr. Emanuela Licandro

Table of contents

Preface

An object is chiral when it cannot be superposed to its mirror image. The word *Chirality* derive from Greek *χειρ* (hand), and indeed our hands are a mirror imagine one of the other and are not superimposable. This concept can be easily extended to molecules, and each of the two mirror images is called enantiomer. This inherent property of some molecules (i.e. chiral molecules) has a dramatic effect on our existence and everyday life: nucleic acids (e.g. DNA, RNA), proteins, amino acids, sugars are all chiral molecules. Sadly, one of the most famous example in our society is thalidomide, a sedative drug prescribed to pregnant women in the 60s. The drug was sold has a mixture of two enantiomers, where the (*R*)-(+)-thalidomide was responsible for the sedative effect and (*S*)-(-)-thalidomide and its derivatives were reported to be teratogenic (Figure 1).[1] Another interesting, less dramatic, example is the different odor perceived for the two enantiomers of carvone. Since olfactory receptors also contain chiral groups, human being can differentiate from (*R*)-carvone (i.e. spearmint leaves smell) and (*S*)-carvone (caraway seeds).

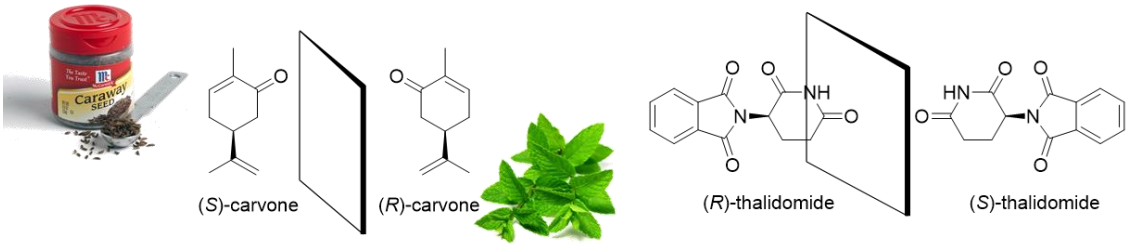

Figure 1. The two enantiomers of thalidomide and carvone.

In 1874, Le Bel and van't Hoff proposed that a carbon atom with four different substituents in a tetrahedral disposition can exist as two enantiomers. Since then, scientists got fascinated by the challenge to achieve full stereocontrol during chemical transformations starting from achiral compounds. In this way, enantioselective synthesis, an important subfield of organic chemistry, was born.

Catalysis is the increase in the rate of a chemical reaction by lowering the energy barrier between the reactants and the products. This is achieved due to the participation of an additional substance called catalyst, which is not consumed in the catalyzed reaction and can continue to act repeatedly. Catalysis has found many applications in our daily life: fermentations (e.g. cheese, beer, wine), cars (i.e. reduction of NOx emissions) and chemical productions (e.g. drugs, fine chemicals). In fact, catalysts are not a human being invention, as enzymes are extremely efficient catalysts present in all organisms.

Asymmetric catalysis is a subfield of catalysis which leads to enantioselective transformations. Among all the enantioselective transformations that have been reported, asymmetric hydrogenation (AH), consisting on the

addition of molecular hydrogen to a compound in a stereoselective way, is so far the most industrially relevant. The first industrial application reported was the production of L-DOPA (Scheme 1) for the treatment of the Parkinson's disease.

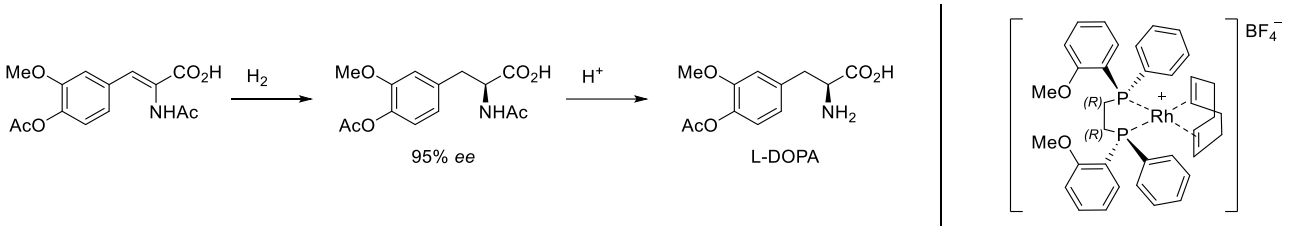

Scheme 1. Industrial process for the synthesis of L-DOPA by Rh-catalyzed asymmetric hydrogenation.

Although AH is operationally simple and shows 100% of atom economy, so far it has been used in a limited number of industrial processes. Most of the hydrogenations are still performed in a non-enantioselective way obtaining a mixture 50:50 of the two enantiomers. This means disposal of half of the reacted material and elevated solvent waste and energy consumption. This paradoxical situation might be explained as results of:

- Time-to-market pressure, no enough time to optimize or to develop new catalytic methods.
- High cost of the catalysts (both the **metal** and the **ligand**) and often relatively low TON.
- Limited availability of noble metals, as long-term supply for the chemical process could exceed their occurrence in nature.
- Lack of efficient methodologies for the AH of challenging substrates.
- Toxicity problems, since even trace amounts of toxic metals are often not allowed to occur in the final products.

A comparison of price of noble metals with base metals shows that the latter are at least 1000 times cheaper (Figure 2),[2] and among them, iron is almost inexpensive.

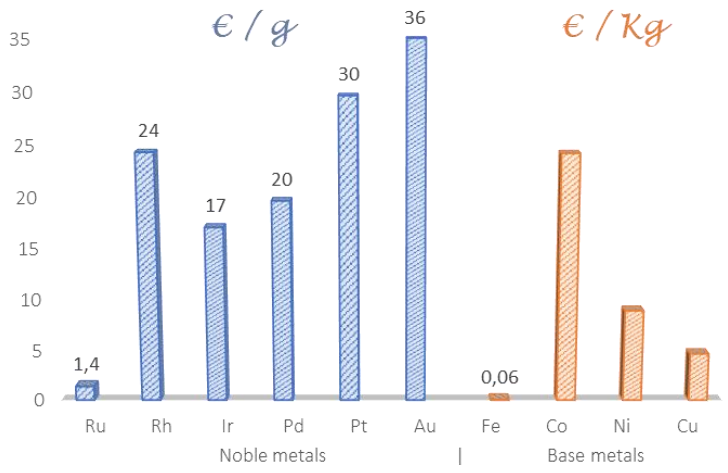

Figure 2. Prices of noble and base metals.

Iron is not only cheap and abundant, it has also practically non-toxicity.[3] The latter peculiarity is attractive especially for pharmaceutical industry. Indeed, the eventual iron traces could be considered less dangerous than the noble metals ones. Therefore, development of new catalysts based on the cheap, environmental friendly and non-toxic iron would be a breakthrough, with an enormous scientific and industrial impact.

This thesis has aimed to develop new hydrogenation and transfer hydrogenation methodologies relying on relatively low-cost and practical iron and ruthenium catalysts.

In the Part A (Chapters 1-5), the development of new iron complexes for hydrogenation and transfer hydrogenation of ketones and imine are described. In the Chapter 1, a general overview on the recent advancements in the homogenous iron catalyzed hydrogenation is reported. In the Chapter 2, two new isonitrile iron complex families are reported. Their synthesis, characterization and reactivity in acetophenone asymmetric reduction is reported. In the Chapter 3, another class of iron complexes called PCCP is described, with particular emphasis on the addressed synthetic problems. In the Chapter 4, the synthesis and characterization of a new member of the (cyclopentadienone)iron complex family is described. Its reactivity towards aldehydes, ketones and activated ester hydrogenation is shown. Furthermore, a transfer hydrogenation methodology with a more challenging substrate (i.e. imines) is also presented. On the same catalytic system, a reductive amination process is reported in this chapter. In the Chapter 5, synthesis, characterization and reactivity of BINOL-derived (cyclopentadienone)iron complexes towards imines reduction is described.

Part B (Chapter 6) is focused on the use of Trost Ligand, a readily available and relatively cheap ligand, for asymmetric hydrogenation of ketones. In the Chapter 6, is described a ketone asymmetric hydrogenation, with the advantage of employing a commercially available chiral ligand (Trost Ligand) and a Ru source $[RuCl_3(H_2O)_x]$.

Part A.
Iron catalysts in reduction of polarized double bonds

CHAPTER 1
IRON CATALYSTS IN HYDROGENATION

Iron is the 4th most abundant element in the earth crust after oxygen, silicon and aluminum, and it is the second most abundant metal. In its elemental state, iron is a lustrous metal, not very hard and quite reactive. Dry air is not effective on massive iron, but when the metal gets in contact with humid air it becomes quickly rust: $Fe_2O_3{\cdot}nH_2O$. In combination with oxygen and halides iron exists mainly in two oxidation states: II and III (Table 1), being III the most stable state. Nevertheless, also oxidation states VI, 0, -I and -II are important. In sharp contrast with osmium and ruthenium (OsO_4, RuO_4), iron does not possess empty *d* orbitals, and it cannot display the +VIII oxidation state. Iron compounds often show octahedral geometry, and in particular Fe^{III} can bind from three to eight different ligands.[4] Usually, Fe^0 complexes coordinate five or six ligands with a trigonal bipyramidal or octahedral geometry. The electron rich iron complexes (0 or -II) show to be more reactive than Fe^{II} or Fe^{III} species, therefore several iron 0 and -II catalysts have been reported.[5]

Table 1. Electronic Configuration and Oxidation States of VIII group Mendeleev's period table[6]

Element	Electronic Structure	Oxidation State[a]
Fe	$[Ar]3d^6\,4s^2$	0 **II** **III** (IV) (V) (VI)
Ru	$[Kr]4d^7\,5s^1$	0 II **III** IV (V) VI (VII) VIII
Os	$[Xe]4f^{14}\,5d^6\,6s^2$	0 (I) (II) (III) **IV** (V) VI (VII) VIII

[a] The common oxidation states are reported in bold.

Iron and its compounds are pervasive in industry, above all in metallurgy and steel production. Notably, the Haber–Bosch process, one of the most important inventions of the 20th century,[7] relies on a heterogenous iron catalyst to produce ammonia from nitrogen and hydrogen. Since then, heterogenous iron catalysis has grown and become relevant (e.g. Fischer-Tropsch process)[8] whereas homogeneous iron catalysis is still relatively underexplored.

Organoiron chemistry started at the end of 19th century, when Mond[9] and Berthelot[10] reported the first iron-pentacarbonyl compound, a very toxic reddish liquid. Another milestone in organoiron chemistry was the synthesis of ferrocene, reported by Pauson in 1951.[11] The first example of homogeneous iron catalyst, promoting the hydroformylation of ethylene, was reported by Reppe *et al.* in 1953.[12] Several years later, in 1971, Kochi and co-workers reported the first example of iron-catalyzed cross-coupling with Grignard reagent and organic halides.[13] Although several reactions promoted by homogeneous iron catalysts have been developed, this research area has still a strong growth potential.

1.1 Difficulties in Iron Catalyst Development

In organometallic chemistry, all the reaction pathways can be described as the sum of simple and sequential steps like, – for example – oxidative addition, reductive elimination, insertion, halogen-metal or ligand exchange and hydride elimination. The sequence of these steps, not necessary in the order in which they have been reported, forms what is called catalytic cycle. As for the geometric figure, in principle the cycle is endless. Therefore, no stable products are formed inside the cycle because this would interrupt it. Usually, oxidative addition is the first step, which results as an oxidation M^{n+2} of the metal. The reactivity towards this reaction is favored by low oxidation states and a vacant coordination site. Nevertheless, the ligands strongly affect the reactivity, too: for example, strong σ-donor (and poor π-acceptor) ligands enhance the reactivity of low-valent iron complexes towards oxidative addition, because they stabilize the oxidized form. Another key reaction is reductive elimination, because it provides the desired compound as product of the cycle.

To obtain an effective iron complex for hydrogenation, a hydride complex species M-H must be formed in the catalytic cycle, which means that an oxidative addition between H_2 (or a different hydrogen donor) and the iron complex must take place. Iron does not show a natural tendency to give oxidative addition, it requires proper ligands to increase its reactivity. The natural tendency of iron is to exist as Fe^{II} (d^6) or Fe^{III} (d^5) species. Indeed, d^5 configuration shows complexes with half-filled *d* shell, more stable due to symmetry reasons. Therefore, iron chemistry is dominated by a single-electron transfer from II to III. To mimic the noble metals behavior, the two-electrons transfer pathway should be preferred, and this would be possible only tuning the electronic properties of the complex using a proper ligand.

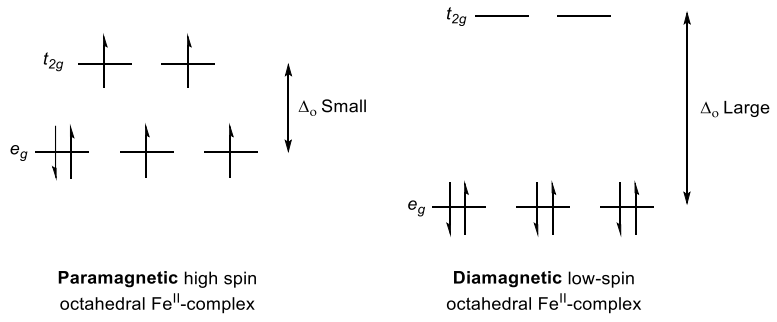

Figure 3. MO diagrams for octahedral crystal field: distribution of the six valence electrons in high-spin and low-spin Fe^{II}-complexes.

Characterization of the complexes is another issue with iron. Indeed, NMR spectroscopy is often useless due to paramagnetism of many iron complexes. As shown in Figure 3, the octahedral energy barrier Δ_o in iron complexes is

often small, thus high-spin paramagnetic complexes form easily. For these reasons, the characterization of Fe complexes often relies on spectrometric techniques such as mass spectrometry and X-Ray diffraction analysis.

1.2 Ligand Features

Homogenous metal-based catalysis has dramatically grown in the last thirty years, leading to the development of highly effective and selective methodologies. In the same period, there has been an increasing concern about how human activities could affect the environment, which has pushed chemists to think their reactions differently. The 'twelve principles of green chemistry' were elaborated to this purpose: in particular, Principle no. 9 claims "Catalytic reagents (as selective as possible) are superior to stoichiometric reagents" and in Principle no. 3 particular emphasis is devoted to the use of non-toxic and environmental friendly substances.[14] Looking from this point of view, the iron catalyzed hydrogenation (the main topic in this PhD thesis) satisfies both these principles, combining a non-toxic and readily available metal with an environmentally friendly and clean reagent (H_2).

Usually, iron complexes are stabilized by chelating ligands possessing nitrogen and/or phosphorus atoms in their binding sites, such as porphyrins or polydentate phosphines. In some cases, these ligands are simple "spectators",[15] and marginally modify the reactivity of the metals. Other kind of ligands can deeply influence the metal's reactivity, overcoming the scarce tendency to undergo two-electron redox chemistry.[16] Some recent advances have been made in the development of these "non-innocent" ligands,[17] which can play a specific role in bond-making and bond-breaking processes. In the presence of these ligands, a cooperation is present between the metal center and the ligand itself during the catalytic cycle. These new ligands are divided in two groups: **redox non-innocent** and **cooperative ligands**, or may exhibit properties of both families.

Innocent ligand is a term introduced by Jørgensen and co-workers, meaning a ligand which does not affect the oxidation state of the metal center, which is clear and not uncertain.[18] On the contrary, **redox non-innocent ligands** form complexes in which the metal's oxidation state is uncertain. The determination of the oxidation state usually requires spectroscopic techniques like: Raman or EPR spectroscopy, X-ray absorption, UV-Vis or Mössbauer spectroscopy. Through resonance or inductive features, redox non-innocent ligands can delocalize the electronic density of the complex and further act as "electronic reservoirs" during the catalytic process. Multi-electronic transformations can be obtained with metals that usually do not show this reactivity, and also radical processes can be initiated and controlled using redox non-innocent ligands.[18] When the delocalization of the electron density moves significantly from the metal to the ligand, the ligand itself becomes able to promote redox processes.[16,17,19]

As stated by Grützmacher *et al.*, **Cooperative ligands** are "participating directly in bond-activation and undergo reversible chemical transformations".[20] In an extreme case, the metal acts only as a binding site bringing together the reactants. Ligand and metal work in a synergistic way to promote the chemical transformation.

More than a kind of structure or sub-structure, non-innocent ligand is a state which can be attributed to any ligand under the proper conditions. Besides, an observed innocent behavior of a ligand in a metal complex does not guarantee that it will act the same with a different metal or under different conditions. Only spectroscopic investigation can confirm a non-innocent behavior of the ligand in a specific transformation.

1.3 Alkene and Alkyne hydrogenation

1.3.1 Iron Carbonyl Complexes

The first iron complexes active in the hydrogenation of alkenes were discovered already in the 1960s. The first example was reported by Frankel *et al.* and consisted in the hydrogenation of fatty ester methyl linoleate.[21] Iron carbonyl complexes were used under 30 atm of hydrogen at 180 °C affording several reduced intermediates and only tiny amounts of the fully reduced methyl stearate. Seven years later, in 1972, Noyori and co-workers reported the first selective alkene hydrogenation of α,β-unsaturated ketones with iron pentacarbonyl.[22] The mechanism behind the hydrogenation of olefins with iron carbonyl complexes was investigated initially by Frankel *et al.*,[21] and later by Grant and co-workers in the late 1980s.[23] The active catalyst consists in an $Fe(CO)_3$ intermediate species which coordinates the double bond of the olefin and promotes the hydrogenation. High temperature (> 150 °C) or UV-light irradiation was needed for generating the active iron species after release of two CO molecules.

Relying on the derived iron carbonyl complex **1**, Nakazawa and co-workers reported an interesting catalyst able to promote the transfer hydrogenation (TH) of aromatic alkynes in the presence of isopropanol.[24] The (hydrido)iron complex **1** (10 mol%), with a Si-H functionalized cyclopentadienyl ligand, allowed to obtain a mixture of alkene and alkane products (Scheme 2). Although no selectivity was shown, the complex is still the first example of (hydroxycyclopentadienyl)iron complex promoting the TH of alkynes. Notably the same complex was found unable to promote the hydrogenation of polar double bonds.

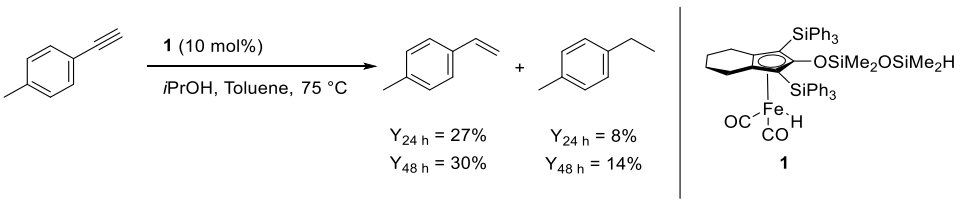

Scheme 2. Nakazawa catalyst for transfer hydrogenation of aromatic alkynes.

1.3.2 Bis(iminopyridine) iron complexes

In 2006, Chirik and co-workers reported the iron-catalyzed hydrogenation of alkenes, which occurred under mild conditions in the presence of the bis(imino)pyridine iron complex **2** (Scheme 3).

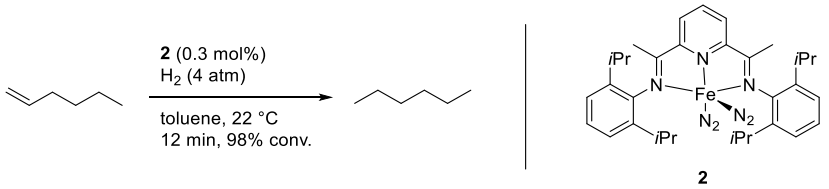

Scheme 3. 1-Hexene reduction using Chirik'catalyst **2.**

Besides being easily synthesized, the bis(imine) ligand of catalyst **2** has the feature to be tunable, which allowed its systematic modification and its use with several metals and different reactions.[25] Iron catalyst **2** showed excellent performance in olefins hydrogenation, with a TOF of 1814 h^{-1} in 1-hexene reduction under 1 bar of H_2 at 22 °C. This result is comparable with the ones obtained with some classical noble metal catalysts such as Pd/C, Wilkinson's $(PPh_3)_3RhCl$[26] or Crabtree's catalyst $[(COD)Ir(PCy_3)Py]PF_6$.[27] Notably, the reactivity is higher for external double bonds, whereas the internal ones require longer reaction time. Moreover, complex **2** was shown to be compatible with neat conditions, and with several functional groups such as amines, esters, ketones and ethers.[28]

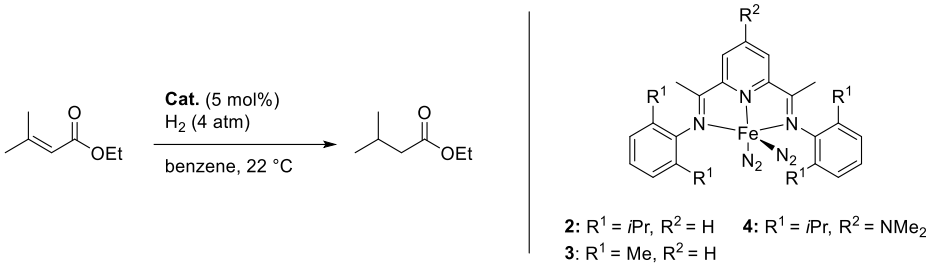

Scheme 4. Effects of ligand modifications on hydrogenation of ethyl-3-methylbut-2-enoate.

Although **2** undergoes decomposition using α,β-unsaturated ketones as substrates, Chirik and co-workers demonstrated that it can be used with conjugated esters, as shown in Scheme 4. Initially, only poor results were obtained (65% conv., 24 h), but carefully tuning the steric hindrance of the ligand allowed to obtain good conversion (>95% conv. in 24 h with complex **3**).[29]

The most remarkable effect was obtained by further tuning the electronic properties of the ligand, i.e. with catalyst **4**. Indeed, upon introduction of electron-donating substituents NMe_2 at the 4-position of the pyridine ring, 95%

conversion was achieved after only 7 hours. Density functional theory (DFT) calculations and spectroscopic data revealed that in **2,** iron has +II oxidation state (Figure 4).

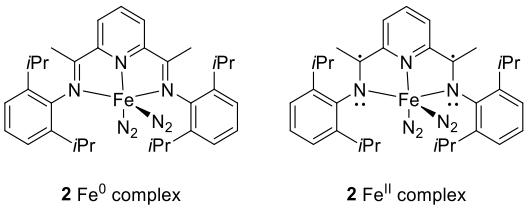

Figure 4. Corrected structure of complex **2** resulted from DFT calculation and spectroscopic data.

Indeed, through the highly conjugated ligand structure, the metal center can transfer two electrons to the ligand, which behaves as redox non-innocent ligand (see Paragraph 1.2).[30]

Chirik and co-workers also synthesized several binuclear bis(imino)pyridine iron dinitrogen complexes (i.e. **5)** which showed activity in reduction of several substrates.[31] The authors investigated also the possibility to exchange the imino moieties with phosphine groups, obtaining a new class of iron pincer complexes **6** (shown in Figure 5).[32] Compared to **2**, iron catalyst **6** shows a different geometry and a hydride replacing the N_2 ligand. Complex **6** showed some activity in the hydrogenation of 1-hexene, but with lower performance than **2** (325 h^{-1} vs. 1814 h^{-1} TOF).

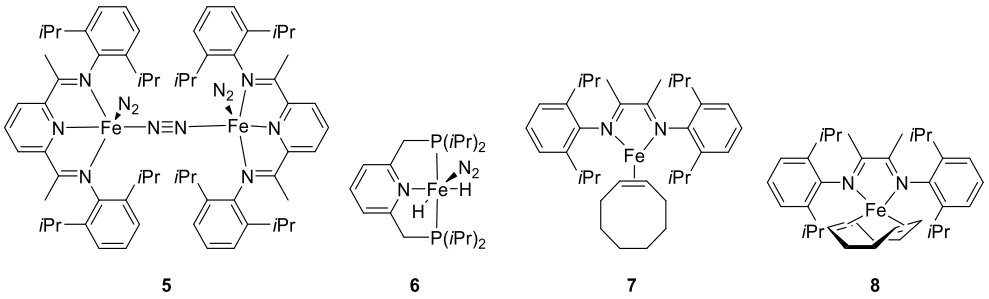

Figure 5. Other catalysts developed by Chirik and co-workers.

Other complexes **7** and **8** were also reported, in which, to increase the stability, the labile N_2 ligands were replaced by an alkene or dialkene species. Also iron complexes **7** and **8** could promote the hydrogenation of 1-hexene, but the results were worse compared to those obtained with **2.**

Despite the excellent performances, the family of Chirik's catalysts suffers from serious practical limitations. Due to their highly air-sensitivity, they must be stored, synthesized and manipulated strictly under inert atmosphere and dry-environment (glove box). These issues, unfortunately, hamper their industrial application.

1.3.3 Multiple P-ligand iron complexes

The first iron catalyst able to hydrogenate alkynes was developed by Bianchini and co-workers in 1992 using the tetradentate phosphine Tetraphos®.[33] Under very mild conditions (room temperature, 1 bar of H_2), terminal alkynes were reduced to alkenes (see Figure 6). Considering the mechanism, ligand Tetraphos® behaves like a cooperative non-innocent ligand. The coordination of the alkyne substrates takes place only after de-coordination of one phosphorus atom from the metal. According to this mechanism, a decreased reaction rate was expected in the presence of bulky substrates, as was confirmed by tests carried out with substituted alkyne substrates. The catalyst was found to be selective towards alkene formation, and no alkane products were detected.

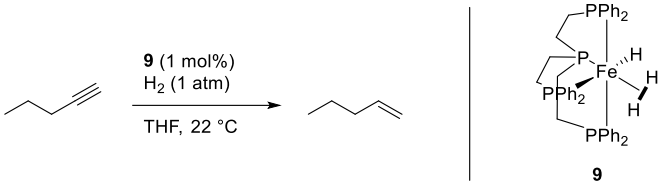

Figure 6. Selective reduction of 1-pentyne using multidentate iron P complex.

Another interesting multidentate P-complex was reported in 2012 by Beller and co-workers using the Tetraphos® ligand to form a Fe-catalyst able to promote the catalytic transfer hydrogenation (CTH) of aromatic alkynes to alkenes.[34] As shown in Scheme 5, the catalytic complex was formed *in situ* from $Fe(BF_4)_2{\cdot}6H_2O$ and Tetraphos® ligand, and formic acid was employed as hydrogen donor. Several aromatic alkynes have been selectively reduced to the corresponding alkenes.

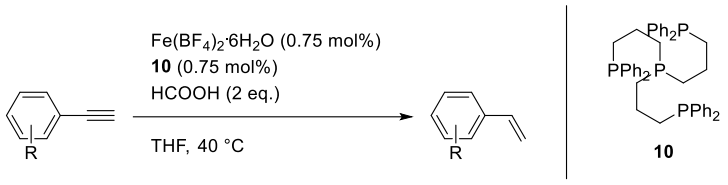

Scheme 5. Catalytic Transfer Hydrogenation (CTH) of aromatic alkynes promoted by an *in situ* formed iron complex.

Another family of multidentate phosphine-iron catalysts **11** active in olefin hydrogenation was developed by Peters and Daida (Scheme 6).[35] To promote the hydrogenation, a catalyst loading of 10 mol% is needed, and **11** is active only in alkene reductions. Indeed, in the presence of catalysts **11** and **12** alkynes undergo polymerization or dimerization. Notably, the authors proposed an unusual Fe^{II} – Fe^{IV} catalytic cycle, beginning with dissociation of a phosphine followed by coordination of the alkene moiety.

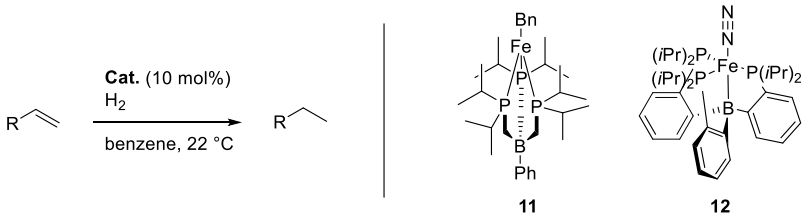

Scheme 6. Multiple P-ligand complexes in hydrogenation of olefins.

In 2013, Peters' group reported another iron boratrane catalyst **12** (Scheme 6), in which Fe is bound to the B and to the P atoms simultaneously.[36] Although it exhibited a modest reactivity, the mechanism of the **12**-catalyzed reduction process is interesting. Indeed, the boron moiety plays an important role acting either as hydride carrier and as a leaving group in order to allow coordination of the alkene moiety.

1.3.4 Biomimetic Complexes

Nature has developed metal-ligand interactions for any use in living system. Porphyrins are one of the molecules that Nature provides for bringing metal co-catalysts into living organisms. Kano and co-workers took inspiration from Nature in the design of their Fe-porphyrin catalyst: using Fe-porphyrin complex and a hydrogen source ($NaBH_4$) they could reduce styrene with a TOF of 81 h^{-1}.[37] Although the reported activity was not outstanding, this Fe-porphyrin catalyst is one of the first used for this kind of reaction. One year later Sakaki and co-workers reported another porphyrin-derived iron complex **13** for hydrogenation of α,β-unsaturated esters (Scheme 7). Good performances were shown with a TOF of 4850 h^{-1}. Some mechanistic studies were carried out and it was found that MeOH is somehow involved in the hydride exchange.[38]

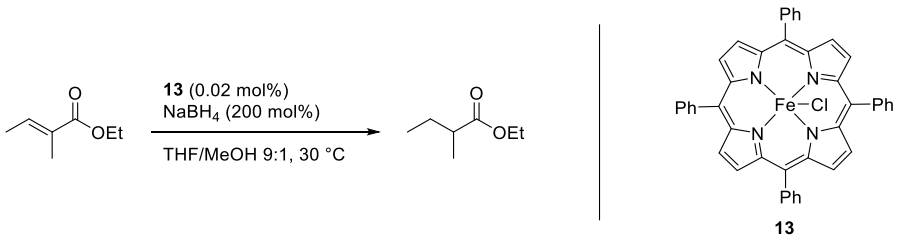

Scheme 7. Hydrogenation of α,β-unsaturated esters with Fe-porphyrin complex.

Another Nature-inspired approach was reported by Inoue, who took inspiration from the iron-sulfur clusters which are present in some hydrogenase enzymes. Using cluster **14**, after activation with PhLi, several alkenes were hydrogenated (see Scheme 8).[39]

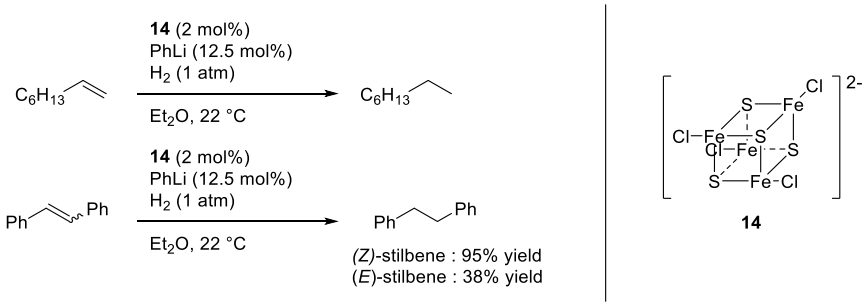

Scheme 8. Fe-S clusters in hydrogenation of olefins.

1.3.5 Iron Nanoparticles

A totally new approach in alkene and alkyne hydrogenation was reported in 2009 by de Vries and co-workers,[40] who discovered the potential of iron nanoparticles FeNPs in the hydrogenation of double bonds. Taking inspiration from a methodology reported by Bedford three years before,[41] FeNPs were prepared reacting $FeCl_3$ with 3 eq. of EtMgCl in a mixture of Et_2O or THF. These iron clusters (~25 nm diameter) were able to reduce at room temperature and under 1 bar of hydrogen pressure norbornene, terminal olefins and disubstituted *Z* alkenes with excellent yields. The catalyst showed to be active also in the alkyne hydrogenation. Although the FeNPs were found to be sensitive to water (less than 1% of water can decrease the reaction rate), this catalyst was successfully applied in a continuous hydrogenation of norbornene. Similar NPs, supported on graphene, were later found active in hydrogenation of cyclic and terminal olefins.[42] The chemoselective reduction of alkynes to *Z*-olefins was performed by Wangelin and co-workers using FeNPs in a biphasic system with heptane and an ionic liquid.[43] For unclear reasons, the presence of a nitrile in the reaction environment was found beneficial for stereoselectivity: a nitrile could be present either as additive (small additions of acetonitrile) or as functional group in the ionic liquid structure.

Another approach using ultra small NPs (~ 2nm diameter) was described by Beller.[44] The ultra-small Fe-NPs were tested in hydrogenation under mild reaction conditions (2.4 mol% of catalyst loading, 10 atm of H_2, in mesitylene at room temperature). The iron nanoparticles were found to be active in the hydrogenation of terminal alkenes and alkynes, as well as of cyclic alkenes. However, no conversion was observed with non-cyclic internal alkenes and alkynes.

1.4 Hydrogenation of Ketones and Aldehydes

As for the reduction of olefins and alkynes, ketone hydrogenation had been dominated by noble metal catalysts for years. In the last thirty years many Rh and Ir catalysts were developed, showing excellent activity in ketone and imine hydrogenation. For a long time, iron catalysis lagged behind in this field, and the few early reports were far away from

the performance of the noble metals. The first breakthrough was obtained in the 1980s by Markó and co-workers, who combined $Fe(CO)_5$ and triethylamine to obtain a catalyst for the reduction of few ketones and aldehydes.[45]

In 2004 Gao *et al.*, using the Markó's catalyst in combination with chiral ligand **15**, were able to perform the asymmetric transfer hydrogenation (ATH) of ketones with modest yields but promising *ee* (Scheme 9). The best enantiomeric excess 98% , was obtained using sterically crowded ketone substrates.[46]The ligand used in this reaction is a PNNP system bearing two phosphine moieties and two nitrogen atoms. From this relatively simple structure a wide number of PNNP ligands have been later developed.

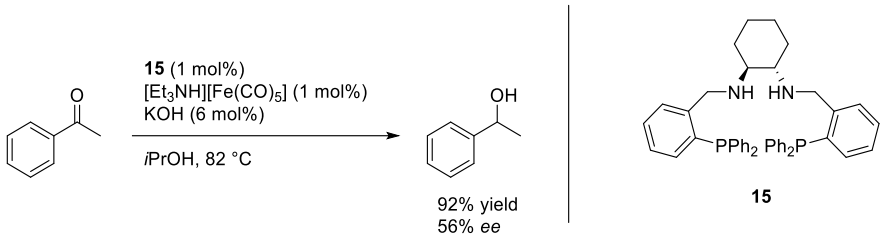

Scheme 9. Gao's ligand and $Fe(CO)_5$ in the ATH of ketones.

1.4.1 PNNP Ligands in iron Catalysts

Ligand **15** had been synthesized several years before (in 1996) by Jing-Xing Gao, a young PhD student in Noyori's group, and used in the ruthenium-catalyzed ATH of aromatic ketones.[47] Ligand **15** bears strong similarity with the most famous 'Trost Ligand', reported by Barry Trost in 1992 (see Figure 7).[48]

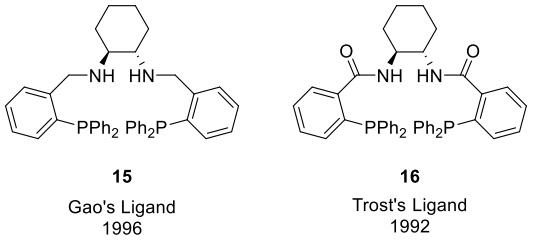

Figure 7. The chiral PNNP ligands developed by Gao (**15**) and Trost (**16**), respectively.

The same author also combined *o*-(diphenylphosphino)benzaldehyde with various chiral diamines to build up a Ru^{II} complex library which was screened in ketone hydrogenation.[49] In 2004, ligand **15** was employed in ketone ATH also with iridium[50] and iron.[46] Perhaps inspired by this findings, in 2008 Morris and co-workers reported the first generation of iron diiminophosphine complexes **17a-b** (Figure 8).[51]

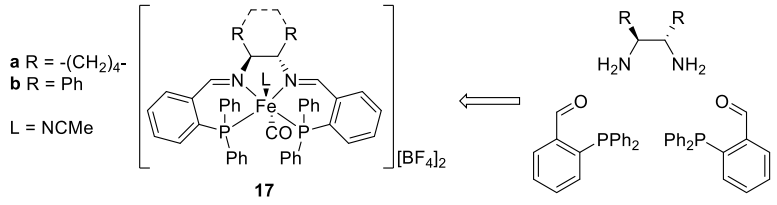

Figure 8. Morris' iron bis-iminophosphine catalysts, first generation.

Complex **17a** showed excellent activity in ATH of ketones and imines, although only modest enantioselectivities could be obtained. Particularly impressive was the TOF of the catalyst, which was up to 907 h^{-1}, a value similar to those obtained with the ruthenium catalysts developed up to that moment. This was one of the first examples of iron catalyst reaching levels of activity similar to those typical of noble metals. A few years later, Morris discovered that the real active species performing the hydrogenation was not the expected homogenous complex **17** but, rather, the FeNPs formed from complex **17a**.[52] This new methodology has represented the first example of FeNPs promoting an enantioselective transformation. In the Authors' opinion, the reason of NPs formation is the flexibility of the six-membered Fe-chelate rings present in complex **17a**. It is possible that, under reductive conditions, de-complexation takes place with release of Fe^0, which then clusters to form the NPs. To test this hypothesis, Morris and co-workers synthesized analog complexes possessing five- instead of six-membered chelate cycles (**18a-e**, Figure 9), which were tested in ATH of acetophenone.

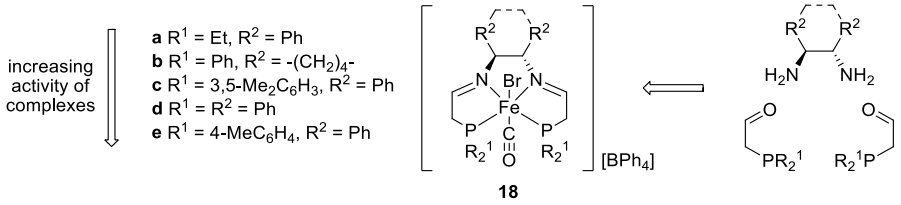

Figure 9. Second generation of Morris' catalysts.

An impressive TOF of 30 000 h^{-1} was obtained with this new generation of Morris's complexes in ATH of ketones and also the *ee* increased, reaching up to 90%. A careful examination of the modifications to the second generation of Morris' complexes shows that the phosphorus moiety is found to have a crucial importance. Indeed, the phosphorus substituents must be of moderate size and quite strong electron donor, otherwise the complexes are catalytically inactive.[53] Complex **18d** proved to be also active in ATH of ketimines, giving high conversions (up to 91%) and excellent enantioselectivity (*ee* = 95-99%).[54]

Several mechanistic studies have been performed to understand the behavior of these complexes in asymmetric hydrogenation.[55] In the catalytic cycle (Scheme 10), ligand **18d** undergoes two transformations: firstly, bis-enamide

18d.1 is formed in the presence of a large excess of *t*BuOK (from 2 to 8 eq.); then, **18d.1** is slowly reduced by *i*PrOH, originating the active complex **18d.2**.

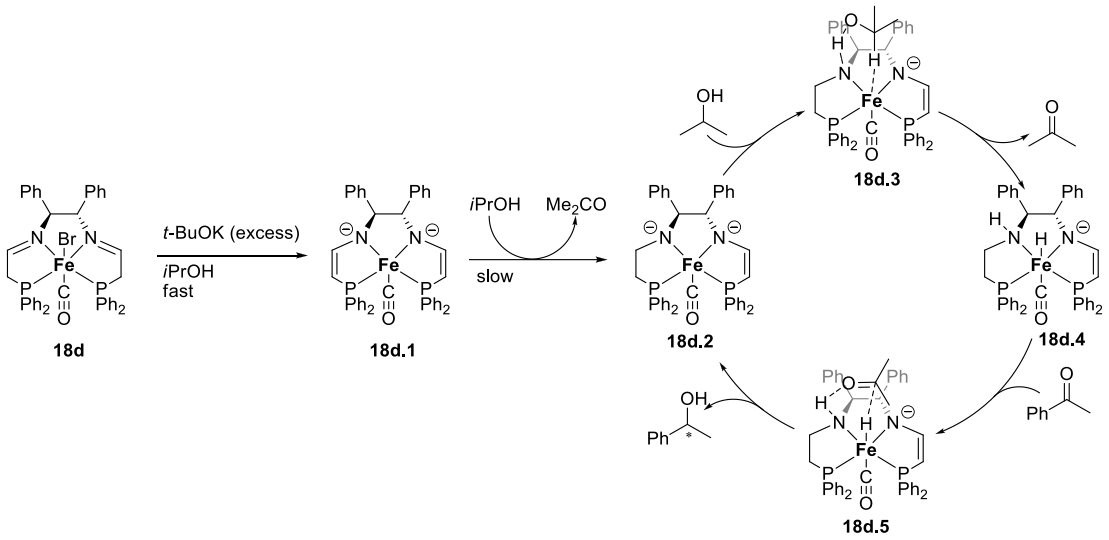

Scheme 10. Proposed activation mechanism of 2nd generation Morris' complex **18d**.

The proposed mechanism is an outer-sphere pathway without coordination of the substrate into the metal center (analogous to that reported by Noyori for his Ru^{II} catalysts possessing amine ligands[56]). In the catalytic cycle the ligand shows a 'non-innocent' behavior, assisting the Fe center in the dehydrogenation of *i*PrOH and substrate hydrogenation through a pericyclic TS. It was found that only the saturated arm of **18d.2** is involved in this kind of mechanism, whereas the unsaturated arm is inert. The authors also synthesized a catalyst with both arms saturated, which curiously was found not catalytically active.[57]

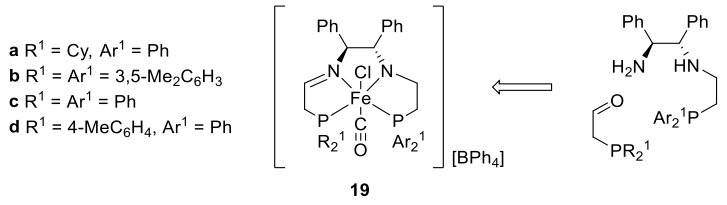

Figure 10. Third generation of Morris' Catalysts.

For this reason, Morris *et al.* developed a third generation of catalyst **19** starting from an unsymmetrical ligand. As expected the new catalysts were much faster than the previous ones. After treatment with an excess of base, the catalyst is directly converted to the active unsymmetrical amide-enamide specie, which can reduce a wide range of ketones and activated ketimines showing a TOF of 150 s^{-1} and a very high enantioselectivity (99% *ee*), as shown in Scheme 11.[57a,c,58]

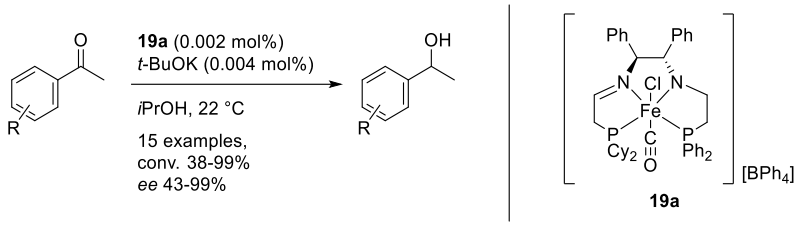

Scheme 11. ATH of ketones with third-generation of Morris' catalysts.

Morris also investigated catalysts for the AH of ketones (i.e., using H_2 instead of *i*PrOH as the reductant).[57b] To this purpose, a new generation of PNP iron catalysts was developed. Complex **20** was synthesized by a condensation between an enantiopure P-NH_2 system and dicyclohexylphosphinoacetaldeyde (Scheme 12). After activation with $LiAlH_4$, compound **20** showed good activity (99% conv) and good enantioselectivity (85% *ee*). Unfortunately, the structure of the real, *in situ* formed catalyst is still unknown at present.

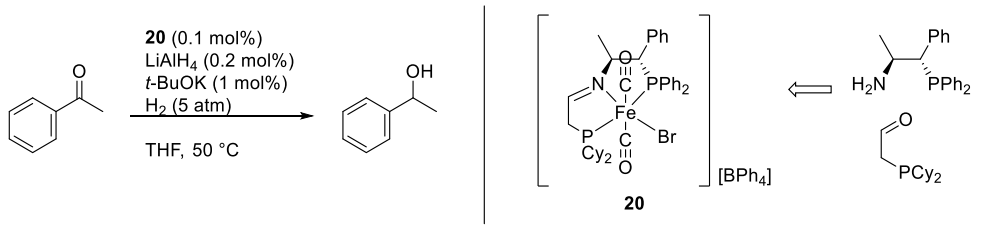

Scheme 12. Fourth-generation of Morris' iron complexes promote asymmetric hydrogenation of acetophenone.

1.4.2 Macrocyclic Ligands (PNNP evolution)

Recently, Mezzetti and co-workers reported a new C_2-symmetric iron complex (**21** in Figure 11) active in the ATH of ketones and featuring a macrocyclic PNNP ligand with stereogenic phosphorus atoms.[59]

Both the diimino (**21f**) and the diamino complexes (**21g**) were synthesized. Besides the macrocyclic ligand, it was found that the isontrile ligands have a strong influence on both activity and enantioselectivity, the best results have been obtained with isonitrile or *N*-isonitrile ligands. The best chiral complexes **21g** showed very good activity and enantioselectivity (*ee* up to 98%) in the ATH of ketones. The reaction scope includes ketones, enones and activated imines. A limitation of these C_2-symmetric PNNP ligands is their preparation, which requires several steps and thus decreases their potential industrial interest.

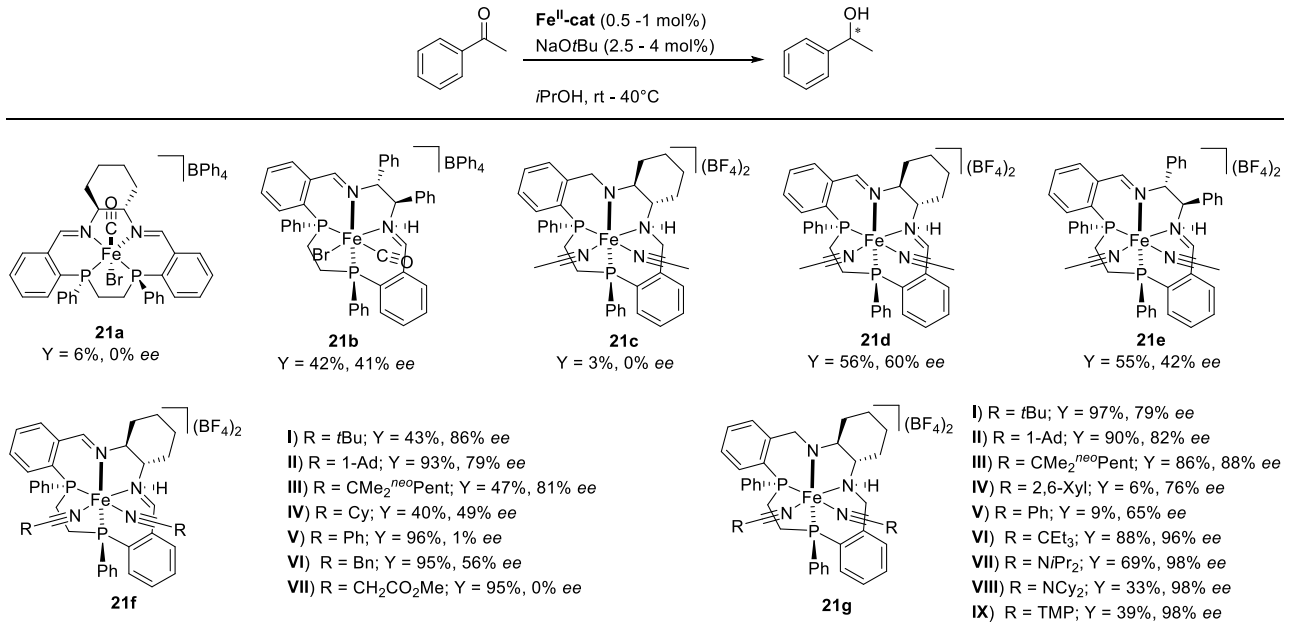

Figure 11. Mezzetti's iron complexes promoting the ATH of acetophenone.

Recently, Gao and co-workers synthesized the new chiral macrocyclic ligands **24** and **25**. Ligand **24** was obtained by condensation of bis(*o*-formylphenyl)-phenylphosphane **22** with the (*S*,*S*)-1,2-cyclohexanediamine **23**. Ligand **25** was obtained from **24** by reduction with sodium borohydride.[60]

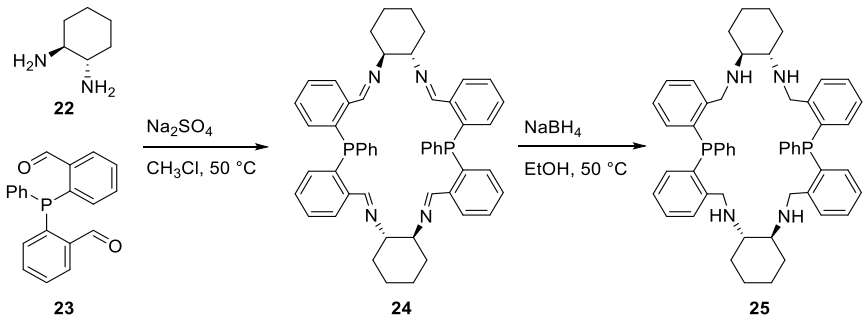

Scheme 13. Synthesis of Gao's macrocyclic ligands.

Using an *in situ* approach, the two ligands were combined with $Fe_3(CO)_{12}$ to promote ATH of propiophenone. Ligand **25** formed a more active catalyst than **24**, yielding 1-phenylpropanol with good yield (93%) and high enantioselectivity (98% *ee*). Several iron sources were screened ($Fe_2(CO)_9$, $FeCl_2$, $FeCl_3$), but only triiron dodecacarbonyl allowed to obtain appreciable conversion. To improve conversions and enantioselectivity some optimization was carried out, and the authors found out that ammonium salts could improve the catalytic performances. With the optimized conditions in their hands, they explored a ketone scope, Scheme 14.

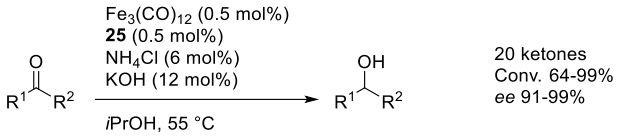

Scheme 14. Fe-catalyzed ATH of ketones in the presence of Gao's macrocyclic ligand **25.**

To understand which was the active catalyst, Gao tried to synthesize an isolated iron complex employing macrocycle **25**. The obtained complex **26** (Scheme 15) showed activity in the ATH of ketones, but with different *ee* and lower conversions, which means that **26** is not the complex involved in the ATH of ketones promoted by the *in situ* catalyst formed from **25** and $Fe_3(CO)_{12}$.[61] Macrocyclic ligand **25** was also tested in the Fe-catalyzed AH of ketones, showing high activity and enantioselectivity. It was found that under hydrogenation conditions formation of FeNPs takes place, meaning that this reaction is promoted by a heterogeneous Fe-complex.[62]

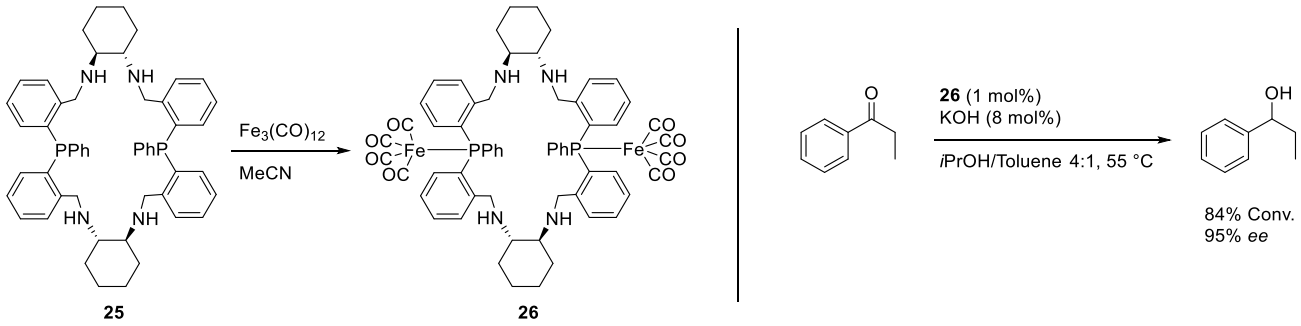

Scheme 15. Synthesis of Fe-complex **26** and catalytic tests in the ATH of ketones.

1.4.3 PNP pincer ligands

Pincer ligands are chelating molecules which bind tightly the metal center through three coplanar atoms.[63] They have been used in combination with several noble metals such as iridium or ruthenium, but the first iron pincer complex was synthesized by Milstein and co-workers in 2011.[64] Pincer complex **27** (Scheme 16) was reported to be an active catalyst in hydrogenation of ketones, with a good TONs of 1880 and low catalyst loading (0.05%).

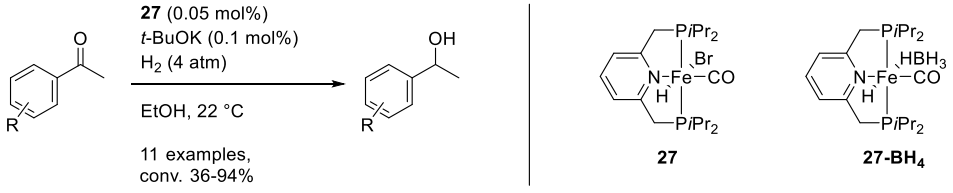

Scheme 16. Milstein's pincer complex **27** in hydrogenation of ketones.

An inner-sphere pathway with the metal center directly involved in the reduction was suggested by the authors for catalyst **27**.

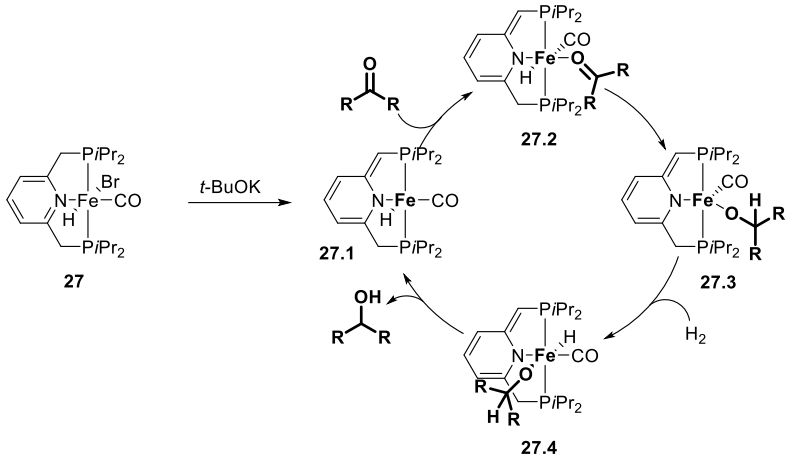

Scheme 17. Proposed catalytic cycle for hydrogenation of ketone promoted by pincer iron complex **27**.

Interestingly the 2,6-bis(diisopropylphosphinomethyl)pyridine ligands shows a 'non-innocent' behavior, flipping between an aromatic and a non-aromatic form (Scheme 17). Milstein proposed also another generation of catalysts **27-BH$_4$,** where the bromide ligand is replaced with a borohydride derivative. This new catalyst system showed the same TON than the previous one without requiring activation with bases.

1.4.4 Multidentate N or P complexes

In 2006 Beller *et. al.* developed an *in situ*-formed catalyst for the transfer hydrogenation of ketones (Scheme 18). Several iron sources [$Fe_3(CO)_{12}$, $FeCl_2$] were combined with 2,6-di(2-pyridyl)pyridine, triphenylphosphine and a base in isopropanol.[65] It was found that the reaction is strongly base-dependent. Use of *i*PrONa or *t*BuONa allowed to obtain excellent yields, independently from what was the iron source.

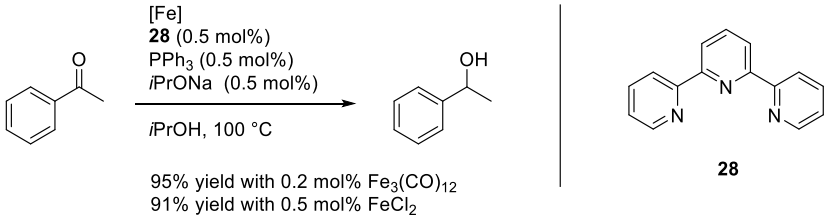

Scheme 18. Transfer hydrogenation of acetophenone promoted by an *in situ* Fe^0 complex.

In another instance from Beller *et al.,* $Fe_3(CO)_{12}$was combinedwith a porphyrin system obtaining the first *in situ* generated iron porphyrins homogeneous catalysts for the transfer hydrogenation of ketones.[66]

1.4.5 Isonitrile iron complexes

From an electronic point of view, isonitrile and carbonyl group are very similar. They are isoelectronic and the MOs of the two structures are comparable. Most of the reported Fe-catalysts for reduction bear at least a CO group in their structure. CO is a strong ligand which behaves as σ donor and strong π-acceptor at the same time. Isonitrile groups share the same features, but with some advantages such as the lower toxicity. Unfortunately, isonitriles usually have an unpleasant smell, and therefore they have to be handled cautiously.

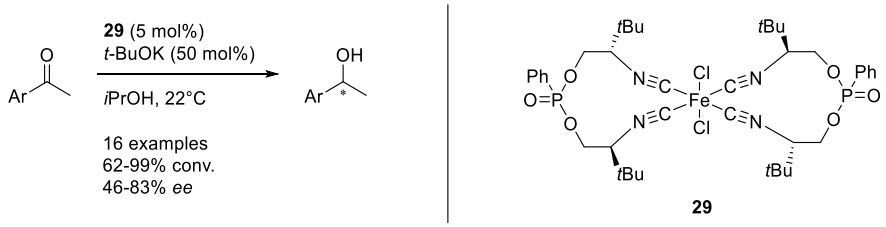

Scheme 19. ATH of aromatic ketones promoted by bis-isonitrile iron(II) complex **29.**

In 2010, a bis-isonitrile iron(II) catalyst for the ATH of aromatic and heteroaromatic ketones was reported by Reiser and co-workers.[67] Under mild reaction conditions, the new catalyst showed good activity with a wide range of ketones (Scheme 19). Unfortunately, only modest *ee* were achieved with this new catalyst.

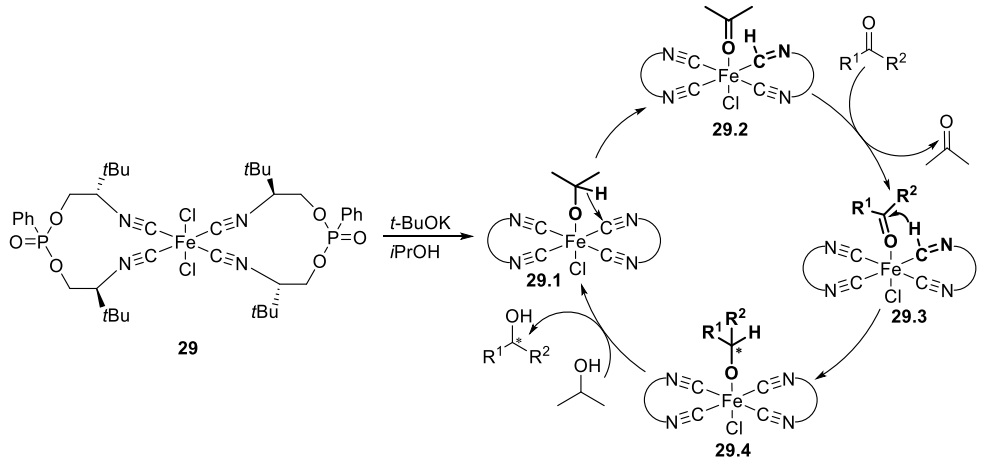

Scheme 20. Proposed mechanism for ketone ATH promoted by complex **29.**

IR investigations suggested that, after addition of the base, the isonitrile group decreases its bond order becoming more an imine bond and also no hydride signals were observed in ^{1}H-NMR spectrum. These evidences suggest that, in the catalytic cycle, the coordinated isonitriles **29** acts as 'non-innocent ligands' (Scheme 20), extracting a hydride from the reductant (*i*PrOH) and then delivering it to the substrate. This kind of mechanism, in which iron bears no

hydride and has the sole role of coordinating the substrate, resembles that of the Meerwein-Ponndorf-Verley reaction.

1.4.6 (Cyclopentadienone)iron complexes

1.4.6.1 Reduction of Aldehydes, Ketones and Imines

(Cyclopentadienone)iron complexes have recently become the object of an increasing interest,[68] being extensively applied in the hydrogenation of aldehydes/ketones, imines and, recently, activated esters. These complexes were originally reported by Reppe and Vetter in 1953,[12] and for many years they received a scarce attention until Knölker[69] and Pearson[70] studied their synthesis and properties in the early 1990s (Figure 12).

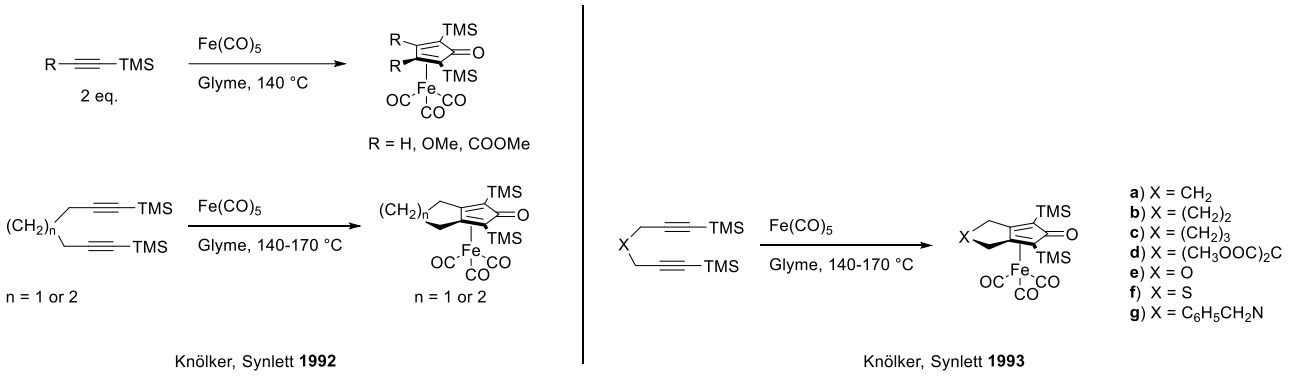

Figure 12. Synthesis of (cyclopentadienone)iron complexes by iron mediated [2+2+1] cycloadditions of alkynes and carbon monoxide proposed by Knölker *et al.*

In 1999, Knölker and co-workers reported the synthesis and characterization of the first (hydrocyclopentadienyl)iron complex **31**, intermediate of the de-metallation of complex **30** (Scheme 21).

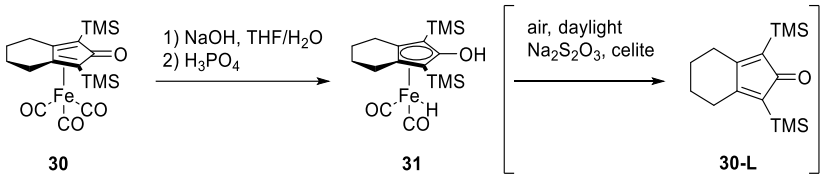

Scheme 21. Synthesis of the first (hydroxycyclopentadienyl)iron complex **31**, and de-metallation to cyclopentadienone **30-L**.

Complex **31** was obtained by treating **30** with an aqueous base (Hieber base reaction) and, unlike its precursor, was found to be highly sensitive to air and daylight, readily forming the corresponding cyclopentadienone **30-L**.[71] In this paper, the potential catalytic properties of complexes **30** and **31** were not tested.

Eight years later (in 2007) Casey and Guan, taking inspiration from the Shvo catalyst **32** (Scheme 22),[72] reported the use of the (hydroxycyclopentadienyl)iron complex **31** as catalyst for ketone hydrogenation and transfer hydrogenation.[73]

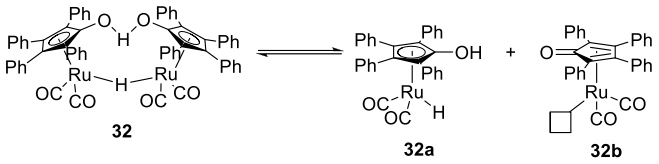

Scheme 22. Shvo dimeric pre-catalyst **32** and its active structures **32a** and **32b.**

Complex **31** turned out to promote the reduction of polarized double bonds (C=O and C=N), leaving alkene, alkyne, nitro, halide and epoxide groups untouched (Scheme 23). Casey and Guan proposed that reduction occurs through a pericyclic TS which the substrate's heteroatom is hydrogen bonded to ligand's hydroxyl group, which explains the inertness of C=C and C≡C bonds and was later confirmed by computational studies carried out by Sun and co-workers.[74]

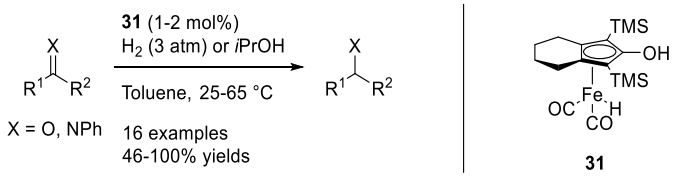

Scheme 23. Hydrogenation and transfer hydrogenation of ketones and imines promoted by Knölker catalyst **31.**

The main limitation of the (hydroxycyclopentadienyl)iron complexes such as **31** is their low stability (high sensitivity to air, moisture and light), which makes a glovebox indispensable for their use/manipulation. For this reason, in the last decade several different strategies have been reported to avoid the direct handling of **31**. *In situ* activation of stable (cyclopentadienone)iron complexes such as **30** has been performed in three different ways: oxidation, light-irradiation, or Hieber base reaction (Scheme 24).

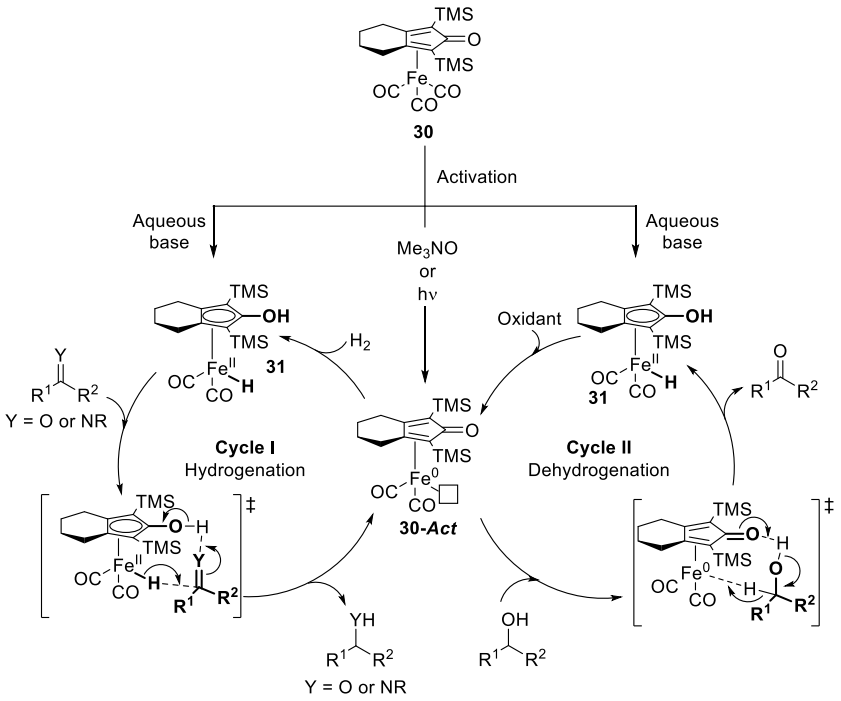

Scheme 24. Activation pathways of stable **30** to **30-*act*** or **31** (Cycle I) hydrogenation of C=O and C=N double bonds and (Cyle II) Oppenauer-type alcohol oxidation.

The first method reported was the oxidative cleavage of one CO group in the presence of Me_3NO,[75] which generates (cyclopetadienone)iron complexes with a vacant coordination site (**30-*act***). Knölker[76] and later Berkessel reported that the same kind of complex **30-*act*** could be obtained by UV irradiation of (cyclopentadienone)iron complexes.[77] Complexes **30-*act*** are able to split molecular hydrogen (H_2) and form the (hydroxycyclopentadienyl)iron complexes **31**. Alternatively, the latter complexes can also be obtained from (cyclopentadienone)iron complexes **30** in the presence of an aqueous base (Hieber base reaction).[78]

The catalytic cycle (reported in Scheme 24) has been deeply investigated and it has been proved that the cyclopentadienone ligand displays a 'non-innocent' behavior.[68] As in the case of the Shvo catalyst **32**, the ligand can flip from cyclopentadienone form (**30-*act***) to the hydroxycyclopentadienyl form **31**, thus enabling a non-ordinary Fe^0/Fe^{II} catalytic cycle. The reaction with **30-*act*** and H_2 produces the (hydroxycyclopentadienyl)iron complex **31**, which then reduces the polarized double bond. The reduction occurs through an outer-sphere, pericyclic TS in which the OH group of the (hydroxycyclopentadienyl)iron complex forms a hydrogen bond with the substrate and the metal hydride attacks the C=Y bond. With the same kind of catalytic cycle, complex **30-*act*** is also able to catalyze the dehydrogenation of alcohols to ketones (Cycle II, Scheme 24), thus performing an Oppenauer-type oxidation.

1.4.6.2 Enantioselective Reductions

Despite the recent success of (cyclopentadienone)iron complexes, only a limited number of chiral complexes belonging to this family have been reported so far. The reason of this scarcity can be found after a critical examination of the general structure of these complexes (Figure 12).

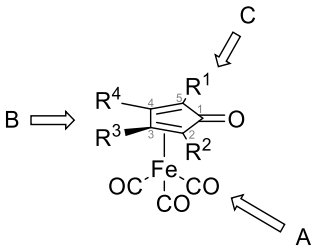

Figure 13. Derivatization sites of Knölker iron pre-catalyst.

Looking through the general structure of these complexes (Figure 13) stereogenic elements can be introduced by modifying three different sites: A) the CO ligands, which can be replaced with a chiral ligand; B) the cyclopentadienone ligand, introducing a chiral backbone; C) the 3,5-substituents of the cyclopentadienone ring (if these substituents are different, then the cyclopentadienone plane becomes stereogenic).

Approach A was initially followed by Berkessel and co-workers, who replaced a CO with a chiral phosphoramidite ligand either under UV irradiation or using Me_3NO (Scheme 25).[77]

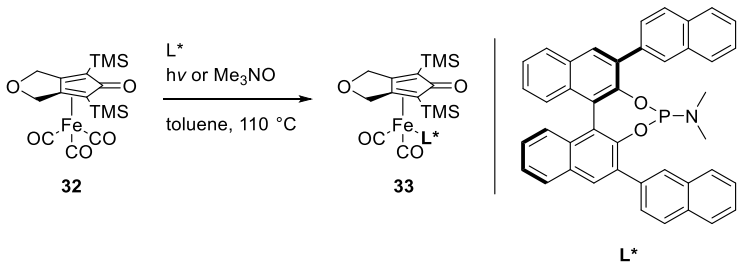

Scheme 25. Berkessel's approach (A): introducing a chiral ligand into the (cyclopentadienone)iron complex **32.**

Pre-catalyst **33** was employed to promote AH of acetophenone, under constant irradiation with UV light, affording 1-phenyletanol with only 31% *ee*. The authors performed a NMR study on catalyst activation in the presence of H_2 under UV irradiation. This experiment revealed that formation of two diastereoisomeric (hydroxycyclopentadienyl)iron complexes **33a-H** and **33b-H** occurs with 1:0.7 ratio + about 2% of achiral catalyst **33c-H** (Scheme 26). This low diastereoselectivity in the active complex formation explains the low observed stereocontrol in ketone ATH.

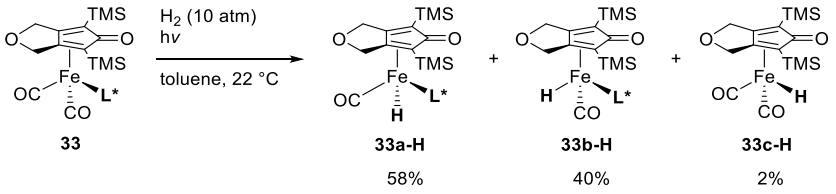

Scheme 26. Formation of diastereoisomeric (hydroxycyclopentadienyl)iron complexes **33-H** from pre-catalyst **33.**

Approach B was followed by Wills, who synthesized the several chiral (cyclopentadienone)iron complexes **34** and **35,** starting from chiral cyclopentadienone bis-propargyl ethers (Scheme 27).[79] The new complexes, possessing both a stereocenter and a stereogenic plane, were tested in the ATH of acetophenone with formic acid and triethylamine as hydrogen donors. The obtained *ee* was around 25%, and similarly poor results were obtained with the corresponding Ru-complexes.

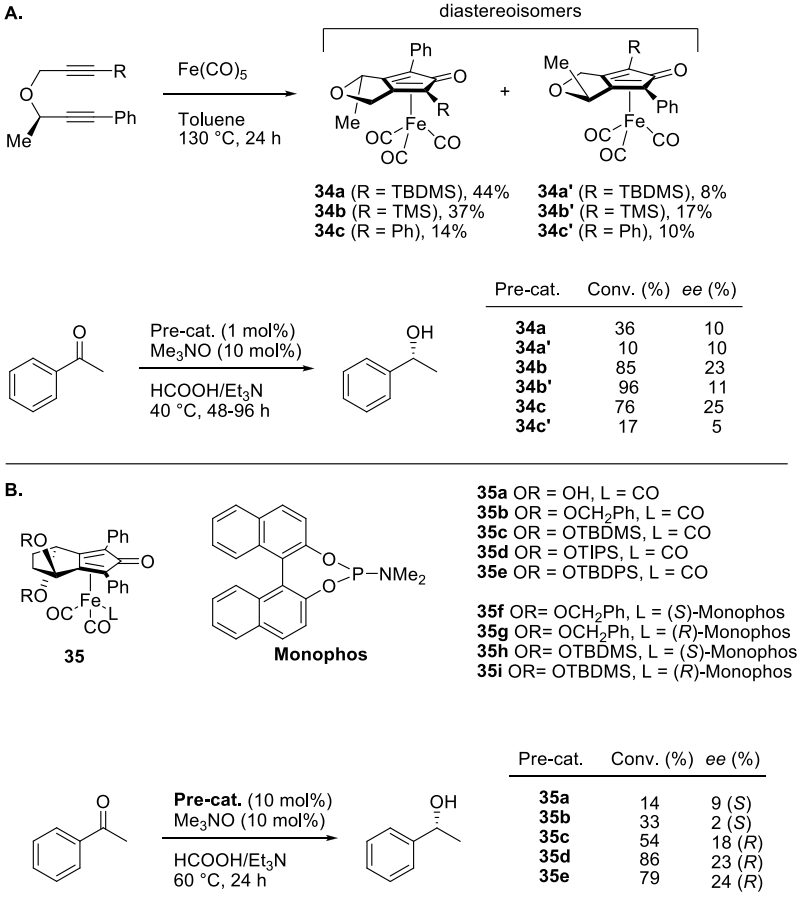

Scheme 27. ATH of acetophenone promoted by Wills' chiral pre-catalyst **34-35.**

Following Approach B, in 2015 our group also developed a new library of seven chiral (cyclopentadienone)iron pre-catalysts (**36** in Scheme 28) for the asymmetric hydrogenation of ketones.[80] Notably, complexes **36c-h** were

prepared by direct functionalization of iron complex **36b**, owing to its high stability to air, moisture and column chromatography. These complexes possess an (*R*)-BINOL-derived chiral backbone fused to the 3,4-positions of the cyclopentadienone ligand. The best pre-catalyst (**36b**) showed a fairly broad scope and gave in most cases *ee* values ranging from 50% to 77% (Scheme 28). Although these *ee* values are clearly inferior to the best literature examples of ketone AH,[81] they still represent the best results obtained so far with chiral (cyclopentadienone)iron complexes.[80]

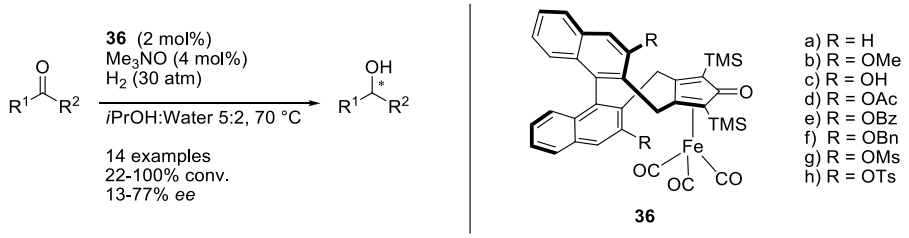

Scheme 28. Asymmetric hydrogenation of ketones promoted by chiral pre-catalyst **36**.

1.5 Hydrogenation of Imines and Amination of Aldehydes, Ketones and Alcohols

Some of the Fe-catalysts already reported were also found active in imine hydrogenation or transfer hydrogenation. Morris' catalysts **18-20** are effective also with some activated imines, and the (cyclopentadienone)iron complex **31** has shown to be active in aromatic imine hydrogenation. Despite these results, the field of imine hydrogenation is still unexplored. To the best of our knowledge, only few examples of iron catalyzed imine transfer hydrogenation process have been reported and only few hydrogenations are reported as well.

An interesting methodology relying on **30** was reported by Beller in 2011.[78b] A combination of the 'Knölker-Casey catalyst' with the chiral phosphoric acid (*S*)-TRIP can afford the reduced amines with good yield and *ee*. According to the proposed mechanism, the Brønsted acid acts as a chiral template, forming hydrogen bonds simultaneously with the catalyst and with the substrate (Figure 14).

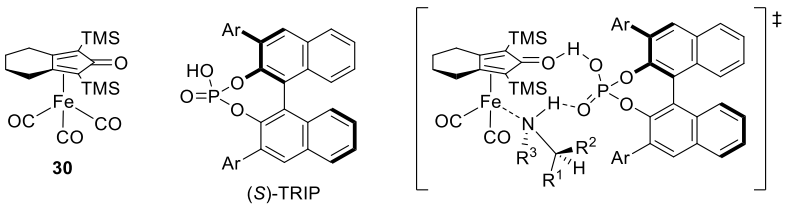

Figure 14. Proposed "Chiral template" transition state with catalyst **30** and chiral acid (*S*)-TRIP.

Beller and co-workers proved that this catalyst system was suitable for a wide number of aromatic ketimines, providing them with excellent yield and *ee*. In another paper, the hydrogenation of quinoxalines and benzoxazines

was reported to occur with high yield and excellent *ee*.[82] The same catalytic system was also employed in a reductive amination protocol using ketones and aniline, and once more high yields and *ee* values were obtained.[83]

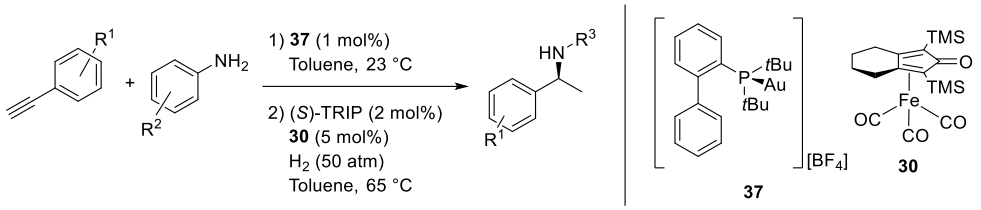

Scheme 29. One-pot hydroamination of alkynes – AH.

In the same paper, a one-pot hydroamination of alkynes followed by asymmetric hydrogenation was reported (Scheme 29). High yields and good *ee* values were obtained.

In 2012, Renaud and co-workers reported a reductive amination protocol based on the (cyclopentadienone)iron pre-catalyst **30**. An aldehyde or ketone was premixed with the desired amine and then the mixture was hydrogenated under 5 atm of hydrogen. Only aliphatic amines were screened, giving yields in the 38- 95% range (Scheme 30). In 2015 the same authors also reported that the more electron-rich pre-catalyst **38** was more effective than **30** in the reductive amination of aldehydes.[75f-i]

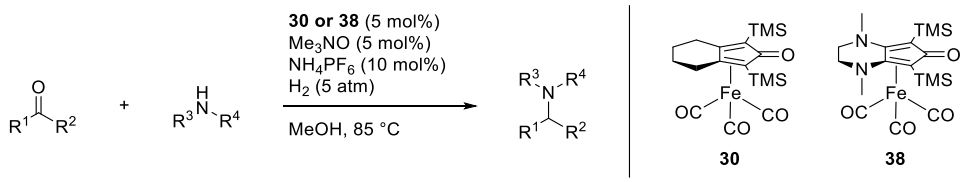

Scheme 30. Ketone and aldehyde reductive amination in the presence of (cyclopentadienone)iron complexes **30** and **38**.

In 2014 Barta and Feringa reported a direct amination of alcohols consisting in a 'hydrogen borrowing' process promoted by complex **30**.[84] With this new methodology, several α-unbranched secondary amines were synthesized with good yields (Scheme 31).

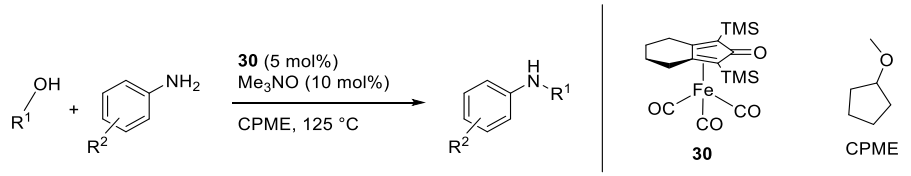

Scheme 31. Direct N-alkylation of alcohols catalyzed by (cyclopentadienone)iron complex **30**.

Several others papers by Kirchner,[85] Basker[86] and Zhao[87] reported analogous hydrogen borrowing processes using either different iron complexes or substrates. Kirchner reported a divergent coupling of alcohols and amines promoted by Fe^{II} pincer complex, giving yields in the 68-90% range. Basker *et al.* using the complex **30**, performed the direct N-alkylation of allylic alcohols. In 2016 Barta *et al.* further explored the scope of alcohol amination, and direct alkylation of benzyl alcohols could be performed.[88] Recently, Zhao successfully employed catalyst **31** to achieve for the first time the iron-catalyzed amination of secondary alcohols affording α-branched amines (Scheme 32). However, in order to achieve conversion it was necessary to employ a large amount of AgF (40 mol%) as co-catalyst, and 10 mol% of iron catalyst.[87]

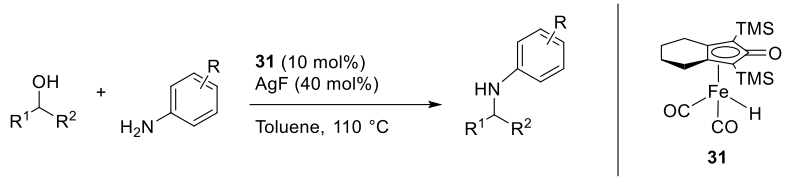

Scheme 32. Iron-catalyzed amination of secondary alcohols promoted by (hydroxycyclopentadienyl)iron complex **31.**

Morris[53] and Beller[46] were able to perform the iron-catalyzed transfer hydrogenation of imines, but the reaction proceeded only with strongly activated complexes (*N*-diphenylphosphinyl-imines). The only example of iron-catalyzed transfer hydrogenation of non-activated imines was reported by Zhao and co-workers in 2016.[89] Combining Funk's (cyclopentadienone)iron complex **39** and a Lewis acid [$Fe(acac)_3$] the transfer hydrogenation of preformed imines proceeded with good yields.

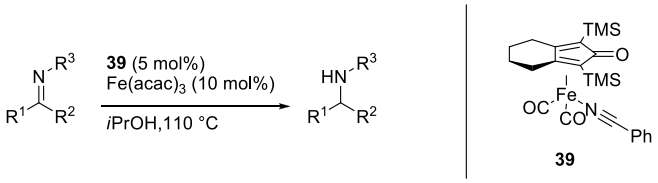

Scheme 33. Transfer Hydrogenation of preformed imines promoted by **39.**

1.6 Ester Hydrogenation

Use of an Fe-catalyst in ester hydrogenation has been reported for the first time in 2014. Milstein and co-workers employed the pincer complex **40**, previously used for CO_2 reduction, to achieve the reduction of trifluoroacetate esters (Scheme 34).[90] Unfortunately, the scope of the new methodology was found to be limited to these strongly activated substrates.

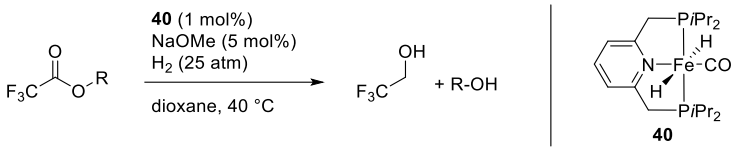

Scheme 34. Hydrogenation of activated ester promoted by Milstein catalyst **40.**

More effective catalysts for iron ester hydrogenation were reported subsequently by the groups of Beller[91] and Guan/Fairweather.[92] Both groups independently discovered that PNP iron complex **41** could hydrogenate esters under base-free conditions (Scheme 35). The substrate scope covered α,β-unsaturated esters, fully saturated esters and even fatty esters (which were hydrogenated under neat conditions).

Recently, our research group also discovered that the (cyclopentadienone)iron pre-catalyst **30** was also able to hydrogenate trifluoroacetate esters with excellent yields.[93] Unfortunately catalyst **30** did not show activity towards non-activated esters.

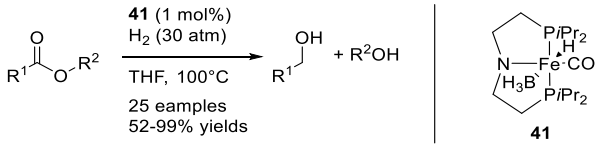

Scheme 35. Hydrogenation of esters promoted by PNP iron complex **41.**

1.7 Summary of Iron Catalyzed Hydrogenation

The aim of this chapter was drawing a general idea about the state of the art in iron catalyzed hydrogenation. More than forty different catalysts are shown, divided by the reaction they can perform. Most of them have been developed in the last ten years, meaning that the field of iron catalysis is still in fast development. A compendium of the most important iron catalysts for hydrogenation of double bonds is shown in Figure 15.

The majority of known homogeneous iron catalysts suffer from difficult synthesis, lack of robustness and/or moderate activity/enantioselectivity. Moreover, most reported catalysts are difficult to handle, due to their air- and moisture-sensitivity, and therefore use of glovebox is often required. These drawbacks need to be overcome to make iron catalysis appealing for industrial manufacturing of fine chemicals.

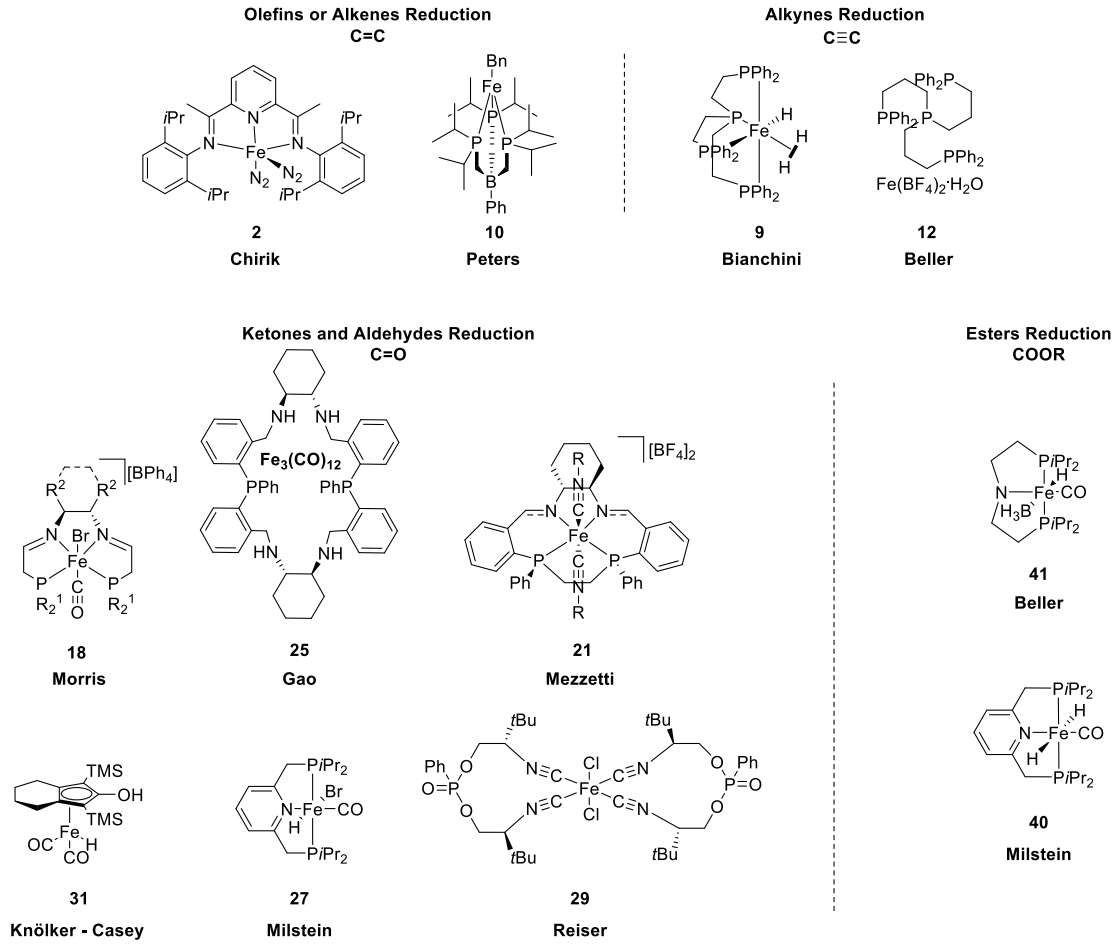

Figure 15. The most important homogeneous iron catalysts for the hydrogenation of double bonds.

CHAPTER 2

ISONITRILE IRON COMPLEXES

Isonitriles or isocyanides are organic molecules bearing a nucleophilic carbon which shows both nucleophilic and electrophilic features.[94] In the zwitterionic form, the carbon atom brings a negative charge (nucleophilic behavior), whereas in the other resonance structure it looks like a carbene and therefore it can be considered an electrophile.

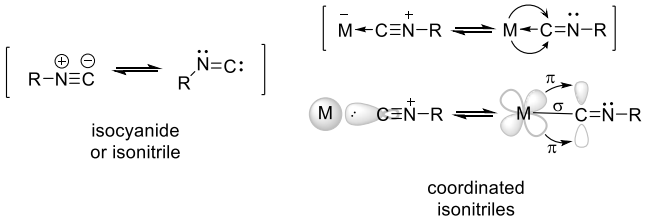

Figure 16. Resonance structures of the isonitrile group.

Isonitrile group has found many applications in coordination chemistry. The lone electron pair on the carbon atom (HOMO) can form σ bond to the metal. Meanwhile, the metal with the right symmetry and full *d* orbitals can fill the empty anti-bonding orbitals (LUMO) of the ligand forming a π-type bond. Thanks to this retrodonation mechanism, isonitrile ligands are able to stabilize metals in low oxidation state. Although isocyanides showed the same stabilization properties of CO and phosphines, only few examples of isonitrile-iron complexes are reported in the literature. A possible reason of this fact is the linear structure of the isontirile group, featuring a sequence of three atoms in a straight line, which makes the design of chelating bis-isontrile ligands difficult. A way to overcome this issue would be building a large-sized and relatively flexible ligand backbone that can allow the isonitrile groups to bind to the same metal center.[95]

2.1 PRELIMINARY RESULTS

As it has been already shown in Paragraph 1.4.5, Reiser and co-workers reported one of the first bis-isonitrile iron complexes for the asymmetric hydrogenation of ketones.[67] Inspired by this report, in 2014 our group synthesized the chiral bis-isonitrile iron complex **42** (Figure 17) , containing a (*S,S*)-2,2'-bipyrrolidine- derived chiral backbone.

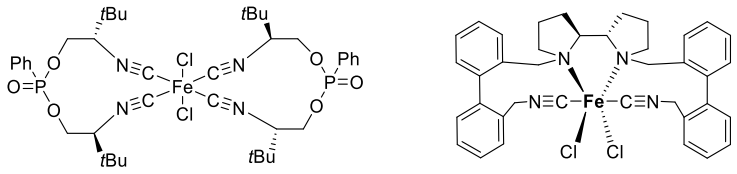

Figure 17. Chiral bis-isonitrile iron complex **29** (reported by Reiser and co-workers[67])and **42** (synthesized by our group).

Complex **42** was designed to work in ATH of ketones as **29** according to a mechanism analogous to the one described by Reiser and co-workers. Indeed, after activation with *t*BuOK, **42** was able to promote the transfer hydrogenation of acetophenone at 50 °C in *i*PrOH, but unfortunately conversion (51-87%) and *ee* (5-16%) were low. We next synthesized the two tetra(isonitrile) complexes **43a** and **43b**, which surprisingly showed no activity in transfer hydrogenation.

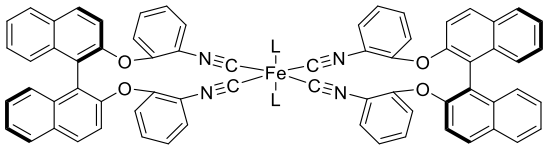

Figure 18. Tetra(isonitrile) iron complexes **43.**

Looking more deeply into the structure of **43**, it can be noted that the isonitrile moiety is directly connected to an aromatic ring. This might change the electronic properties of the isonitrile group, and thus explain the lack of activity of **43**. Indeed, in the catalytic cycle the hydride transfer from the imine to the substrate (**43a.3, Scheme 36)** might be disfavored when R is aromatic (i.e., less electron-rich).

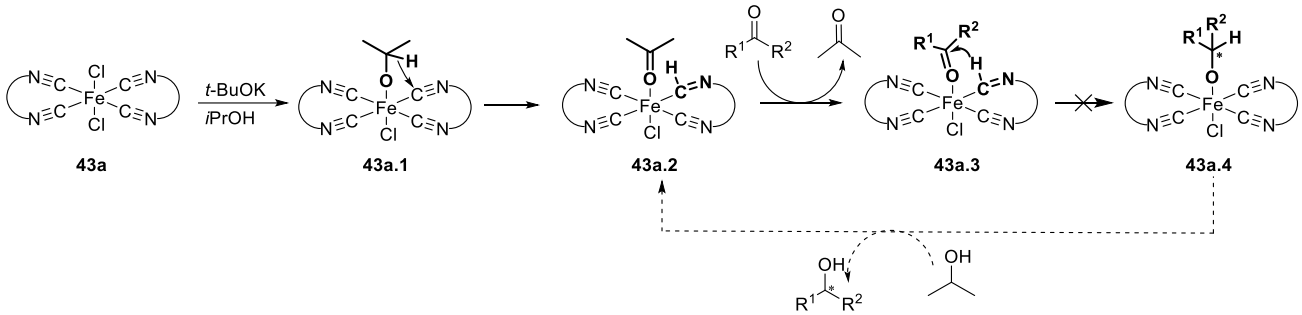

Scheme 36. Catalytic cycle of the ATH of ketones promoted by isonitrile iron complexes proposed by Reiser and co-workers.

2.2 New families of tetra(isonitrile) Iron Complexes for the ATH of Ketones

Considering the possible reasons of failure of complex **43** (see above), a new class of aliphatic BINOL-derived complexes was designed and synthesized: two sub-families **A** and **B** (shown in Figure 19), differing in the length of the 'arms' bearing the isonitrile groups. On the basis of molecular models, an alkyl chain formed by two carbon atoms (compounds **A**) was expected to facilitate chelation of the Fe-center by the isocyanide groups. On the other hand, the expected advantage of compounds **B** consisted in a lower distance between the stereogenic unit and the iron center, which would possibly facilitate the transfer of stereochemical information during the ATH process.

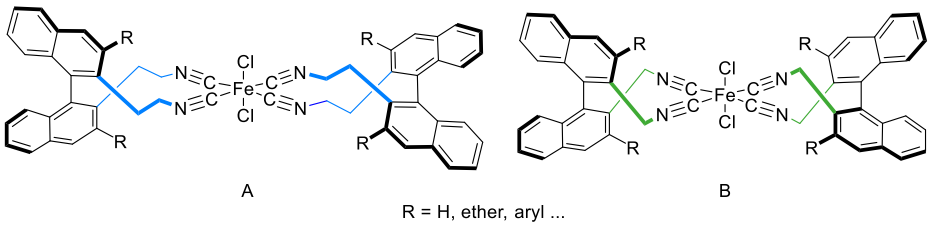

Figure 19. Two families of BINOL-derived isonitrile complexes **A** and **B**.

The ligand synthesis started from (*R*)-BINOL and allowed to introduce different substituents at the 3,3'-positions of the binaphthyl moiety, thus creating a tunable hindered structure. By varying the length of the 2,2'-"arms" and the 3,3'-substituents of the binaphthyl moiety, it was possible to build a library of tetra(isonitrile) iron catalysts. Ligands **56a,b** and **58a,b** (Scheme 38) were prepared starting from the bis-bromides **47a** and **47b**, synthesized as described, respectively, by Maruoka[96] and Cramer.[97]

It should be noted that some of these intermediates were already available in our research group, because they had been used due the synthesis of chiral (cyclopentadienone)iron complexes.[80b,c]

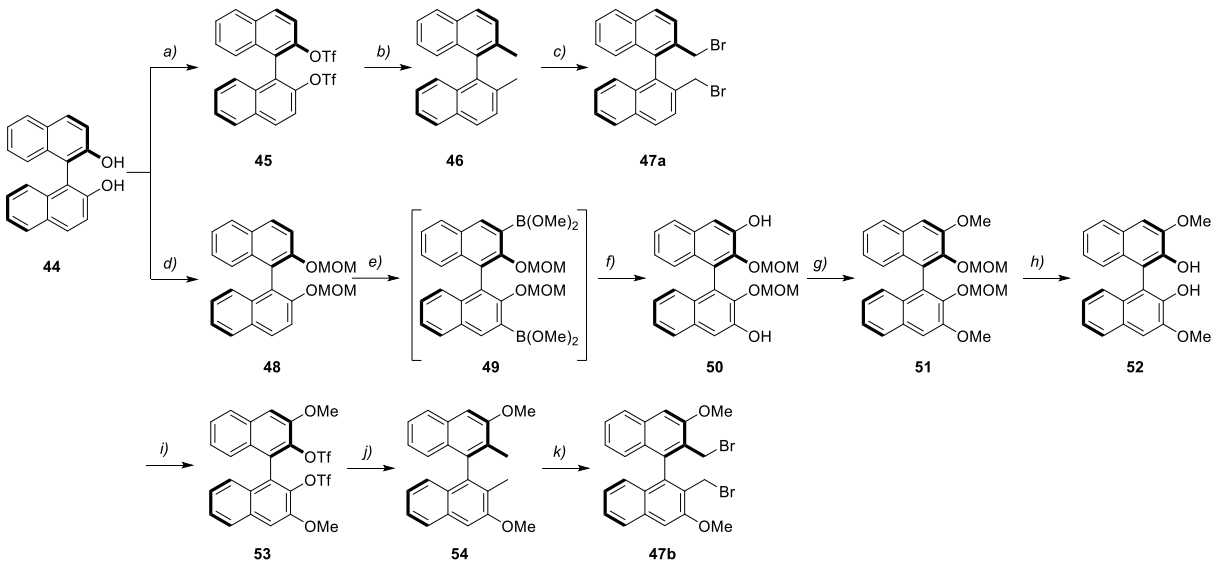

Scheme 37. Synthetic plan for synthesis of bis-bromide **47a,b**. REAGENTS and CONDITIONS: *a*) Tf_2O, TEA, DCM, -78 °C to 23°C, 2 h, Y.: quant. (**45**); *b*) MeMgI, $NiCl_2$(dppp), Et_2O, 0 to 40 °C, overnight, Y.: quant. (**46**); *c*) NBS, Benzoyl peroxide, CCl_4, vis-light, 75 °C, overnight, Y.: 70% (**47a**); *d*) NaH, MOMCl, THF, 0 °C to 23°C, overnight, Y.: 82% (**48**); *e*) I) *n*-BuLi, THF, -78 °C to 0 °C; II) $B(OMe)_3$, THF, -78 °C to 23 °C, overnight; *f*) H_2O_2, benzene, 0 °C to 80 °C, 2h; *g*) MeI, K_2CO_3, acetone, 56 °C, overnight, Y.(*e*-*g*): 60% (**51**); *h*) HCl 37%, dioxane, 40 °C, 4h; *i*) Tf_2O, TEA, DCM, -78 °C to 23°C, 2 h, Y.(*h*-*i*): 82% (**53**); *j*) MeMgI, $NiCl_2$(dppp), Et_2O, 0 to 40 °C, overnight, Y.: 81% (**54**); *k*) NBS, Benzoyl peroxide, CCl_4, vis-light, 75 °C, overnight, Y.: 89% (**47b**).

The synthesis of bis-bromide **47a** proceeded straightforward from (*R*)-BINOL **44**, which was deprotonated with TEA and reacted with triflic anhydride yielding the bis-triflate derivative **45**. A nickel Kumada coupling[98] was used to synthesize the dimethyl binaphthyl **46** which, after chromatography purification, was subjected to radical Wohl-Ziegler bromination to give bis-bromide **47a**. To prepare the bis-bromide **47b**, featuring OMe substituents at the 3,3' binaphthyl positions, a slightly different synthetic pathway was followed. BINOL was firstly protected with MOMCl, followed by *orto*-lithiation and borylation with $B(OMe)_3$ affording the intermediate **49**, which was not isolated but immediately oxidized with hydrogen peroxide to give the bis-phenol **50**. Under basic conditions, **50** was alkylated with MeI affording the bis-methoxy-MOM-protected compound **51**, which was hydrolyzed with HCl to give the unprotected bis-phenol **52**. Following the same synthetic sequence used for preparing **47a**, bis-phenol **52** was converted into **47b** with 30% overall yield.

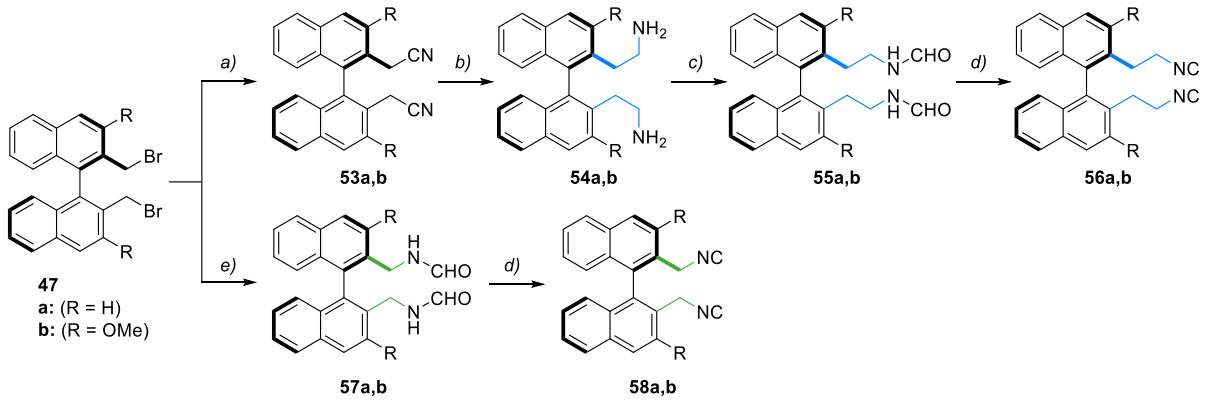

Scheme 38. Synthetic plan of isonitrile ligands. REAGENTS AND CONDITIONS: *a*) NaCN, EtOH, water, reflux overnight, Y.: 49% (**53a**) Y.: 92% (**53b**); *b*) $AlCl_3$, $LiAlH_4$, Et_2O, THF, r.t., Y.: 92% (**54a**) Y.: 77% (**54b**); *c*) Ethyl formate, reflux, overnight, Y.: 60% (**55a**) Y.: 80% (**55b**); *d*) $POCl_3$, TEA, THF, r.t., overnight, Y.: 86% (**56a**), Y.: 89% (**56b**), Y.: 46% (**58a**) Y.: 55% (**58b**); *e*) $NaN(CHO)_2$, DMF, 100 °C, overnight, Y.: 70% (**57a**), Y.: 88% (**57b**).

The synthesis of bis-isonitriles **56a,b** was carried out as shown in Scheme 38. In the former case, compounds **47a,b** were reacted with NaCN to yield the bis-nitriles **53a,b**, which were then reduced to yield the diamines **54a,b**. Several reductants were tried ($LiAlH_4/H_2SO_4$, BH_3THF, $(CH_3)_2S{\cdot}BH_3$, H_2 over Pd/C or Nickel Ranaey) but only the use of $LiAlH_4/AlCl_3$ (*in situ* formation of AlH_3) allowed to obtain a good yield. Diamines **54a,b** were converted in the corresponding formamides **55a,b**, which were dehydrated to form the isonitriles **56a,b**. The synthesis of ligands **58a,b** was shorter and involved the conversion of **47a,b** into the corresponding bis-formamides (**57a,b**), followed by dehydration with $POCl_3$.

Purification of compounds **56a,b** and **58a,b** turned out to be problematic due to their poor stability to silica gel. Flash chromatography, indispensable to isolate the ligand with sufficient purity for using it in the subsequent complexation, initially afforded low yields (< 40%). To circumvent this problem, the purification was carried out at low temperature with chilled eluent (-15 °C) and dry-ice cover around the column.

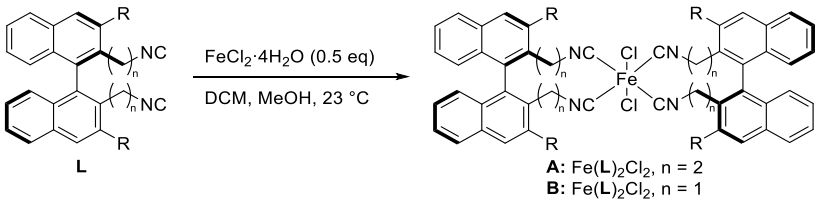

Scheme 39. General procedure for the synthesis of (tetra)isonitrile iron complexes, $Fe(L)_2Cl_2$.

The isonitrile complexes were prepared according to the procedure reported by Reiser and co-workers,[67] i.e. by mixing 1 eq. of $FeCl_2 \cdot 4H_2O$ and 2 eq. of ligand (Scheme 39). As all the complexes synthesized are paramagnetic, it was not possible characterize them by NMR, but only with ESI mass spectrometry.

The new isonitrile iron complexes were tested in the ATH of ketones following the procedure reported by Reiser.[67] Acetophenone was chosen as model substrate for testing the catalytic activity of our catalysts. A standard catalyst loading of 5 mol% and *t*BuOK (50 mol%) in isopropanol were used. The catalytic test results are reported in Table 2. All complexes showed catalytic activity, and some promising enantiomeric excesses were obtained.

Table 2. Catalytic results in ATH of acetophenone.[a]

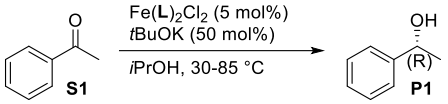

#	Complex $Fe(\mathbf{L})_2Cl_2$	L	30 °C		60 °C		85 °C	
			Conv. (%)[b]	*ee* (%)[b]	Conv. (%)[b]	*ee* (%)[b]	Conv. (%)[b]	*ee* (%)[b]
1	**A1**	**56a**	6	15	74	27		
2	**A2**	**56b**	51	14	73	17		
3	**B1**	**58a**	55	5	81	5	82	5
4	**B2**	**58b**	28	8	57	16	82	11

[a] **S1**/Catalyst/*t*BuOK = 1/0.05/0.5; Solvent: *i*PrOH, $C_{Sub,0}$ = 0.2 mol L^{-1} (0.1 mmol); [b] conversion and *ee* determined by GC.

To gain the enantioselectivity, it was expected that the installation of bulky substituents in 3,3'-position of the binaphthyl moiety could improve the transfer of stereochemical information to the active center. Thus, starting from bis-formamide **57b**, a new synthetic way that could introduce a versatile functional group in 3,3'-positions of the binaphthyl moiety was designed (Scheme 40). Deprotection of **57b** gave the free diol **59**, which allowed us to diversify the synthesis. On one hand, isonitrile **62** was synthesized by triflation of **59** followed by Suzuki coupling. Several boronic acids were screened, but only with phenylboronic acid the reaction gave a reasonable yield. On the other hand, ester isonitrile **64** was obtained by acylation of **59** followed by formamide dehydration.

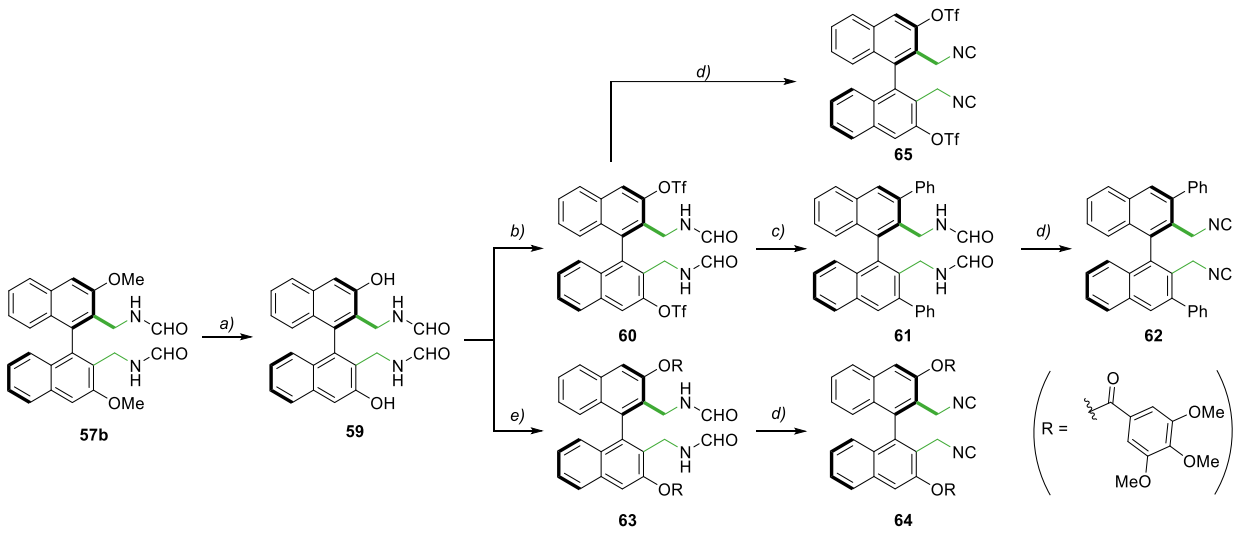

Scheme 40. Synthetic plan for the functionalization of 3,3'-position of BINOL moiety. REAGENTS AND CONDITIONS: *a*) BBr_3, DCM, -70 °C to 23 °C, overnight, Y.: 80% (**59**); *b*) Comins' Reagent, TEA, DMAP, THF, 23 °C, overnight, Y.: 81% (**60**); *c*) $Pd(OAc)_2$, PPh_3, K_3PO_4, Phenylboronic acid, KBr, dioxane, 87 °C, overnight, Y.: 55% (**61**); *d*) $POCl_3$, TEA, THF, 23 °C, overnight, Y.: 86% (**62**), Y.: 17% (**64**), Y.: 84% (**65**); *e*) 3,4,5-trimethoxybenzoyl chloride, TEA, DMAP, THF, 70 °C, 4 h, Y.: 72% (**63**).

The new complexes **B3-5** were also synthesized following the same procedure reported in Scheme 39. All of them were tested in ATH of ketones under the same conditions of the previous screening, and results are shown in Table 3.

Table 3. Catalytic results in ATH of acetophenone.[a]

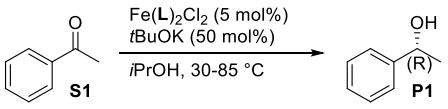

#	Complex $Fe(L)_2Cl_2$	L	30 °C		60 °C		85 °C	
			Conv. (%)[b]	*ee* (%)[b]	Conv. (%)[b]	*ee* (%)[b]	Conv. (%)[b]	*ee* (%)[b]
1	**B3**	**62**	3	28	22	0	62	0
2	**B4**	**65**	2	6	6	0		
3	**B5**	**64**	1	2	7	3		

[a] **S1**/Catalyst/*t*BuOK = 1/0.05/0.5; Solvent: *i*PrOH, $C_{Sub,0}$ = 0.2 mol L^{-1} (0.1 mmol); [b] conversion and *ee* determined by GC.

Very low conversions were obtained with all the new catalysts, small increases being observed at higher temperatures. Moreover, quite unexpectedly the bulky substituents at the 3,3'-positions of the binaphthyl residue had the only effect of reducing the conversion, without any benefit in terms of stereocontrol. Initially, it was suspected that the

poor conversions might be due to low solubility of complexes **B3** [Fe(**62**)$_2$Cl$_2$] and **B4** [Fe(**65**)$_2$Cl$_2$] in isopropanol, therefore the reaction was performed either in the presence of a co-solvent (e.g. THF, DCM) or in a different reducing medium (HCOOH/TEA). However, none of these approaches led to improvement. Moreover, also complex **B5** [Fe(**64**)$_2$Cl$_2$], freely soluble in *i*PrOH owing to the presence of polar gallic ester groups, displayed poor catalytic activity. Thus, we concluded that the observed low activity was not due to solubility issues. It is possible that the presence of bulky 3,3'-substituents on the binaphthyl moiety creates too much steric crowd around the metal center, thus limiting its accessibility.

2.3 Tetra(isonitrile) Iron Complexes in Isomerization of Allylic Alcohols

Although some of the tetra(isonitrile) iron complexes have shown acceptable conversion and promising *ee* in transfer hydrogenation of acetophenone, most of them turned out to be poorly active. Recently, a paper was published by Renaud and co-workers which reports isomerization of allylic alcohol catalyzed by iron isonitrile complexes.[99] Inspired by this work, tetra(isonitrile) iron catalysts have been tested in isomerization of 1-octen-3-ol to 3-octanone (Scheme 41).

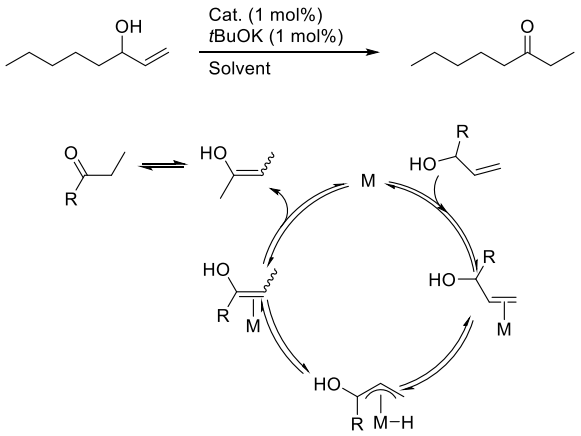

Scheme 41. Isomerization of 1-octen-3-ol to 3-octanone and its hypothetical catalytic cycle.

Only the catalysts which had shown the highest activity in ATH were tested: **A1** (Fe(**56a**)$_2$Cl$_2$), **A2** (Fe(**56b**)$_2$Cl$_2$), **B1** (Fe(**58a**)$_2$Cl$_2$) and **B2** (Fe(**58b**)$_2$Cl$_2$). With a catalyst loading of 1% we tried the reaction employing different conditions (Table 4). Unfortunately, no appreciable conversion was obtained.

Table 4. Summary of conditions which have been used in isomerization of 1-octen-3-ol.[a]

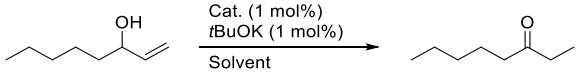

#	Catalysts	Solvent	Base	Temperature (°C)[a]	Time (h)	Conv. (%)[b]
1	**A1, A2, B1, B2**	*i*PrOH	*t*BuOK	80	24	0
2	**A1, A2, B1, B2**	*i*PrOH	*t*BuOK	120	50	0
3	**A1, A2, B1, B2**	*i*PrOH	-	80	24	0
4	**A1, A2, B1, B2**	*i*PrOH	-	120	50	0
5	**A1, A2, B1, B2**	Toluene	*t*BuOK	80	24	0
6	**A1, A2, B1, B2**	Toluene	*t*BuOK	120	50	0
7	**A1, A2, B1, B2**	Toluene	-	80	24	0
8	**A1, A2, B1, B2**	Toluene	-	120	50	0

[a] 1-octen-3-ol/Cat./Base = 100:1:1, Solvent: Toluene or *i*PrOH; [b] the conversion is obtained by GC analysis with dodecane as internal standard.

2.4 Tetra(isonitrile) iron complexes in Asymmetric Hydrogenation of Ketones

To further expand the application of (tetra)isonitrile iron complexes, asymmetric hydrogenation (AH) of ketones was also investigated. Using acetophenone as model substrate, a first attempt under 30 bar of H_2 (other conditions in Table 5) was carried out. Complexes **A1**, **A2**, **B1** and **B2** turned out to be catalytically active in the AH of this benchmark substrate, although with low or no enantioselectivity.

Table 5. Catalytic results in asymmetric hydrogenation of acetophenone.[a]

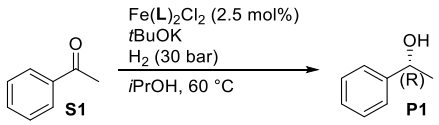

#	Complex $Fe(L)_2Cl_2$	Base	Conv. (%)[b]	*ee* (%)[b]
1	**56a, A1**	*t*BuOK	39	8
2	**56a, A1**	-	0	0
3	**56b, A2**	*t*BuOK	42	4
4	**56b, A2**	-	0	0
5	**58a, B1**	*t*BuOK	11	1
6	**58a, B1**	-	0	0
7	**58b, B2**	*t*BuOK	49	21
8	**58b, B2**	-	0	0

[a] **S1**/Catalyst/*t*BuOK = 1/0.025/0.25; Solvent: *i*PrOH, $C_{Sub,0}$ = 0.2 mol L^{-1} (0.1 mmol), p_{H2} = 30 bar, 60 °C, overnight. [b] Conversion and *ee* determined by GC.

In order to improve the hydrogenation performance, employing **B2** as model catalyst a base screening was carried out. Several bases and different base/catalyst ratios were tested, and the best results were achieved with *t*BuOK (Table 6).

Table 6. Base optimization in AH of acetophenone promoted by **B2.**[a]

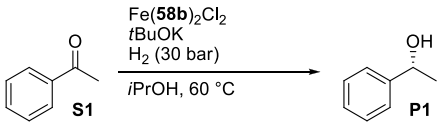

#	**Complex** $Fe(\mathbf{L})_2Cl_2$	**Base**	**Conv. (%)** [b]	***ee* (%)** [b]
1	**58b, B2**	*t*BuOK (25% mol)	5	15
2	**58b, B2**	*t*BuOK (50% mol)	12	4
3	**58b, B2**	*t*BuOK (125% mol)	25	2
4	-	*t*BuOK (25% mol)	5	-
5	-	*t*BuOK (125% mol)	0	-
6	**58b, B2**	Cs_2CO_3 (25% mol)	3	17
7	-	Cs_2CO_3 (25% mol)	2	0
8	**58b, B2**	K_2CO_3 (25% mol)	2	8
9	-	K_2CO_3 (25% mol)	0	-
10	**58b, B2**	KOH (25% mol)	12	11
11	-	KOH (25% mol)	5	-

[a] **S1**/Catalyst/*t*BuOK = 1/0.025/see table; Solvent: *i*PrOH, $C_{Sub,0}$ = 0.2 mol L^{-1} (0.1 mmol), p_{H2} = 30 bar, 60 °C, overnight.; [b] conversion and *ee* determined by GC.

Different solvents were also tested (Table 7), but the data obtained were found to be poorly reproducible: comparing the results in the Table 5-Table 7 it can be found that different conversion and *ee* values were obtained with the same catalyst and experimental condition.

Table 7. Solvent screening in the AH of acetophenone promoted by $Fe(\mathbf{58b})_2Cl_2$.[a]

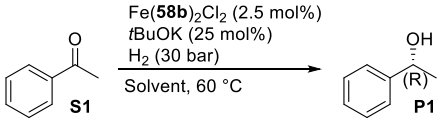

#	**Solvent**	**Conv. (%)**[b]	***ee* (%)**[b]
1	*i*PrOH	5	4
2	MeOH	1	2 (*S*)
3	Toluene	0	-
4	THF	0	-

[a] **S1**/Catalyst/*t*BuOK = 1/0.025/0.25; Solvent: *i*PrOH, $C_{Sub,0}$ = 0.2 mol L^{-1} (0.1 mmol), p_{H2} = 30 bar, 60 °C, overnight.; [b] conversion and *ee* determined by GC.

Looking for the reason of this lack of reproducibility, the purity of the catalysts was tested. Due to the paramagnetic character of these iron (tetra)isonitrile complexes, NMR spectroscopy does not provide any useful information. The only way to analyze the synthesized complexes **A1**, **A2**, **B1** and **B2** was by high resolution mass spectrometry, and the

results are shown in Figure 20. The analytical data obtained do not fit with the expected ones, the major compound is the trimeric complex **66** followed by the Cl-bridged complex **67** and less of 5% of the desired complex **68**.

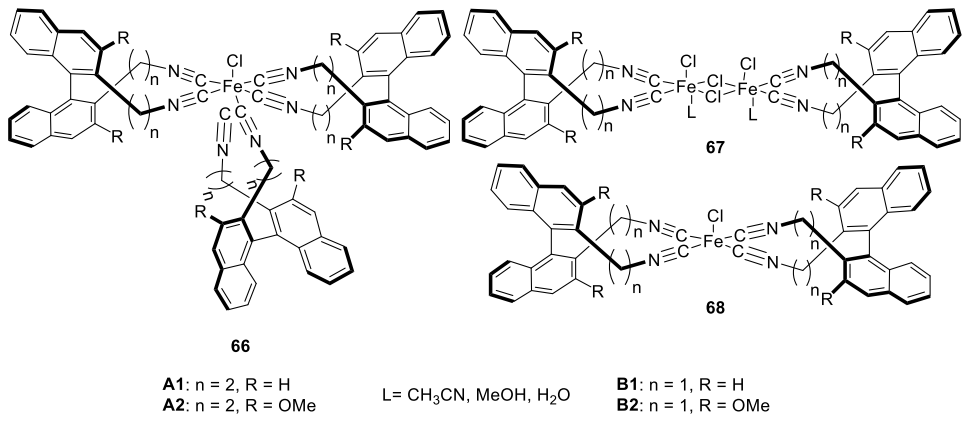

Figure 20. Proposed structures for iron complexes based on HRMS data.

2.5 Summary of isonitrile iron complexes

A new class of chiral iron tetra(isonitrile)complexes was synthesized. In particular, two families of catalysts were reported: family **A** and **B** (Figure 19). The first catalytic tests demonstrated that the catalysts were active in ATH of acetophenone with promising conversions and *ee*s. Although it was expected that installing bulkier substituents on the 3,3'-position of the binaphthyl scaffold could improve the enantioselectivity, in fact it only decreased the activity leaving the enantioselectivity nearly unaffected. The most active iron complexes were then tested in ketone asymmetric hydrogenation and in the isomerization of allylic alcohols. While the latter reaction did not show any appreciable results under a number of different conditions, the asymmetric hydrogenation of acetophenone under 30 bar of hydrogen gave promising conversion. However, the tetra(isonitrile)iron complexes showed poor reproducibility, the conversions swinging from 50% to 4% using the same catalyst under the same reaction conditions. Further investigations revealed that the catalyst structure differs from the expected one. Indeed, instead of one defined specie, several different catalysts were produced as it has shown in Figure 20. Considering the above, no further studies were performed with these isonitrile iron complexes.

2.6 Experimental section

General remarks

All reactions were carried out in flame-dried glassware with magnetic stirring under nitrogen, unless otherwise stated. The solvents for reactions were distilled over the following drying agents and transferred under nitrogen: CH_2Cl_2

(CaH_2), MeOH (CaH_2), THF (Na), dioxane (Na), Et_3N (CaH_2). Dry Et_2O, acetone and $CHCl_3$ (over molecular sieves in bottles with crown cap) were purchased from Sigma Aldrich and stored under nitrogen. The reactions were monitored by analytical thin-layer chromatography (TLC) using silica gel 60 F254 pre-coated glass plates (0.25 mm thickness). Visualization was accomplished by irradiation with a UV lamp and/or staining with a potassium permanganate alkaline or ninhydrin stain solution. Flash column chromatography was performed using silica gel (60 Å, particle size 40-64 μm) as stationary phase, following the procedure by Still and co-workers.[100] Proton NMR spectra were recorded on a spectrometer operating at 400.13 MHz. Proton chemical shifts are reported in ppm (δ) with the solvent reference relative to tetramethylsilane (TMS) employed as the internal standard ($CDCl_3$ δ = 7.26 ppm; CD_2Cl_2 δ = 5.32 ppm; acetone-d_6 δ = 2.05 ppm; DMSO-d_6 δ = 2.50 ppm; CD_3OD δ = 3.33 ppm). The following abbreviations are used to describe spin multiplicity: *s* = singlet, *d* = doublet, *t* = triplet, *q* = quartet, *m* = multiplet, *br* = broad signal, *dd* = doublet-doublet, *td* = triplet-doublet. ^{13}C-NMR spectra were recorded on a 400 MHz spectrometer operating at 100.56 MHz, with complete proton decoupling. Carbon chemical shifts are reported in ppm (δ) relative to TMS with the respective solvent resonance as the internal standard ($CDCl_3$ δ = 77.16 ppm; CD_2Cl_2 δ = 54.00 ppm; acetone-d_6 δ = 29.84 ppm, 206.26 ppm; DMSO-d_6 δ = 39.51 ppm; CD_3OD δ = 49.05 ppm). The coupling constant values are given in Hz. Infrared spectra were recorded on a standard FT/IR spectrometer. Optical rotation values were measured on an automatic polarimeter with a 1 dm cell at the sodium D line (λ = 589 nm). Gas chromatography was performed on a GC instrument equipped with a flame ionization detector, using a chiral capillary column. High resolution mass spectra (HRMS) were performed on a Fourier Transform Ion Cyclotron Resonance (FT-ICR) Mass Spectrometer APEX II & Xmass software (Bruker Daltonics) – 4.7 T Magnet (Magnex) equipped with ESI source, available at CIGA (Centro Interdipartimentale Grandi Apparecchiature) c/o Università degli Studi di Milano. Low resolution mass spectra (MS) were acquired either on a Thermo-Finnigan LCQ Advantage mass spectrometer (ESI ion source) or on a VG Autospec M246 spectrometer (FAB ion source). Elemental analyses were performed on a Perkin Elmer Series II CHNS/O Analyzer 2000.

Materials

Commercially available reagents were used as received. Ethynyltrimethylsilane, ethylmagnesium bromide (1M in THF), *n*-BuLi (1.6M in hexane), BBr_3 (1M in DCM), Bu_4NI, NaI, CuI, $Fe_2(CO)_9$ and the ketones used in the substrate screening were purchased from commercial suppliers (TCI Chemicals, ACROS, Sigma Aldrich) and used as received.

[1,1'-Binaphthalene]-2,2'-diyl bis(trifluoromethanesulfonate) (45):

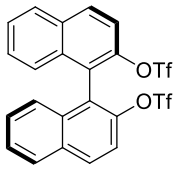

At -78 °C, under argon atmosphere, Tf_2O (2.59 mL, 15.4 mmol, 2.2 eq.) was added dropwise to a stirred mixture of (*R*)-BINOL (2.00 g, 7.0 mmol, 1 eq.) and TEA (2.92 mL, 21.0 mmol, 3 eq.) in dry DCM (17.5 mL). After the addition was over, the cooling bath was removed and the mixture is stirred for 2 h at r.t.. Then it was poured into ice-cold 1M HCl (40 mL) and extracted with hexane (4 × 20 mL) and washed with $NaHCO_3$, brine and dried over Na_2SO_4. Quantitative yield. The crude is pure enough to be used in the next step without further purification.

^{1}H-NMR (400 MHz, $CDCl_3$) δ 8.14 (d, J = 9.1 Hz, 1H), 8.01 (dt, J = 8.2, 0.7 Hz, 1H), 7.66-7.58 (m, 1H), 7.62-7.54 (m, 1H), 7.41 (dt, J = 8.3, 6.9, 1.3 Hz, 1H), 7.27-7.24 (m, 1H). The reported ^{1}H-NMR data fit with the one reported in the literature.[80]

2,2'-Dimethyl-1,1'-binaphthalene (46):

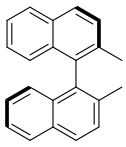

In a Schlenk vessel, under argon atmosphere, **45** (3.85g, 7 mmol, 1 eq.) and $NiCl_2$(dppp) (0.51 g, 0.94 mmol, 6.7 mol%) were dissolved in dry Et_2O (55 mL). A 3M ethereal solution of MeMgI (23.5 mL, 70 mmol, 5 eq.) was added dropwise at 0 °C. After addition was complete, reaction was stirred overnight at 40°C. The day after, the mixture was cooled with an ice bath, then it was poured slowly into ice-cold 1M HCl (80 mL). The obtained mixture was filtered through celite® 545 (rinsing with Et_2O, not DCM because it dissolves the Ni cat.) to remove the catalyst. After filtration, the two phases were transferred into a separating funnel and separated with AcOEt. The combined organic phases were washed with brine and then dried over Na_2SO_4. The desired product was purified by column chromatography (86:14 hexane/DCM) to give 3.88 g (11.34 mmol, 81% yield) of **46**.

^{1}H-NMR (300 MHz, $CDCl_3$) δ 7.89 (d, J = 8.4 Hz, 2H), 7.88 (d, J = 8.4 Hz, 2H), 7.51 (d, J = 8.4 Hz, 2H), 7.39 (ddd, J = 8.4, 6.9, 1.2 Hz, 2H), 7.20 (ddd, J =8.4, 6.9, 1.2 Hz, 2H), 7.04 (d, J = 8.4 Hz, 2H), 2.03 (s, 6H). The reported ^{1}H-NMR data fit with the one reported in the literature.[80]

2,2'-Bis(bromomethyl)-1,1'-binaphthalene (47a):

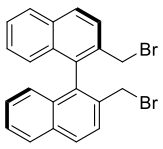

In a Schlenk vessel fitted with a gass-tight screw cap, compound **46** (3.08 g, 10.9 mmol, 1 eq.), NBS (4.26 g, 23.9 mmol, 2.2 eq.) and benzoyl peroxide (0.085 g, 3.2 mol%) were dissolved in dry CCl_4 (60 mL). The solution was heated to 80 °C while irradiating with a 100 W lamp. After 22 h the reaction was cooled down and filtered on a frit (rinsing with CCl_4) to remove solid succinimide. The solvent was evaporated off to obtain a foamy solid. The residue was purified by recrystallization from Et_2O/hexane to give **47a** as a yellow pale powder 4.27 g (9.70 mmol, 89% yield).

^{1}H NMR (300 MHz, $CDCl_3$) δ 8.03 (d, J = 8.7 Hz, 2H), 7.94 (d, J = 8.1 Hz, 2H), 7.66 (d, J = 8.4 Hz, 2H), 7.50 (ddd, J = 8.1, 6.9, 1.2 Hz, 2H), 7.28 (ddd, J = 8.4, 6.9, 1.2 Hz, 2H), 7.08 (d, J = 8.7 Hz, 2H), 4.26 (s, 4H). The reported ^{1}H-NMR data fit with the those reported in the literature.[80]

2,2'-Bis(methoxymethoxy)-1,1'-binaphthalene (48):

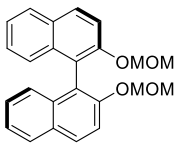

In 1 L round bottom flask, under argon atmosphere, NaH (6.89 g, 60% in oil, 171.3 mmol, 2.3 eq.) was washed several time with dry hexane and further suspended in dry THF (300 mL) at 0 °C. A solution of (*R*)-BINOL (21.3 g, 74.5 mmol, 1 eq.) in THF (100 mL) was added dropwise and the mixture was stirred at 0 °C for 1 h. The stirred solution was allowed to warm up to r.t. in 15 min and afterwards was re-cooled to 0 °C. Chloromethyl methyl ether MOMCl (13.3 mL, 172.3 mmol, 2.3 eq.) was slowly dropped into the cooled stirred solution. After addition, the reaction mixture was stirred at r.t. overnight. After quenching of unreacted NaH with a saturated solution of NH_4Cl (100 mL), THF was removed *in vacuo* and the residue was extracted with DCM (3 × 100 mL). The combined organic phases were washed with brine, dried over Na_2SO_4 and solvent was removed under reduced pressure. Product **48** (26 g, 70 mmol, 99%) was obtained as a yellow foam and used without any further purification.

^{1}H NMR (400 MHz, CD_2Cl_2) δ 7.99 (d, ^{3}J = 9.1 Hz, 2H), 7.91 (d, ^{3}J = 8.2 Hz, 2H), 7.61 (d, ^{3}J = 9.1 Hz, 2H), 7.36 (t, ^{3}J= 7.5 Hz, 2H), 7.24 (t, ^{3}J = 7.6 Hz, 2H), 7.12 (d, ^{3}J = 8.5 Hz, 2H), 5.10 (d, ^{2}J = 6.8 Hz, 2H), 5.03 (d, ^{2}J = 6.8 Hz, 2H), 3.19 (s, 6H). The reported ^{1}H-NMR data fit with the ones reported in the literature.[80]

2,2'-Bis(methoxymethoxy)-[1,1'-binaphthalene]-3,3'-diol (50):

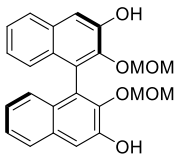

In a Schlenk tube, at -78 °C under argon atmosphere, a solution of *n*BuLi (1.6M in hexane 112 mL, 178.8 mmol, 2.4 eq.) was added dropwise to a stirred solution of **48** (26 g, 74.5 mmol, 1 eq.) in dry THF (220 mL). The mixture was allowed to warm at 0 °C and stirred for 1 hour.

After cooling at -78 °C, trimethylborate (24.9 mL, 223.5 mmol, 3 eq.) was added dropwise and left reacting at r.t. overnight. THF was removed under high vacuum and crude borate **49** was suspended in benzene (260 mL). 30% H_2O_2 (22.9 mL, 224 mmol, 3 eq.) was added dropwise at 0 °C; the mixture was then refluxed for 2 hours, cooled at -10 °C and poured in 150 mL of ice-cooled saturated solution of Na_2SO_3; after extraction with AcOEt (3 × 150 mL), the organic layers were washed with brine (100 mL), dried over Na_2SO_4 and evaporated under reduced pressure, affording **50** (32.8 g) as a pale orange foam, used without any further purification.

^{1}H NMR (400 MHz, CD_2Cl_2) δ 7.78 (d, ^{3}J = 8.4 Hz, 2H), 7.49 (d, ^{3}J = 4.9 Hz, 2H), 7.37 (t, ^{3}J = 7.6 Hz, 2H), 7.11 (t, ^{3}J = 7.0 Hz, 2H), 7.00 (d, ^{3}J = 9.0 Hz, 2H), 4.73 (d, ^{2}J = 6.3 Hz, 2H), 4.67 (d, ^{2}J = 6.3 Hz, 2H), 3.39 (s, 6H). The reported ^{1}H-NMR data fit with the ones reported in the literature.[80]

3,3'-Dimethoxy-2,2'-bis(methoxymethoxy)-1,1'-binaphthalene (51):

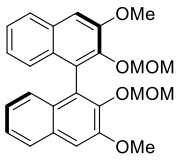

In a Schlenk vessel under argon, crude compound **50** (32.8 g) was dissolved into acetone (500 mL) with suspended Na_2CO_3 (45.4 g, 328 mmol, 4.5 eq.). MeI (22.7 mL, 365 mmol, 5 eq.) was added and mixture was left stirring at reflux overnight. Solvent was then removed under reduced pressure and crude dissolved in AcOEt (300 mL), which was washed with water. Aqueous phases were extracted (2 × 100 mL) with AcOEt. Organic phases were washed with brine and dried over Na_2SO_4. Evaporation the solvent under reduced pressure afforded crude **51** (31.9 g) as a white foam, which was used without any further purification.

^{1}H NMR (400 MHz, CD_2Cl_2) δ 7.80 (d, ^{3}J = 8.1 Hz, 2H), 7.40-7.33 (m, 4H), 7.10 (m, 4H), 4.90 (d, ^{2}J = 5.5 Hz, 2H), 4.83 (d, ^{2}J = 5.5 Hz, 2H), 4.03 (s, 6H), 2.57 (s, 6H). The reported ^{1}H-NMR data fit with the one reported in the literature.[80]

3,3'-Dimethoxy-[1,1'-binaphthalene]-2,2'-diol (52):

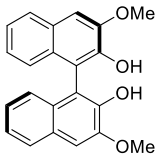

Crude **51** (31.9 g) was dissolved in dioxane (150 mL) and 37% aq. HCl (3 mL) was added. Mixture was heated at 40 °C for 3 hours. Solvent was evaporated under reduced pressure; water (300 mL) was added and then extracted with AcOEt (3 × 120 mL). Organic layers were dried over Na_2SO_4 and solvent was removed under high vacuum, affording crude **52** (30.2 g) as a yellow foam, which was used without any further purification.

^{1}H NMR (400 MHz, CD_2Cl_2) δ 7.80 (d, ^{3}J = 8.2 Hz, 2H), 7.32 (m, 4H), 7.17-7.10 (m, 2H), 7.07 (d, ^{3}J = 8.0 Hz, 2H), 4.09 (s, 6H). The reported ^{1}H-NMR data fit with the one reported in the literature.[80]

3,3'-Dimethoxy-[1,1'-binaphthalene]-2,2'-diyl bis(trifluoromethanesulfonate) (53):

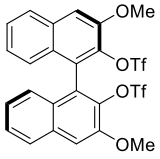

In a Schlenk vessel, under argon atmosphere, crude compound **52** (30.2 g, 109.3 mmol, 1 eq.) was dissolved in dry DCM (180 mL) and dry TEA (30 mL, 328 mmol, 3 eq.). After cooling at -78 °C, Tf_2O (27 mL, 160 mmol, 2.2 eq.) was added dropwise, then mixture was allowed reacting 2 h at r.t.. Mixture was then poured into ice-cooled 1 M HCl (300 mL); after extraction with DCM (3 × 100 mL), organic layer was washed with $NaHCO_3$ solution (100 mL) and brine (100 mL), then dried over Na_2SO_4. After evaporation of

solvent, the crude was dissolved in the minimal amount of CH_2Cl_2 and diethyl ether was added to precipitate triflate salts, which were filtered off. After another precipitation of triflate salts, product **53** (35.0 g, as a black viscous oil) was purified by flash chromatography (8:2 hexane/DCM). Bis-triflate **53** (15.09 g, 37.2 mmol) was obtained as a white foam in 34% yield, over six steps.

^{1}H NMR (400 MHz, $CDCl_3$) δ 7.87 (d, ^{3}J = 8.1 Hz, 2H), 7.54-7.49 (m, 4H), 7.24 (t, ^{3}J = 8.0 Hz, 2H), 7.14 (d, ^{3}J = 8.5 Hz, 2H), 4.11 (s, 6H). The reported ^{1}H-NMR data fit with the one reported in the literature.[80]

3,3'-Dimethoxy-2,2'-dimethyl-1,1'-binaphthalene (54):

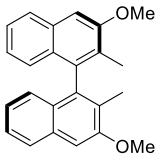

In a scaled Schlenk under argon, bis-triflate **53** (15.09 g, 24.7 mmol, 1 eq.) and $NiCl_2$(dppp) (896 mg, 1.65 mmol, 6.7 mol%) were dissolved in dry Et_2O (100 mL). MeMgI (41.2 mL, 3 M in Et_2O, 123.6 mmol, 5 eq.) was added dropwise at 0 °C; the reaction was left at 40 °C for 3 days (control by TLC, 7:3 hexane/DCM). After cooling in an ice bath, the mixture was slowly poured in 1M HCl solution (200 mL) and filtered over a celite® pad, rinsing with Et_2O, to remove catalyst. Organic and aqueous phases were separated, without shaking, in a funnel. The aqueous phases were extracted twice with AcOEt (100 mL) and then with DCM (50 mL). Organic layers were washed once with brine and dried over Na_2SO_4. The pale rose crude foam was purified by flash chromatography (9:1 hexane/DCM), affording **54** (4.60 g, 15.1 mmol) as a white-yellowish solid in 61% yield. The reported ^{1}H-NMR data fit with the one reported in the literature.[80]

Product of mono-coupling was purified by flash chromatography (8:2 hexane/DCM) and obtained in 4.1% yield as a white solid (0.480 mg, 1.0 mmol).

^{1}H NMR (400 MHz, $CDCl_3$) δ 7.91 (dd, ^{3}J = 8.2, ^{4}J = 1.1 Hz, 2H), 7.46 (ddd, ^{3}J = 8.1, 6.6 Hz, ^{4}J = 1.4 Hz, 2H), 7.34 (s, 2H), 7.18 (ddd, ^{3}J = 7.9, 6.7 Hz, ^{4}J = 1.3 Hz, 2H), 7.13 (d, J = 8.2 Hz, 2H), 4.09 (s, 6H), 2.09 (s, 6H).

2,2'-Bis(bromomethyl)-3,3'-dimethoxy-1,1'-binaphthalene (47b):

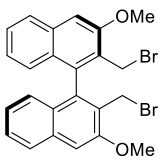

Under argon, in a Schlenk tube, compound **54** (5.15 g, 14.0 mmol, 1 eq.) was dissolved in CCl_4 (85 mL); NBS (6.06 g, 34.0 mmol, 2.2 eq.) and benzoyl peroxide (117 mg, 0.481 mmol, 3.2%mol) were added as solid, and mixture was heated at 80 °C, while irradiating with a 300 W lamp. After 22 hours the reaction was cooled down and filtered on a frit, rinsing with CCl_4, to remove the insoluble succinimide. Solvent was removed under vacuum, and the **47b** crude was obtained as a white pale brown foam. Purification was done by crystallization, dissolving crude **47b** in the minimal amount of Et_2O under sonication and adding hexane. Precipitate **47b** (6.63 g) was decanted and obtained in 88% yield. Remaining solvent was removed under high vacuum, affording impure **47b** (1.400 g), which was used without any further purification.

^{1}H NMR (400 MHz, $CDCl_3$) δ 7.82 (d, ^{3}J = 8.2 Hz, 2H), 7.44 (ddd, ^{3}J = 8.3, 6.8, ^{4}J = 1.3 Hz, 2H), 7.34 (s, 2H), 7.11 (ddd, ^{3}J = 8.2, 6.8, ^{4}J = 1.2 Hz, 2H), 7.00 (d, ^{3}J = 8.4 Hz, 2H), 4.36 (d, ^{2}J = 9.5 Hz, 2H), 4.29 (d, ^{2}J = 9.5 Hz, 2H), 4.12 (s, 6H). The reported ^{1}H-NMR data fit with the one reported in the literature.[80]

2,2'-([1,1'-Binaphthalene]-2,2'-diyl)diacetonitrile (53a):

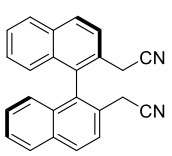

In a Schlenk, under argon, compound **47a** (1.3 g, 2.95 mmol, 1 eq.) was suspended in EtOH (6 mL). NaCN (330 mg, 10 mmol, 3.4 eq.) was added as solution in water (3.8 mL). The suspension was heated to reflux and stirred overnight. After monitoring the conversion by TLC (8:2 hexane:AcOEt), the reaction was extracted with ethyl acetate (3 × 20 mL), then the organic layer was washed with brine (20 mL) and dried over Na_2SO_4. After evaporation under reduced pressure, crude product was obtained as a white-yellowish powder. The product was purified with flash chromatography (9:1 → 8:2 DCM/hexane). **53a** (480 mg, 1.44 mmol) was obtained as a white powder in 49% yield.

^{1}H NMR (400 MHz, $CDCl_3$) δ 8.1 (d, J = 8.8 Hz, 2H), 8.0 (d, J = 8.4 Hz, 2H), 7.8 (d, J = 8.4 Hz, 2H), 7.6 (ddd, J = 7.2 1.2 Hz, 2H), 7.4 (dt, J = 7.2, 1.2 Hz, 2H), 7.1 (d, J = 8.8 Hz, 2H), 3.4 (d, J = 9.5 Hz, 2H), 3.3 (d, J = 9.5 Hz, 2H).

2,2'-([1,1'-Binaphthalene]-2,2'-diyl)bis(ethan-1-amine) (54a):

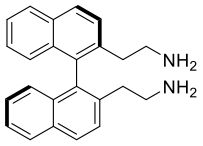

To a solution of $AlCl_3$ (0.81 g, 6.1 mmol, 4.2 eq.) and $LiAlH_4$ (0.23 g, 6.1 mmol, 4.2 eq.) in 15 mL of THF, a solution of **53a** (0.48 g, 1.44 mmol, 1 eq.) was added dropwise. The mixture was stirred overnight under a gentle flow of N_2. The reaction was diluted with 5 mL of water, then 3M H_2SO_4 (8 mL) was added dropwise under N_2 flow. The reaction mixture was diluted with CH_2Cl_2, phases were separated and the aqueous layer was extracted with CH_2Cl_2 (3 × 15 mL). The combined organic phases were dried with Na_2SO_4, filtered and evaporated. Crude **54a** was used without purification in the following step.

^{1}H NMR (400 MHz, $CDCl_3$): δ 7.9 (m, 2H), 7.7 (m, 2H), 7.6 (m, 2H), 7.5 (m, 2H), 7.4 (m, 2H), 7.1 (m, 2H), 2.8 (m, 4H), 2.6 (m, 4H), 1.6 (br, 4H).

***N,N'*-([1,1'-Binaphthalene]-2,2'-diylbis(ethane-2,1-diyl))diformamide (55a):**

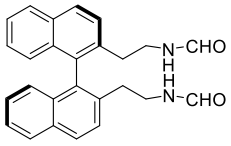

Crude compound **54a** (490mg, 1.44 mmol, 1 eq.) was dissolved in ethyl formate (5 mL) and refluxed for 48 h. Purification of the crude by flash column chromatography (97:3 DCM/MeOH) afforded product **55a** (343 mg, 0.86 mmol) with 60% yield.

^{1}H NMR (400 MHz, $CDCl_3$): δ 8.0 (d, J = 8.8 Hz, 2H), 7.9 (d, J = 8.4 Hz, 2H), 7.7 (d, J = 8.4 Hz, 2H), 7.5 (ddd, J = 7.2, 1.2 Hz, 2H), 7.3 (dt, J = 7.2, 1.2 Hz, 2H), 7.0 (d, J = 8.8 Hz, 2H), 3.5 (m, 2H), 3.3 (m, 2H), 2.6 (m, 2H).

ESI-MS in CH_3CN: $[M+Na]^+$ *m/z* 419.6.

2,2'-Bis(2-isocyanoethyl)-1,1'-binaphthalene (56a):

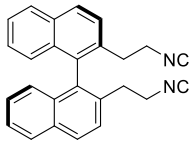

$POCl_3$ (90 μL, 0.9 mmol, 2.2 eq.) was dropped into a stirred solution of **55a** (165 mg, 0.42 mmol, 1 eq.) and TEA (0.3 mL, 3.35 mmol, 8 eq.) in DCM (6 mL). After stirring at r.t. for 3 h, the reaction mixture was poured into ice-chilled Na_2CO_3 aqueous solution and CH_2Cl_2 was added. Phases were separated and the aqueous layer was extracted with CH_2Cl_2 (3 × 10 mL). The combined organic phases were dried with Na_2SO_4, filtered and evaporated. Purification by flash column chromatography (using chilled eluents) afforded ligand **56a** (151 mg, 3.6 mmol) as an off-white foam in 86% yield.

^{1}H NMR (400 MHz, $CDCl_3$): δ 8.1 (d, J = 8.8 Hz, 2H), 8.0 (d, J = 8.4 Hz, 2H), 7.6 (d, J = 8.4 Hz, 2H), 7.5 (m, Hz, 2H), 7.3 (m, 2H), 7.0 (d, J = 8.4 Hz, 2H), 3.3 (m, 4H), 2.8 (m, 4H).

ESI-MS in CH_3CN: $[M+Na]^+$ *m/z* 383.16.

2,2'-(3,3'-Dimethoxy-[1,1'-binaphthalene]-2,2'-diyl)diacetonitrile (53b):

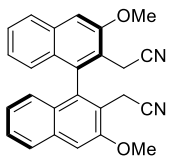

Compound **47b** (694 mg, 1.39 mmol, 1 eq.) was suspended in EtOH (8.6 mL) under argon atmosphere; NaCN (330 mg, 6.73 mmol, 4.85 eq.) was added as a water solution (3.8 mL). The suspension was stirred overnight, under reflux. The reaction was extracted with AcOEt (3 × 20 mL), and the organic layer was washed with brine (20 mL) and dried over sodium sulfate. After evaporation under reduced pressure, crude was obtained as a white-yellowish powder (532 mg). The product was purified by flash column chromatography (9:1→8:2 DCM/hexane) and **53b** (501.5 mg, 1.28 mmol) was obtained as a white powder in 92% yield.

^{1}H NMR (400 MHz, $CDCl_3$) δ 7.88 (d, J = 8.2 Hz, 2H), 7.51 (t, J = 7.1 Hz, 2H), 7.40 (s, 2H), 7.21 (t, J = 7.6 Hz, 2H), 7.04 (d, J = 8.4 Hz, 2H), 4.14 (s, 6H), 3.40 (d, J = 3.8 Hz, 4H). ^{13}C NMR (101 MHz, $CDCl_3$) δ 155.06, 136.05, 134.59, 127.65, 127.15, 125.97, 125.19, 120.59, 117.22, 106.59, 55.98, 29.75, 16.78.

HRMS in CH_3CN = $[C_{26}H_{20}N_2O_2Na_{Calc.} = 415.147]$ *m/z* 415.14118.

2,2'-(3,3'-Dimethoxy-[1,1'-binaphthalene]-2,2'-diyl)bis(ethan-1-amine) (54b):

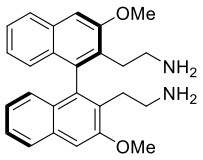

$LiAlH_4$ (664 mg, 17.5 mmol, 4.0 eq.) was suspended under stirring in Et_2O (40 mL), in a sealed Schlenk tube. After cooling in an ice bath, $AlCl_3$ (2.22 g, 17.5 mmol, 4 eq.) was added. Compound **53b** (1.71 g, 4.36 mmol, 1 eq.) was added as THF solution (25 mL). The mixture was allowed to warm up to r.t. and stirred overnight. After cooling in an ice bath 0.66 mL of water were slowly added under stirring; after 20 minutes 0.66 mL of NaOH (15% w/w) was added and then 2 mL of water (Fieser Rule's). The mixture was filtered through celite®, the filtrate containing the desired product **54b**. Some additional product **54b** was obtained from the solid which remained on the filter. The latter was removed from the filter with a spatula, dissolved in 15%w. NaOH (50 mL) and then extracted with Et_2O (150 mL) and DCM (120 mL). Finally, Celite was removed from the frit, suspended in DCM was washed under sonication (10 min) with DCM (4 × 10 mL) and MeOH (2 × 10 mL). The combined organic phases containing the desired product **54b** were dried over sodium sulfate and evaporated under reduced pressure. Compound **54b** (1.55 g) was obtained as a white-yellowish foam and used without any further purification.

^{1}H NMR (400 MHz, $CDCl_3$) δ 7.77 (d, J = 8.2 Hz, 2H), 7.34 (ddd, J = 8.1, 6.7, J = 1.2 Hz, 2H), 7.24 (s, 2H), 7.03 (ddd, J = 8.2, 6.8, J = 1.3 Hz, 2H), 6.91 (d, J = 8.4 Hz, 2H), 4.01 (s, 6H), 2.75-2.60 (m, 4H), 2.55-2.41 (m, 4H), 1.99 (b, 4H).

ESI-MS in CH_3CN: $[M]^+$ *m/z* 400.5.

***N,N'*-((3,3'-Dimethoxy-[1,1'-binaphthalene]-2,2'-diyl)bis(ethane-2,1-diyl))diformamide (55b):**

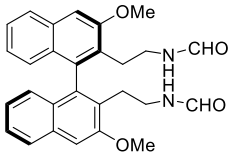

In a Schlenk tube, compound **54b** (365 mg, 0.91 mmol) was dissolved under argon in ethyl formate (10 mL). After addition of two drops of triethylamine, mixture was heated at 65 °C overnight. After control by TLC (95:5 DCM/MeOH), ethyl formate was removed by evaporation under reduced pressure: a yellow solid was obtained. The crude was purified by flash chromatography (98:2 → 95:5 DCM/MeOH) and product **55b** (335 mg, 0.73 mmol) was obtained as a yellow foam in 80% yield.

^{1}H NMR† (400 MHz, $CDCl_3$) δ 7.82 (d, J = 8.0 Hz, 2H), 7.58 (br, 2H), 7.41 (dt, J = 14.7, 7.5 Hz, 2H), 7.29 (t, J = 4.7 Hz, 2H), 7.15-7.05 (m, 2H), 7.01-6.92 (m, 2H), 5.67 –5.44 (br, 2H), 4.04 (s, 3H), 4.03 (s, 3H), 3.33 (ddd, J = 12.6, J = 6.1 Hz, 1H), 3.18 (tt, J = 21.9, J = 7.7 Hz, 1H), 2.99 (dt, J = 13.4, J = 5.8 Hz, 1H), 2.91-2.71 (m, 1H), 2.53-2.42 (m, 1H), 2.40-2.30 (m, 1H). † Chain hydrogens multiplicity is due to the presence of conformational isomers (formamide moiety)

ESI-MS in CH_3CN: $[M+Na]^+$ *m/z* 479.3.

2,2'-Bis(2-isocyanoethyl)-3,3'-dimethoxy-1,1'-binaphthalene (56b):

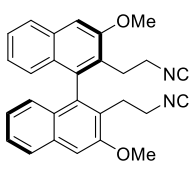

$POCl_3$ (60 µL, 0.6 mmol, 2.2 eq.) was dropped into a stirred solution of compound **55b** (134 mg, 0.3 mmol, 1 eq.) and TEA (0.3 mL, 2.3 mmol, 8 eq.) in 3.5 mL of dry THF. After stirring for 3 h at r.t., the reaction mixture was poured into chilled 10% aqueous solution of Na_2CO_3, and AcOEt was added. Phases were separated and the aqueous layer was extracted with AcOEt (3 × 5 mL). The combined organic phases were dried with Na_2SO_4, filtered and evaporated. Purification of the crude was performed by chilled flash column chromatography (DCM) affording ligand **56b** (112 mg, 0.27 mmol) with 89% yield.

^{1}H NMR (400 MHz, CD_2Cl_2) δ 7.86 (dt, *J* = 8.2, 0.9 Hz, 2H), 7.43 (ddd, *J* = 8.2, 6.8, 1.3 Hz, 2H), 7.37 (s, 2H), 7.10 (ddd, *J* = 8.2, 6.8, 1.3 Hz, 2H), 6.87 (dq, *J* = 8.4, 0.9 Hz, 2H), 4.07 (s, 6H), 3.50-3.37 (m, 2H), 3.18-3.10 (m, 2H), 3.00 (ddd, *J* = 12.3, 10.9, 5.2 Hz, 2H), 2.71-2.64 (m, 2H). ^{13}C NMR (101 MHz, CD_2Cl2) δ 156.11, 136.67, 134.19, 128.28, 127.02, 126.61, 125.94, 124.23, 105.83, 55.55, 39.92, 29.53.

***N,N'*-([1,1'-Binaphthalene]-2,2'-diylbis(methylene))diformamide (57a):**

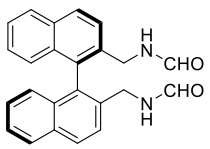

In a Schlenk, under argon, compound **47a** (400 mg, 0.9 mmol, 1 eq.) and sodium diformylamide (259 mg, 2.73 mmol, 3 eq.) were dissolved in dry DMF (5 mL). The mixture was stirred overnight at 100 °C. The following day, AcOEt was added and the mixture was washed several times with water in order to remove the remaining DMF. The organic phases were combined, washed with brine and dried over Na_2SO_4. The crude was purified by column chromatography (99:1 → 95:5 DCM/MeOH) affording **57a** (255 mg, 0.69 mmol) with 77% yield.

^{1}H NMR (400 MHz, $CDCl_3$) δ 8.16 (d, *J* = 1.7 Hz, 1H), 7.97 (dd, *J* = 23.9, 8.4 Hz, 2H), 7.72 (d, *J* = 8.6 Hz, 1H), 7.48 (ddd, *J* = 8.1, 6.8, 1.2 Hz, 1H), 7.31-7.26 (m, 1H), 7.12-7.04 (m, 1H), 6.98 (s, 1H), 4.30 (dd, *J* = 15.3, 7.2 Hz, 1H), 3.98 (dd, *J* = 15.3, 5.6 Hz, 1H).

ESI-MS in CH_3CN: $[M+Na]^+$ *m/z* 391.2.

2,2'-Bis(isocyanomethyl)-1,1'-binaphthalene (58a):

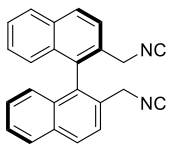

$POCl_3$ (89 µL, 0.96 mmol, 2.2 eq.) was dropped into a stirred solution of **55a** (160 mg, 0.44 mmol, 1 eq.) and TEA (0.48 mL, 3.5 mmol, 8 eq.) in 4 mL dry THF. After stirring for 3 h at r.t., the reaction mixture was poured into chilled 10% aqueous solution of Na_2CO_3 and rinsed with AcOEt. Phases were separated and the aqueous layer was extracted with AcOEt (3 × 5 mL). The combined organic phases

were dried with Na_2SO_4, filtered and evaporated. Purification of the crude was performed by chilled flash column chromatography (8:2 DCM/hexane) affording ligand **58a** (80 mg, 0.24 mmol) with 55% yield.

^{1}H NMR (400 MHz, CD_2Cl_2) δ 8.20 (dd, *J* = 8.6, 0.8 Hz, 1H), 8.07 (ddd, *J* = 8.4, 1.0 Hz, 1H), 7.89 (d, *J* = 8.6 Hz, 1H), 7.60 (ddd, *J* = 8.2, 6.8, 1.2 Hz, 1H), 7.38 (ddd, *J* = 8.3, 6.8, 1.3 Hz, 1H), 7.08 (dq, *J* = 8.5, 1.0 Hz, 1H), 4.39-4.26 (m, 2H). ^{13}C NMR (101 MHz, CD_2Cl_2) δ 158.51, 133.52, 132.77, 132.10, 129.89, 129.47, 128.43, 127.57, 127.01, 125.45, 125.02, 43.87.

***N,N′*-((3,3'-Dimethoxy-[1,1'-binaphthalene]-2,2'-diyl)bis(methylene))diformamide (57b):**

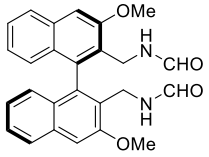

In a Schlenk vessel, under argon, compound **47b** (500 mg, 1 mmol, 1 eq.) and sodium diformylamide (285 mg, 3 mmol, 3 eq.) were dissolved in dry DMF (5 mL). The mixture was stirred for 27h at 100 °C. The following day, AcOEt was added and the mixture was washed several times with water in order to remove the remaining DMF. The organic phases were combined, washed with brine and dried over Na_2SO_4. The crude was purified by column chromatography (97:3 → 95:5 DCM/MeOH) affording **57b** (373 mg, 0.87 mmol) with 87% yield.

^{1}H NMR (400 MHz, $CDCl_3$) δ 8.00-7.90 (m, 1H), 7.84-7.78 (m, 1H), 7.44-7.41 (m, 1H), 7.34 (s, 1H), 7.10 (dt, *J* = 8.2, 6.8, 1.3 Hz, 1H), 7.00 (s, 1H), 6.91 (d, *J* = 8.5 Hz, 1H), 4.16-4.01 (m, 5H).

ESI-MS in CH_3CN: $[M+Na]^+$ *m/z* 451.3.

2,2'-Bis(isocyanomethyl)-3,3'-dimethoxy-1,1'-binaphthalene (58b):

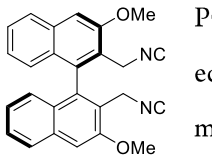

$POCl_3$ (204 μL, 2.2 mmol, 2.2 eq.) was dropped into a stirred solution of **57b** (366 mg, 1 mmol, 1 eq.) and TEA (1.11 mL, 8 mmol, 8 eq.) in 5.2 mL dry THF. After stirring 3 h at r.t., the reaction mixture was poured into chilled 10% solution of Na_2CO_3 and diluted with AcOEt. Phases were separated and the aqueous layer was extracted with AcOEt (3 × 5 mL). The combined organic phases were dried with Na_2SO_4, filtered and evaporated. Purification of the crude was performed by chilled flash column chromatography (DCM) affording ligand **58b** (216 mg, 0.55 mmol) with 55% yield.

^{1}H NMR (400 MHz, CD_2Cl_2) δ 7.94 (d, *J* = 8.2 Hz, 1H), 7.54 (ddd, *J* = 8.1, 6.8, 1.2 Hz, 1H), 7.49 (s, 1H), 7.21 (ddd, *J* = 8.2, 6.8, 1.2 Hz, 1H), 7.03 (d, *J* = 8.4 Hz, 1H), 4.35 (dd, *J* = 15.1, 7.6 Hz, 2H), 4.17 (s, 3H).

ESI-MS in CH_3CN: $[M+1]^+$ *m/z* 393.3.

***N,N'*-((3,3'-Dihydroxy-[1,1'-binaphthalene]-2,2'-diyl)bis(methylene))diformamide (59):**

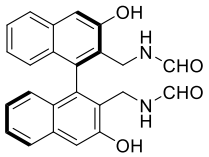

Into a Schlenk vessel, under argon, **57b** (91 mg, 0.21 mmol, 1 eq.) was dissolved in dry DCM (1 mL). At 0 °C a 1 M BBr_3 solution in DCM (0.84 mL, 0.84 mmol, 4.7 eq.) was added. The mixture was stirred overnight at r.t.. With an ice-bath the solution was cooled and water was dropped into the crude solution. The solution changed color from orange-red to milky white. Phases were extracted with AcOEt (the free bis-alcohol is poorly soluble in DCM) and the combined organic phases were washed with brine and dried over Na_2SO_4. After evaporation of the solvent, the crude was purified by flash column chromatography (99:1 → 95:5 DCM/MeOH), affording compound **59** (68 mg, 0.17 mmol) with 80% yield.

^{1}H NMR (400 MHz, $CDCl_3$) δ 7.98 (s, 1H), 7.83 (d, *J* = 8.3 Hz, 1H), 7.57 (s, 1H), 7.45 (ddd, *J* = 8.2, 6.7, 1.2 Hz, 1H), 7.15 (ddd, *J* = 8.1, 6.7, 1.2 Hz, 1H), 6.98 (d, *J* = 8.5 Hz, 1H), 5.77 (s, 1H), 4.45 (dd, *J* = 14.8, 7.5 Hz, 1H), 3.92 (dd, *J* = 14.8, 5.6 Hz, 1H).

2,2'-Bis(formamidomethyl)-[1,1'-binaphthalene]-3,3'-diyl bis(trifluoromethanesulfonate) (60):

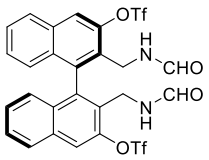

In a Schlenk vessel, under argon, compound **59** (294 mg, 0.73 mmol, 1 eq.), TEA (0.41 mL, 2.93 mmol, 4 eq.) and a tip of spatula of DMAP were dissolved in dry THF (4 mL). A solution of Comins' reagent (720 mg, 1.84 mmol, 2.5 eq.) in dry THF (3 mL) was slowly dropped into the stirred solution containing **59**. The reaction was stirred at r.t. overnight. The mixture, rinsed with DCM, was washed with 1M HCl (3 × 5 mL), NaOH 1M (3 × 5 mL), brine and dried over Na_2SO_4. After evaporation of the solvent, the crude product was columned using a mixture of (98:2 DCM/MeOH) affording **60** (393 mg, 0.59 mmol) with 81% yield.

^{1}H NMR (400 MHz, $CDCl_3$) δ 8.06 (s, 1H), 8.01 (d, *J* = 8.2 Hz, 0H), 7.92-7.89 (m, 1H), 7.63 (ddd, *J* = 8.2, 6.9, 1.2 Hz, 1H), 7.44 (ddd, *J* = 8.3, 6.9, 1.3 Hz, 1H), 7.05 (dt, *J* = 8.6, 0.9 Hz, 1H), 6.67-6.57 (m, 1H), 4.45 (dd, *J* = 15.1, 6.2 Hz, 1H), 4.16 (dd, *J* = 15.2, 5.5 Hz, 1H). ^{13}C NMR (101 MHz, $CDCl_3$) δ 160.76, 146.21, 136.90, 132.95, 131.96, 128.74, 128.69, 128.29, 127.88, 125.70, 120.89, 117.04, 36.12.

***N,N'*-((3,3'-Diphenyl-[1,1'-binaphthalene]-2,2'-diyl)bis(methylene))diformamide (61):**

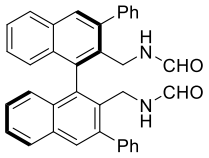

In a Schlenk vessel, under argon, compound **60** (200 mg, 0.3 mmol, 1eq.), $Pd(OAc)_2$ (13.5 mg, 0.06 mmol, 0.02 eq.), PPh_3 (31.6 mg, 0.12 mmol, 0.04 eq.), K_3PO_4 (191.7 mg, 0.9 mmol, 3 eq.), phenylboronic acid (91.7 mg, 0.75 mmol, 2.5 eq.) and KBr (78 mg, 0.66 mmol, 2.2 eq.) were dissolved in dry dioxane (8 mL). The mixture was stirred overnight at 87 °C. The day after the mixture was washed with 1 M NaOH, water, brine and dried over Na_2SO_4. After filtration and solvent evaporation, the crude product **61**

was purified by flash column chromatography (98:2 → 9:1 DCM/MeOH) affording pure **61** (100 mg, 0.19 mmol) with 63% yield.

^{1}H NMR (400 MHz, $CDCl_3$) δ 8.02-7.90 (m, 2H), 7.75-7.66 (m, 1H), 7.60-7.44 (m, 6H), 7.42-7.34 (m, 1H), 7.25-7.18 (m, 1H), 5.82 (s, 1H), 4.53-3.92 (m, 2H).

TOF-MS-ESI in CH_3CN: Calculated$[M+Na]^+$ = *m/z* 543.204. Experimental = *m/z* 543.331.

2,2'-Bis(isocyanomethyl)-3,3'-diphenyl-1,1'-binaphthalene (62):

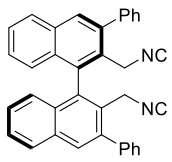

$POCl_3$ (39 μL, 0.42 mmol, 2.2 eq.) was dropped into a stirred solution of **61** (99.6 mg, 0.19 mmol, 1 eq.) and TEA (0.21 mL, 1.53 mmol, 8 eq.) in dry THF (2.5 mL). After stirring for 3 h at r.t., the reaction mixture was poured into a chilled 10% aqueous solution of Na_2CO_3 and diluted with AcOEt. Phases were separated and the aqueous layer was extracted with AcOEt (3 × 3 mL). The combined organic phases were dried with Na_2SO_4, filtered and evaporated. Purification of the product was performed by flash column chromatography using chilled (DCM) as eluent and affording ligand **62** (79 mg, 0.163 mmol) with 86% yield.

^{1}H NMR (400 MHz, CD_2Cl_2) δ 8.09 (s, 1H), 8.06 (dd, *J* = 8.3, 1.1 Hz, 1H), 7.68-7.49 (m, 6H), 7.41 (ddd, *J* = 8.2, 6.8, 1.3 Hz, 1H), 7.23 (d, *J* = 8.2 Hz, 1H), 4.34 (dd, *J* = 15.7, 8.6 Hz, 2H).

ESI-MS in CH_3CN: $[M+Na+Fe]^+$ *m/z* 579.0.

2,2'-Bis(formamidomethyl)-[1,1'-binaphthalene]-3,3'-diyl bis(3,4,5-trimethoxybenzoate) (63):

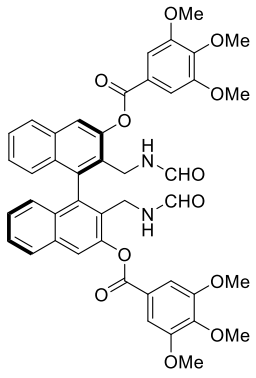

In a Schlenk vessel, under argon, compound **59** (50 mg, 0.125 mmol, 1 eq.) and tip of spatula of DMAP were dissolved in dry THF (0.125 mL). TEA (50 μL, 0.39 mmol, 3 eq.) was then added at r.t. followed by 3,4,5-trimethoxybenzoyl chloride (72 mg, 0.312 mmol, 2.5 eq.). The mixture was stirred for 4 h at 70 °C and its progress was monitored by TLC. When the starting material disappeared, the mixture was diluted with AcOEt and washed with 1 M HCl, water, brine and dried over Na_2SO_4. After filtration and evaporation of the solvent, crude **63** was purified by flash column chromatography (99:1 → 95:5 DCM/MeOH). Compound **63** (71 mg, 0.1 mmol) was obtained in 72% yield.

^{1}H NMR (400 MHz, $CDCl_3$) δ 7.97-7.91 (m, 1H), 7.89 (s, 1H), 7.72 (s, 1H), 7.55-7.51 (m, 3H), 7.32 (s, 1H), 7.14 (dd, *J* = 8.5, 1.0 Hz, 1H), 6.14 (s, 1H), 4.35 (dd, *J* = 14.4, 5.5 Hz, 1H), 4.22 (dd, *J* = 14.4, 4.9 Hz, 1H), 3.96 (s, 9H).

ESI-MS in CH_3CN: $[M-1]^+$ *m/z* 787.2.

2,2'-Bis(isocyanomethyl)-[1,1'-binaphthalene]-3,3'-diyl bis(3,4,5-trimethoxybenzoate) (64):

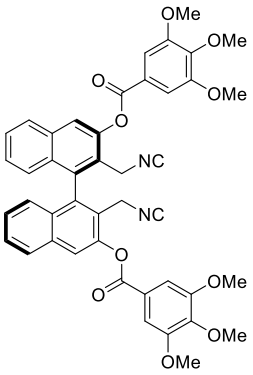

$POCl_3$ (18.5 μL, 0.2 mmol, 2.2 eq.) was dropped into a stirred solution of **63** (71 mg, 0.1 mmol, 1 eq.) and TEA (0.1 mL, 0.72 mmol, 7.2 eq.) in dry THF (2 mL). After stirring for 3 h at r.t., the reaction mixture was poured into chilled 10% aqueous solution of Na_2CO_3 and diluted with AcOEt. Phases were separated and the aqueous layer was extracted with AcOEt (3 × 2 mL). The combined organic phases were dried with Na_2SO_4, filtered and evaporated. Purification of the crude was performed by chilled flash column chromatography (95:5 → 8:2 DCM/AcOEt) affording ligand **64** (13 mg, 0.017 mmol) in 17% yield.

^{1}H NMR (400 MHz, CD_2Cl_2) δ 8.17 (d, *J* = 0.7 Hz, 1H), 8.08 (d, *J* = 8.4 Hz, 1H), 7.67 (ddd, *J* = 8.2, 6.9, 1.2 Hz, 1H), 7.65 (s, 3H), 7.43 (ddd, *J* = 8.3, 6.9, 1.3 Hz, 1H), 7.20 (dd, *J* = 8.5, 0.9 Hz, 1H), 4.39 (s, 2H), 3.98 (s, 6H), 3.94 (s, 3H).

2,2'-Bis(isocyanomethyl)-[1,1'-binaphthalene]-3,3'-diyl bis(trifluoromethanesulfonate) (65):

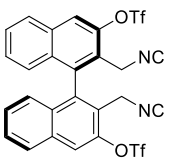

$POCl_3$ (31 μL, 0.33 mmol, 2.2 eq.) was dropped into a stirred solution of **60** (100 mg, 0.15 mmol, 1 eq.) and TEA (0.17 mL, 1.2 mmol, 8 eq.) in dry THF (2 mL). After stirring 3 h at r.t., the reaction mixture was poured into chilled 10% aqueous solution of Na_2CO_3 and diluted with AcOEt. Phases were separated and the aqueous layer was extracted with AcOEt (3 × 5 mL). The combined organic phases were dried with Na_2SO_4, filtered and evaporated. Purification of the crude was performed by chilled flash column chromatography (DCM) affording ligand **65** (79 mg, 0.126 mmol) with 84% yield.

^{1}H NMR (300 MHz, CD_2Cl_2) δ 8.21 (s, 1H), 8.1 (d, *J* = 8.23 Hz, 1H), 7.72 (t, *J* = 7.15 Hz, 1H), 7.49 (t, *J* = 7.35 Hz, 1H), 7.10 (d, *J* = 8.43 Hz, 1H), 4.38 (m, 2H).

ESI-MS in CH_3CN: $[M+Na]^+$ *m/z* 651.1.

Iron Complex (A1) $Fe(\mathbf{56a})_2Cl_2$**:**

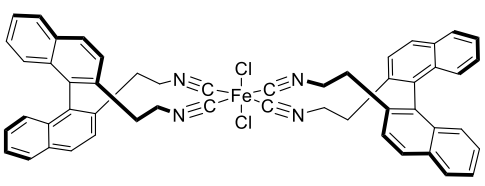

Under Ar, a solution of ligand **56a** (111 mg, 0.39 mmol, 2 eq.) in CH_2Cl_2 (5 mL) was added via cannula into a stirred solution of $FeCl_2{\cdot}4H_2O$ (39 mg, 0.20 mmol, 1 eq.) in MeOH (7 mL). The mixture suddenly took a red color. The reaction mixture was stirred overnight at r.t., then solvents were removed under high vacuum and the solid residue was washed with hexane (2 × 5 mL),

decanting off the supernatant solvent. Complex **A1**, Fe(**56a**)$_2$Cl$_2$ (125 mg, 0.148 mmol) was obtained as an orange solid in 76% yield.

ESI-MS in CH_3CN: $[M(\mathbf{L})_2Cl+CH_3CN]^+$ *m/z* 851.9.

Iron Complex (A2) Fe(**56b**)$_2$Cl$_2$**:**

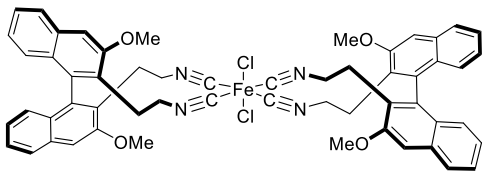

Under Ar, a solution of ligand **56b** (85 mg, 0.2 mmol, 2 eq.) in CH_2Cl_2 (5 mL) was added via cannula into a stirred solution of $FeCl_2{\cdot}4H_2O$ (20 mg, 0.10 mmol, 1 eq.) in MeOH (7 mL). The mixture suddenly took a red color. The reaction was stirred overnight at r.t., then solvents were removed under high vacuum and the residue was washed with hexane (2 × 5 mL), decanting off the supernatant solvent. Complex **A2,** Fe(**56b**)$_2$Cl$_2$ (73 mg, 0.076 mmol) was obtained as an orange solid in 76% yield.

ESI-MS in CH_3CN: $[Fe(\mathbf{L})_2Cl]^+$ *m/z* 931.0; $[Fe(\mathbf{L})Cl]^+$ *m/z* 511.1; $[Fe(\mathbf{L})_3Cl]^+$ *m/z* 1351.2.

Iron Complex (B1) Fe(**58a**)$_2$Cl$_2$**:**

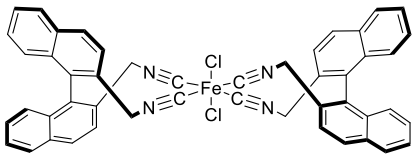

Under Ar, a solution of ligand **58a** (85 mg, 0.25 mmol, 2 eq.) in CH_2Cl_2 (5 mL) was added via cannula into a stirred solution of $FeCl_2{\cdot}4H_2O$ (25.3 mg, 0.13 mmol, 1 eq.) in MeOH (7 mL). The mixture suddenly took a red color. The reaction was stirred overnight at r.t., then solvents were removed under high vacuum and the residue was washed with hexane (2 × 5 mL), decanting off the supernatant solvent. Complex **B1**, Fe(**58a**)$_2$Cl$_2$ (97 mg, 0.122 mmol) was obtained as a red solid in 98% yield.

ESI-MS in CH_3CN: $[Fe(\mathbf{L})_2Cl]^+$ *m/z* 755.1; $[Fe(\mathbf{L})Cl_3Na]^+$ *m/z* 921.9; $[Fe(\mathbf{L})_3Cl]^+$ *m/z* 1087.0.

Iron Complex (B2) Fe(**58b**)$_2$Cl$_2$**:**

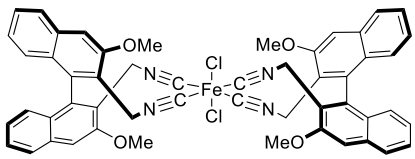

Under Ar, a solution of ligand **58b** (100 mg, 0.25 mmol, 2 eq.) in CH_2Cl_2 (5 mL) was added via cannula into a stirred solution of $FeCl_2{\cdot}4H_2O$ (25.3 mg, 0.13 mmol, 1 eq.) in MeOH (7 mL). The mixture suddenly took a red color. The reaction was stirred overnight at r.t., then solvents were removed under high vacuum and the residue was washed with hexane (2 × 5 mL), decanting off the supernatant solvent. Complex **B2**, Fe(**58b**)$_2$Cl$_2$ (104 mg, 0.113 mmol) was obtained as a red solid in 91% yield.

ESI-MS in CH_3CN: $[Fe(\mathbf{L})_2Cl]^+$ *m/z* 875.2; $[Fe(\mathbf{L})_3Cl]^+$ *m/z* 1267.2.

Iron Complex (B3) $Fe(\mathbf{62})_2Cl_2$**:**

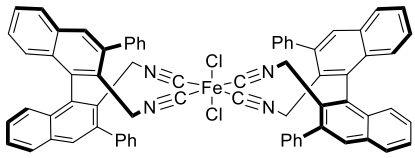

Under Ar, a solution of ligand **62** (66 mg, 0.14 mmol, 2 eq.) in CH_2Cl_2 (1.7 mL) was added via cannula into a stirred solution of $FeCl_2{\cdot}4H_2O$ (13.5 mg, 0.07 mmol, 1 eq.) in MeOH (2.4 mL). The mixture suddenly took a red color. The reaction was stirred overnight at r.t., then solvents were removed under high vacuum and the residue was washed with hexane (2 × 2 mL), decanting off the supernatant solvent. Complex **B3**, $Fe(\mathbf{62})_2Cl_2$ (51 mg, 0.047 mmol) was obtained as a red solid in 67% yield.

ESI-MS in CH_3CN: $[Fe(\mathbf{L})_2Cl]^+$ *m/z* 1059.2; $[Fe(\mathbf{L})_2Cl(CH_3CN)]^+$ *m/z* 1099.3; $[Fe(\mathbf{L})_3Cl]^+$ *m/z* 1543.2.

Iron Complex (B4) $Fe(\mathbf{65})_2Cl_2$**:**

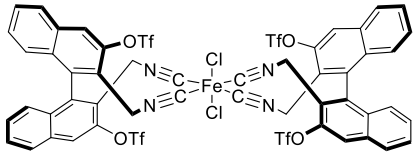

Under Ar, a solution of ligand **65** (77 mg, 0.11 mmol, 2 eq.) in CH_2Cl_2 (1.7 mL) was added via cannula into a stirred solution of $FeCl_2{\cdot}4H_2O$ (11.1 mg, 0.06 mmol, 1 eq.) in MeOH (2.4 mL). The mixture suddenly took a red color. The reaction mixture was stirred overnight at r.t., then solvents were removed under high vacuum and the residue was washed with hexane (2 × 2 mL), decanting off the supernatant solvent. Complex **B4**, $Fe(\mathbf{65})_2Cl_2$ (46mg, 0.033 mmol) was obtained as a red solid in 61% yield.

ESI-MS in CH_3CN: $[Fe(\mathbf{L})_2Cl(CH_3CN)]^+$ *m/z* 1387.9; $[Fe(\mathbf{L})_3Cl]^+$ *m/z* 1974.8.

Iron Complex (B5) $Fe(\mathbf{64})_2Cl_2$**:**

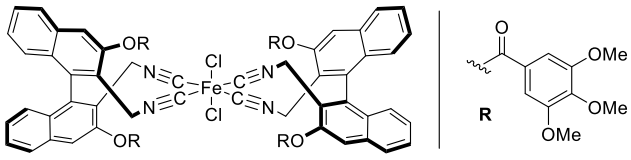

Under Ar, a solution of ligand **64** (11.3 mg, 0.015 mmol, 2 eq.) in CH_2Cl_2 (0.63 mL) was added via cannula into a stirred solution of $FeCl_2{\cdot}4H_2O$ (1.5 mg, 0.008 mmol, 1 eq.) in MeOH (0.1 mL). From a yellow solution, a reddish suspension formed. The reaction mixture was stirred overnight at r.t., then solvents were removed under high vacuum and the residue was washed with hexane (2 × 0.2 mL), decanting off the supernatant solvent. Complex **B5**, $Fe(\mathbf{64})_2Cl_2$ (10mg, 0.006 mmol) was obtained as a red-orange solid in 82% yield.

ESI-MS in CH_3CN: $[Fe(\mathbf{L})_2Cl(CH_3CN)]^+$ *m/z* 1387.9; $[Fe(\mathbf{L})_3Cl]^+$ *m/z* 1974.8.

2.6.1 Catalytic Tests

General Procedure for Asymmetric Transfer Hydrogenation

In oven-dried Schlenk, the selected iron complex (0.005 mmol, 0.05 eq.) and *t*BuOK (5.8 mg, 0.05 mmol, 0.5 eq.), were subjected to 3 vacuum-argon cycles, and dissolved in 0.52 mL of dry *i*PrOH. The mixtures were stirred for 1 min and then acetophenone (12 μL, 0.1 mmol, 1 eq.) was dispensed into the Schlenk. The Schlenk was heated at desired temperature and stirred for 22 h. A small aliquot of reaction crude was analyzed by GC to determine conversion and *ee*.

General Procedure for Asymmetric Hydrogenation

In oven-dried vials, iron complex (0.005 mmol, 0.05 eq.) and *t*BuOK (5.8 mg, 0.05 mmol, 0.5 eq.), were subjected to 3 vacuum-argon cycles, and dissolved in 0.52 mL of dry *i*PrOH. The mixtures were stirred for 1 min and then acetophenone (12 μL, 0.1 mmol, 1 eq.) was dispensed into the vials. The vials were then transferred into an autoclave, which was purged three times with H_2, then pressurized to 30 bar, heated at desired temperature and magnetically stirred for 22 h. After cooling down and venting H_2, hexadecane (0.1 mmol) was added in each vial and GC analysis was performed. The *ee* values and conversion were determined by GC.

General Procedure for isomerization of allylic alcohols

In oven-dried pressure proof vials, iron complex (0.001 mmol, 0.01 eq.) and *t*BuOK (if required) (0.8 mg, 0.001 mmol, 0.01 eq.), were subjected to 3 vacuum-argon cycles, and dissolved in 0.52 mL of dry solvent. The mixture was stirred for 15 minutes and afterwards, 1-octen-3-ol (15 μL, 0.1 mmol, 1 eq.) was added under argon to the mixture. The solution was heated at desired temperature and stirred for the proper time. The conversion is obtained by GC analysis with dodecane as internal standard.

GC-Analysis

(*S*)-1-Phenylethanol[80]

Capillary column: MEGADEX DACTBSβ, diacetyl-*tert*-butylsilyl-β-cyclodextrin, 0.25 μm; diameter = 0.25 mm; length = 25 m; carrier: hydrogen; inlet pressure: 1 bar; oven temperature: 95 °C for 20 min: $t_{\mathbf{S1}}$ = 6.0 min; $t_{(R)\text{-}\mathbf{P1}}$ = 13.8 min; $t_{(S)\text{-}\mathbf{P1}}$ = 14.8 min.

CHAPTER 3

PCCP IRON COMPLEXES

As already mentioned, a very important feature of ligands to be suitable for iron catalysis is their ability to stabilize the metal center: along with the synthesis of chelating and macrocyclic ligands, the use of strong field ligands is widely used both to bind strongly with the metal center and to finely tune electronic properties of the complex. Phosphines – in particular arylphosphines – in addition to σ donation of the phosphorus lone pair, have a nonnegligible π backbonding feature, which can enhance their ability to split t_{2g} and e_g orbitals. Along with their electronic properties (Tolman Electronic Parameter), steric bulk can be also modified by the substitution on the phosphorus atom (Tolman Cone Angle).

Probably due to their awful smell and their high sensitivity to acids, isonitriles are ligands whose chemistry is still relatively underdeveloped, compared to their tight relative carbon monoxide.[101] Compared to carbonyl, isocyanides are better σ-donors (as shown in Figure 21),[102] their HOMO 2σ is localized on the carbon atom, because nitrogen is less electron attracting (compared to oxygen); their π backbonding ability greatly varies with the oxidation state of the metal center: complexed to metal in low oxidation number backbonding is comparable to CO, but at medium or high oxidation state is almost negligible.

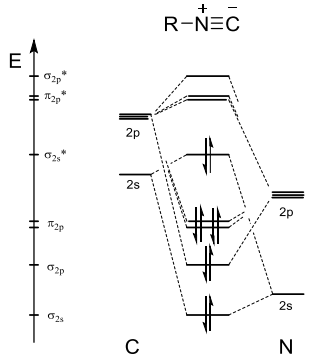

Figure 21. Molecular orbital structure of isonitriles.

Although these carbene-like features have recently attracted some interest (e.g. Reiser's complex **29**),[67] up to now isocyanides use has been confined to the role of ancillary ligands. However, recent contributions by Mezzetti and co-workers has shown that, in PNNP iron complexes, replacing acetonitrile ligands with simple monodentate isonitriles can lead to a dramatic increase of catalytic activity and enantioselectivity.[59c,d,51].

Based on the chiral binaphthyl backbone which has already been described in Chapter 2, we decided to incorporate the isonitrile group into a multidentate ligand, thus developing a PCCP ligand which – to the best of our knowledge –

has no precedents in the literature. **C** and **D** are chiral tetradentate PCCP (phosphine-isonitrile) ligands with a C_2 axis; two arms attached at the 2,2' positions of the binaphthyl system and phosphines bonded at 3,3' positions by ethereal bonds.

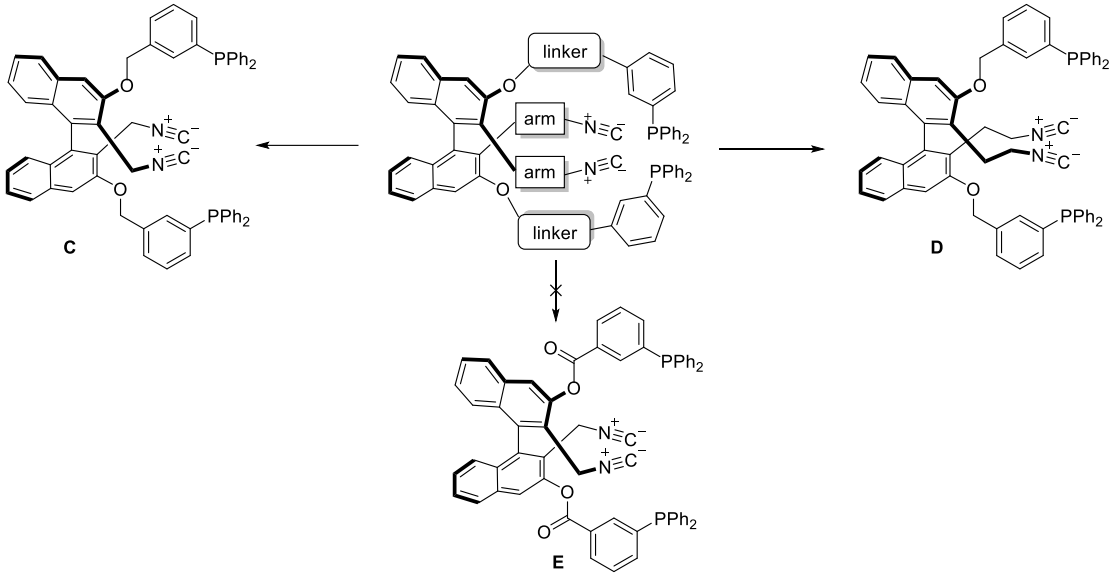

Figure 22. Designed structure of PCCP ligands.

3.1 PCCP IRON LIGAND, FIRST GENERATION

The first attempt to prepare a PCCP ligand was performed according to the retrosynthetic strategy shown in Scheme 42. Installation of the phosphine groups as an ester was thought to be tried as a late stage transformation, because attempts of dehydration of the formamide in presence of the phosphine were producing several side products (e.g. mono-oxidation, bis-oxidation, closing cycle).

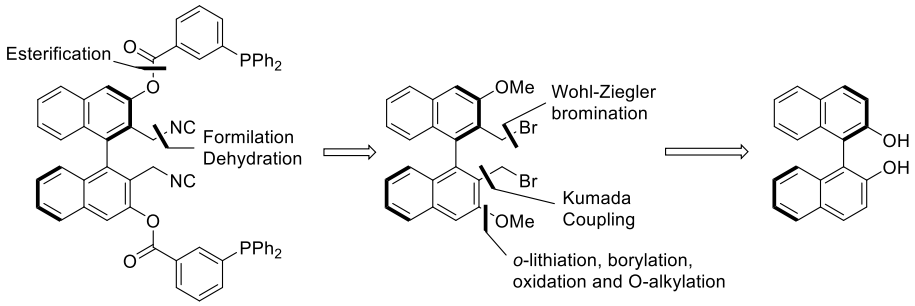

Scheme 42. Retrosynthesis of first generation of PCCP ligand.

The isonitrile group was obtained by functional group interconversion, starting from formamide, which was synthesized from the bis-bromide intermediate from nucleophilic substitution with sodium diformylamide $NaN(CHO)_2$. The carbon-carbon bonds at the 2,2'-positions of the binaphthyl backbone were introduced using

Kumada coupling, followed by functionalization of the benzylic positions by radical Wohl-Ziegler bromination. As first synthetic steps, formation of phenol at the 3,3'-positions was obtained by one-pot directed ortho-lithiation, borylation and oxidation, followed by O-alkylation in order to protect phenol moiety (see Scheme 37, pag. 36).

The strategy just described proved troublesome since the beginning. When the synthesis of the phosphine synthon by palladium-catalyzed coupling between diphenylphosphine and *m*-iodobenzoic acid was attempted (Scheme 43),[103] more than 68% of phosphine oxide was detected by ^{31}P NMR (sharp signal at 27 ppm, see 3.4 Experimental section). Flash column chromatography and crystallization technique failed to give pure **70**. Since free carboxylic acid are not easily purified by chromatography, from mixture of **70** + **70a** a methyl ester derivative was synthesized in order to further purify the product. Surprisingly, during the Steglich esterification, the phosphine was fully oxidized to phosphine oxide, giving **70a-OMe** as the sole product. The latter was deprotected with LiOH to afford the free acid **70a**, which was reduced quantitatively following a procedure reported by Beller and co-workers (TMDS, $Cu(OTf)_2$ in toluene).[104] Several other reducing methodologies were tried but none of them worked (e.g. Pd/C hydrogenation, trichlorosilane).

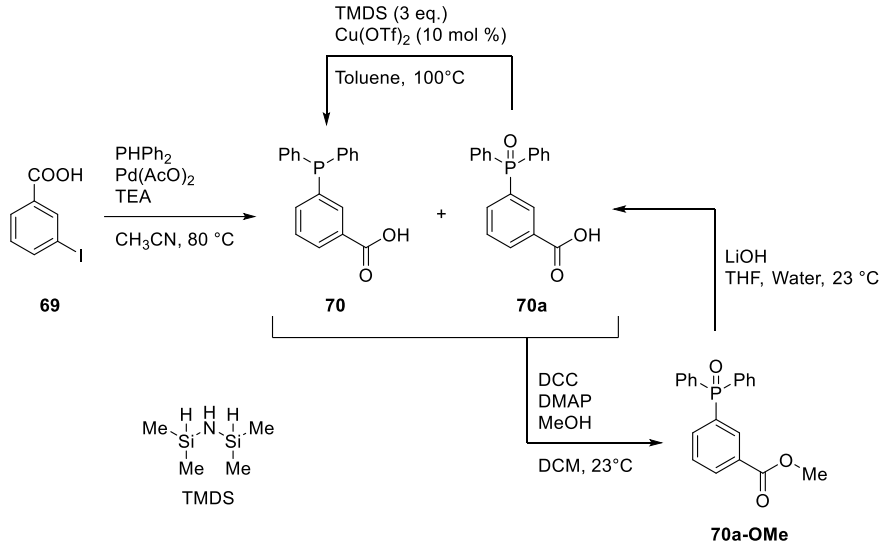

Scheme 43. Synthesis of 3-(diphenylphosphanyl)benzoic acid **70**.

For the formation of the ester bonds, the acyl chloride route was firstly attempted. Unfortunately, both thionyl chloride and oxalyl chloride afforded the acyl chloride **70a-Cl**, with full oxidation of phosphine moiety. The reduction of **70a-Cl** did not lead to any successful results. Furthermore, the reaction of bis-phenol **59** with the acyl chloride derivative **70a-Cl** gave no desired product, but only side-products (Scheme 44). The activated esters **70a-NHS** and **70-pNO2** were then synthesized and reacted with compound **59**, but none of them afforded the desired ester **71**. Using the Yamaguchi's reagent, anhydride **70-TCBC** was synthesized without oxidation of phosphine moiety, but again the coupling with bis-alcohol **59** did not afford the desired bis-ester product.

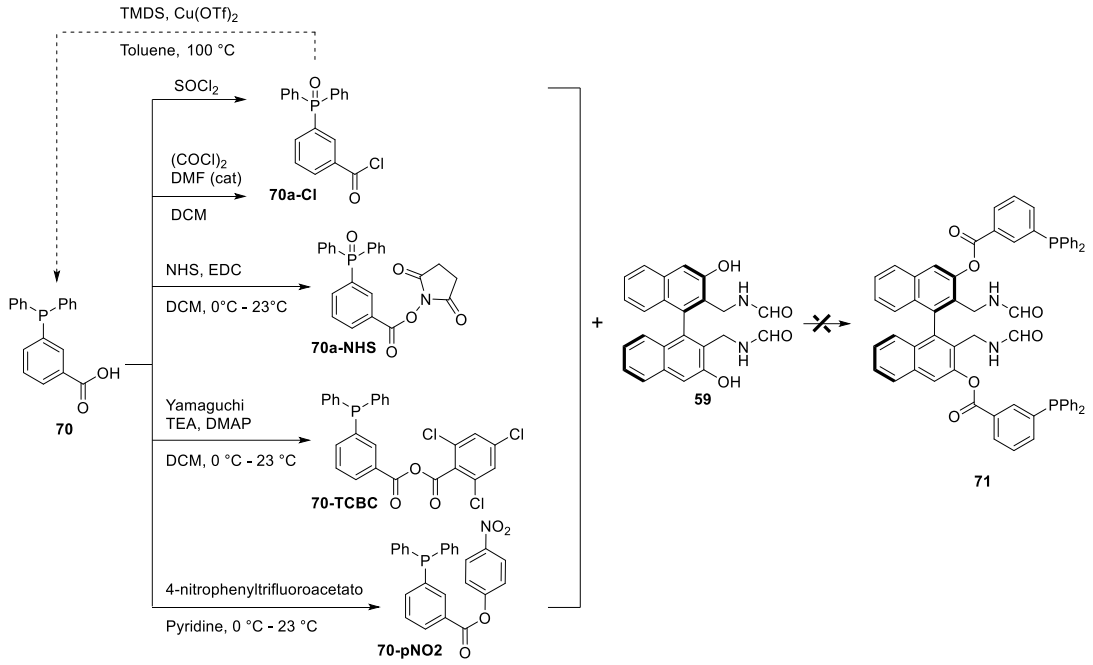

Scheme 44. Unfruitful attempts to prepare bis-formamide **71.**

The direct condensation of free alcohol **59** with phosphine **70** was also tried. Different condensing agents (e.g. DCC, EDC, DIC) were screened, but none of them yielded the desired ester. It was thus decided to replace the ester linkages with ethers. The synthesis of the bis-ether **C** was attempted starting from the bis-isonitrile **74** rather than from bis-formamide **59** (Scheme 45). Synthesis of **74** required some specific precautions. Indeed, dehydration with $POCl_3$ in the presence of free alcohol yielded a stable adduct, which could be hydrolyzed only in basic medium (isonitriles are acid-sensitive). Thus, the desired compound was obtained only in very low yield. We then followed a procedure reported by Bauer *et al.*[105] and involving protection of bis-phenol oxygens as trimethylsilyl ethers followed by dehydration of formamide groups. This reaction yielded the desired product **74** pure enough to proceed in the further steps (Scheme 45).

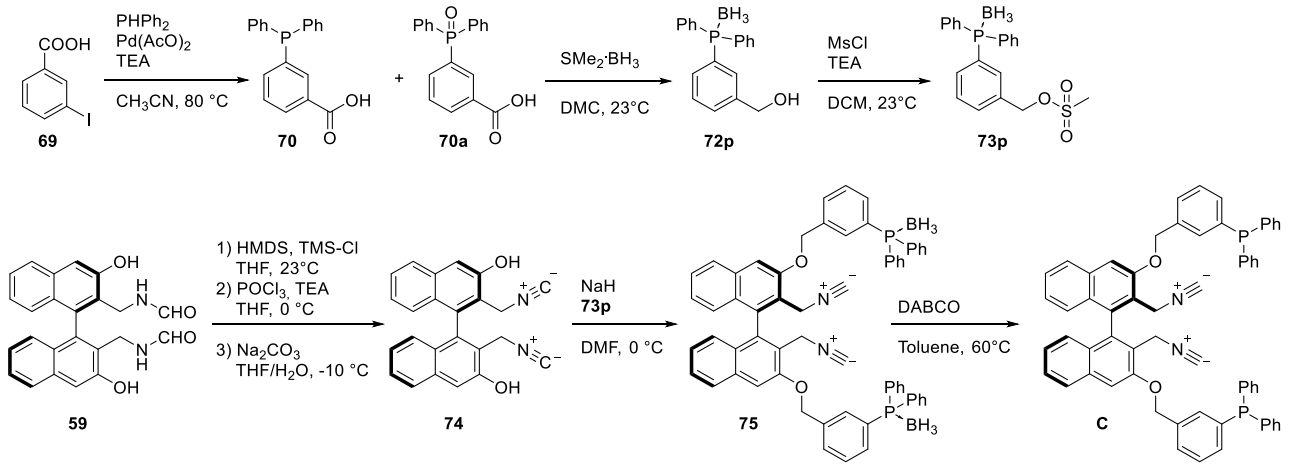

Scheme 45. Synthesis of PCCP ligand **75.**

To avoid the oxidation of the reagent to be used for ether formation, it was protected at phosphorus as a BH_3 complex. Reacting the **70/70a** mixture with borane, carboxy group reduction, phosphine oxide reduction and protection were simultaneously obtained. Benzyl alcohol **72p** was then converted in the corresponding mesylate **73p**.

Using compound **73p**, synthesis of the C_2-symmetric ligand **C** proceeded in a straightforward manner. Bis-isonitrile **74** was coupled under basic conditions with mesylate **73p**. No side products were observed. After deprotection with DABCO and chromatography purification, pure ligand **C** was obtained in 51% of yield (over three steps).
The iron complex $[Fe(\mathbf{C})(CH_3CN)_2](BF_4)_2$ was synthesized from ligand **C** on a small scale. The ESI mass spectrum showed the aqua-adduct at *m/z* 987,2. The ^{1}H-NMR spectrum presents very broad signals, due to the presence of paramagnetic Fe^{II}. In order to better understand the structure of the complex, several crystallization attempts were tried in Leibniz Institute for Catalysis, but it was not possible to grow suitable crystals for XRD. The complex was analyzed by ^{31}P NMR: only one signal was observed, lying in the region typical of metal-bound phosphines. This finding leads to think that both the phosphorus atoms of **C** bind to iron, and the complex is probably C_2-symmetric.

Table 8. Solvent screening in AH of acetophenone promoted by $[Fe(\mathbf{C})(CH_3CN)_2](BF_4)_2$.[a]

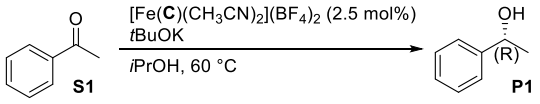

#	Base Loading (mol%)	Time (h)	Conv. (%)[b]	*ee* (%)[b]
1	25	18	4	0
2	25	30	10	0
3	50	18	4	0
4	50	30	35	0

[a] **S1**/Cat./*t*BuOK = 1/0.025/0.25(0.5), Solvent: *i*PrOH, 60 °C, $C_{Sub,0}$ = 0.2 mol L^{-1}; [b] conversion and *ee* determined by GC.

Complex $[Fe(\mathbf{C})(CH_3CN)_2](BF_4)_2$ was tested in the ATH of acetophenone in the presence of *t*BuOK. Unfortunately, the complex showed very poor or no activity: only racemic 1-phenylethanol was obtained with 5% of yield, probably due to the background reaction catalyzed by *t*BuOK itself.

A possible explanation for such low activity is that the isonitrile groups might not coordinate directly the iron center, and thus they would not play the expected role in promoting the transfer hydrogenation.[67] This might be due to the insufficient dimension of the chelate cycle incorporating the two isonitriles. IR-analysis focused at the isonitrile stretching would allow to clarify if there is any coordination of the isonitrile into the iron. Unfortunately, the iron complex and the ligand **C** are not available anymore to perform other investigations. Indeed, the poor results

observed in catalysis do not justify the effort that would be necessary to re-synthesize them. On the contrary, ligand **D** is still interesting because it is able to form a larger chelating cycle, thus ensuring that both isonitrile bind to the Fe-center. Preliminary attempts to prepare ligand **D** have been already done.

3.2 PCCP LIGAND, SECOND GENERATION

The synthetic strategy designed for **C** did not work with **D**. The main issue was found to be the deprotection of the methyl ether group on the 3,3'-position of the binaphthyl scaffold. When the bis-formamide-bis-methoxy derivative **55b** (Scheme 38, pag. 37) was treated with BBr_3, only a very low yield of desired free phenol was obtained. Several side-products were detected, mainly involving a reaction between the formamide moiety and the phenol forming cyclic-derivatives (5 or 6-member rings). Several different conditions were tried, but still the yields were too low to be synthetically meaningful. Hence, a new synthetic strategy was designed (Scheme 46). Notably, the synthetic intermediate **79** also provides access to a PNNP ligand (**F**) which might be tested in catalysis in its own right. The bis-amines **54b** was successfully deprotected, affording the bromide salt **76** in excellent yield. Before carrying out the O-alkylation at the 3,3'-position with phosphine **73p**, the amine moieties of **76** were firstly Boc protected. Under the experimental conditions adopted, both phenol and amine moieties were protected.

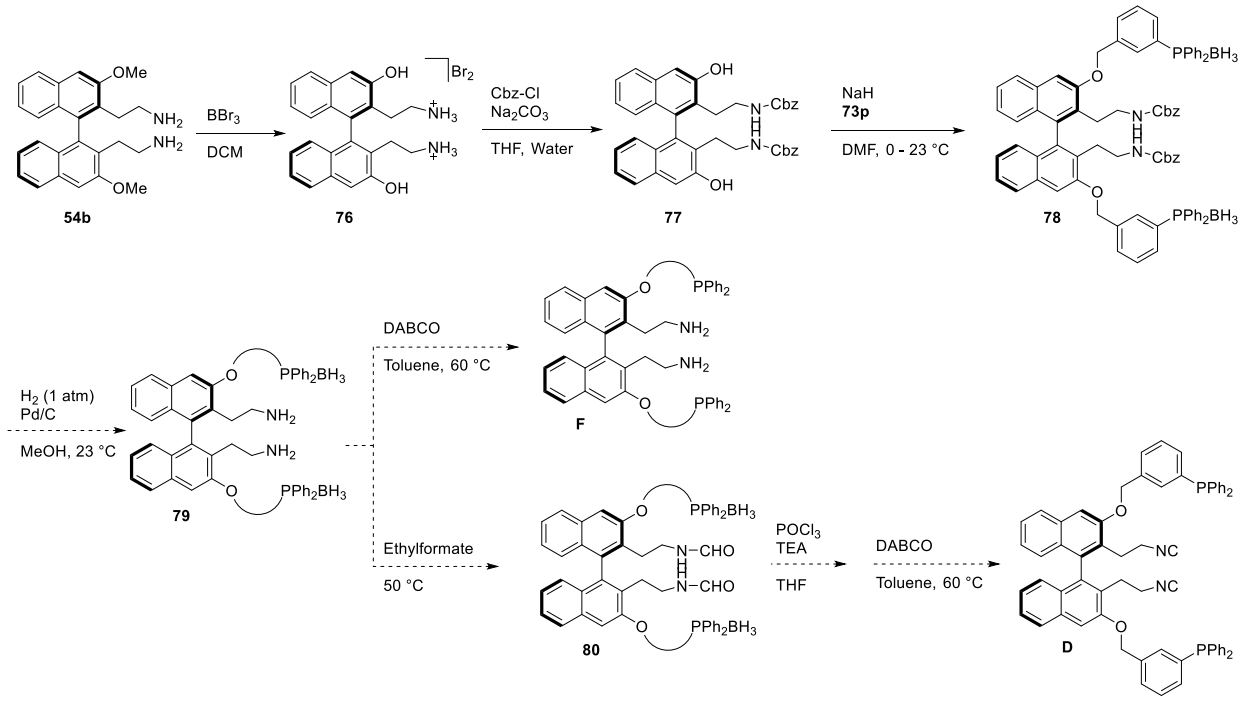

Scheme 46. Synthetic plan of PNNP ligand **F** and PCCP ligand **D.**

Since the stability of the carbamate (N-Boc) and carbonate (O-Boc) should be slightly different, selective deprotection of the phenol moieties was tried. Unfortunately, all attempts were unsuccessful, giving low yields of desired product and a number of byproducts including the fully deprotected bis-phenol-diamine. Thus, the Cbz

protecting group was chosen instead of Boc, and the desired carbamate **77** was selectively formed. Compound **77** was alkylated with **73d**, affording the protected amine-phosphine **78** with 21% yield. Unfortunately, since the amount of **78** available was not sufficient to carry out the synthesis of **F** and **D**, a scale up of the synthesis is currently ongoing.

3.3 Summary of PCCP ligands

Two new ligands combining the π-acceptor properties of the isonitrile groups with the σ-donating ability of phosphine ligands have been designed, i.e. the PCCP ligands **C** and **D** (Figure 22). The two ligands differ in the length of the "arms" bearing the isonitrile group. The linkage between the phosphine moiety and the binaphthyl scaffold was initially planned to be an ester bond, but only an ether linkage was later found to be synthetically accessible. The reaction proceeded in a straightforward manner, affording the deprotected ligand **C** with reasonable yield. The iron complex $[Fe(\mathbf{C})(CH_3CN)_2](BF_4)_2$ was synthesized from ligand **C** on a small scale, and then tested in ATH of acetophenone. Unfortunately, only a small amount of racemic product was obtained from this reaction. The synthesis of ligand **D**, able to bind iron with a larger chelate cycle, and of the related PNNP ligand **F** are currently ongoing.

3.4 Experimental section

General remarks

All reactions were carried out in flame-dried glassware with magnetic stirring under nitrogen atmosphere, unless otherwise stated. The solvents for reactions were distilled over the following drying agents and transferred under nitrogen: CH_2Cl_2 (CaH_2), MeOH (CaH_2), CH_3CN (CaH_2), THF (Na), dioxane (Na), Et_3N (CaH_2). Dry Et_2O, acetone and $CHCl_3$ (over molecular sieves in bottles with crown cap) were purchased from Sigma Aldrich or Across Chemical and stored under nitrogen. The reactions were monitored by analytical thin-layer chromatography (TLC) using silica gel 60 F254 pre-coated glass plates (0.25 mm thickness). Visualization was accomplished by irradiation with a UV lamp and/or staining with a potassium permanganate alkaline or ninhydrin stain solution. Flash column chromatography was performed using silica gel (60 Å, particle size 40-64 μm) as stationary phase, following the procedure by Still and co-workers.[100] ^{1}H-NMR spectra were recorded on a spectrometer operating at 300 MHz, 400.13 MHz and 500 MHz. Proton chemical shifts are reported in ppm (δ) with the solvent reference relative to tetramethylsilane (TMS) employed as the internal standard ($CDCl_3$ δ = 7.26 ppm; CD_2Cl_2 δ = 5.32 ppm; CD_3OD δ = 3.33 ppm). The following abbreviations are used to describe spin multiplicity: *s* = singlet, *d* = doublet, *t* = triplet, *q* = quartet, *m* = multiplet, *br* = broad signal, *dd* = doublet-doublet, *td* = triplet-doublet. ^{13}C-NMR spectra were recorded on a 400 MHz spectrometer operating at 100.56 MHz, with complete proton decoupling. Carbon chemical shifts are

reported in ppm (δ) relative to TMS with the respective solvent resonance as the internal standard ($CDCl_3$ δ = 77.16 ppm; CD_2Cl_2 δ = 54.00 ppm; CD_3OD δ = 49.05 ppm). The coupling constant values are given in Hz.

^{31}P-NMR spectra were recorded on a 400 MHz or 500 MHz spectrometer operating at 161.976 or 202.404 MHz, with complete proton decoupling. Phosphorus chemical shifts are reported in ppm (δ) relative to H_3PO_4.The coupling constant values are given in Hz. Gas chromatography was performed on a GC instrument equipped with a flame ionization detector, using a chiral capillary column. High resolution mass spectra (HRMS) were performed on a Fourier Transform Ion Cyclotron Resonance (FT-ICR) Mass Spectrometer APEX II & Xmass software (Bruker Daltonics) – 4.7 T Magnet (Magnex) equipped with ESI source, available at CIGA (Centro Interdipartimentale Grandi Apparecchiature) c/o Università degli Studi di Milano. Low resolution mass spectra (MS) were acquired either on a Thermo-Finnigan LCQ Advantage mass spectrometer (ESI ion source) or on a VG Autospec M246 spectrometer (FAB ion source).

3.4.1 Synthetic procedure and NMR data of reported compounds.

3-(Diphenylphosphanyl)benzoic acid (70):[103]

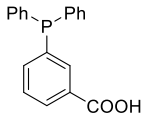

In a dried two necked flask, under argon, 3-iodobenzoic acid (2 g, 8 mmol, 1 eq.) and palladium(II) acetate (4 mg, 0.018 mmol, 0.002 eq.) were dissolved in dry acetonitrile (13 mL). Triethylamine (5 mL, 35.5 mmol, 4.4 eq.) and diphenylphosphine (3.25 mL, 17.74 mmol, 2.2 eq.) were added to the solution, which was brought to reflux and stirred overnight. On the next day, the solution had turned reddish. Volatiles were evaporated under reduced pressure, and the brown-red residue was treated with water (7 mL) and potassium hydroxide (526 mg). The aqueous phase was washed with diethyl ether (3 × 18 mL), acidified with 2 M HCl to pH ~ 3, and extracted with diethyl ether (3 × 15 mL). The combined organic layers were washed with water (13 mL) and then dried over Na_2SO_4. The solvent was then removed under vacuum. Notably, the reaction cannot be followed by TLC because the starting material and the desired product share the same *rf*. A mixture of phosphine oxide **70b** and desired product **70** were obtained.

NMR data must be recorded with CD_2Cl_2, since in $CDCl_3$ spontaneous oxidation of phosphorous was observed.

***70** NMR data:*

^{1}H NMR (400 MHz, CD_2Cl_2) δ 8.04 (ddt, *J* = 11.2, 7.6, 1.6 Hz, 2H), 7.54 (ddt, *J* = 8.1, 6.7, 1.5 Hz, 1H), 7.46 (td, *J* = 7.7, 1.5 Hz, 1H), 7.40-7.30 (m, 9H).^{13}C NMR (101 MHz, CD_2Cl2) δ 170.75, 138.75, 138.58, 135.06, 134.85, 133.83, 133.63, 130.23, 129.04, 128.66, 128.60. ^{31}P NMR (162 MHz, CD_2Cl_2) -4.29.

***70b** NMR data:*

^{1}H NMR (500 MHz, $CDCl_3$) δ 8.55 (dtd, *J* = 12.6, 1.7, 0.7 Hz, 1H), 8.30 (dq, *J* = 7.9, 1.4 Hz, 1H), 7.83 (ddt, *J* = 11.9, 7.8, 1.5 Hz, 1H), 7.74-7.66 (m, 4H), 7.64-7.56 (m, 3H), 7.54-7.49 (m, 4H). ^{31}P NMR (202 MHz, $CDCl_3$) δ 33.82. ^{31}P NMR (162 MHz, CD_2Cl2) δ 27.28.

Methyl 3-(diphenylphosphoryl)benzoate (70a-OMe):

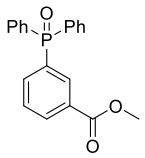

To a stirred solution of **70** and **70b** (1 g, 3.2 mmol, 1 eq.) DCM (15 mL), DIC (473.8 mg, 3.75 mmol, 1.15 eq.) and DMAP (19.9 mg, 0.16 mmol, 0.05 eq.) and dry MeOH (0.145 mL, 3.6 mmol, 1.1 eq.) wer added dropwise at 0 °C. The mixture was stirred overnight at r.t.. On the following day, the crude product was filtered and washed with DCM. Compound **70a-OMe** was purified by flash column chromatography (95:5 → 1:1 hexane/AcOEt) affording 810 mg (2.37 mmol) of a white solid, 74% yield.

^{1}H NMR (500 MHz, $CDCl_3$) δ 8.37 (d, *J* = 12 Hz, 1H), 8.23 (d, *J* = 8 Hz, 1H), 7.93 (t, *J* = 8.5 Hz, 1H), 7.71-7.67 (m, 4H), 7.61-7.57 (m, 3H), 7.52-7.50 (m, 4H), 3.91 (s, 3H). ^{31}P NMR (500 MHz, $CDCl_3$) δ 28.7.

(3-(Diphenylphosphanyl)phenyl)methanol borane complex (72p):[106]

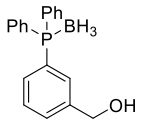

In a Schlenk vessel, BH_3·SMe_2 (2.79 mL, 29.4 mmol, 20 eq.) was added to a solution of the free phosphorus compound **70** (450 mg, 1.47 mmol, 1 eq.) in dry DCM (1 mL). After stirring for 16 h at 50 °C, a saturated aqueous NH_4Cl solution (3 mL) was gently added. The mixture was stirred for 1 h, then poured into water (10 mL), and extracted with DCM (15 mL). The combined organic phase was washed with a saturated aqueous $NaHCO_3$ solution (15 mL), dried over Na_2SO_4, filtered, and concentrated. Filtration over silica gel and elution with DCM (100 mL) yielded the borane adduct in nearly quantitative yield after evaporation and removal of the solvents under high vacuum.

^{1}H NMR (400 MHz, CD_2Cl_2) δ 7.62-7.51 (m, 8H), 7.50-7.42 (m, 6H), 4.67 (s, 2H). ^{31}P NMR (162 MHz, CD_2Cl_2) δ 21.82 (br, coupling with boron).

ESI-MS in CH_3CN: $[M+Na]^+$ *m/z* 390.9.

3-(Diphenylphosphanyl)benzyl methanesulfonate borane complex (73p):

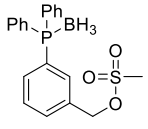

In a Schlenk vessel, the benzyl alcohol derivative **72p** (232 mg, 0.76 mmol, 1 eq.) was combined with dry dichloromethane (3.3 mL) and TEA (222 µL, 1.59 mmol, 2.1 eq.). The mixture was cooled to −10 °C (ice + NaCl), and methanesulfonyl chloride (104 µL, 1.61 mmol, 1.4 eq.) was added to the

mixture while being stirred vigorously. The reaction was monitored by TLC (95:5 DCM/AcOEt). When the starting material disappeared, the reaction mixture was washed with a 0.05 M HCl solution (3 × 10 mL) and a saturated aqueous $NaHCO_3$ solution (3 × 5 mL). The organic layer was dried (Na_2SO_4), filtered and the solvent was removed *in vacuo*. Pure product **73p** was obtained with quantitative yield.

^{1}H NMR (400 MHz, CD_2Cl_2) δ 7.65-7.42 (m, 14H), 5.21 (s, 2H), 0.8-1.7 (bm, 3H). ^{13}C NMR (101 MHz, CD_2Cl_2) δ 135.23 (d, *J*[C,B] = 10.1 Hz) 134.27 (d, *J*[C,B] = 8.8 Hz), 133.59 (d, *J*[C,B] = 9.7 Hz), 133.31 (d, *J*[C,B] = 10.7 Hz), 131.98 (d, *J*[C,B] = 11.6 Hz), 130.88 (d, *J*[C,B] = 57.1 Hz), 129.87 (d, *J*[C,B] = 10.2 Hz), 129.42 (d, *J*[C,B] = 10.2 Hz). ^{31}P NMR (162 MHz, CD_2Cl_2) δ 21.69 (d, 1*J*[P,B] = 62.5 Hz).

ESI-MS in CH_3CN: $[M+Na]^+$ *m/z* 407.12.

(*R*)-2,2'-Bis(isocyanomethyl)-[1,1'-binaphthalene]-3,3'-diol (74):[105]

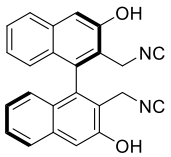

In a Schlenk vessel under argon, bis-formamide **59** (50 mg, 0.125 mmol, 1 eq.) was dissolved in dry THF (0.125 mL) followed by addition of HMDS (44.3 mg, 0.275 mmol, 2.2 eq.) and TMS-Cl (1 drop). The mixture was stirred at 40 °C overnight. The day after, the solution was cooled to -10 °C and dry TEA (87 µl, 0.62 mmol, 5 eq.) was added followed by slow addition of a solution of $POCl_3$ (23 µL, 0.25 mmol, 2 eq.) in dry THF (0.125 mL). The reaction was kept at 0 °C for 2 h and monitored by TLC. The solution was cooled down to -10 °C and 10% w/w of Na_2CO_3 solution was added dropwise. After stirring at r.t. for 10 min, the aqueous layer was extracted with AcOEt (3 × 2 mL, water was added if necessary). The combined organic layers were dried over Na_2SO_4, filtered and concentrated *in vacuo*. Crude product **74** was pure enough to be used in the next step.

^{1}H NMR (400 MHz, CD_2Cl_2) δ 7.82 (d, J = 8.2 Hz, 1H), 7.57-7.39 (m, 2H), 7.17 (dd, J = 8.4, 6.9 Hz, 1H), 7.00 (d, J = 8.5 Hz, 1H), 6.04 (s, 1H), 4.43-4.27 (m, 2H).

(*R*)-((((2,2'-Bis(isocyanomethyl)-[1,1'-binaphthalene]-3,3'-diyl)bis(oxy))bis(methylene))bis(3,1-phenylene))bis(diphenylphosphane) borane complex (75):

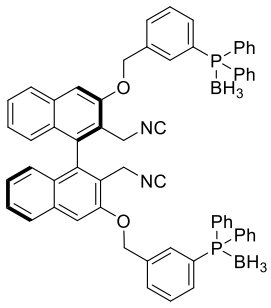

In a Schlenk vessel, under argon, bis-phenol-bis-isonitrile **74** (10 mg, 0.025 mmol, 1 eq.) was dissolved in dry DMF (0.125 mL). The solution was cooled down to 0 °C and NaH (60% in mineral oil, 2.2 mg, 0.056 mmol, 2.2 eq.) was added. The reaction was stirred for 30 minutes at 0 °C. Then 2.2 eq. of compound **73p** (21.5 mg, 0.056 mmol, 2.2 eq.) was dissolved in DMF (0.125) and added slowly to the reaction mixture, which was stirred for 3 hours at r.t.. After addition of AcOEt, the reaction mixture was washed with $NaHCO_3$,

water and brine. The organic phase was dried over Na_2SO_4, filtered and concentrated under reduced pressure. Crude compound **75** product was pure enough to be used in the next step.

^{1}H NMR (400 MHz, $CDCl_3$) δ 7.87-7.78 (m, 3H), 7.67-7.39 (m, 14H), 7.21 (ddd, *J* = 8.3, 6.8, 1.1 Hz, 1H), 7.03 (d, *J* = 8.5 Hz, 1H), 5.40 (s, 2H), 4.36-4.20 (m, 2H). ^{31}P NMR (162 MHz, $CDCl_3$) δ 21.88 (br).

ESI-MS in CH_3CN: $[M+Na]^+$ *m/z* 963.3.

(*R*)-((((2,2'-bis(isocyanomethyl)-[1,1'-binaphthalene]-3,3'- diyl)bis(oxy))bis(methylene))bis(3,1-phenylene))bis(diphenylphosphane) (C):

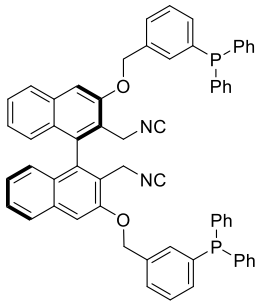

In a Schlenk vessel under argon, compound **75** (62.8 mg, 0.067 mmol, 1 eq.) was dissolved in dry toluene (5 mL). DABCO (22.4 mg, 0.2 mmol, 3 eq.) was added as a solid and the mixture was heated at 60 °C for 2 hours. The reaction was monitored by TLC. When the starting material disappeared, volatiles were removed under vacuum and the crude was purified by flash column chromatography (DCM). Pure compound **C** (33 mg, 0.036 mmol) was obtained in 52% yield.

^{1}H NMR (400 MHz, CD_2Cl_2) δ 7.85 (d, *J* = 8.2 Hz, 1H), 7.61 (d, *J* = 7.6 Hz, 1H), 7.54-7.42 (m, 5H), 7.38-7.25 (m, 13H), 7.21-7.12 (m, 1H), 6.97 (d, *J* = 8.4 Hz, 1H), 5.35 (s, 2H), 4.30-4.17 (m, 2H). ^{31}P NMR (162 MHz, CD_2Cl2) δ -4.28. ^{13}C NMR (101 MHz, CD_2Cl_2) δ 157.14 , 154.63 , 138.70 (d, *J* = 12.4 Hz), 137.76 (dd, *J* = 11.5, 2.5 Hz), 137.37 (d, *J* = 6.3 Hz), 136.88 , 135.43 , 134.42 (d, *J* = 1.4 Hz), 134.23 (d, *J* = 1.3 Hz), 134.04 (d, *J* = 20.4 Hz), 132.99 , 129.50 (d, *J* = 7.2 Hz), 129.41 , 129.15 (d, *J* = 6.9 Hz), 128.36 (d, *J* = 10.6 Hz), 127.67 , 127.05 , 125.57 , 123.37 , 108.72 , 70.91 , 39.42 , 30.30.

ESI-MS in CH_3CN: $[M+Na]^+$ *m/z* 935.0.

Iron Complex $[Fe(\mathbf{C})(CH_3CN)_2](BF_4)_2$:

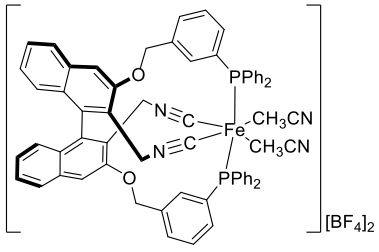

In a Schlenk vessel under argon, a solution of $[Fe(H_2O)_6](BF_4)_2$ (11.6 mg, 0.034 mmol, 1 eq.) in dry CH_3CN (0.92mL) was added dropwise to a solution of ligand **C** (33 mg, 0.036 mmol, 1.05 eq.) in DCM (0.46 mL). After stirring for 2.5 hours at r.t., the solvent was removed under reduced pressure. The resulted reddish complex, was washed with Et_2O (0.3 mL). Yield: 10.5 mg (0.008 mmol, 24%).

^{1}H NMR (400 MHz, CD_2Cl_2, paramagnetic) δ 8.22, 7.97, 7.95, 7.72, 7.64, 7.45, 7.30, 7.23, 7.11, 6.82, 6.79, 6.53, 5.99, 5.96, 5.82, 5.79, 4.67, 4.63, 3.20. ^{31}P NMR (162 MHz, CD_2Cl2) δ 46.94.

ESI-MS in CH_3CN: $[Fe(\mathbf{L})(H_2O)]^+$ *m/z* 987.2; $[Fe(\mathbf{L})]^{2+}$ *m/z* 484.2; $[Fe(\mathbf{L})(H_2O)(CH_3CN)]^+$ *m/z* 1027.28; $\{[Fe(\mathbf{L})(CH_3CN)_2][BF_4]_2+Na\}^+$ *m/z* 1248.7.

2,2'-(3,3'-Dihydroxy-[1,1'-binaphthalene]-2,2'-diyl)bis(ethan-1-aminium) dibromide (76):

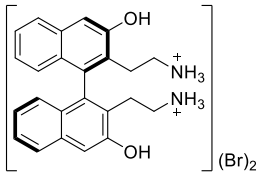

To solution of **54b** (153 mg, 0.38 mmol, 1 eq.) in DCM (2 mL) kept at 0 °C, a BBr_3 solution (1 mol L^{-1} solution, 2.29 mmol, 6 eq.) in DCM was added dropwise. The mixture soon became yellow, and then a white precipitate quickly formed. After 5 h, the unreacted BBr_3 was quenched with 1 mL water. The white-grey solid was filtered on a Buchner and washed with DCM. The desired salt was obtained with 89% yield.

^{1}H NMR (400 MHz, MeOD-δ4) δ 7.78 (d, *J* = 8.2 Hz, 1H), 7.43 (s, 1H), 7.38 (ddd, *J* = 8.1, 6.7, 1.2 Hz, 1H), 7.08 (ddd, *J* = 8.2, 6.8, 1.3 Hz, 1H), 6.92-6.86 (m, 1H), 3.01 (ddt, *J* = 15.5, 12.0, 5.1 Hz, 2H), 2.83-2.60 (m, 2H).

ESI-MS in CH_3CN: $[M]^{2+}$ *m/z* 187.0.

Dibenzyl ((3,3'-dihydroxy-[1,1'-binaphthalene]-2,2'-diyl)bis(ethane-2,1-diyl))dicarbamate (77):

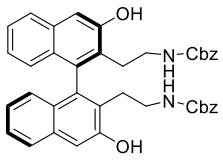

To a solution of **76** (23.9 mg, 0.035 mmol, 1 eq.) kept at 0 °C, in a mixture of water (0.1 mL) and THF (0.1 mL), Na_2CO_3 (30.1 mg, 0.28 mmol, 8 eq.) was added. Benzyl chloroformate, **Cbz-Cl** (10 µL, 0.075 mmol, 2.1 eq.) was added dropwise. The brown suspension was stirred for 30 min at r.t., and the THF was removed *in vacuo*. The brown solution was diluted with water and extracted with AcOEt. The organic phases were combined, washed with brine and dried over Na_2SO_4. The solvent was removed under reduced pressure, and the crude product was used without further purification.

^{1}H NMR (400 MHz, $CDCl_3$) δ 7.77 (d, *J* = 8.3 Hz, 1H), 7.49-7.30 (m, 8H), 7.03 (t, *J* = 7.5 Hz, 1H), 6.92 (d, *J* = 8.4 Hz, 1H), 5.12 (s, 2H), 4.92 (s, 1H), 3.22-3.01 (m, 1H), 2.85 (s, 1H), 2.76-2.65 (m, 1H), 2.59 (d, *J* = 14.5 Hz, 1H).

ESI-MS in CH_3CN: $[M+Na+H]^+$ *m/z* 664.61.

Dibenzyl ((3,3'-bis((3-(diphenylphosphanyl)benzyl)oxy)-[1,1'-binaphthalene]-2,2'-diyl)bis(ethane-2,1-diyl))dicarbamate borane complex (78):

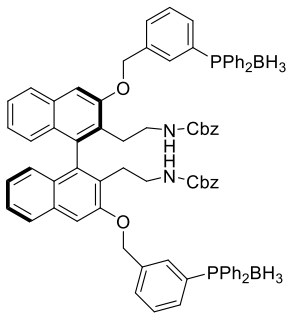

In a Schlenk vessel, compound **77** (22.4 mg, 0.035 mmol, 1 eq.) was dissolved i dry DMF (0.125 mL). The solution was cooled down to 0 °C and NaH (60% dispersed in mineral oil, 3.1 mg, 0.067 mmol, 2.2 eq.) was added. The mixture was stirred for 30 minutes at 0 °C and then the borane-protected-mesyl-derivative **73p** (29.6 mg, 0.077 mmol, 2.2 eq.) dissolved in DMF (0.125) was added slowly. The mixture was allowed to slowly reach r.t., and the reaction was monitored by TLC. Then AcOEt was added to the reaction mixture and the solution was washed with saturated solution of $NaHCO_3$, water and brine. The organic phase was dried over Na_2SO_4, filtered and concentrated under reduced pressure. The desired product **78** (9 mg, 0.007 mmol) was obtained with 21% yield.

^{1}H NMR (400 MHz, CD_2Cl_2) δ 7.82-7.60 (m, 2H), 7.56-7.23 (m, 18H), 7.15 (s, 2H), 7.07 (s, 2H), 6.94 (t, *J* = 7.5 Hz, 1H), 6.78 (d, *J* = 8.4 Hz, 1H), 4.73 (s, 2H), 4.65-4.47 (m, 2H), 3.09-2.85 (m, 1H), 2.69-2.55 (m, 1H), 2.40 (dd, *J* = 13.0, 6.7 Hz, 1H), 1.54-0.76 (m, 3H). ^{13}C NMR (101 MHz, CD_2Cl_2) δ 155.97 (d, *J* = 57.5 Hz), 138.01 (d, *J* = 89.1 Hz), 133.69 (d, *J* = 9.3 Hz), 133.25 , 132.69 , 132.22 (d, *J* = 10.2 Hz), 131.94 , 131.74 (d, *J* = 10.6 Hz), 130.88 , 130.35 , 129.79 (d, *J* = 10.0 Hz), 129.40 (d, *J* = 9.7 Hz), 128.86 , 128.32 , 127.41 , 126.76 , 124.80 , 107.33 , 70.05 , 66.50 , 65.01 , 40.65 , 30.05 .

ESI-MS in MeOH: $[M+Na+MeOH]^{2+}$ *m/z* 635.17; $[M+Na]^+$ *m/z* 1239.22.

3.4.2 General Procedure for Asymmetric Transfer Hydrogenation

In a Schlenk vessel, the iron complex (0.025 eq.) and *t*BuOK (2.9 mg, 0.026 mmol, 0.25 eq.) were added as solid in the empty flask. 3 vacuum-argon cycles were made, and then dry *i*PrOH (0.4 mL) and acetophenone (12 μL, 0.1 mmol, 1 eq.) were added. The mixture was stirred overnight at 60 °C. The day after, a reaction crop was diluted in DCM and the conversion and *ee* were determined by GC-analysis.

GC-Analysis:

(*S*)-1-Phenylethanol[80]

Capillary column: MEGADEX DACTBSβ, diacetyl-*tert*-butylsilyl-β-cyclodextrin, 0.25 μm; diameter = 0.25 mm; length = 25 m; carrier: hydrogen; inlet pressure: 1 bar; oven temperature: 95 °C for 20 min: $t_{\mathbf{S1}}$ = 6.0 min; $t_{(R)\text{-}\mathbf{P1}}$ = 13.8 min; $t_{(S)\text{-}\mathbf{P1}}$ = 14.8 min.

CHAPTER 4

A NEW (CYCLOPENTADIENONE)IRON PRE-CATALYST

Very early during their development, (cyclopentadienone)iron complexes were shown to be readily tunable: several modifications on their structure were made even before their catalytic applications became known.[69,70] Later on, structural modifications of these complex were introduced with the aim to achieve specific catalytic properties, such as enhanced activity or enantioselectivity (by means of chiral complexes).

The first and perhaps most obvious approach was the replacement of carbonyl(s) with other type of ligands (Figure 23, A). Nitriles[71,107], pyridines,[108] NHCs,[109] phosphines,[70b] and chiral phosphoramidites[110] have been already used as potential candidates for replacing the carbonyl group. Another approach consisted in the modification of the cyclopentadienone ring. Positions 2,5[111] and 3,4[75g-h, 79, 80, 110a] can be differently functionalized affording new cyclopentadienone catalysts/complexes (Figure 23, B). According to the latter approach, the synthesis of [bis(hexamethylene)cyclopentadienone]iron tricarbonyl **81** – bearing modifications at both the 2,3 and the 4,5 positions of cyclopentadienone ring – was carried out.[112]

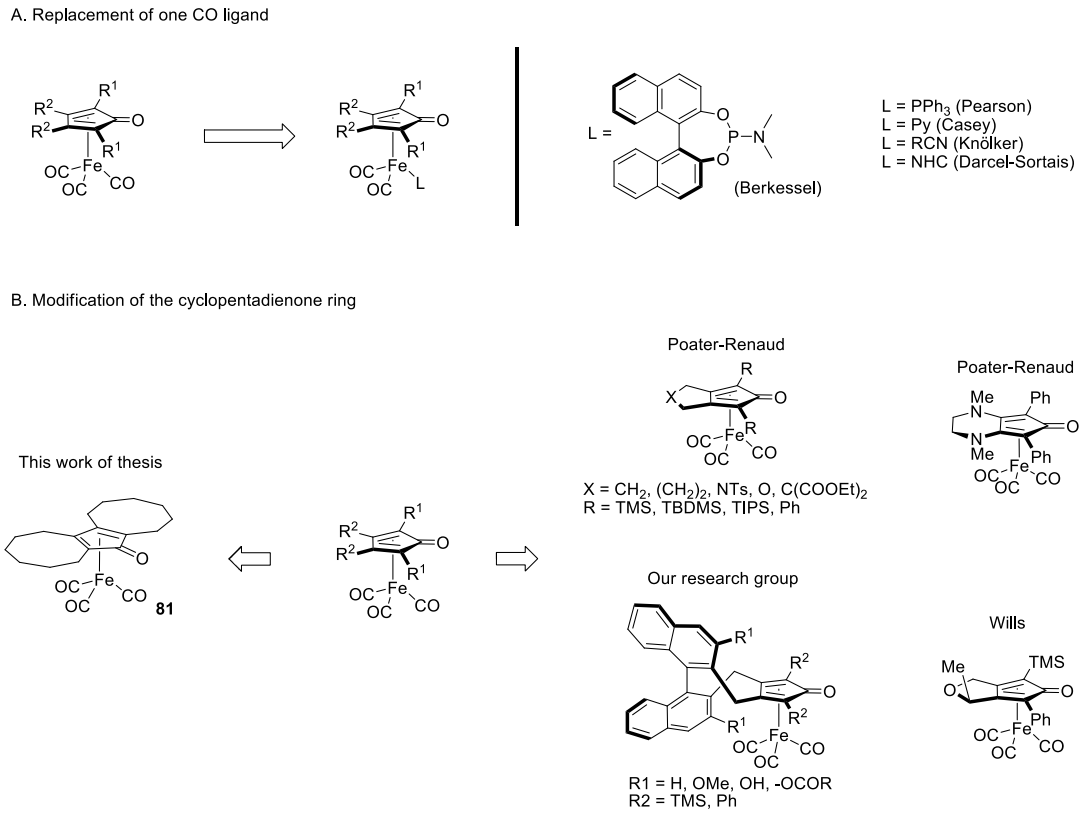

Figure 23. Examples of structural variation of (cyclopentadienone)iron complexes, and the new [bis(hexamethylene) cyclopentadienone] iron complex **81.**

4.1 Synthesis of [bis(hexamethylene)cyclopentadienone]iron complex **81**

The most commonly used strategy for the synthesis of (cyclopentadienone)iron complexes involves a tethered cyclative carboxylation of diynes with a large excess of an iron carbonyl complex [e.g. $Fe(CO)_5$ or $Fe_2(CO)_9$]. This one-pot reaction affords the half-sandwich iron tricarbonyl complex. Since $Fe(CO)_5$ is inexpensive, its use in large excess is still acceptable. This approach involves a significant effort to prepare a diyne precursor with the proper functionalization, which somehow limits the possibility to tune the substitution pattern at the cyclopentadienone ring. In principle, starting from two distinct alkynes an intermolecular cyclative carbonylation/complexation could be used to synthesize a functionalized (cyclopentadienone)iron complex. The latter strategy has been shown to give acceptable results only with alkynes bearing very specific type of substituents such as silyl groups,[69] -Cl, -CF_3 and -O*t*Bu. [113] Notably, with common alkynes (e.g. phenylacetylene, diphenylacetylene) the desired (cyclopentadienone)iron complexes were obtained only with very low yield.[114]

Cyclooctyne **85** is the smallest isolated cyclic alkyne. Due to the strain in its structure, it is known to be very reactive and to undergo a relatively fast degradation (it survives a few days at -19 °C). For this reason, **85** is not commercially available, although it can be easily synthesized from a relatively cheap *cis*-ciclooctene **82** as reported by Brandsma and Verkruijsse in 1978.[115]

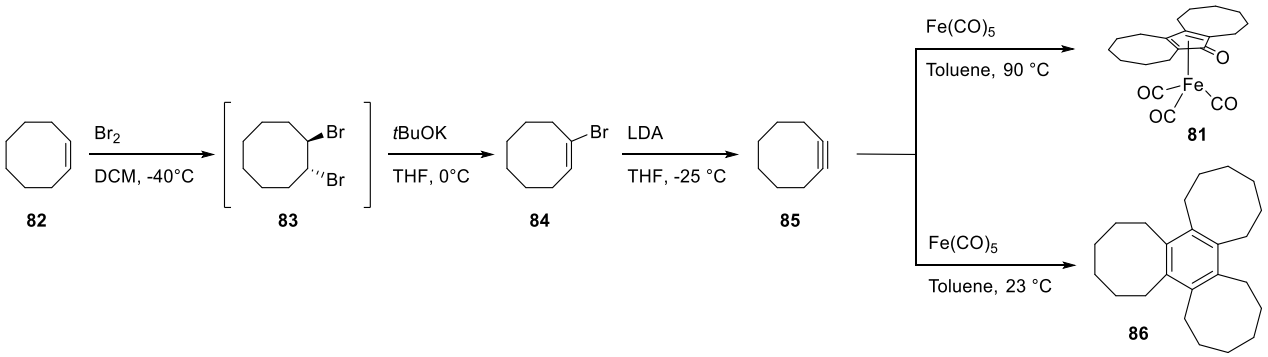

82 83 84 85 81 86

Scheme 47. Synthesis of [bis(hexamethylene)cyclopentadienone]iron complex **81** from *cis*-cyclooctene **82.**

Bromination with Br_2 affords *trans*-1,2-dibromocicloocatane **83,** which undergoes two elimination steps. The first equivalent of HBr is released using *t*BuOK, affording 1-bromocyclooctene **84** with 80% yield. The second elimination step requires a stronger base: LDA. Notably, the original paper reports a 1:2 LDA:**84** ratio,[115] giving **85** with 80% of yield (based on LDA, limiting reagent). However, we were able to achieve 86% yield using a 1:1 ratio LDA:**84**.

According to the literature,[116] the combination of cyclooctyne **85** with nickel, tungsten, cobalt and iron carbonyl complexes produce several products. Among them, using $Fe(CO)_5$ substantial amounts of tris(hexamethylene) benzene **86** (derived from cyclotrimerization) and minor quantities of the [bis(hexamethylene)cyclopentadienone] iron complex **81** were formed. The reaction was investigated and temperature turned out to be a key issue. Indeed, running the cyclative carbonylation at r.t. or 90 °C could change the product distribution. At lower temperature, the benzene derivative **86** was obtained as the major product, whereas at higher temperature (i.e. 90 °C) the iron complex **81** was formed with respectable yield (56%).

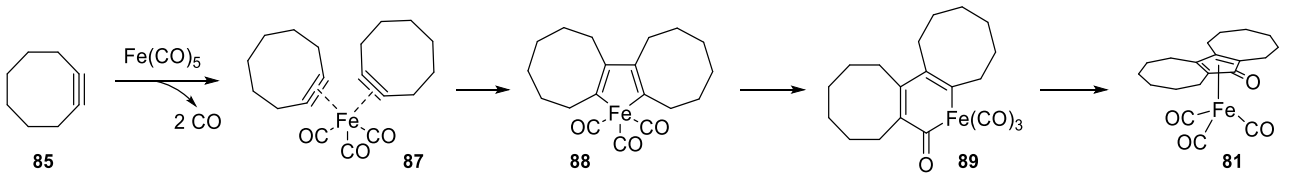

Scheme 48. Proposed mechanism for the formation of complex **81.**

The proposed mechanism for the formation of **81** (Scheme 48) consists of a stepwise iron-mediated [2+2+1] cycloaddition which is initiated by the sequential replacement of two carbon monoxides by the two alkyne molecules, thus generating the tricarbonyl[bis-η^2-alkyne] iron complex **87**. At this stage, Fe^0 promotes the oxidative coupling of the two bound alkynes to form the intermediate ferrocyclopentadiene structure **88**. Insertion of a molecule of carbon monoxide into the iron-carbon bond followed by a subsequent rearrangement of the ferrohexadienone **89** affords the tricarbonyliron-complexed cyclopentadienone **81**. The driving force guiding the cyclative carbonylation/complexation process is probably the release of strain present in the cyclooctyne ring. Indeed, cyclododecyne **90**, which has a less strained ring than **85**, forms the related complex **91** only with 5% of yield (under the same cyclative carbonylation/complexation condition). Notably that, no improvements were achieved changing temperature or solvents (e.g. toluene, xylene).

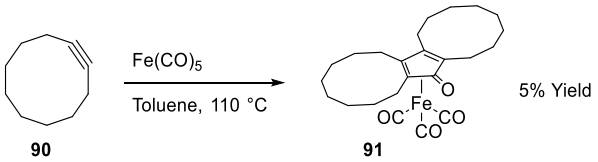

Scheme 49. Synthesis of [bis(decamethylene)cyclopentadienone]iron complex **91.**

[Bis(hexamethylene)cyclopentadienone]iron complex **81** was thoroughly characterized spectroscopically, and crystals suitable for X-ray diffraction analysis could be grown by cooling a saturated solution of the **81** in *n*-hexane/DCM. The X-ray structure reveals the usual piano-stool geometry with a significant deviation from planarity of the cyclopentadienone ring.

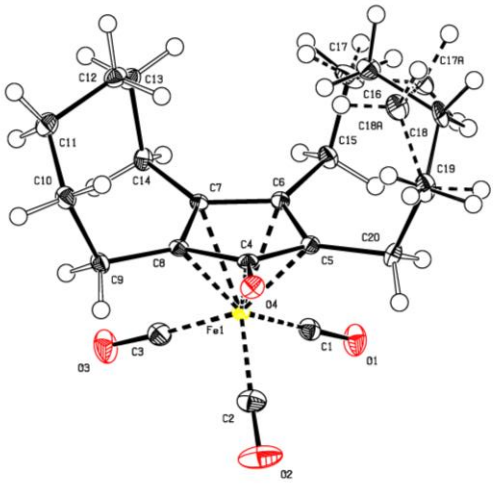

Figure 24. X-ray structure of [bis(hexamethylene)cyclopentadienone]iron complex **81.**

4.2 Aldehyde, Ketone and Ester Hydrogenation

(Cyclopentadienone)iron complex **81** was tested in the hydrogenation of acetophenone after *in situ* activation, showing good conversions at 10 and 30 bar of hydrogen pressure (Table 9).

Table 9. Hydrogenation of acetophenone promoted by pre-catalyst **81**.[a]

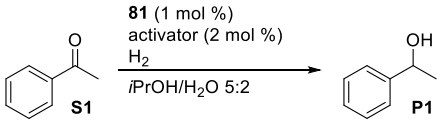

#	Activator	p H_2 (atm)	Temperature (°C)	Conversion (%) [b]
1	K_2CO_3	10	70	< 5
2	hν[c]	10	40	>99
3	Me_3NO	10	70	52
4	K_2CO_3	30	70	51
5	Me_3NO	30	70	>99

[a] Reaction conditions: **S1**/**81**/activator = 100:1:2, solvent: 5:2 *i*PrOH/ H_2O, $C_{0,S}$ = 1.43 mol L^{-1}, reaction time = 16 h ; [b] Determined by using GC ; [c] Reaction vessel irradiated at λ_{max} = 352 nm and 8 W; solvent: toluene.

Firstly, we screened different protocols for the *in situ* activation of pre-catalyst **81**. Use of K_2CO_3 (*in situ* Hieber reaction)[71] only led to a moderate conversion (Table 9, entry 1). However, other activation strategies (entries 2–3) gave better results: UV photolysis of a CO ligand[77] led to full conversion, and oxidative cleavage with Me_3NO[75] allowed to obtain 52% conversion. Increasing the P_{H2} to 30 bar allowed us to reach 51% conversion in the presence of K_2CO_3 (entry 4) and full conversion with Me_3NO (entry 5).

As the equipment to perform pressure hydrogenation under UV irradiation is not readily available in any lab/company, we decided to perform the reaction scope evaluation using the activation protocol involving Me_3NO. As shown in Table 10, several different ketones were tested: a wide number of 4-, 3- and 2-substituted acetophenone, regardless of EWG or EDG property of the substituents, were fully hydrogenated (entries 1-7, 9-11, 14-19). In particular, nitro and halogen groups were tolerated (entries 2, 4 and 6). Notably, 2-acetylpyridine (entry 7) was fully hydrogenated despite the presence of a coordinating atom, which in principle might poison the catalyst. Hindered α-tetralone was the only ketone which was only partially reduced (entry 8). With aliphatic ketones (entries 9-10) excellent conversions were also observed. The α,β-unsaturated ketone **S11** (entry 11) was fully converted to a 1:1 mixture of 4-phenyl-3-buten-2-ol **P11** (C=O reduction) and 4-phenylbutan-2-ol **P11b** (reduction of both C=O and C=C). In a control experiment (entry 12), reduction of 4-phenyl-3-buten-2-ol **S12** did not afford 4-phenylbutan-2-ol, which leads to conclude that the reduction of both the C=O and the C=C bond (shown in entry 11) took place following a 1,4-reduction pathway. Instead, with a hindered cyclic α,β-unsaturated ketone such as isophorone (entry 13), only the C=O group was reduced in low yield. All tested aldehydes (entries 15-18) were hydrogenated quantitively. Notably, in the case of cinnamaldehyde full conversion was achieved with only 5% of over-hydrogenated product (i.e., 4-phenylbutanol). The latter byproduct is probably obtained through a 1,4-reduction pathway that, due to the higher reactivity of aldehydes compared to ketones, competes with the 1,2-reduction pathway less efficiently than in the case of isophorone reduction (entry 13). As the classical cyclopentadienone **30**,[93] also pre-catalyst **81** can fully hydrogenate activated esters (entry 19). An amide substrate (phenyl acetamide **S20**) was also tested and, in accordance with the usual activity of Knölker-type complexes,[68,117] no conversion was observed.

Table 10. Substrate screening for C=O hydrogenation in the presence of pre-catalyst **81.**[a]

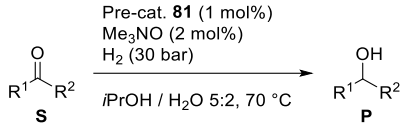

#	Substrate		Conversion [%][b]	#	Substrate		Conversion [%][b]
1	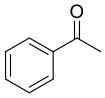	**S1**	> 99 (98)[c]	11	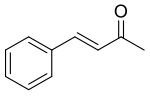	**S11**	> 99[c]
2	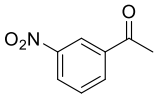	**S2**	> 99	12	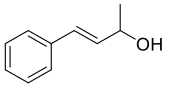	**S12**	0
3	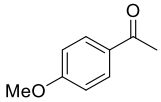	**S3**	> 99 (98)[c]	13	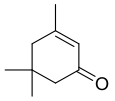	**S13**	15
4	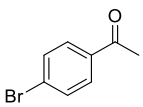	**S4**	> 99 (98)[c]	14		**S14**	> 99 *cis:trans* = 60:40

5	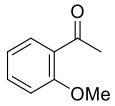	**S5**	> 99	15	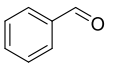	**S15**	> 99 (94)[c]
6	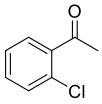	**S6**	> 99	16	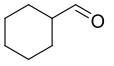	**S16**	> 99 (86)[c]
7	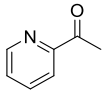	**S7**	> 99	17	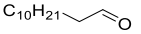	**S17**	> 99
8	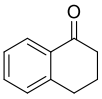	**S8**	80	18	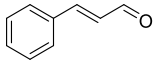	**S18**	> 99[d]
9	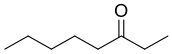	**S9**	> 99	19	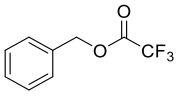	**S19**	99
10		**S10**	> 99	20	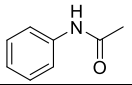	**S20**	0

[a] Reaction conditions: S/**81**/Me_3NO = 100:1:2, p_{H2} = 30 bar, solvent: 5:2 *i*PrOH/H_2O, $C_{0,sub.}$ = 1.43 mol L^{-1}, T = 70 °C, reaction time = 16 h; [b] Determined by GC or ^{1}H-NMR of the crude reaction mixture; [c] In brackets, isolated yields of 2 mmol-scale reactions; [d] 1:1 4-phenyl-3-buten-2-ol / 4-phenylbutan-2-ol; [e] 95:5 cinnamyl alcohol / 3-phenyl-1-propanol.

Performances of the 'Knölker complex' **30** and of [bis(hexamethylene)cyclopentadienone]iron complex **81** were compared at decreased the catalyst loading (0.1 mol%). Remarkably, the cyclooctyne-derived pre-catalyst **81** showed higher activity than **30** (Table 11), with a TON 5 times higher than that of complex **30**. This evidence justified a deeper investigation of the kinetic properties of complex **81**. The kinetics of acetophenone hydrogenation promoted by pre-catalysts **30** and **81** (after activation with Me_3NO) were studied. Using a computer-controlled Parr autoclave system, from the hydrogen uptake conversions *vs.* time were measured (Figure 25).

Table 11. Comparison of Knölker catalyst **30** and **81** in the hydrogenation of acetophenone.[a]

#	Catalyst	Conversion (%)[b]	TON	TOF (h^{-1})
1	**30**	13	130	7.5
2	**81**	62	620	35.9

[a] Reaction conditions: S1/**Cat**/Me_3NO = 100:0.1:0.2, solvent: 5:2 *i*PrOH/H_2O, $C_{0,s}$ = 1.43 mol L^{-1}, p_{H2} = 30 bar, T = 70 °C, reaction time = 17h; [b] Determined by using GC.

The plot conversion *vs.* time of Figure 25 shows in the initial part (t < 23 min) that complexes **30-*act*** and **81-*act*** formed *in situ* possess similar activities with pseudo-first-order kinetic profiles (Table 12). Indeed, the two curves are practically superimposable. However, after approximately 23 min, the two catalysts started to behave very differently: although **81-*act*** continued to follow pseudo-first-order kinetics (Figure 25, green diamonds), the catalyzed **30-*act*** reaction slowed down (Figure 25, blue square) and then proceeded until completion at a reduced rate.

Table 12. Kinetic parameters of the hydrogenation of acetophenone in the presence of **30** and **81**.[a,b]

#	Pre-Catalyst	k_{app} (min^{-1})[c]	$t_{1/2}$ (min)	k ($L\ mol^{-1}\ min^{-1}$)[c]
1	**30**	0.042	16.3	8.5
2	**81**	0.034	20.5	6.8

[a] **S1**/Pre-catalyst/Me_3NO = 100:1:2; solvent: 5:2 *i*PrOH/H_2O; $C_{0,\ Sub.}$ = 0.501 mol L^{-1}; p_{H2} = 30 bar; T= 70 °C; C_{cat} = 5 mmol L^{-1}. [b] Kinetic parameters calculated for the following time/conversion intervals: 1–23 min (1–63% conversion) for **30**, 3–57 min (1–83% conversion) for **81**. [c] $k_{app} = k_{Ccat}$.

These findings seem to suggest that the "classical" **30**-derived catalyst undergoes quite a fast decomposition so that most of it is transformed into a less active or inactive species before the hydrogenation of acetophenone is complete.[118] Conversely, the catalyst derived from **81** seems to be more robust and does not undergo substantial decomposition before the hydrogenation is finished (see decomposition pathway Scheme 50). The lower stability of catalyst **30-*act*/30** compared to **81-*act*/81** would also explain the lower TON, TOF and conversion obtained with **30** and **81** at 0.1 mol% catalytic loading (Table 11).

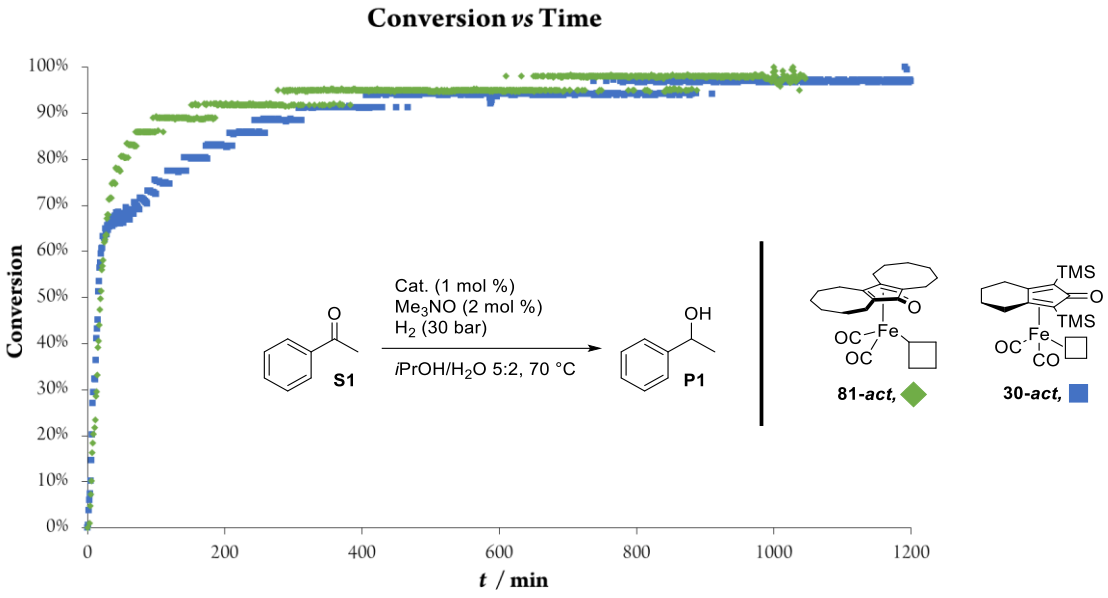

Figure 25. Kinetics of acetophenone hydrogenation promoted by **30** (■) and **81**(◆) activated with Me_3NO. Reaction conditions: **S1**/pre-catalyst/Me_3NO=100:1:2; solvent: 5:2 *i*PrOH/H_2O; $C_{0,\ Sub.}$ = 0.501 mol L^{-1}; p_{H2} =30 bar; T = 70 °C; $C_{cat.}$=5 mmol L^{-1}.

The catalytic cycle proposed for the (cyclopentadienone)iron like complexes is the one proposed by Casey (Scheme 50).[119,77b,108] Initially, the stable complex **81** is activated *in situ* by reaction with Me_3NO releasing CO_2 and trimethylamine. The obtained complex **81-*act*** then reacts with the reductant (either H_2 or *i*PrOH) generating the

(hydroxycyclopentadienyl)iron complex **81.3**. The latter reacts with the substrate through the concerted pericyclic transition state **81.4**, re-generating the catalytic complex **81-*act*** together with the reaction product.

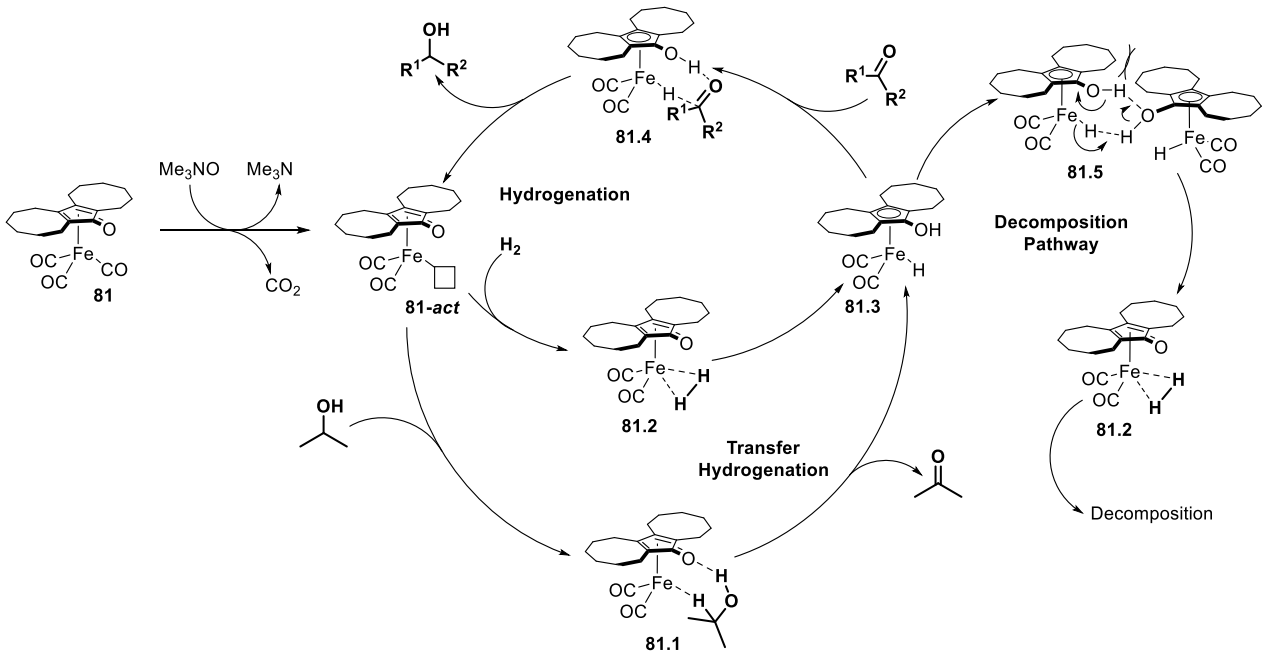

Scheme 50. Proposed mechanisms involved **81** in ketone hydrogenation, transfer hydrogenation and catalyst decomposition pathway.

On the basis of the catalytic cycle shown above (Scheme 50), catalyst **81-*act*** was also expected to promote the transfer hydrogenation of ketones in the presence of *i*PrOH. Again, complexes **30** and **81** were directly compared under the same reaction conditions. As it was expected, [bis(hexamethylene)cyclopentadienone] iron complex **81** was found active in transfer hydrogenation of acetophenone, and it showed better performance than **30** (Table 13).

Table 13. Transfer hydrogenation of acetophenone with *i*PrOH in the presence of pre-catalysts **30** and **81**.[a]

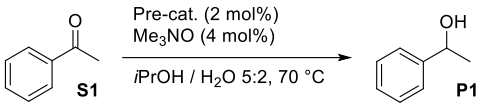

#	Pre-cat.	Conv. [%][b]
1	**30**	34
2	**81**	90

[a] **S1**/Pre-cat./Me_3NO = 100:2:4, $C_{0,\,Sub.}$ = 0.7 mol L^{-1}, T = 70 °C, 17 h, solvent: 5:2 *i*PrOH/H_2O; [b] Determined by GC.

4.3 Transfer Hydrogenation of Imines with Cyclooctyne-derived Iron Complex

Encouraged by the results obtained in the reduction of ketones, we tested the new pre-catalyst **81** also in the reduction of imines to amines. Indeed, from an industrial point of view catalytic hydrogenation (CH)[120] and catalytic transfer hydrogenation (CTH)[121] can be considered a very attractive way to prepare this important class of products, commonly used in the synthesis of bioactive compounds, dyes, fibers and materials.[122] In most instances noble metal catalysts are employed, but in recent years cost and toxicity issues have stimulated the investigation of base metal catalysis[61] in general, and iron catalysis[123] in particular. While several Fe-catalysts for the hydrogenation of imines/iminium ions,[124,125] to amines have been developed, quite surprisingly, the number of iron catalysts reported for the CTH of imines is very limited (see Chapter 1.5 and Scheme 51).[126]

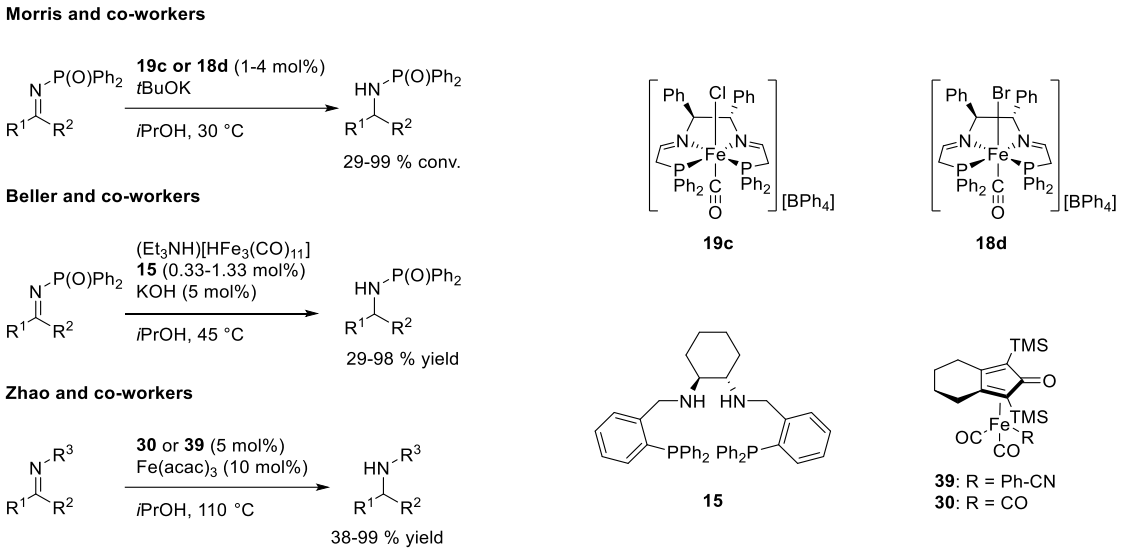

Scheme 51. State of the art in iron catalyzed transfer hydrogenation of imines.

Thus, in a preliminary experiment, complex **81**, recently developed,[112] and the classical 'Knölker complex' **30**[69a] were tested in the CTH of *N*-(1-phenylethylidene)-*p*-anisidine **S21** (Scheme 51).

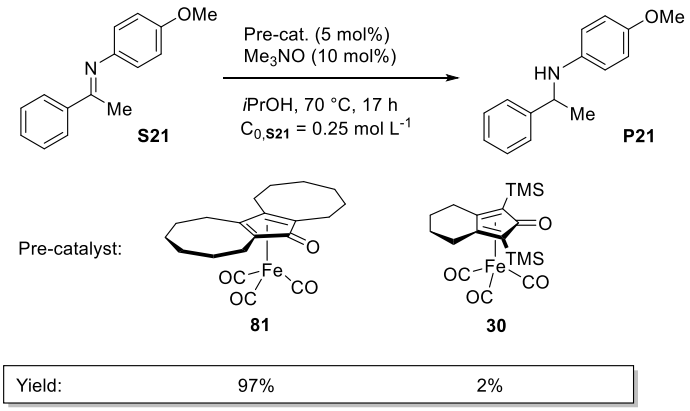

Scheme 52. Preliminary tests of pre-catalysts **81** and 30 in the CTH of a ketimine.

As in ketone hydrogenation (see Paragraph 4.2), the pre-catalytic complexes **81** and **30** were activated by reaction with Me_3NO.[75] This activation step was found to be delicate and crucial to achieve reproducibility. Under optimized conditions, the pre-catalyst was dissolved in *i*PrOH ($C_{pre\text{-}cat.}$ = 0.1 M or higher) and reacted with Me_3NO for 20 min at r.t., before adding the substrate and heating. The catalyst derived from **81** was found to be much more active than the one derived from **30** (97% *vs.* 2% yield, Scheme 52). This difference in activity is remarkable, and more pronounced than that observed in ketone CH and CTH (see Paragraph 4.2).[112] Moreover, these results confirm what reported by Zhao *et al.* for pre-catalyst **39** (precursor of the same catalytic species as pre-catalyst **30**), which is able to promote ketimine CTH only in the presence of a substantial amount of Lewis acid.[126a] To investigate further the applicability of **81** in the reduction of ketimine **S21**, different hydrogen donors were also tested (Table 14).

Table 14. Reduction of *N*-(1-phenylethylidene)-p-anisidine **S21** promoted by pre-catalysts **81**.[a]

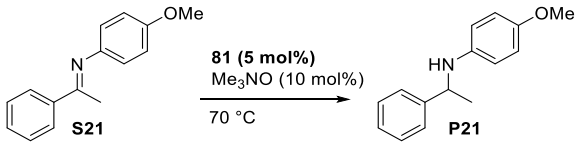

#	Hydrogen donor	Cat. Loading (mol%)	Conc. (mol L^{-1})	Solvent	Conv. (%)[b]
1	H_2 (20 atm)	10	0.5	Toluene	98
2	H_2 (20 atm)	10	0.5	MeOH	>99
3	H_2 (20 atm)	5	0.5	Toluene	22
4	H_2 (20 atm)	5	0.5	MeOH	60
5	FA/TEA[c]	5	0.5		38
6	*i*PrOH	5	0.5	*i*PrOH	70

[a] **S21**/**81**/Me_3NO = 100:5:10, T = 70 °C, 17 h; [b] Determined by ^{1}H-NMR of the crude reaction mixture; [c] Formic Acid/Triethylamine 5:2.

As expected, pre-catalyst **81** promoted the hydrogenation of **S21** with excellent yield in MeOH and a catalyst loading of 10%. However, decreasing the loading strongly affected the yield. With 5 mol% of catalyst loading, using the formic acid/triethylamine azeotrope as hydrogen donor, transfer hydrogenation of **S21** took place with a reasonable yield. Switching to *i*PrOH, the yield of the desired amine rose to 70%. Encouraged by the promising results obtained with pre-catalyst **81**, we set to optimize the reaction conditions using two different model substrates, i.e. ketimine **S21** and aldimine **S22**. Catalyst loading, concentration and temperature were varied as shown in Table 15. Conversions were determined by ^{1}H NMR analysis of the crude reaction mixtures.

Table 15. Reduction of benchmark imines promoted by pre-catalysts **81**.[a]

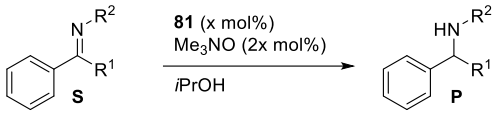

21: R^1 = Me, R^2 = 4-MeO-Ph
22: R^1 = H, R^2 = Ph

#	Sub	Loading (mol%)	[Substrate] (mol L^{-1})	Conv.[b] (%)
1	**S21**	5	0.40	72
2	**S21**	5	0.25	97
3	**S21**	5	0.13	89
4	**S21**	2	0.40	71
5	**S21**	2	0.25	>99
6	**S21**	1	0.25	8
7	**S21**	1	0.25	98[c]
8	**S21**	0.5	0.25	4
9	**S21**	0.5	0.25	95[c]
10	**S21**	0.1	0.25	0[c]
11	**S22**	5	0.40	>99
12	**S22**	5	0.25	>99
13	**S22**	5	0.13	>99
14	**S22**	2	0.40	90
15	**S22**	2	0.25	>99
16	**S22**	1	0.25	74
17	**S22**	1	0.25	>99[c]
18	**S22**	0.5	0.25	28
19	**S22**	0.5	0.25	>99[c]
20	**S22**	0.1	0.25	17[c]

[a] Reaction conditions: **81**/Me_3NO = 1:2, T = 70 °C, 18 h, solvent: *i*PrOH.
[b] Determined by ^{1}H-NMR of the crude reaction mixture.
[c] Reaction run at 100 °C.

With ketoimine **S21**, the initial substrate concentration ($C_{0,sub.}$) strongly affected the conversion, and 0.25 M was found to be the optimal value (Table 15, entry 2 *vs.* entries 1 and 3). Lowering the catalyst loading to 2 mol% did not impact on conversion (Table 15, entries 4-5), whereas at 1 mol% and at 0.5 mol% the reaction became slow (Table

15, entries 6 and 8). However, when the latter experiments were run at higher temperature (100 °C, Table 15, entries 7 and 9) high conversions were restored (TON up to 190). When the catalyst loading was further lowered to 0.1 mol%, no conversion was observed. As expected, aldimine **S22** was found more reactive than ketimine **S21**, giving full conversion with 5 mol% catalyst loading, irrespective of $C_{0,sub.}$ (Table 15, entries 10-12). Experiments run at 2 mol% confirmed that 0.25 M is the optimal $C_{0,sub.}$ value (Table 15, entries 14 *vs.* 15).

Further lowering the catalyst loading led to a decrease of the rate less evident than in the case of **S21** (Table 15, entries 16 and 18 *vs.* 6 and 8), and full conversion could be obtained running the reaction at 100 °C (entries 17 and 19, TON up to 200). At 0.1 mol% catalyst loading, the conversion dropped to 17% (Table 15, entry 20).

On the basis of this optimization, $C_{0,sub.}$ = 0.25 M, 2 mol% loading of **81**, and T = 100 °C were selected as conditions for investigating the substrate scope. The screening was carried out on a 2 mmol scale, and isolated yields were assessed for each product (Table 16). To our delight, excellent yields were obtained with all substrates except ketimines **S26**, **S27** and **S31** (Table 16, entries 5, 6 and 11), which gave only partial conversion. Particularly remarkable are the results obtained with the sterically encumbered imines such as **S35** (Table 16, entry 15), **S39** (entry 19), **S41** (entry 21).

Table 16. Substrate scope of **81** in transfer hydrogenation of preformed imines.[a]

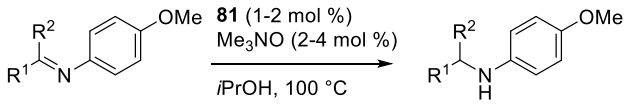

S **P**

#	Substrate		Yield[b](%)	#	Substrate		Yield[b](%)
1	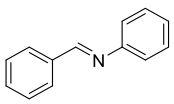	**S22**	>99	12	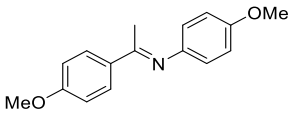	**S32**	98
2	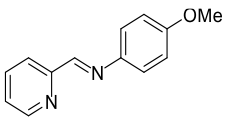	**S23**	>99	13	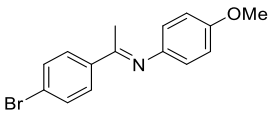	**S33**	>99
3	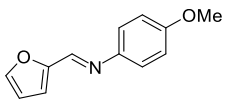	**S24**	>99	14	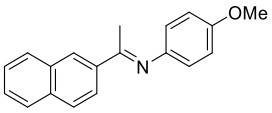	**S34**	>99
4	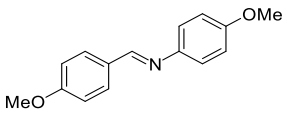	**S25**	>99	15	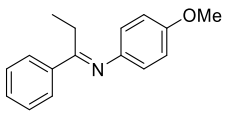	**S35**	99

5	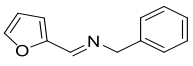	**S26**	36	16	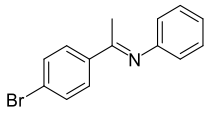	**S36**	68
6	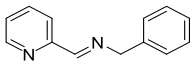	**S27**	66	17	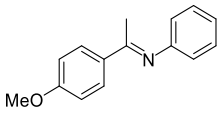	**S37**	99
7	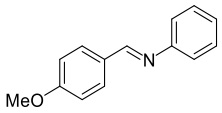	**S28**	99	18	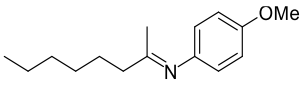	**S38**	99
8	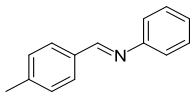	**S29**	99	19	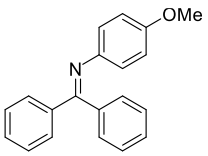	**S39**	83
9	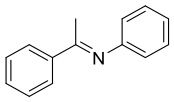	**S30**	>99	20	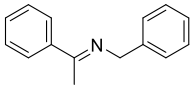	**S40**	99
10	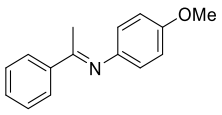	**S21**	>99	21	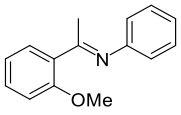	**S41**	95
11	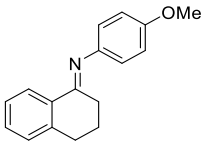	**S31**	57	22	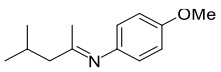	**S42**	99

[a] Entries 1-9: S/**81**/Me_3NO = 100:1:2, entries 10-23: S/**81**/Me_3NO = 100:2:4, $C_{0,\,Sub}$= 0.25 M (5 mmol), T = 100 °C, 18 h, solvent: *i*PrOH; [b] Isolated yields.

Encouraged by the results obtained with imine CTH, we then investigated the feasibility of a reductive amination methodology involving imine synthesis transfer hydrogenation in one pot. This kind of reaction, pioneered by Renaud and co-workers in the case of imine catalytic hydrogenation (CH),[124b,e,h] would avoid the need for imine isolation and purification, thus extending the substrate scope to imines that cannot be readily isolated.

We found that successful imine formation is crucial for success of reductive amination. Indeed, whenever the conversion to imine was lower than 90%, the CTH gave complex mixtures. Thus, condensation of benzaldehyde with 4-methoxyaniline was monitored by ^{1}H-NMR. Reaction in toluene for 1 h in the presence of 3 Å molecular sieves (MS) allowed quantitative aldimine synthesis (Table 17).

Table 17. NMR studies on the *in situ* formation of imine **S43.**

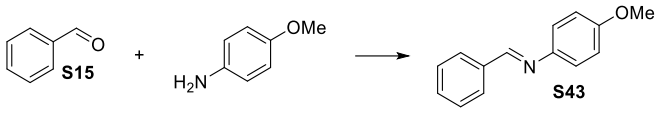

#	Anisidine	Time	T (°C)	Solvent	Additive	Conv. (%)[a]
1	1 eq.	1 h	r.t.	MeOD-d4		0
2	1 eq.	o/n	r.t.	MeOD-d4		0
3	1 eq.	1	r.t.	MeOD-d4	NH_4PF_6	96
4	1 eq.	1 h	100 °C	Toluene-d8	4 Å 200 mg MS[b]	91
5	1.5 eq.	1 h	100 °C	Toluene-d8	3 Å 200 mg MS[b]	>99
6	1 eq.	1 h	50 °C	MeOD-d4	3 Å 200 mg MS[b]	87

[a] Determined by ^{1}H-NMR; [b] under vacuum overnight activated molecular sieves and kept under argon.

Reductive amination tests were then carried out (Table 18): pre-catalyst **81** was activated with Me_3NO in *i*PrOH, and then added to the imine formed *in situ* in different solvents. As expected on the basis on the NMR study shown in Table 17, the best result was observed when the imine was formed in toluene (Table 18, entry 3), whereas lower conversions were observed when other solvents were used for imine formation (entries 1 and 2).

Table 18. Reductive Amination – Transfer hydrogenation promoted by pre-catalyst **81.**[a]

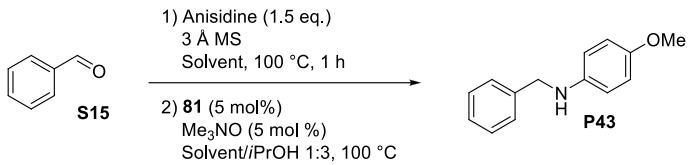

#	Solvent 1	Solvent mixture in the Step 2 (CTH)	Isolated Yield (%)
1	*i*PrOH	*i*PrOH	70
2	MeOH	1:3 MeOH/*i*PrOH	60
3	Toluene	1:3 toluene/*i*PrOH	>99

[a] 1) **S15**/Anisidine = 1:1.5; 3 Å M.S. 400 mg; 2) **S15**/**81**/Me_3NO = 100:5:5, $C_{S,f}$ = 0.25 mol L^{-1} (5 mmol), Solvent/*i*PrOH = 1:3, T = 100 °C, 18 h.

Under these optimized conditions, a substrate scope was performed (Table 19). Different aldehydes were screened in combination with *p*-anisidine or other amines. Remarkably, the *in situ* formed imines **S23** and **S24** gave the same results as the corresponding pre-formed ones (Table 19, entries 2-3 *vs.* Table 16, entries 2-3).

Table 19. Substrates scope of reductive amination – Transfer hydrogenation promoted by pre-catalyst **81.**[a]

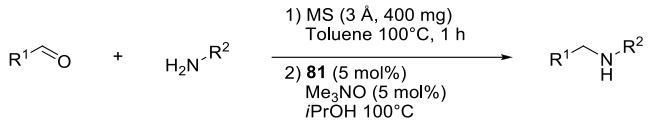

#	Substrate[b]		Yield[s](%)	#	Substrate[b]		Yield[c](%)
1	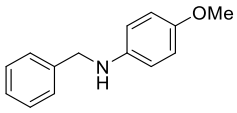	**P43**	>99	7	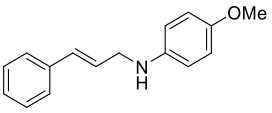	**P47**	75
2	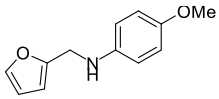	**P24**	98	8	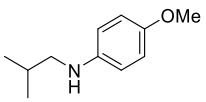	**P48**	17
3	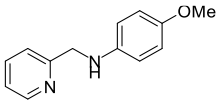	**P23**	93	9	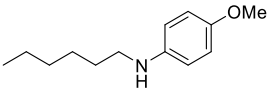	**P49**	0
4	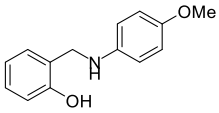	**P44**	44	10	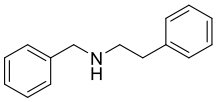	**P50**	38
5	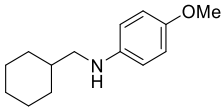	**P45**	74	11	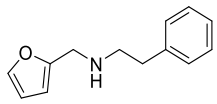	**P51**	67
6	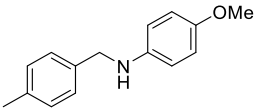	**P46**	>99	12	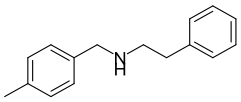	**P52**	90

[a]1) Aldehyde/Anisidine = 1:1.5, 3Å M.S. 400 mg, Solvent: Toluene, T = 100 °C, 1 h; 2) Aldehyde/**81**/Me_3NO = 100:5:5, $C_{S,f}$= 0.25 mol L^{-1} (5 mmol), Toluene/*i*PrOH = 1:3, T = 100 °C, 18 h; [b] All the aldehydes were used freshly distilled over PPh_3; [c] Isolated Yield.

The *in situ* formed imines **S45**, **S46** and **S47** were reduced with good yields (Table 19, entries 5-7), whereas the salicylaldehyde-derived imine **S44** (entry 4) was reduced to the corresponding amine **P44** only with 44% isolated yield (66% of imine left in the crude). Notably, amine **P47** was obtained selectively (no 1,4-reduction took place), and only unreacted imine was found in the reaction crude (neither starting aldehyde nor its reduction product were detected). Unfortunately, the unstable imines derived from carbonyl compounds gave either 17% of isolated yield **P48** (Table 19, entry 8) or no desired product **P49** (entry 9). On the contrary, the imines deriving from an aromatic carbonyl compound and an aliphatic amine were reduced with yields in the 38-90% range (Table 19, entries 10-12).

The *in situ* formation of ketimines was also investigated by NMR, choosing acetophenone and anisidine as benchmark substrate (see Table 20). These NMR studies showed that the use of molecular sieves was not sufficient

to ensure the high-yielding formation of imine **S21**, acid catalysis being also needed (entries 3-20). Among the tested acids, TFA (10 mol%) allowed to obtain the highest conversion to the desired imine (entry 15).

Table 20. NMR studies *in situ* formation of imine **S21**.[a]

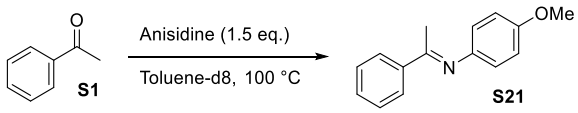

#	Time	Acid (mol%)	MS[b]	Conv. (%)[c]
1	1 h		3 Å 200mg	37
2	o.n.		3 Å 200mg	71
3	1 h	2% NH_4PF_6	3 Å 200mg	35
4	o.n.	2% NH_4PF_6	3 Å 200mg	63
5	1 h	5% NH_4PF_6	3 Å 200mg	52
6	1 h	10% NH_4PF_6	3 Å 200mg	53
7	1 h	10% NH_4PF_6	3 Å 400mg	71
8	1 h	10% NH_4PF_6	3 Å 400mg smashed	71
9	1 h	5% NH_4PF_6	3 Å 400mg smashed	89
10	2 h	5% NH_4PF_6	3 Å 400mg smashed	88
11	1 h	5% *p*-toluenesulfonic acid	3 Å 400mg smashed	86
12	1 h	5% HCl in methanol ~1M	3 Å 400mg smashed	80
13	1 h	5% CH_3COOH	3 Å 400mg smashed	57
14	1 h	5% HCl in dioxane 4N	3 Å 400mg smashed	85
15	**2 h**	**10% TFA**	**3 Å 400mg smashed**	**93**
16	2 h	5% TFA	3 Å 400mg smashed	86
17	1 h	5% TFA	4 Å 400mg smashed	68
18	1 h	5% NH_4PF_6	4 Å 400mg smashed	71
19	1 h	5% TFA	3 Å 500mg	71
20	1 h	5% NH_4PF_6	3 Å 500mg	79

[a] **S1**/Anisidine = 1:1.5, solvent: Toluene, T = 100 °C, $C_{S,i}$= 0.25 mol L^{-1} (5 mmol);
[b] The employed molecular sieves were activated under vacuum and kept under argon;
[c] Determined by ^{1}H-NMR.

Once established the optimal conditions for ketimine formation, we performed preliminary tests by adding the activated catalyst (*i*PrOH solution) to the newly formed imine. However, only moderate yields were obtained under these conditions (Table 21, entries 1-3). Assuming that this was due to progressive catalyst decomposition in the

presence of TFA, we carried out several experiments in which a slight excess of base (with respect to the catalyst) was added after imine formation had taken place and before adding the activated catalyst (Table 21, entries 4-6). Use of an excess *N,N*-diisopropylethylamine (DIPEA, 15 mol%) allow to obtain the best yield (Table 21, entry 4).

Table 21. Reductive Amination – Transfer Hydrogenation of branched imines, promoted by pre-catalyst **81**.[a]

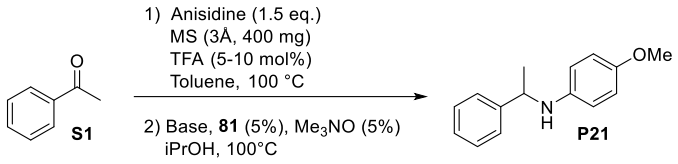

#	TFA (mol%)	Base	Time (h)	Conv. NMR (%)	Isolated Yield (%)
1	5		o/n	40	40
2	10		o/n	10	10
3	10		48	22 (60% imine left)	22 (60% imine left)
4	**10**	**DIPEA (15 mol%)**	**o/n**	**>99**	**98**
5	10	K_2CO_3 (15 mol%)	o/n	89	70
6	10	$K_2CO_{3\,(aq)}$ (15 mol%)	o/n	nd	Nd

[a] 1) **S1**/Anisidine/TFA = 1:1.5:10; 3 Å M.S. 400 mg; 2) **S1**/**81**/Me_3NO/Base = 100:5:5:15, $C_{S,f}$ = 0.25 mol L-1 (5 mmol), Solvent/*i*PrOH = 1:3, *T* = 100 °C, 22 h.

In the substrate screening (Table 22), this iron-catalyzed reductive amination methodology afforded the desired amines with appreciable yields. Aromatic (entries 1, 2 and 4) and aliphatic ketones (entries 5-6) gave synthetically useful yields. Surprisingly, even hindered aliphatic ketones (Table 22, entries 3 and 7) afforded the desired amines with promising yields. From the excess of anisidine (0.5 eq.) used to increase the rate of imine formation, the side product **SP** was generated (and then isolated from the reaction mixture). This isopropylaniline derivative is probably formed by reductive amination of the excess *p*-anisidine with acetone (coproduct of the CTH process).

In conclusion, the first catalytic transfer hydrogenation (CTH) of non-activated N-aryl and N-alkyl imines promoted by a Fe-complex in the absence of Lewis acid co-catalysts has been developed. Thanks to pre-catalyst **81** – displaying much higher activity than the classical 'Knölker complex' **30** – it was possible to reduce a number of imines with a cheap reductant (*i*PrOH) using a relatively low catalyst loading (0.5-2 mol%). Remarkably, very good yields were obtained also with non-activated ketimines, whose reduction with a Fe-complex as the only catalyst has little precedents. Based on this CTH methodology, a reductive amination protocol was also developed, which leads to the one-pot formation of secondary amines in high yield starting from an aldehyde/ketone and a primary amine.

Table 22. Substrates scope of Reductive Amination – Transfer Hydrogenation of branched imines promoted by pre-catalyst **81.**[a,b]

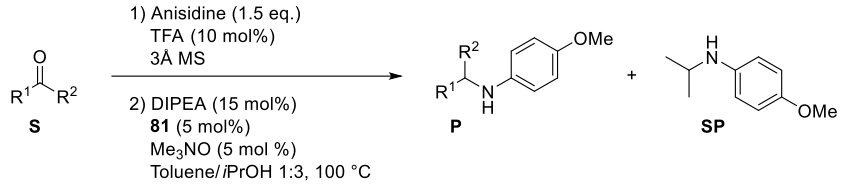

#	Product		Isolated Yield (%)
1	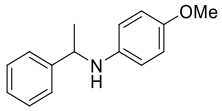	**P21**	98
2	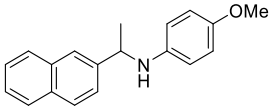	**P34**	31
3	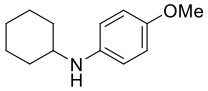	**P53**	41
4	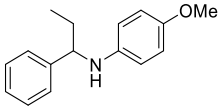	**P35**	68
5	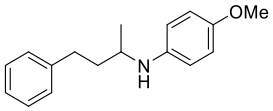	**P54**	52
6	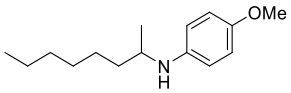	**P38**	60
7	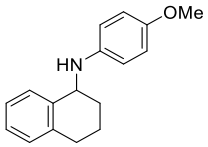	**P31**	51

[a] 1) **S**/Anisidine/TFA = 1:1.5:10; 3Å M.S. 400 mg, solvent: Toluene, T = 100 °C, 2 h; 2) **81**/Me_3NO/DIPEA = 5:5:15, C_S = 0.25 mol L^{-1} (5 mmol), solvent: Toluene/*i*PrOH = 1:3, T = 100 °C, 22 h; [b] Toluene and DIPEA were freshly distilled.

4.4 Summary of [bis(hexamethylene)cyclopentadienone] Iron Complex **81**

The first efficient synthesis and full characterization of the [bis(hexamethylene)cyclopentadienone]iron complex **81** have been reported. The latter compound has been obtained in preparatively useful yield (56%) by reaction of cyclooctyne with $Fe(CO)_5$. The yield obtained is remarkable for this kind of intermolecular cyclative carbonylation/complexation, which usually gives good results only with a few, properly substituted alkynes.[69a, 113, 114] The observed reactivity of cyclooctyne – the smallest cyclic alkyne – is probably due to ring strain, as suggested by the lack of reactivity of its unstrained higher homolog cyclododecyne. Complex **81** has been tested as pre-catalyst in the hydrogenation of ketones, in which, after activation with Me_3NO, it displayed a catalytic activity superior (in terms of TON and TOF) to that of the well-known complex **30**. The same trend was observed also in the transfer hydrogenation of acetophenone, in which **81** allowed to obtain a higher conversion compared to **30**. Further exploration of the pre-catalyst's scope showed that **81** can promote also the hydrogenation of aldehydes and trifluoroacetate esters. Kinetic studies on the hydrogenation of acetophenone in the presence of complexes **30** and **81** suggest that this difference is due to the higher stability of the **81**-derived catalyst compared to the "Knölker-Casey catalyst" generated *in situ* from **30**.

Furthermore, [bis(hexamethylene)cyclopentadienone]iron complex **81** has been tested in transfer hydrogenation of imines, with a catalyst loading of 1-2 mol%. The substrate scope was investigated and excellent yields were obtained in many cases. To further expand the reactivity of the complex, a reductive amination protocol has been developed. The one-pot imine formation–transfer hydrogenation methodology reported has been proved to give good results also in the formation of α-branched secondary amines. To the best of our knowledge, this is the first efficient and practical catalytic transfer hydrogenation (CTH) of non-activated imines promoted by a Fe-catalyst in the absence of other additives.

4.5 Experimental Section

4.5.1 General remarks

All reactions were carried out in flame-dried glassware with magnetic stirring under inert atmosphere (nitrogen or argon), unless otherwise stated. Solvents for reactions were distilled over the following drying agents and transferred under nitrogen: CH_2Cl_2 (CaH_2), MeOH (CaH_2), THF (Na), dioxane (Na), toluene (Na), Et_3N (CaH_2). Dry dichloroethane (DCE), *N*,*N*-dimethylformamide (DMF), dimethoxyethane (DME), 2-propanol, ethanol, acetone and $CHCl_3$ (over molecular sieves in bottles with crown cap) were purchased from Sigma Aldrich and stored under nitrogen. The reactions were monitored by analytical thin-layer chromatography (TLC) using silica gel 60 F254 pre-coated glass plates (0.25 mm thickness). Visualization was accomplished by irradiation with a UV lamp and/or staining with a potassium permanganate alkaline solution. Flash Column Chromatography was performed using silica gel (60 Å, particle size 40-64 μm) as stationary phase, following the procedure by Still and co-workers.[100]

^{1}H-NMR spectra were recorded on a spectrometer operating at 400.13 MHz. Proton chemical shifts are reported in ppm (δ) with the solvent reference relative to tetramethylsilane (TMS) employed as the internal standard ($CDCl_3$, δ = 7.26 ppm; CD_2Cl_2 δ = 5.32 ppm; acetone-d_6, δ = 2.05 ppm; toluene-d_8, δ = 2.08 ppm; CD_3OD, δ = 3.31 ppm). The following abbreviations are used to describe spin multiplicity: s = singlet, d = doublet, t = triplet, q = quartet, m = multiplet, br = broad signal, dd = doublet-doublet, ddd = doublet-doublet-doublet, td = triplet-doublet. ^{13}C-NMR spectra were recorded on a 400 MHz spectrometer operating at 100.56 MHz, with complete proton decoupling. Carbon chemical shifts are reported in ppm (δ) relative to TMS with the respective solvent resonance as the internal standard ($CDCl_3$ δ = 77.16 ppm; CD_2Cl_2 δ = 54.00 ppm; acetone-d_6 δ = 29.84 ppm, 206.26 ppm; CD_3OD, δ = 49.00 ppm). The coupling constant values are given in Hz. Infrared spectra were recorded on a standard FT/IR spectrometer. High resolution mass spectra (HRMS) were performed on a Fourier Transform Ion Cyclotron Resonance (FT-ICR) Mass Spectrometer APEX II & Xmass software (Bruker Daltonics) – 4.7 T Magnet (Magnex) equipped with ESI source, available at CIGA (Centro Interdipartimentale Grandi Apparecchiature) c/o Università degli Studi di Milano.

Materials: commercially available reagents were used as received. The ketones used in the substrate screening were purchased from commercial suppliers (TCI Chemicals, ACROS, Sigma Aldrich) and distilled over PPh_3 before use. The other commercially available reagents were used as received.

4.5.2 Synthesis of Ligands and Complexes

(*E*)-1-Bromocyclooct-1-ene (84):

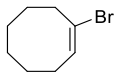

To a solution of cyclooctene (33.2 mL, 0.25 mol, 1 eq.) in CH_2Cl_2 (100 mL) at -40 °C, a solution of Br_2 (0.25 mol) in CH_2Cl_2 (12 mL) was added dropwise until the yellow color persisted. The reaction mixture was quenched with 10% aq. $Na_2S_2O_3$ solution (50 mL) and extracted with CH_2Cl_2 (2 × 100 mL). The organic layer was dried over Na_2SO_4 and concentrated *in vacuo* to give *trans*-1,2-dibromocyclootane in quantitative yield, which was used in the following step without further purification.

^{1}H NMR (400 MHz, $CDCl_3$): δ 4.59-4.57 (m, 2H, CHBr), 2.46-2.37 (m, 2H), 2.15-2.05 (m, 2H), 1.88-1.81 (m, 2H), 1.70-1.56 (m, 4H), 1.54-1.46 (m, 2H). ^{13}C NMR (100 MHz, $CDCl_3$): 61.6, 33.3, 26.0, 25.5.

Trans-1,2-dibromocyclootane (65.78 g, 244 mmol, 1 eq.) was dissolved in THF (100 mL) and the resulting solution was added to a suspension of *t*BuOK (41.07 g, 370 mmol, 1.52 eq.) in THF (40 mL) at 0 °C. The reaction mixture was quenched with a saturated aq. NH_4Cl solution (100 mL), and THF was evaporated off. The resulting crude was extracted with CH_2Cl_2 (2 × 100 mL). The organic layer was dried over Na_2SO_4 and concentrated *in vacuo*. The residue was purified by distillation (bp: 73-80 °C / 10 mbar), and 1-bromocyclooctene **84** was obtained as a colorless liquid. Yield: 36.8 g (227 mmol, 80%).

^{1}H NMR (400 MHz, $CDCl_3$): δ 6.03 (t, ^3J = 8.5 Hz, 1H), 2.58-2.64 (m, 2H), 2.08-2.19 (m, 2H), 1.51-1.62 (m, 8H). ^{13}C NMR (100 MHz, $CDCl_3$): 131.7, 35.2, 29.9, 28.6, 27.5, 26.4, 25.5.

Cyclooctyne (85):

A lithium diisopropylamide (LDA) solution was prepared by adding *n*-butyllithium (1.58 M hexane solution, 43 mmol, 26.7 mL) to a solution of dry diisopropylamine (4.77 g, 47 mmol) in dry THF (20 mL). 1-Bromocyclooctene **2** (8.1 g, 43 mmol) was added at once to the LDA solution cooled at -25 °C. The temperature of the reaction mixture was allowed to rise to 15 °C gradually over a period of 45 min and was kept at this level for another 90 min. It was then poured into a cold solution of 3 N HCl. The solution was extracted with hexane and the combined extracts were washed several times with water to remove the THF. The organic layer was dried over Na_2SO_4 and concentrated *in vacuo*. Careful distillation of the residue gave cyclooctyne (b.p. 50-55 °C / 20 torr). Yield of **85**: 3.9 g (37 mmol, 86%).

^{1}H NMR (400 MHz, CD_2Cl_2): δ 2.13 (m,4H), 1.85 (m, 4H), 1.61 (m, 4H). ^{13}C NMR (75 MHz, CD_2Cl_2): δ 94.90, 35.13, 30.32, 21.90. IR (Nujol, selected band): ν = 2216 cm^{-1} (C≡C stretch).

[Bis(hexamethylene)cyclopentadienone] iron tricarbonyl (81):

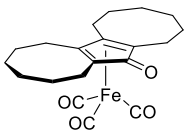

Cyclooctyne **4** (2.7 mL, 21 mmol) and $Fe(CO)_5$ (14.6 mL, 111 mmol, 5.3 eq.) were dissolved in dry toluene (20 mL), under argon, and heated to 90 °C overnight in a sealed glass tube. Evaporation of the solvent gave the crude product, which was then purified by flash chromatography (7:3 hexane/AcOEt). Yellow crystals. Yield of **81**: 1.55 g (4 mmol, 38%). m.p. = 156 °C.

^{1}H NMR (400 MHz $CDCl_3$): δ 1.44-1.59 (m, 10H), 1.74-1.92 (m, 8H), 2.40-2.49 (m, 2H), 2.59-2.64 (m, 2H), 2.76-2.78 (m, 2H). ^{13}C NMR (100 MHz $CDCl_3$): δ 23.43, 23.70, 25.77, 26.24, 28.81, 31.29, 85.54, 102.42 171.42, 209.35.

FT-IR: ν = 2924.1, 2856.6, 2050.3, 1978.9, 1950.0, 1620.2, 1585.5, 1456.3, 1354.0, 1278.8, 1203.6, 1118.7, 1097.5, 1031.9, 987.5, 817.8, 736.8, 648.1, 621.1 cm^{-1}.

HRMS (ESI+): calcd. for $C_{21}H_{24}O_4Fe$: *m/z* 385,1102; $C_{20}H_{24}O_4FeNa$: *m/z* 407.0922. Experimental: $[M+H]^+$ *m/z* 385.1098; $[M + Na]^+$ *m/z* 407.0919.

(*E*)-Cyclododecenyl trifluoromethanesulfonate:

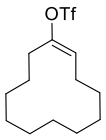

To a solution of cyclododecanone (1.0 g, 5.48 mmol, 1 eq.) in 2 mL of dry THF kept at -78 °C lithium diisopropylamide (6.03 mL, 6.03 mmol, 1.1 eq.) in 6 mL of THF was added. The resulting solution was stirred at -78 °C for 2 h at which time a solution of *N*-phenyltriflimide (2.09 g, 5.86 mmol, 1.07 eq.) in 10 mL of THF was added and the reaction was allowed to warm to 0 °C. The reaction was maintained at this temperature until completion, as observed by TLC. The workup consisted of filtering the reaction solution through a plug of silica gel using ether as eluent. The solvent was removed under reduced pressure and the residue was purified by flash column chromatography (Hexane) furnishing an 85% yield of the corresponding vinyl triflate (1.47 g, 4.66 mmol).

^{1}H NMR (400 MHz, $CDCl_3$): δ 5.37 (*t*, J = 8.3 Hz, 1H), 2.41 (t, J = 6.3 Hz, 2H), 2,25 (m, 2H), 1.55-1.25 (16H). ^{13}C NMR (100 MHz, $CDCl_3$): δ 184.6, 123.8, 118.4 (*q*, J = 319 Hz), 33.2, 26.2, 25.7, 25.4, 25.3, 25.2, 24.5, 24.4, 24.2, 22.9.

IR ($CHCl_3$): ν = 1692, 1411, 1221, 1142 cm^{-1}.

HRMS (ESI+): calcd. for $C_{13}H_{21}F_3O_3S$: *m/z* 314.1163. Experimental: $[M+H]^+$ *m/z* 314.1160.

^{1}H NMR data of the contaminated *E*-isomer (8%) δ: 5.48 (t, J = 8.3 Hz, 1H), 2.45 (t, J = 6.8 Hz, 2H), 2.15 (dt, J = 8.3, 6.8 Hz, 2H), 1.70-1.25 (16H).

Cyclododecyne (90):

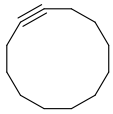

To a solution of (*E*)-cyclododecenyl trifluoromethanesulfonate (0.8 g, 2.54 mmol, 1 eq.) in 1 mL of dry THF kept at -78 °C, a solution of LDA (5.08 mL, 5.08 mmol, 2 eq.) in 1 mL of THF was added over 5 min. The reaction mixture was stirred at -78 °C for 2 h and then poured onto hexane/H_2O. The aqueous phase was extracted with pentane (3 × 10 mL) and the combined organic layers were washed with brine, dried over $NaSO_4$, filtered and concentrated *in vacuo*. Purification of the resulting oil by flash chromatography (hexane) gave cyclododecyne **90**. Yield: 396 mg (2.16 mmol, 95%).

^{1}H NMR (400 MHz, $CDCl_3$): *δ* 2.20-2.17 (m, 4H), 1.58-1.51 (m, 8H), 1.47-1.40 (m, 8H).

^{13}C NMR (100 MHz, $CDCl_3$): *δ* 81.6, 25.7, 25.5, 24.9, 24.6, 18.5. IR ($CHCl_3$): ν = 1461, 1447, 1322 cm^{-1}.

HRMS (ESI+): Calcd. for $C_{12}H_{20}$: $[M+H]^+$ *m/z* 164.1565. Experimental: *m/z* 164.1531 $[M+H]^+$.

[bis(decamethylene)cyclopentadienone]irontricarbonyl (91):

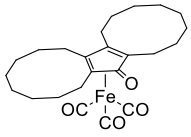

Cyclododecyne **6** (167μL, 0.91 mmol) and $Fe(CO)_5$ (613 μL, 4.6 mmol, 5 eq.) were dissolved in dry toluene (5 mL), under argon and heated to 110 °C overnight in a sealed glass tube. Evaporation of the solvent gave the crude product, which was then purified by flash chromatography (6:4 hexane/AcOEt). Orange solid. Yield: 12 mg (0.02 mmol , 5%).

^{1}H NMR (400 MHz, $CDCl_3$): *δ* 2.37-2.35 (*br*, 4H), 2.10-2.08 (*br*, 2H), 1.94-1.97 (*br*, 2H), 1.78 (*br*, 2H), 1.56-1.30 (*m*, 27H), 1.21-1.19 (*br*, 3H).

MS (ESI+): Calcd. for $C_{28}H_{41}O_4Fe$: $[M + H]^+$ *m/z* 497.24; $C_{28}H_{40}O_4FeNa$: $[M + Na]^+$ *m/z* 519.22. Experimental: $[M + H]^+$ *m/z* 497.11; $[M + Na]^+$ *m/z* 519.11.

4.5.3 Synthesis of pre-isolated imines

4.5.3.1 General Procedure

Aldehyde/ketone (4.5 mmol) was added to a solution of amine (3 mmol) in anhydrous toluene (5 mL) in the presence of 3 Å molecular sieves (0.6 g). The reaction was heated to 110 °C, stirred overnight and monitored by ^{1}H-

NMR. The molecular sieves were removed by filtration, and the solvent was evaporated to afford the crude imine. The imine was purified by reduced pressure distillation (Kugelrohr).

4.5.3.1 Characterization data

Imine (name, chemical formula)	^{1}H NMR
***N*-(4-Methoxy-phenyl)-(1-phenyl-ethylidene)-amine (S21):**[131]	
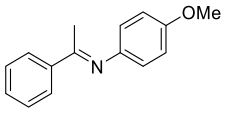	^{1}H NMR (400 MHz, $CDCl_3$) δ 7.95-7.99 (m, 2H), 7.44-7.46 (m, 3H), 6.90-6.93 (m, 2H), 6.75-6.78 (m, 2H), 3.82, (s, 3H), 2.26 (s, 3H).
(*E*)-*N*-Benzylidenebenzenamine (S22):[127]	
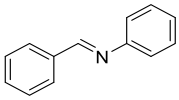	^{1}H NMR (300 MHz, $CDCl_3$) δ 7.18–7.30 (m, 3H), 7.35–7.55 (m, 5H), 7.86–7.96 (m, 2H), 8.46 (s, 1H).
(*E*)-*N*-(4-Methoxyphenyl)-1-(pyridin-2-yl)methanimine (S23):[128]	
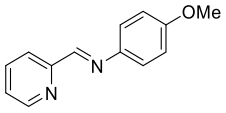	^{1}H NMR (300 MHz, $CDCl_3$) δ 8.61 (d, J = 4.7 Hz, 1H), 8.56 (s, 1H), 8.10 (d, J = 7.9 Hz, 1H), 7.68 (t, J = 7.7 Hz, 1H), 7.27 (d, J = 8.8 Hz, 3H), 6.86 (d, J = 8.8 Hz, 2H), 3.72 (s, 3H).
***N*-(Furan-2-ylmethylene)-4-methoxyaniline (S24):**[128]	
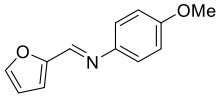	^{1}H NMR (300 MHz, $CDCl_3$) δ 8.30 (s, 1H), 7.59 (s, 1H), 7.26 (d, J = 9.1 Hz, 2H), 6.92 (d, J = 9.0 Hz, 3H), 6.57–6.51 (m, 1H), 3.82 (s, 3H).
***N*-(4-Methoxybenzylidene)-4-methoxyaniline (S25):**[128]	
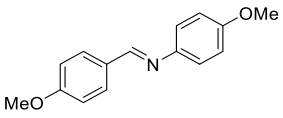	^{1}H NMR (300 MHz, $CDCl_3$) δ 8.41 (s, 1H), 7.30 (d, J = 8.7 Hz, 2H), 6.89 (d, J = 8.7 Hz, 2H), 6.79 (d, J = 9.0 Hz, 2H), 6.61 (d, J = 9.0 Hz, 2H), 3.81 (s, 3H), 3.75 (s, 3H).
***N*-Furfurylidenebenzylamine (S26):**[129]	
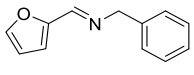	^{1}H NMR (400 MHz, $CDCl_3$) δ 8.10 (s, 1H), 7.44 (m, 1H), 7.28-7.24 (m, 4H), 7.20-7.17 (m, 1H), 6.70 (d, J = 3.3 Hz, 1H), 6.40 (dd, J = 3.3, 1.7 Hz, 1H), 4.72 (s, 2H).
(*E*)-*N*-Benzyl-1-(pyridin-2-yl)methanimine (S27):[129]	
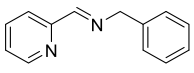	^{1}H NMR (400 MHz, $CDCl_3$) δ 8.66 (d, J = 4.6 Hz), 8.49 (s, 1H), 8.07 (d, J = 7.9 Hz, 1H), 7.75 (dd, J = 11.1, 4.3 Hz, 1H), 7.37-7.27 (m, 6H), 4.89 (s, 2H).

(p-Methoxybenzylidene)aniline (S28):[130]

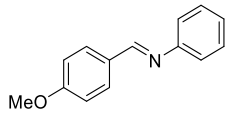

^{1}H-NMR (300 MHz, $CDCl_3$) δ 8.43 (s, 1H), 7.90 (d, J= 8.8 Hz, 2H), 7.46-7.41 (m, 2H), 7.30-7.24 (m, 3H), 7.03 (d, J= 8.8 Hz, 2H), 3.92 (s, 3H).

(*E*)-*N*-(4-Methylbenzylidene)benzenamine (S29):[127]

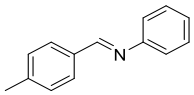

^{1}H NMR (300 MHz, $CDCl_3$) δ 2.36 (s, 3H), 7.16–7.31 (m, 5H), 7.34–7.43 (m, 2H), 7.76–7.83 (m, 2H), 8.40 (s, 1H).

(*E*)-(Phenyl)(1-phenylethylidene)amine (S30):[131]

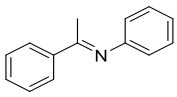

^{1}H NMR (400 MHz, $CDCl_3$) δ 8.01-8.04 (m, 2H), 7.48-7.51 (m, 3H), 7.37-7.41 (m, 2H), 7.11-7.15 (m, 1H), 6.84-6.86 (m, 2H), 2.27 (s, 3H).

[3,4-Dihydro-2*H*-naphthalenylidene]-(4-methoxyphenyl)amine (S31):[132]

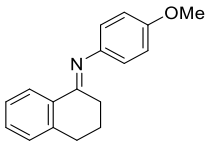

^{1}H NMR (400 MHz, $CDCl_3$) δ 8.33 (dd, J= 8.0, 1.1 Hz, 1 H), 7.19-7.39 (m, 3 H), 6.91 (m, 2 H), 6.77 (mc, 2 H), 3.02(s, 3 H), 2-89-2.92 (m, 2 H), 2.55-2.59 (m, 2 H), 1.89-1.95 (m, 2 H).

(*E*)-*N*,1-Bis(4-methoxyphenyl)ethan-1-imine (S32):[133]

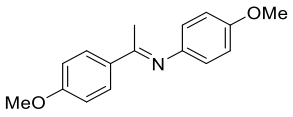

^{1}H NMR (400 MHz, $CDCl_3$) δ 7.93 (m, 2H), 6.97 (m, 2H), 6.92 (m, 2H), 6.74 (m, 2H), 3.86 (s, 3H), 3.81 (s, 3H), 2.21 (s, 3H).

***N*-(1-(4-Bromophenyl)ethylidene)-4-methoxyanil (S33):**[134]

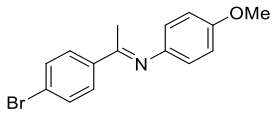

^{1}H NMR (400 MHz, $CDCl_3$) δ 7.85–7.80 (m, 2H), 7.57–7.34 (m, 2H), 6.92–6.89 (m, 2H), 6.76–6.72 (m, 2H), 3.81 (s, 3H), 2.22 (s, 3H).

(4-Methoxy-phenyl)-[1-naphthalen-2-yl-ethylidene]-amine (S34):[133]

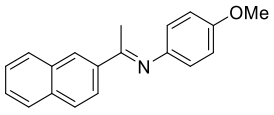

^{1}H NMR (400 MHz, $CDCl_3$) δ 8.33 (s, 1H), 8.25 (dd, J = 1.6, 8.6 Hz), 7.89-7.97 (m, 3H), 7.53-7.59 (m, 2H), 6.96 (m, 2H), 6.83 (m, 2H), 3.86 (s, 3H) 2.41 (s, 3H).

[1-Phenylpropylidene]-(4-methoxyphenyl)-amine (S35):[133]

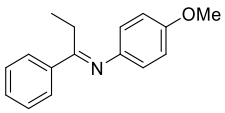

E/*Z* = 88:12

E: ^{1}H NMR (400 MHz, $CDCl_3$) δ 7.88-7.96 (m, 2H), 7.41-7.49 (m, 3H), 6.91 (m, 2H), 6.74 (m, 2H), 3.81 (s, 3H), 2.68 (q, J 7.6 Hz, 2H),1.08 (t, J 7.6 Hz, 3H);

Z: ^{1}H NMR (400 MHz, $CDCl_3$) δ 7.19-7.23 (m, 3H), 7.05-7.08 (m, 2H), 6.52-6.68 (m, 4H), 3.70 (s, 3H), 2.79 (q, J 7.6 Hz, 2H),1.20 (t, J 7.6 Hz, 3H).

(*E*)-1-(4-Bromophenyl)-*N*-phenylethan-1-imine (S36):[134]

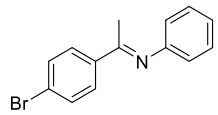

^{1}H NMR (400 MHz, $CDCl_3$) δ 7.85 (d, J = 8.7 Hz, 2H), 7.58 (d, J =8.7 Hz, 2H), 7.36 (t, J = 8.1 Hz, 2H), 7.10 (t, J = 7.2 Hz, 1H), 6.78 (d, J = 7.5 Hz, 2H), 2.21 (s, 3H).

(*E*)-1-(4-Methoxyphenyl)-*N*-phenylethan-1-imine (S37):[135]

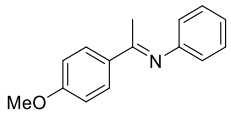

^{1}H NMR (400 MHz, $CDCl_3$) δ 7.95 (d, J = 8.0 Hz, 2H), 7.35 (t, J = 8.0 Hz, 2H), 7.08 (t, J= 8.0 Hz, 1H), 6.96 (d, J = 8.0 Hz, 2H), 6.80 (d, J = 8.0 Hz, 2H), 3.88 (s, 3H), 2.21 (s, 3H).

(*E*)-*N*-(4-Methoxyphenyl)octan-2-imine (S38):[136]

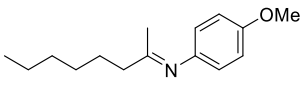

^{1}H NMR (400 MHz, CD_2Cl_2) δ 6.83 (m, 2H), 6.59 (m, 2H), 3.77 (s, 3H), 2.37-2.12 (m, 2H), 2.10-1.75 (s, 3H), 1.65-1.47 (m, 2H), 1.42-1.14 (m, 6H), 0.91-0.85 (t, J = 7.0 Hz, 3H).

***N*-(4-Methoxyphenyl)-1,1-diphenylmethanimine (S39):**[137]

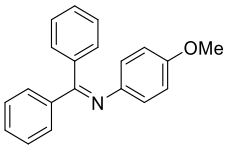

^{1}H NMR (400 MHz, acetone-d6) δ 7.71-7.73 (m, 2 H), 7.47-7.51 (m, 1 H), 7.41-7.45 (m, 2 H), 7.32-7.36 (m, 3 H), 7.14-7.17 (m, 2 H), 6.69-6.72 (m, 2 H), 6.64-6.67 (m, 2H), 3.68 (s, 3 H).

***N*-(1-Phenylethylidene)benzenemethanamine (S40):**[138]

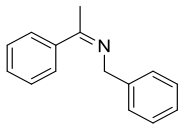

^{1}HNMR (300 MHz, $CDCl_3$) δ 7.80-7.77 (m, 2H), 7.50-7.25 (m, 8H), 4.83 (s, 2H), 1.25 (s, 3H).

(*E*)-1-(2-Methoxyphenyl)-*N*-phenylethan-1-imine (S41):

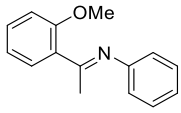

Ratio: *E*/*Z* = 7:3

E: ^{1}H NMR (400 MHz, Acetone-d_6) δ 7.68-7.50 (m, 1H), 7.40-7.35 (m, 2H), 7.14-7.00 (m, 4H), 6.84-6.79 (m, 2H), 3.93 (s, 3H), 2.17 (s, 3H);

Z: ^{1}H NMR (400 MHz, Acetone-d_6) δ 7.43 (ddd, *J* = 8.3, 7.4, 1.8 Hz, 2H), 7.22-7.15 (m, 1H), 6.95-6.88 (m, 2H), 6.66-6.59 (m, 2H), 3.79 (s, 3H), 2.39 (s, 3H).

(*E*)-*N*-(4-Methoxyphenyl)-4-methylpentan-2-imine (S42):

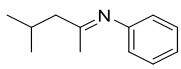

Ratio: *E*/*Z* = 8:2

E: ^{1}H NMR (400 MHz, Acetone-d_6) δ 6.88 (d, *J* = 8.8 Hz, 2H), 6.61 (d, *J* = 8.8 Hz, 2H), 3.78 (s, 3H), 2.29-2.24 (m, 2H), 2.18 (dq, *J* = 7.8, 6.5 Hz, 1H), 1.00 (d, *J* = 6.5 Hz, 9H);

Z: ^{1}H NMR (400 MHz, Acetone-d_6) δ 6.88 (d, *J* = 8.8 Hz, 2H), 6.61 (d, *J* = 8.8 Hz, 2H), 3.75 (s, 3H), 2.29-2.24 (m, 2H), 2.18 (dq, *J* = 7.8, 6.5 Hz, 1H), 0.82 (d, *J* = 6.5 Hz, 2H).

4.5.4 Catalytic Tests - Reduction of Aldehydes and Ketones

4.5.4.1 Hydrogenation of acetophenone with activation by UV irradiation

Hydrogenation experiments were carried out in a custom-made glass autoclave equipped with a thick-walled glass reaction vessel (total capacity 20 mL, maximum pressure 25 bar), a single inlet valve, a manometer, and safety relieve valve. UV irradiation experiments were carried out in a Rayonet RPR-100 (Southern New England UV Company, USA). The UV lamps used have the specification F8T5BLB, 8 W, 352 nm (Sanyo Denki, Japan).

Acetophenone **S1** (5.50 μL, 47.1 μmol, 1 eq.) and dodecane (8.0 μL, 44.0 μmol) were dissolved in toluene (1.0 mL) in a glass autoclave (20 mL capacity) under a stream of argon. A 0.0236 mM toluene stock solution of the iron pre-catalyst **81** (0.1 mL, 2.36 μmol, 0.05 eq.) was added. The autoclave was sealed and filled with and then carefully discharged from argon (14 to 1 bar) and it was purged for three times with hydrogen (14 bar). After the last fill/vent cycle, the autoclave was loaded with hydrogen (14 bar) and discharged to the desired reaction pressure (10 bar). The vessel was placed in a Rayonet RPR-100 (Southern New England UV Company) and irradiated (λ_{max} = 350 nm). The reaction mixture was stirred under hydrogen pressure and 40 °C as indicated by the total reaction time. Conversions were determined by GC using dodecane as internal standard.

4.5.4.2 Transfer hydrogenation of acetophenone

A 10 mL Schlenk was charged with a stir bar and the iron complex (0.01 mmol, 0.02 eq.) in *i*PrOH 1 mL), followed by addition of a stock solution of Me_3NO (1.5 mg, 0.02 mmol, 0.04 eq.) in H_2O (0.4 mL). After stirring for 5 min, acetophenone **S1** (117 μL, 120.2 mg, 1.0 mmol, 1 eq.) was added, and the obtained mixture was heated at 70 °C and stirred for 16 h. Conversions were determined by GC using dodecane as internal standard.

4.5.4.3 General procedure for hydrogenation reactions with Me_3NO as activator

Hydrogenations were run in a 450 mL Parr autoclave equipped with a removable aluminum block that can accommodate up to fifteen magnetically stirred 7 mL-glass vials. The pre-catalyst (0.005 mmol, 0.01 eq.) was weighed in glass vials, which were accommodated in the aluminum block after adding magnetic stirring bars in each of them. The block was placed in a Schlenk tube, where it was subjected to three vacuum/nitrogen cycles. *i*PrOH (0.25 mL) was added to each vial, and stirring was started. Me_3NO (0.75 mg, 0.01 mmol, 0.02 eq.) was added to each vial as a stock solution in H_2O (0.1 mL). After stirring at r.t. under nitrogen for 10 min, the substrate (0.5 mmol, 1 eq.) was added to the mixtures. Each vial was capped with a Teflon septum pierced by a needle, the block was transferred into the autoclave, and stirring was started. After purging four times with hydrogen at the selected

pressure, heating was started. The reactions were stirred under hydrogen pressure overnight and then filtered throgh a pad of celite and analyzed for determining the conversion.

Conversions were determined by ^{1}H NMR for products: **P2**, **P3**, **P4**, **P5**, **P6**, **P7**, **P8**, **P9**, **P10**, **P11**, **P12**, **P13**, **P19**, ^{19}F NMR for product **P18** or by GC for products **P1**, **P14**, **P15**, **P16**, **P17** (Table 10, page 78).

4.5.4.4 Alcohol Conversions:

NMR conversions were calculated from the signal integrals (all the substrates and reduction products are known compounds, and our spectra are superimposable to those reported in the literature). The NMR spectra were measured taking $d1$ = 20 s.

Alcohol (name, chemical formula)	^{1}H NMR
1-Phenylethanol (P1):[139] 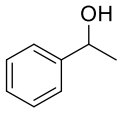	^{1}H-NMR (300 MHz, $CDCl_3$): δ 7.43-7.34 (m, 4H), 7.33-7.28 (m, 1H), 4.92 (q, J = 6.5 Hz, 1H), 1.91 (s, 1H), 1.53 (d, J = 6.5 Hz, 3H).
1-(3-Nitrophenyl)ethanol (P2):[139] 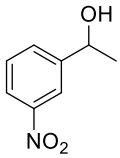	^{1}H-NMR (300 MHz, $CDCl_3$): δ 8.22 (s, 1H), 8.09 (d, J = 6.8 Hz, 1H), 7.70 (d, J = 6.8 Hz, 1H), 7.49 (t, J = 6.0 Hz, 1H), 5.01 (q, J = 6.0 Hz, 1H), 2.73 (br s, 1H), 1.52 (d, J = 6.0 Hz, 3H).
1-(4-Methoxyphenyl)ethanol (P3):[139] 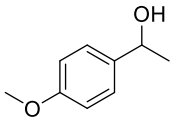	^{1}H-NMR (300 MHz, $CDCl_3$): δ 7.32 (d, J = 8.7 Hz, 2H), 6.91 (d, J = 8.7 Hz, 2H), 4.88 (q, J = 6.4 Hz, 1H), 3.83 (s, 3H), 1.82 (br s, 1H), 1.50 (d, J = 6.4 Hz, 3H).
1-(4-Bromophenyl)ethanol (P4):[140] 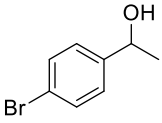	^{1}H-NMR (300 MHz, $CDCl_3$): δ 7.49 (d, J = 8.4 Hz, 2H), 7.27 (d, J = 8.4 Hz, 2H), 4.89 (q, J = 6.5 Hz, 1H), 1.85 (s, 1H), 1.49 (d, J = 6.5 Hz, 3H).

1-(2-Methoxyphenyl)ethanol (P5):[140]

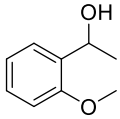

^{1}H-NMR (300 MHz, $CDCl_3$): δ 7.33 (d, *J* = 7.6 Hz, 1H), 7.24 (dt, *J* = 7.6, 1.6 Hz, 1H), 6.95 (t, *J* = 7.6 Hz, 1H), 6.87 (d, *J* = 7.6 Hz, 1H), 5.09 (q, *J* = 6.4 Hz, 1H), 3.84 (s, 3H), 2.74 (br s, 1H), 1.49 (d, *J* = 6.4 Hz, 3H).

1-(2-Chlorophenyl)ethanol (P6):[140]

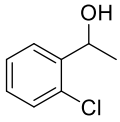

^{1}H-NMR (300 MHz, $CDCl_3$): δ 7.56 (d, *J* = 7.6 Hz, 1H), 7.29 (m, 2H), 7.18 (d, *J* = 7.6 Hz, 1H), 5.26 (d, *J* = 6.4 Hz, 1H), 2.45 (br s, 1H), 1.45 (d, *J* = 6.4 Hz, 3H).

1-(Pyridin-2-yl)ethanol (P7):[139]

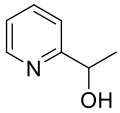

^{1}H-NMR (300 MHz, $CDCl_3$): δ 8.52 (d, *J* = 7.7 Hz, 1H), 7.69 (t, *J* = 7.9 Hz, 1H), 7.30 (d, *J* = 7.9 Hz, 1H), 7.19 (t, *J* = 7.9 Hz, 1H), 4.90 (d, *J* = 6.5 Hz, 1H), 4.46 (br s, 1H), 1.50 (d, *J* = 6.5 Hz, 3H).

1,2,3,4-Tetrahydronaphthalen-1-ol (P8):[140]

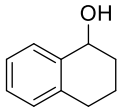

Product **P8** (conv. = 80%): ^{1}H-NMR (300 MHz, $CDCl_3$): δ 7.44 (m, 1H), 7.24-7.19 (m, 2H), 7.13-7.10 (m, 1H), 4.76 (s, 1H), 2.87-2.70 (m, 2H), 2.01-1.76 (m, 5H).

Residual **S8** (20%): ^{1}H-NMR (300 MHz, $CDCl_3$): δ 8.03 (d, *J* = 8.0 Hz, 1H), 7.46 (t, *J* = 7.6 Hz, 1H), 7.30 (t, *J* = 7.6 Hz, 1H), 7.25 (d, *J* = 7.6 Hz, 1H), 2.96 (t, *J* = 6.0 Hz, 2H), 2.65 (t, *J* = 6.4 Hz, 2H), 2.17-2.10 (m, 2H).

Octan-3-ol (P9):[141]

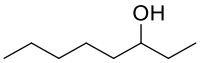

^{1}H-NMR (300 MHz, $CDCl_3$): δ 3.53 (br s, 1H), 1.25-1.56 (m, 11H), 0.86-0.97 (m, 6H).

1-Cyclopropylethanol (P10):[142]

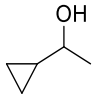

^{1}H-NMR (300 MHz, $CDCl_3$): δ 3.05 (dq, *J* = 8.3, 6.2 Hz, 1H), 1.85 (s, 1H), 1.25 (d, *J* = 6.2 Hz, 3H), 0.91-0.84 (m, 1H), 0.48-0.46 (m, 2H), 0.26-0.23 (m, 1H), 0.17-0.15 (m, 1H).

4-Phenylbut-3-en-2-ol (P11):[143]

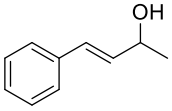

^{1}H-NMR (300 MHz, $CDCl_3$): δ 7.18-7.39 (5H, m), 6.53-6.58 (1H, m), 6.22-6.29 (1H, m), 4.46-4.50 (1H, m), 1.36 (d, *J* = 6.0 Hz, 3H)

4-Phenylbutan-2-ol (P11b):[144]

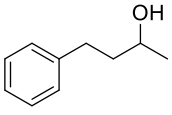

^{1}H-NMR (300 MHz, $CDCl_3$): δ 7.18-7.39 (m, 5H), 3.78-3.85 (m, 1H), 2.63-2.75 (m, 2H), 3.78-3.85 (m, 1H), 1.78 (br s, 1H), 1.75-1.77 (m, 2H), 1.22 (d, *J* = 6.0 Hz, 3H)

3,5,5-Trimethylcyclohex-2-enol (P13):[143]

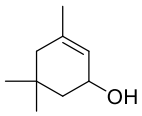

Product **P12** (conv. = 15%): ^{1}H-NMR (300 MHz, $CDCl_3$): δ 5.89 (s, 1H), 2.20 (2H, s), 2.17 (2H, s), 1.94 (s, 3H), 1.04 (s, 6H).

Residual **S12** (85%): ^{1}H-NMR (300 MHz, $CDCl_3$): δ 5.43 (m, 1H), 4.25 (m, 1H), 1.87-1.74 (m, 10H), 1.68 (s, 3H), 1.96-2.10 (m, 1H).

2-Methylcyclopentan-1-ol (P14, mixture of *trans* and *cis* isomer):[145]

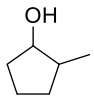

Trans isomer: ^{1}H-NMR (300 MHz, $CDCl_3$): δ 3.73 (q, J = 6.0 Hz, 1 H), 1.31-1.89 (m, 8H), 1.20 (d, *J* = 7.0 Hz, 3H).

Cis isomer: ^{1}H-NMR (300 MHz, $CDCl_3$): δ 4.06 (m, 1 H), 1.31-1.89 (m, 5H), 1.16 (m, 1 H), 0.96 (d, *J* = 7.0 Hz, 3H).

No attempts were made to separate the two isomers.

Benzyl alcohol (P15):[139]

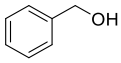

^{1}H-NMR (300 MHz, $CDCl_3$): δ 7.30-7.42 (m, 5H), 4.73 (s, 2H), 1.66 (s, 1H).

Cyclohexylmethanol (P16):[146]

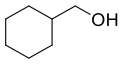

^{1}H-NMR (300 MHz, $CDCl_3$): δ 3.47 (d. *J* = 6.4 Hz, 2H), 1.83 -1.66, (m, 5H), 1.56-1.39 (m, 2H), 1.35-1.12 (m, 3H), 0.97 (m, 2H).

Dodecan-1-ol (P17):[147]

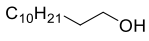

^{1}H-NMR (300 MHz, $CDCl_3$): δ 3.39 (t, *J* = 6.6 Hz, 2H), 1.61-1.68 (m, 2H), 1.57-1.59 (m, 2H), 1.24-1.34 (m, 16H), 0.88 (t, *J* = 6.81 Hz, 3H).

3-Phenylprop-2-en-1-ol (P18):[148]

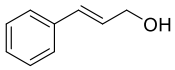

^{1}H NMR (300 MHz, $CDCl_3$): δ 4.36 (d, *J* = 5.7, 2H), 6.37-6.43 (m, 1H), 6.65 (d, *J* = 15.9 Hz, 1H), 7.22-7.43 (m, 5H).

3-Phenyl-1-propanol (P18b):[149]

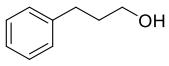

^{1}H NMR (300 MHz, $CDCl_3$): δ 7.22-7.31 (m, 5H), 3.71 (t, *J* = 6.4 Hz, 2H), 2.74 (t, *J* = 7.2 Hz, 2H), 1.93 (m, 2H).

Benzyl alcohol and 2,2,2-trifluoroethanol (P19):[150]

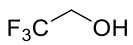

For benzyl alcohol, see above (**P15**).

2,2,2-Trifluoroethanol **P19** (conv. = 99%): ^{1}H-NMR (300 MHz, $CDCl_3$): δ 3.92 (q, *J* = 8.4 Hz, 2H), 3.40 (br s, 1H). ^{19}F NMR (300 MHz, $CDCl_3$): δ -76.93 (s, 3F).

Residual **P19** (1%): ^{1}H-NMR (300 MHz, $CDCl_3$): δ 7.40 (s, 5H), 5.36 (s, 2H). ^{19}F NMR (282 MHz, $CDCl_3$): δ -75.96 (s, 3F).

4.6.4.5 GC conversions

1-Phenylethanol (P1):[139]

Capillary column: MEGADEX DACTBSβ, diacetyl-*tert*-butylsilyl-β-cyclodextrin, 0.25 μm; diameter = 0.25 mm; length = 25 m; carrier: hydrogen; inlet pressure: 1 bar; oven temperature: 95 °C for 20 min: $t_{\mathbf{S1}}$ = 6.0 min; $t_{(R)\text{-}\mathbf{P1}}$ = 13.2 min; $t_{t(S)\text{-}\mathbf{P1}}$ = 15.1 min.

Benzyl alcohol (P15):[139]

Capillary column: MEGADEX DACTBSβ, diacetyl-*tert*-butylsilyl-β-cyclodextrin, 0.25 μm; diameter = 0.25 mm; length = 25 m; carrier: hydrogen; inlet pressure: 1 bar; oven temperature: 95 °C for 20 min: $t_{\mathbf{S14}}$ = 3.54 min; $t_{\mathbf{P14}}$ = 11 min.

Cyclohexylmethanol (P16):[146]

Capillary column: MEGADEX DACTBSβ, diacetyl-*tert*-butylsilyl-β-cyclodextrin, 0.25 μm; diameter = 0.25 mm; length = 25 m; carrier: hydrogen; inlet pressure: 1 bar; oven temperature: 95 °C for 20 min: $t_{\mathbf{S15}}$ = 2.98 min; $t_{\mathbf{P15}}$ = 18.9 min.

Dodecan-1-ol (P17):[147]

Capillary column: MEGADEX DACTBSβ, diacetyl-*tert*-butylsilyl-β-cyclodextrin, 0.25 μm; diameter = 0.25 mm; length = 25 m; carrier: hydrogen; inlet pressure: 1 bar; oven temperature: 95 °C for 17 min, then 30 °C/min ramp to 200 °C: $t_{\mathbf{S16}}$ = 19.5 min; $t_{\mathbf{P16}}$ = 20.1 min.

3-Phenylprop-2-en-1-ol / 3-Phenyl-1-propanol (P18/P18b):

Capillary column: MEGADEX DACTBSβ, diacetyl-*tert*-butylsilyl-β-cyclodextrin, 0.25 μm; diameter = 0.25 mm; length = 25 m; carrier: hydrogen; inlet pressure: 1 bar; oven temperature: 95 °C for 20 min: $t_{\mathbf{S17}}$ = 19.6 min; $t_{\mathbf{P17b}}$= 19.2 min; $t_{\mathbf{P17a}}$ = 20.1 min.

4.5.4.6 Isolated Yields

The hydrogenation of substrates **S1**, **S3**, **S4**, **S15** and **S16** was carried out on a 2 mmol scale following the General Procedure, in order to determine the isolated yields.

1-Phenylethanol (P1):

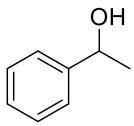

After the hydrogenation, the volatiles were evaporated and the residue was purified by flash column chromatography (9:1 hexane/AcOEt). The product was isolated as a colorless oil. Yield: 239 mg (98%). Its physical and spectroscopic data are superimposable with those reported in the literature.[142] 1H-NMR (300 MHz, $CDCl_3$): δ 7.43-7.34 (m, 4H), 7.33-7.28 (m, 1H), 4.92 (q, J = 6.5 Hz, 1H), 1.91 (s, 1H), 1.53 (d, J = 6.5 Hz, 3H).

1-(4-Methoxyphenyl)ethanol (P3):

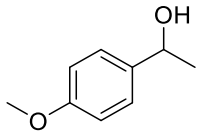

After the hydrogenation, the volatiles were evaporated and the residue was purified by flash column chromatography (9:1 hexane/AcOEt). The product was isolated as a colorless oil. Yield: 298 mg (98%). Its physical and spectroscopic data are superimposable with those reported in the literature.[139] ^{1}H-NMR (300 MHz, $CDCl_3$): δ 7.32 (d, *J* = 8.7 Hz, 2H), 6.91 (d, *J* = 8.7 Hz, 2H), 4.88 (q, *J* = 6.4 Hz, 1H), 3.83 (s, 3H), 1.82 (br s, 1H), 1.50 (d, *J* = 6.4 Hz, 3H).

1-(4-Bromophenyl)ethanol (P4):

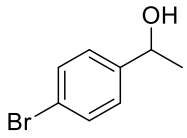

After the hydrogenation, the volatiles were evaporated and the residue was purified by flash column chromatography (9:1 hexane/AcOEt). The product was isolated as a white solid. Yield: 390 mg (97%). Its physical and spectroscopic data are superimposable with those reported in the literature.[140] ^{1}H-NMR (300 MHz, $CDCl_3$): δ 7.49 (d, *J* = 8.4 Hz, 2H), 7.27 (d, *J* = 8.4 Hz, 2H), 4.89 (q, *J* = 6.5 Hz, 1H), 1.85 (s, 1H), 1.49 (d, *J* = 6.5 Hz, 3H).

Benzyl alcohol (P15):

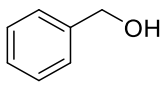

After the hydrogenation, the volatiles were evaporated and the residue was purified by flash column chromatography (9:1 hexane/AcOEt). The product was isolated as a colorless liquid. Yield: 203 mg (94%). Its physical and spectroscopic data are superimposable with those reported in the literature.[139] ^{1}H-NMR (300 MHz, $CDCl_3$): δ 7.30-7.42 (m, 5H), 4.73 (s, 2H), 1.66 (s, 1H).

Cyclohexylmethanol (P16):

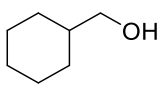

After the hydrogenation, the reaction mixture was diluted with water and extracted with Et_2O (3 × 10 mL). The combined organic extracts were dried over Na_2SO_4 and then the solvent was removed by rotary evaporator (temperature, pressure and time of evaporation had to be carefully controllled, as compound

P15 is quite volatile). The residue was purified by flash column chromatography (DCM), giving a a colorless liquid. Yield: 196 mg (86%). Its physical and spectroscopic data are superimposable with those reported in the literature.[146] ^{1}H-NMR (300 MHz, $CDCl_3$): δ 3.47 (d. *J* = 6.4 Hz, 2H), 1.83 -1.66, (m, 5H), 1.56-1.39 (m, 2H), 1.35-1.12 (m, 3H), 0.97 (m, 2H).

4.5.5 X-Ray Crystal Structure Analysis of Iron Complex 81

Crystals suitable for X-ray diffraction analysis have been obtained by cooling a saturated solution of the [bis(hexamethylene)cyclopentadienone]iron complex **81** in *n*-hexane/DCM solution. Crystal data and details of data collection and refinement are given in Table 23 and Table 24. X-Ray structure analysis was conducted using a Bruker D8 Venture equipped with a copper micro focus source and Photon 100 detector. The analysis program used was Apex 3. The structures were solved with Shelxt and refined using the program Shelxl.[151]

Table 23. X-Ray Crystal data and structure refinement of complex **81.**

Object	Values	Additional Values
Empirical formula	$C_{20}H_{24}FeO_4$	
Moiety formula	$C_{20}H_{24}FeO_4$	
Formula weight	384.24	
Temperature	100(2) K	
Wavelength	1.54178 Å	
Crystal system	Monoclinic	
Space group	$P2_1/n$	
Unit cell dimensions	a = 9.7015(3) Å	α= 90°
	b = 16.0131(5) Å	β= 102.5480(10)°
	c = 11.9162(4) Å	γ = 90°
Volume	1806.98(10) Å^3	
Z	4	
Density (calculated)	1.412 Mg/m^3	
Absorption coefficient	6.869 mm^{-1}	
F(000)	808	
Crystal size	0.100 × 0.100 × 0.050 mm^3	
Theta range for data collection	4.699 to 72.289°.	
Index ranges	-10<=h<=11, -19<=k<=19, -14<=l<=14	
Reflections collected	18911	
Independent reflections	3539 [R(int) = 0.0385]	
Completeness to θ = 67.679°	99.5%	

Absorption correction	Multiscan
Max. and min. transmission	0.7536 and 0.5330
Refinement method	Full-matrix least-squares on F^2
Data / restraints / parameters	3539 / 0 / 244
Goodness-of-fit on F^2	0.739
Final R indices [I>2σ(I)]	R1 = 0.0315, ωR2 = 0.0803
R indices (all data)	R1 = 0.0347, ωR2 = 0.0836
Extinction coefficient	n/a
Largest diff. peak and hole	0.308 and -0.389 e.$Å^{-3}$

Table 24. Selected bond lengths [Å] and angles [°] for complex **81.**

Atoms	Bond length and angles	Atoms	Bond length and angles
Fe(1)-C(3)	1.799(2)	Fe(1)-C(2)	1.801(2)
Fe(1)-C(1)	1.8004(19)	Fe(1)-C(3)	1.799(2)
Fe(1)-C(2)	1.801(2)	Fe(1)-C(1)	1.8004(19)
Fe(1)-C(7)	2.0718(17)	Fe(1)-C(2)	1.801(2)
Fe(1)-C(6)	2.0789(17)	Fe(1)-C(7)	2.0718(17)
Fe(1)-C(8)	2.1140(17)	Fe(1)-C(6)	2.0789(17)
Fe(1)-C(5)	2.1246(18)	Fe(1)-C(8)	2.1140(17)
Fe(1)-C(4)	2.3968(18)	Fe(1)-C(5)	2.1246(18)
O(1)-C(1)	1.138(2)	Fe(1)-C(4)	2.3968(18)
O(2)-C(2)	1.142(3)	O(1)-C(1)	1.138(2)
O(3)-C(3)	1.140(2)	O(2)-C(2)	1.142(3)
O(4)-C(4)	1.241(2)	O(3)-C(3)	1.140(2)
C(4)-C(8)	1.471(2)	O(4)-C(4)	1.241(2)
C(4)-C(5)	1.478(2)	C(4)-C(8)	1.471(2)
C(5)-C(6)	1.439(2)	C(4)-C(5)	1.478(2)
C(6)-C(7)	1.429(3)	C(5)-C(6)	1.439(2)
C(7)-C(8)	1.439(2)	C(6)-C(7)	1.429(3)
C(8)-C(4)-C(5)	103.53(15)	C(7)-C(8)	1.439(2)
C(6)-C(5)-C(4)	108.36(15)	C(8)-C(4)-C(5)	103.53(15)
C(7)-C(6)-C(5)	107.95(15)	C(6)-C(5)-C(4)	108.36(15)
C(6)-C(7)-C(8)	107.96(15)	C(7)-C(6)-C(5)	107.95(15)
C(7)-C(8)-C(4)	108.58(15)	C(6)-C(7)-C(8)	107.96(15)
Fe(1)-C(3)	1.799(2)	C(7)-C(8)-C(4)	108.58(15)

Fe(1)-C(1)	1.8004(19)		
Atoms	**Selected torsion angles [°]**	**Atoms**	**Selected torsion angles [°]**
C(4) C(5) C(6) C(7)	-11.83(19)	C(7) C(6) C(15) C(16)	90.3(2)
C(5) C(6) C(7) C(8)	0.03(19)	C(6) C(5) C(20) C(19)	82.4(2)
C(6) C(7) C(8) C(4)	11.84(18)	C(8) C(7) C(14) C(13)	87.9(2)
C(8) C(4) C(5) C(6)	18.37(18)	C(7) C(8) C(9) C(10)	-79.7(2)
C(5) C(4) C(8) C(7)	-18.38(18)		

Planarity of 5-membered ring:

Distance from C(4) to lspl (C(5) C(6) C(7) C(8)) : 0.287(2)

see Listing

Least-Squares Planes - P*X+Q*Y+R*Z=S :: First Line Orthogonal(XO,YO,ZO), Second Line Fractional(X,Y,Z)

========== Ring/Plan/Resd/Lspl N Indicates that the Ring/Plane/Residue Involves N Atoms

Sigref - R.M.S-Error of the Contributing Atoms

The Deviation D of an Atom with Sigpln - Sqrt(Sum(j=1:N)(D(j)**2/(N-3))

Chisq - Chi-Squared = Sum(j=1:N)(D(j)**2)/Sigref**2

Fractional Coordinates X,Y,Z may be Pl.Hyp. - Result of the Chi.Sq. Test for Planarity (See Stout & Jensen, p424)

Calculated via Substitution in

**** - Atoms Deviating by More Than 1.5 Angstrom and Hydrogen Atoms are NOT Listed

D = P*X + Q*Y + R*Z - S (2nd Line) Note - Weights : UNIT

**** - Maximum Metal Containing Ring Size: 6

- Maximum Number of Bonds to Ring Metal: 6

- Deviations from planes are in Ångström Units

- The Plane determining Atoms have been Marked #

- DISTANCES TO PLANES ROUNDED TO 3 DECIMALS

Nr 1 P Q R S Sigref 0.002 Sigpln 0.127 Chisq 10186.9 Pl.Hyp. P<5

Lspl 0.1670(9) 0.9829(2) 0.0781(9) 5.653(4) #C(4) 0.112(2) #C(5) -0.092(2) #C(6) 0.037(2) #C(7) 0.036(2)

A 5 1.620(8) 15.739(3) 0.476(10) 5.653(4) #C(8) -0.092(2) O(4) 0.292(1) C(9) -0.086(2) C(10) 1.318(2)

C(14) 0.267(2) C(15) 0.219(2) C(19) 1.371(2) C(20) -0.060(2)

Nr 2 P Q R S Sigref 0.002 Sigpln 0.001 Chisq 0.2 Pl.Hyp.

Lspl 0.2121(10) 0.9643(3) 0.1586(11) 6.016(5) #C(5) 0.000(2) #C(6) 0.000(2) #C(7) 0.000(2) #C(8) 0.000(2)

A 4 2.058(9) 15.441(5) 1.296(13) 6.016(5) O(4) 0.582(1) C(4) 0.287(2) C(9) 0.052(2) C(10) 1.461(2)

C(14) 0.121(2) C(15) 0.071(2) C(20) 0.076(2)

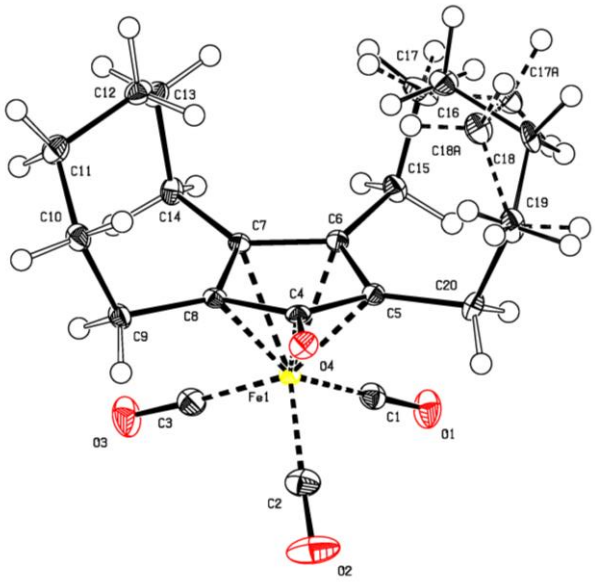

Figure 26. ORTEP diagram of the molecular structure of the [bis(hexamethylene)cyclopentadienone]iron complex **81** (CCDC 1511079).

4.5.6 Determination of the Hydrogenation Kinetics of Acetophenone

Abbreviations used: $R_{sub.,t}$ = fraction of unreacted substrate Acetophenone ($R_{sub.,0} = 1$); $C_{cat.}$ = catalyst concentration; $C_{0,S4}$ = initial substrate concentration.

Experimental parameters: T = 243.15 K; $C_{0,S}$ = 0.501 M; $C_{cat.}$ = 5 mM; solvent: 5:2 *i*PrOH/H_2O; $P_{hydrogen}$ = 30 bar.

General procedure. The kinetic experiments were carried out using a computer-controlled Parr multireactor. Each reaction was set up as follows: the pre-catalyst (0.03508 mmol, 0.01 eq.) was weighted in a glass vessel and, after purging with argon for 2 minutes, it was dissolved in dry *i*PrOH (5 mL), and then a solution of Me_3NO (5.3 mg, 0.07016 mmol, 0.02 eq.) in H_2O (2 mL) was added. The resulting solution was stirred for 10 minutes, and then the vessel was placed into the autoclave, evacuated and filled with hydrogen (P = 30 bar). Mechanical stirring (300 rpm) was immediately started together with heating (70 °C), and the reaction was run overnight measuring the hydrogen uptake, from which conversion values were calculated. The final conversion was confirmed by GC analysis of the crude reaction mixture.

Note: time = 0 was marked when the reactor was filled with hydrogen. Pseudo-first order rate constants k_{app} and corresponding half-lives $t_{1/2}$ were determined from the slope of a linear least squares fit to the graph of $\ln(R_{sub.,t}) = -kt$. Second order constants k were calculated dividing k_{app} by c_{cat} (assumed to be constant).

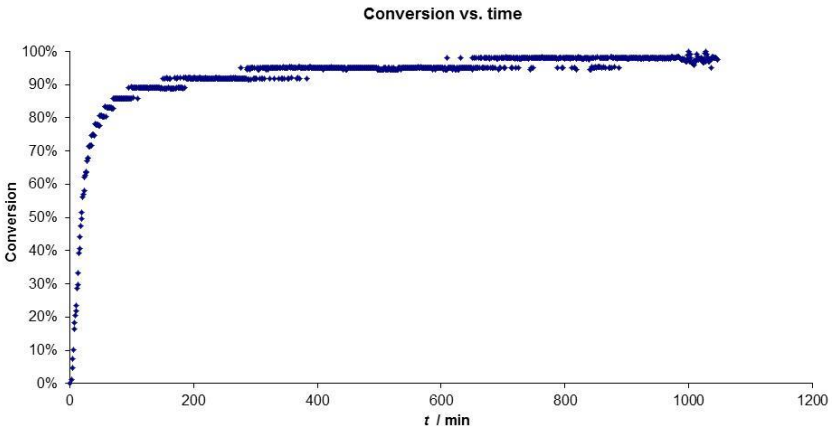

Figure 27. Kinetics of the hydrogenation of acetophenone promoted by pre-catalyst **81** activated with Me_3NO.

Table 25. Kinetic parameters of the hydrogenation of acetophenone promoted by pre-catalyst **81** activated with Me_3NO.

Regression interval = 12-24 min		
Linear regression	**Slope**	**Intercept**
	-0,0360	0,0000
Standard error =	0,0010	#N/D
R^2 =	0,9899	0,0695
F index =	1174,7910	12,0000
	5,6825	0,0580
k_{app} (min^{-1}) =	**0,036**	
$t_{1/2}$ (min) = ln(2) / k =	**19,27**	
k ($L\ mol^{-1}\ min^{-1}$) =	**7,19**	

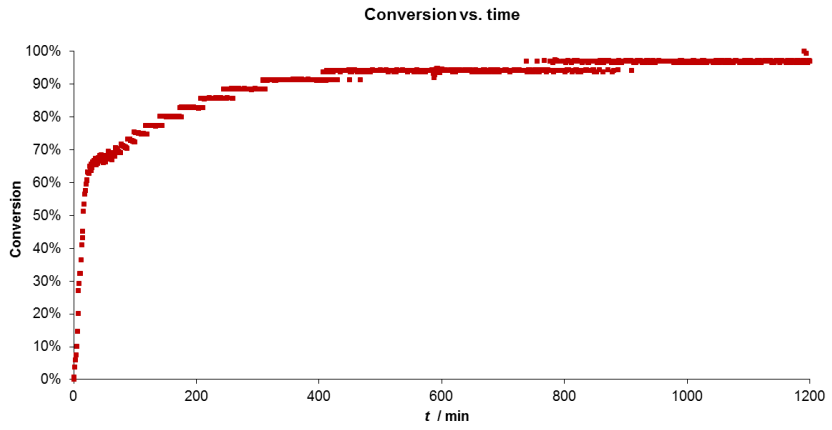

Figure 28. Kinetics of the hydrogenation of acetophenone promoted by pre-catalyst **30** activated with Me_3NO.

Table 26. Kinetic parameters of the hydrogenation of acetophenone promoted by pre-catalyst **30** activated with Me_3NO

Regression interval = 6 - 16 min		
Linear regression	Slope -0,0396	Intercept 0,0000
Standard error =	0,0012	#N/D
R^2 =	0,9916	0,0439
F index =	1174,5795	10,0000
	2,2630	0,0193
k_{app} (min^{-1}) =	0,040	
$t_{1/2}$ (min) = ln(2) / k =	17,49	
k (L mol^{-1} min^{-1}) =	7,93	

4.5.7 Catalytic Tests – Transfer Hydrogenation of Imines – General Procedure

4.5.7.1 General Procedure for the CTH of pre-formed aldimines

Pre-catalyst **81** (1.9 mg, 0.005 mmol, 0.01 eq.) and Me_3NO (0.8 mg, 0.010 mmol, 0.02 eq.) were dissolved in dry *i*PrOH (0.05 mL) and the resulting solution, which gradually turned from yellow to dark red, was stirred for 20 minutes at r.t.. The imine substrate (0.5 mmol, 1 eq.) was added, followed by dry *i*PrOH (1.9 mL). The reaction vessel was sealed and stirred in a pre-heated oil bath at 100 °C for 18 h. The volatiles were removed and the crude was purified by flash column chromatography (hexane/AcOEt).

4.5.7.2 General Procedure for the CTH of pre-formed ketimines

Pre-catalyst **81** (3.8 mg, 0.010 mmol, 0.02 eq.) and Me_3NO (1.6 mg, 0.020 mmol, 0.04 eq.) were dissolved in dry *i*PrOH (0.1 mL) and the resulting solution, which gradually turned from yellow to dark red, was stirred for 20 minutes at r.t.. The imine substrate (0.5 mmol, 1 eq.) was added, followed by dry *i*PrOH (1.9 mL). The reaction vessel was sealed and stirred in a pre-heated oil bath at 100 °C for 18 h. The volatiles were removed and the crude was purified by flash column chromatography (hexane/AcOEt).

4.5.7.3 General Procedure for the reductive amination of aldimines

3 Å MS (400 mg), the aldehyde (0.5 mmol, 1 eq.) and the amine (0.75 mmol, 1.5 eq.) were dissolved in dry toluene (0.5 mL) and the mixture was stirred for 1 h at 100 °C. Meanwhile, in another vessel, pre-catalyst **81** (9.6 mg, 0.025 mmol, 0.05 eq.) and Me_3NO (1.9 mg, 0.025 mmol, 0.05 eq.) were dissolved in dry *i*PrOH (0.25 mL). The activated catalyst solution was dispensed into the vessel containing the imine, followed by dry *i*PrOH (1.2 mL). The reaction vessel was sealed and stirred in a pre-heated oil bath at 100 °C for 18 h. The volatiles were removed and the crude was purified by flash column chromatography (hexane/AcOEt).

4.5.7.4 General Procedure for the reductive amination of ketimines

3 Å MS (400 mg), the aldehyde (0.5 mmol, 1 eq.), the amine (0.75 mmol, 1.5 eq.) and TFA (4 μL, 0.05 mmol, 0.1 eq., dispensed as a stock solution in toluene) were dissolved in dry toluene (final total volume: 0.5 mL) and stirred for 2 h at 100 °C. Meanwhile, in another vessel, pre-catalyst **81** (9.6 mg, 0.025 mmol, 0.05 eq.) and Me_3NO (1.9 mg, 0.025 mmol, 0.05 eq.) were dissolved in dry *i*PrOH (0.25 mL). Freshly distilled DIPEA (13 μL, 0.075 mmol, 0.15 eq.) and then the activated catalyst solution was dispensed into the vessel containing the imine, followed by dry *i*PrOH (1.2 mL). The reaction vessel was sealed and stirred at 100 °C for 18 h. The volatiles were removed and the crude was purified by flash column chromatography (hexane/AcOEt).

4.5.7.5 Imines Conversions

NMR conversions were calculated from the signal integrals (all the substrates and reduction products are known compounds, and our spectra are superimposable to those reported in the literature). The NMR spectra were measured taking $d1$ = 20 s.

Amines (name, chemical formula)	**^{1}H NMR**
4-Methoxy-*N*-(1-phenylethyl)aniline (P21):[152]	
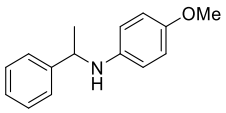	^{1}H NMR (400 MHz, CD_2Cl_2) δ 7.62-7.10 (m, 5H), 6.71 (d, *J* = 8.9 Hz, 2H), 6.51 (d, *J* = 8.9 Hz, 2H), 4.47 (q, *J* = 6.7 Hz, 1H), 3.91 (d, *J* = 18.4 Hz, 1H), 3.71 (s, 3H), 1.52 (d, *J* = 6.7 Hz, 3H).
***N*-Benzylaniline (P22):**[153]	
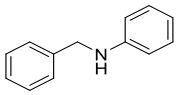	^{1}H NMR (400 MHz, CD_2Cl_2) δ 7.46-7.33 (m, 4H), 7.32-7.23 (m, 1H), 7.16-7.07 (m, 2H), 6.70-6.61 (m, 1H), 6.59-6.52 (m, 2H), 4.59-4.51 (m, 1H), 4.19 (s, 1H), 1.55 (d, *J* = 6.8 Hz, 3H).
4-Methoxy-*N*-(pyridin-2-ylmethyl)aniline (P23):[128]	
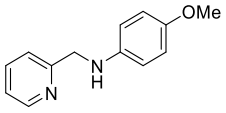	^{1}H NMR (400 MHz, $CDCl_3$) δ 8.63-8.56 (m, 1H), 7.67 (td, *J* = 7.7, 1.8 Hz, 1H), 7.37 (d, *J* = 7.8 Hz, 1H), 7.21 (ddd, *J* = 7.6, 4.9, 1.1 Hz, 1H), 6.85-6.76 (m, 2H), 6.70-6.62 (m, 2H), 4.51 (s, 1H), 4.45 (s, 2H), 3.75 (s, 3H).
***N*-(Furan-2-ylmethyl)-4-methoxyaniline (P24):**[128]	
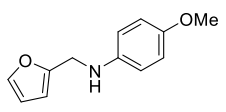	^{1}H NMR (400 MHz, $CDCl_3$) δ 7.38 (dd, *J* = 1.8, 0.9 Hz, 1H), 6.85-6.79 (m, 2H), 6.77-6.71 (m, 2H), 6.39-6.24 (m, 2H), 4.31 (s, 2H), 3.77 (s, 3H).

4-Methoxy-*N*-(4-methoxybenzyl)aniline (P25): [128]

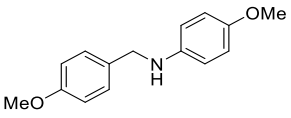

^{1}H NMR (400 MHz, Acetone-d_6) δ 7.32 (d, J = 8.6 Hz, 2H), 6.93-6.84 (m, 2H), 6.77-6.67 (m, 2H), 6.67-6.56 (m, 2H), 4.94 (s, 1H), 4.23 (d, J = 4.6 Hz, 2H), 3.78 (s, 3H), 3.68 (s, 3H).

***N*-Benzyl-1-(furan-2-yl)methanamine (P26):**[154]

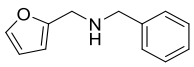

^{1}H NMR (400 MHz, Acetone-d_6) δ 7.47 (dd, J = 1.9, 0.9 Hz, 1H), 7.39-7.21 (m, 5H), 6.37 (dd, J = 3.2, 1.9 Hz, 1H), 6.24 (dd, J = 3.1, 0.9 Hz, 1H), 3.78 (s, 2H), 3.75 (s, 2H).

***N*-Benzyl-1-(pyridin-2-yl)methanamine (P27):** [155]

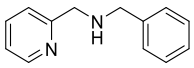

^{1}H NMR (400 MHz, Acetone-d_6) δ 8.54-8.52 (m, 1H), 7.74 (td, J = 7.6, 1.8 Hz, 1H), 7.49-7.19 (m, 7H), 3.88 (s, 2H), 3.83 (s, 2H).

***N*-(4-Methoxybenzyl)aniline (P28):**[153]

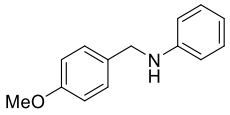

^{1}H NMR (400 MHz, Acetone-d_6) δ 7.32 (d, J = 8.3 Hz, 2H), 7.15-7.02 (m, 2H), 6.91-6.86 (m, 2H), 6.66 (d, J = 8.0 Hz, 2H), 6.57 (t, J = 7.3 Hz, 1H), 5.31 (s, 1H), 4.28 (d, J = 5.6 Hz, 2H), 3.78 (s, 3H).

***N*-(4-Methylbenzyl)aniline (P29):** [156]

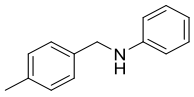

^{1}H NMR (400 MHz, Acetone-d_6) δ 7.29 (d, J = 7.8 Hz, 2H), 7.14 (d, J = 7.8 Hz, 2H), 7.08 (dd, J = 8.6, 7.2 Hz, 2H), 6.66 (dd, J = 8.6, 1.1 Hz, 2H), 6.61-6.54 (m, 1H), 5.36 (s, 1H), 4.31 (d, J = 5.7 Hz, 2H), 2.31 (s, 3H).

***N*-(1-Phenylethyl)aniline (P30):**[153]

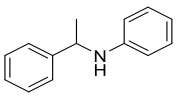

^{1}H NMR (400 MHz, CD_2Cl_2) δ 7.49-7.33 (m, 4H), 7.31-7.24 (m, 1H), 7.11 (dd, J = 8.6, 7.3 Hz, 2H), 6.71-6.61 (m, 1H), 6.61-6.51 (m, 2H), 4.60-4.48 (m, 1H), 4.19 (s, 1H), 1.55 (d, J = 6.8 Hz, 3H).

***N*-(4-Methoxyphenyl)-1,2,3,4-tetrahydronaphthalen-1-amine (P31):**[157]

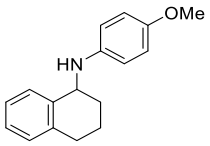

^{1}H NMR (400 MHz, CD_2Cl_2) δ 7.45-7.36 (m, 1H), 7.23-7.11 (m, 3H), 6.82 (d, J = 8.9 Hz, 2H), 6.71-6.65 (m, 2H), 4.58 (t, J = 5.1 Hz, 1H), 3.78 (s, 3H), 2.91-2.74 (m, 2H), 2.03-1.81 (m, 4H).

4-Methoxy-*N*-(1-(4-methoxyphenyl)ethyl)aniline (P32):[158]

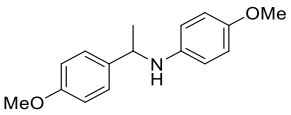

^{1}H NMR (400 MHz, CD_2Cl_2) δ 7.32 (d, J = 8.1 Hz, 2H), 6.90 (d, J = 8.1 Hz, 2H), 6.72 (d, J = 8.2 Hz, 2H), 6.52 (d, J = 8.3 Hz, 2H), 4.43 (q, J = 6.7 Hz, 1H), 3.97-3.85 (m, 1H), 3.82 (s, 3H), 3.72 (s, 3H).

_N_-(1-(4-Bromophenyl)ethyl)-4-methoxyaniline (P33):[158]

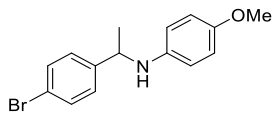

^{1}H NMR (400 MHz, CD_2Cl_2) δ 7.52-7.45 (m, 2H), 7.30 (d, *J* = 8.4 Hz, 2H), 6.75-6.67 (m, 2H), 6.51-6.44 (m, 2H), 4.42 (q, *J* = 6.7 Hz, 1H), 3.90 (d, *J* = 8.8 Hz, 1H), 3.71 (s, 3H), 1.50 (d, *J* = 6.7 Hz, 3H).

4-Methoxy-_N_-(1-(naphthalen-2-yl)ethyl)aniline (P34): [159]

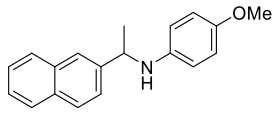

^{1}H NMR (400 MHz, CD_2Cl_2) δ 7.89-7.83 (m, 4H), 7.56 (dd, *J* = 8.4, 1.7 Hz, 1H), 7.54-7.45 (m, 2H), 6.70 (d, *J* = 8.9 Hz, 2H), 6.56 (d, *J* = 8.9 Hz, 2H), 4.63 (q, *J* = 6.7 Hz, 1H), 4.03 (s, 1H), 3.69 (s, 3H), 1.61 (d, *J* = 6.7 Hz, 3H).

4-Methoxy-_N_-(1-phenylpropyl)aniline (P35): [160]

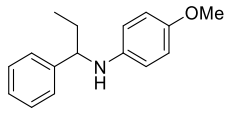

^{1}H NMR (400 MHz, $CDCl_3$) δ 7.36-7.28 (m, 5H), 7.25-7.18 (m, 1H), 6.73-6.64 (m, 2H), 6.52-6.39 (m, 2H), 4.15 (t, *J* = 6.7 Hz, 1H), 3.69 (s, 3H), 1.92-1.67 (m, 2H), 0.94 (t, *J* = 7.4 Hz, 3H).

_N_-(1-(4-Bromophenyl)ethyl)aniline (P36):[161]

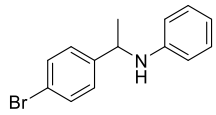

^{1}H NMR (400 MHz, CD_2Cl_2) δ 7.44-7.34 (m, 8H), 7.32-7.26 (m, 2H), 6.77-6.67 (m, 2H), 6.60-6.49 (m, 2H), 4.21-4.07 (m, 1H), 3.71 (s, 3H), 1.57 (s, 3H).

_N_-(1-(4-Methoxyphenyl)ethyl)aniline (P37):[162]

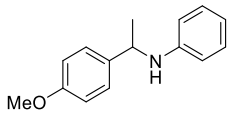

^{1}H NMR (400 MHz, Acetone-d_6) δ 7.34 (d, *J* = 8.3 Hz, 2H), 7.00 (t, *J* = 7.7 Hz, 2H), 6.87 (d, *J* = 8.3 Hz, 2H), 6.63-6.44 (m, 3H), 5.29 (d, *J* = 6.1 Hz, 1H), 4.49 (p, *J* = 6.6 Hz, 1H), 3.77 (s, 3H), 1.47 (d, *J* = 6.8 Hz, 3H).

4-Methoxy-_N_-(octan-2-yl)aniline (P38):[163]

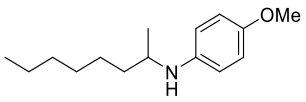

^{1}H NMR (400 MHz, Acetone-d_6) δ 6.73 (d, *J* = 9.0 Hz, 2H), 6.57 (d, *J* = 9.0 Hz, 2H), 4.14 (s, 1H), 3.69 (s, 3H), 3.39 (q, *J* = 6.1 Hz, 1H), 1.50-1.23 (m, 5H), 1.13 (d, *J* = 6.3 Hz, 3H), 0.94-0.82 (m, 3H).

_N_-Benzhydryl-4-methoxyaniline (P39):[164]

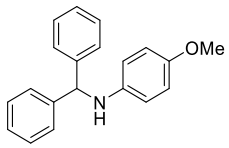

^{1}H NMR (400 MHz, CD_2Cl_2) δ 7.47-7.33 (m, 9H), 7.33-7.24 (m, 2H), 6.77-6.67 (m, 2H), 6.58-6.48 (m, 2H), 5.48 (s, 1H), 3.71 (s, 3H).

_N_-Benzyl-1-phenylethan-1-amine (P40):[165]

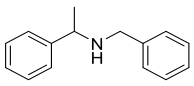

^{1}H NMR (400 MHz, $CDCl_3$) δ 7.44-7.22 (m, 10H), 3.85 (q, *J* = 6.6 Hz, 1H), 2.19 (s, 2H), 1.41 (d, *J* = 6.6 Hz, 3H).

_N_-(1-(2-Methoxyphenyl)ethyl)aniline (P41):

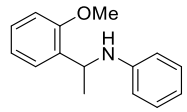

^{1}H NMR (400 MHz, Acetone-d_6) δ 7.37 (dd, J = 7.7, 1.8 Hz, 1H), 7.18 (td, J = 7.8, 1.8 Hz, 1H), 6.99 (dd, J = 8.6, 7.3 Hz, 3H), 6.85 (td, J = 7.5, 1.1 Hz, 1H), 6.58-6.45 (m, 3H), 5.31 (d, J = 6.9 Hz, 1H), 4.89 (p, J = 6.8 Hz, 1H), 3.94 (s, 3H), 1.44 (d, J = 6.7 Hz, 3H)

_N_-(4-Methylpentan-2-yl)aniline (P42):[166]

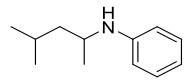

^{1}H NMR (400 MHz, Acetone-d_6) δ 6.77-6.67 (m, 2H), 6.63-6.55 (m, 2H), 3.69 (s, 3H), 3.55-3.42 (m, 1H), 1.81 (dt, J = 13.5, 6.7 Hz, 1H), 1.49 (dt, J = 14.0, 7.1 Hz, 1H), 1.34-1.19 (m, 2H), 1.12 (d, J = 6.2 Hz, 3H), 0.93 (dd, J = 12.1, 6.6 Hz, 7H).

_N_-Benzyl-4-methoxyaniline (P43):[167]

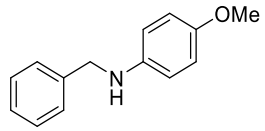

^{1}H NMR (400 MHz, $CDCl_3$) δ 7.53-7.20 (m, 6H), 6.90-6.77 (m, 2H), 6.74-6.63 (m, 2H), 4.32 (s, 2H), 3.77 (s, 3H).

2-(((4-Methoxyphenyl)amino)methyl)phenol (P44):[168]

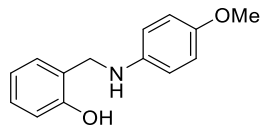

^{1}H NMR (400 MHz, $CDCl_3$) δ 7.21 (t, J = 7.7 Hz, 1H), 7.09 (d, J = 7.3 Hz, 1H), 6.93 (d, J = 8.1 Hz, 1H), 6.88-6.77 (m, 5H), 4.37 (s, 2H), 3.76 (s, 3H).

_N_-(Cyclohexylmethyl)-4-methoxyaniline (P45):[167]

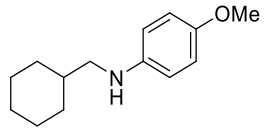

^{1}H NMR (400 MHz, $CDCl_3$) δ 6.81 (d, J = 8.9 Hz, 2H), 6.69 (dd, J = 7.3, 4.8 Hz, 2H), 3.77 (s, 3H), 2.95 (d, J = 6.6 Hz, 2H), 1.90-1.81 (m, 2H), 1.82-1.56 (m, 3H), 1.35-1.14 (m, 4H), 1.00 (qd, J = 11.9, 3.4 Hz, 2H).

4-Methoxy-_N_-(4-methylbenzyl)aniline (P46):[169]

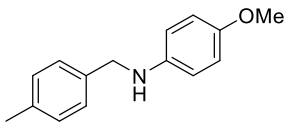

^{1}H NMR (400 MHz, $CDCl_3$) δ 7.29 (d, J = 7.7 Hz, 2H), 7.18 (d, J = 7.9 Hz, 2H), 6.87-6.76 (m, 2H), 6.71-6.61 (m, 2H), 4.27 (s, 2H), 3.77 (s, 3H), 2.37 (s, 3H).

_N_-Cinnamyl-4-methoxyaniline (P47):[86]

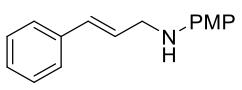

^{1}H NMR (400 MHz, $CDCl_3$) δ 7.42-7.38 (m, 2H), 7.36-7.31 (m, 2H), 7.29-7.25 (m, 1H), 6.83 (d, J = 9.0 Hz, 2H), 6.70 (d, J = 8.9 Hz, 2H), 6.69-6.60 (m, 1H), 6.37 (dt, J = 15.9, 5.9 Hz, 1H), 3.93 (dd, J = 5.9, 1.6 Hz, 2H), 3.78 (s, 3H).

_N_-Isobutyl-4-methoxyaniline (P48):[170]

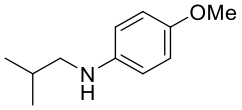

^{1}H NMR (400 MHz, $CDCl_3$) δ 6.89-6.64 (m, 4H), 3.77 (s, 3H), 2.93 (d, J = 6.8 Hz, 2H), 1.91 (dq, J = 13.5, 6.7 Hz, 1H), 1.01 (d, J = 6.7 Hz, 6H).

_N_-Benzyl-2-phenylethan-1-amine (P50):[171]

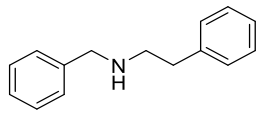

^{1}H NMR (400 MHz, $CDCl_3$) δ 7.39-7.16 (m, 10H), 3.84 (s, 2H), 2.98-2.91 (m, 2H), 2.91-2.83 (m, 2H).

_N_-(Furan-2-ylmethyl)-2-phenylethan-1-amine (P51):[172]

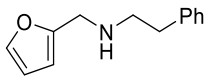

^{1}H NMR (400 MHz, $CDCl_3$) δ 7.39-7.37 (m, 1H), 7.34-7.29 (m, 1H), 7.26-7.19 (m, 3H), 6.36-6.28 (m, 1H), 6.21 (d, J = 3.0 Hz, 1H), 3.85 (s, 2H), 2.98-2.81 (m, 3H), 1.94 (bs, 1H).

_N_-(4-Methylbenzyl)-2-phenylethan-1-amine (P52):[173]

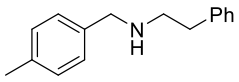

^{1}H NMR (400 MHz, $CDCl_3$) δ 7.36-7.10 (m, 9H), 3.80 (s, 2H), 2.97-2.82 (m, 4H), 2.35 (s, 3H), 1.80 (s, 1H).

_N_-Cyclohexyl-4-methoxyaniline (P53):[169]

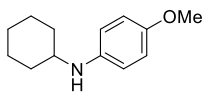

^{1}H NMR (400 MHz, $CDCl_3$) δ 6.76 (d, J = 8.8 Hz, 2H), 6.56 (d, J = 8.8 Hz, 2H), 3.72 (s, 3H), 3.16-3.11 (m, 2H, including an NH), 2.05-2.02 (m, 2H), 1.77-1.72 (m, 2H), 1.71-1.62 (m, 1H), 1.36-1.08 (m, 5H).

4-Methoxy-_N_-(4-phenylbutan-2-yl)aniline (P54):[174]

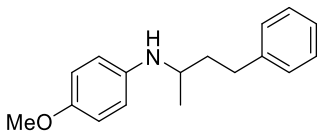

^{1}H NMR (400 MHz, $CDCl_3$) δ 7.35-7.27 (m, 2H), 7.25-7.18 (m, 3H), 6.64-6.50 (m, 4H), 3.77 (d, J = 0.9 Hz, 3H), 3.43 (h, J = 6.3 Hz, 1H), 2.76 (t, J = 7.9 Hz, 2H), 1.97-1.85 (m, 1H), 1.83-1.70 (m, 1H), 1.22 (d, J = 6.3 Hz, 3H).

CHAPTER 5

ASYMMETRIC REDUCTION OF IMINES WITH A CHIRAL KNÖLKER CATALYST

In 2015, our research group reported a new class of chiral (cyclopentadienone)iron pre-catalysts **36** (Figure 29) for the enantioselective hydrogenation of ketones (see Chapter 1).[80] Building on the experience gained in the hydrogenation of imines with pre-catalyst **81**, we tested complexes **36** also in the asymmetric hydrogenation of ketoimines.

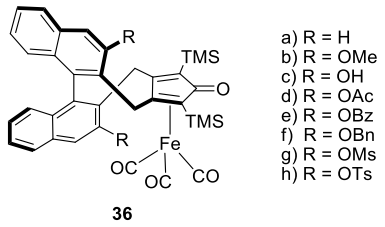

Figure 29. Asymmetric hydrogenation of ketones promoted by chiral complex **36.**

5.1 SYNTHESIS OF CHIRAL (CYCLOPENTADIENONE)IRON COMPLEXES

First, we re-synthesized several of the chiral complexes shown in Figure 29 from (*R*)-BINOL, following the published methodology.[80] The synthesis of pre-catalyst (*R*)-**36a** (Scheme 53) starts with a BINOL triflation with trifluoromethanesulfonic anhydride to afford 2,2'-bis-triflate **45**. With a Kumada coupling, 2,2'-bis-triflate **45** was converted to (*R*)-2,2'-dimethyl-1,1'-bisnaphthalene **46**. Bismethylnaphthalene **46** was brominated under Wohl-Ziegler conditions to afford the bis-bromide **47a**. A Finkelstein substitution gave the bis-iodide **92a** which serves as precursor for the copper(I)-catalyzed displacement of the iodide with ethinyltrimethylsilyl magnesium bromide.

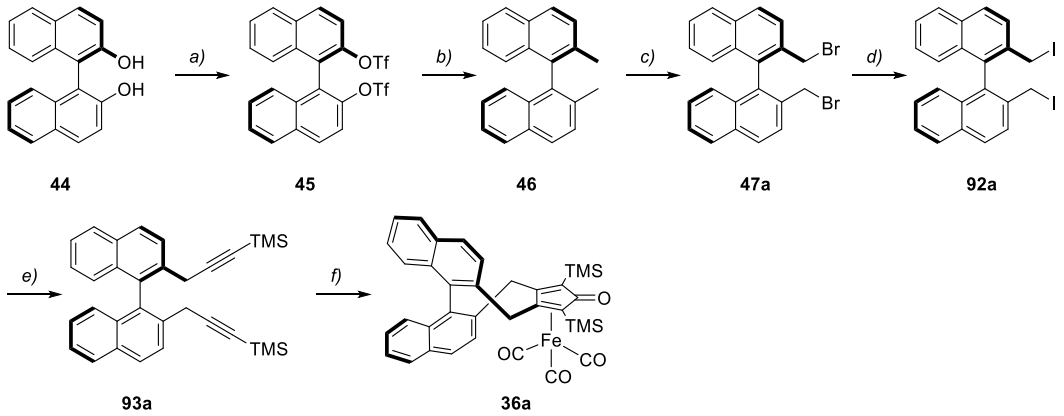

Scheme 53. Synthetic pathway followed for complex **36a**. REAGENTS and CONDITIONS: *a*) Tf_2O, TEA, DCM, -78 °C to 23°C, 2 h, Y.: quant. (**45**); *b*) MeMgI, $NiCl_2$(dppp), Et_2O, 0 to 40 °C, overnight, Y.: quant. (**46**); *c*) NBS,

Benzoyl peroxide, CCl_4, vis-light, 75 °C, overnight, Y.: 70% (**47a**); *d*) NaI, acetone, reflux, Y.: 96% (**92a**); *e*) TMS-acetylene, EtMgBr, CuI, dry THF, -60 °C – 23 °C, overnight; f) $Fe_2(CO)_9$, toluene, 80 °C, 5h, Y.: 53% over two steps (**36a**).

In the following step, the diyne **93a** was subjected to cyclative carbonylation to afford the pentadieneone iron complex (*R*)-**36a**.

Pre-catalysts (*R*)-**36b** and (*R*)-**36c** also derive from (*R*)-BINOL (Scheme 54). Using *n*-butyllithium, the MOM-protected (*R*)-BINOL **48** was *ortho*-lithiated in 3-3' positions and then converted into the 3,3'-bis-boronate **49**. Oxidation of bis-boronate **49** afforded the 3,3'-bisphenol **50** which, after alkylation with methyl iodide, yielded the 3,3'-bismethoxy substituted (*R*)-BINOL **51**. MOM-deprotection (**52**), triflation (**53**) and Kumada coupling afforded the 2,2'-dimethyl-3,3'-dimethoxy derivative **54**. Bromination under Wohl-Ziegler conditions and Finkelstein reaction allowed to obtain bis-iodide **92b**. A nucleophilic displacement of iodide by lithium TMS-acetylide gave the diyne **93b**, which represents the starting material for the cyclisation in the presence of diironnonacarbonyl. Following the mechanism of a Pauson-Khand reaction, the chiral Knölker-derived iron complex (*R*)-**36b** was formed. Moreover, the corresponding 3,3'-dihydroxy (*R*)-**36c** was obtained by BBr_3-induced demethylation.

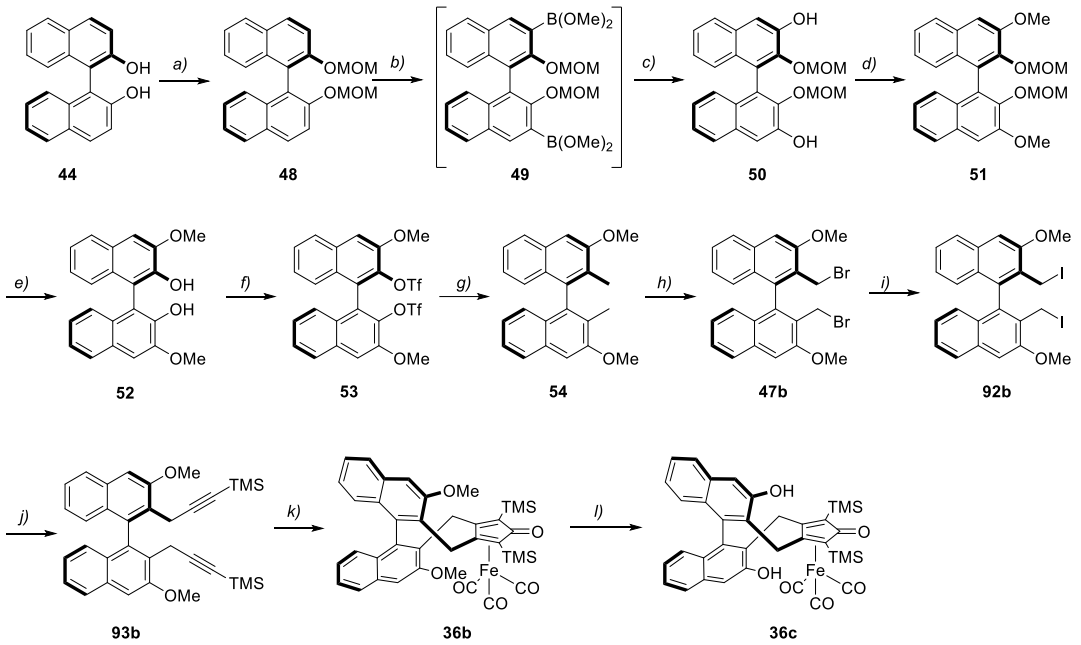

Scheme 54. Synthetic route for synthesis of Iron complexes **36b** and **36c**. REAGENTS and CONDITIONS: a) NaH, MOMCl, THF, 0 °C to 23°C, overnight, Y.: 82% (**48**); b) I) *n*-BuLi, THF, -78 °C to 0 °C; II) $B(OMe)_3$, THF, -78 °C to 23 °C, overnight; *c*) H_2O_2, benzene, 0 °C to 80 °C, 2h; *d*) MeI, K_2CO_3, acetone, 56 °C, overnight, Y.(*b-d*): 60% (**51**); *e*) HCl 37%, dioxane, 40 °C, 4h; *f*) Tf_2O, TEA, DCM, -78 °C to 23°C, 2 h, Y.(*e-f*): 82% (**53**); g) MeMgI, $NiCl_2$(dppp), Et_2O, 0 to 40 °C, overnight, Y.: 81% (**54**); *h*) NBS, Benzoyl peroxide, CCl_4, vis-light, 75 °C, overnight, Y.: 89% (**47b**); *i*) NaI, acetone, reflux, overnight, Y.: quantitative (**92b**); *j*) TMS-acetylene, *n*BuLi, THF, -60 °C to 23 °C, overnight, Y.:

93% (**93b**); *k*) $Fe_2(CO)_9$, Toluene, 80 °C, overnight, Y.: 48% (**36b**); *l*) BBr_3, *n*TBAI, DCE, 0 °C to 84 °C, 3 days, Y.: 80% (**36c**).

As reported by Funk and co-workers in 2012,[107b] it is possible to replace one CO ligand of (cyclopentadienone)iron complexes with a nitrile. The resulting complexes can be activated by thermal dissociation of the labile nitrile ligand (with formation of an empty coordianation site), without need to add an activator such as Me_3NO. Although not always nitrile-substituted (cyclopentadienone)iron complexes perform better than their parent complexes, they are certainly more practical, because the use of an activator is not required in this case. Zhao *et al.* successfully used a nitrile-substituted complex (**39** in Scheme 34) in the transfer hydrogenation of imines.[89] Therefore, we synthesized the acetonitrile and benzonitrile derivatives of complex **36b**. The synthesis is straightforward, and it is shown in Scheme 55.

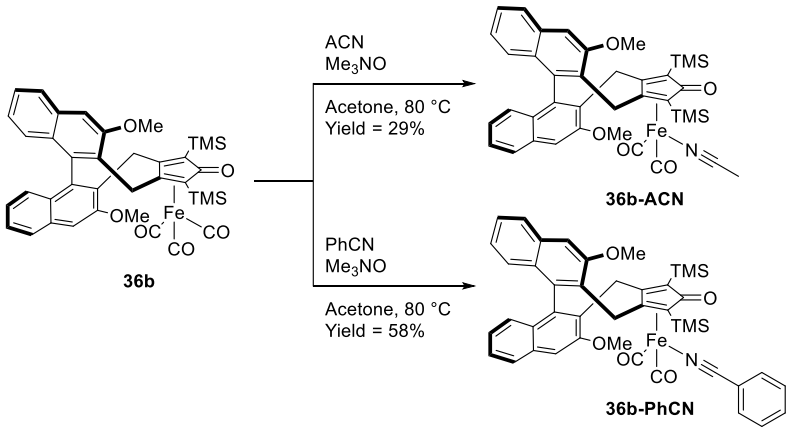

Scheme 55. Synthesis of nitrile-substituted derivatives of the iron complex **36b**.

5.2 Asymmetric Hydrogenation of Imines *in situ* approach – Reductive Amination

Taking inspiration from the reductive amination protocol developed by Renaud and co-workers,[75f] the reactivity of the achiral (cyclopentadienone)iron **30** was tested in the reaction between 4-phenyl-2-butanone and *N*-methyl benzylamine.

Table 27. Attempts for the reductive amination of benzyl acetone promoted by Knölker pre-catalyst 30.[a]

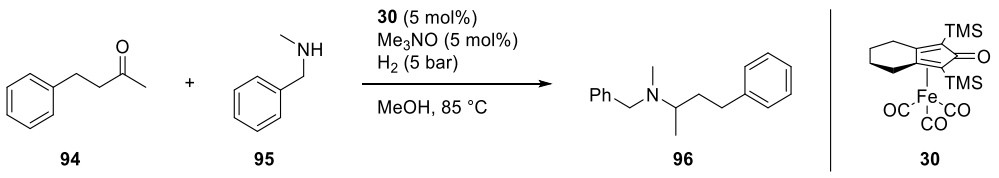

#	95 (eq.)	$C_{0,94}$ (mol L^{-1})	NH_4PF_6	Conv. (%)[b]
1	1.2	1.3	-	12
2	1.2	0.3	-	74
3	1	0.3	-	42
4	1.2	0.3	**10 mol%**	24
5	0.9	0.3	-	27

[a] Reaction conditions: **94**/**30**/Me_3NO = 100:5:5, solvent: MeOH, p_{H2} = 5 atm, T = 85 °C, 16 h, 1 mmol of **95**; [b] Conversion determined by ^1H NMR.

The results in Table 27 show a conversion up to 74%, which is an acceptable starting point for a further optimization. To improve the conversions and compare chiral and achiral pre-catalysts, a screening of different iron complexes was performed. Furthermore, the influence of Lewis acids, different catalytic complexes, different activation procedures and higher hydrogen pressure was assessed. These catalytic attempts (Table 28) were performed using 50 bar of H_2 pressure, which allowed to obtain a notable increase of conversions compared to the results shown in Table 27. Comparison between the Me_3NO-activation of (*R*)-**36b** (Table 28, entry 4) and the use of the isolated (*R*)-**36b-PhCN** (entry 6) shows no dramatic differences: both catalysts lead to very good yields. Instead, (*R*)-**36b-ACN** gave minor conversion (entry 5). The use of additional Lewis acids [$Sc(OTf)_3$, $Fe(acac)_3$, $Ti(OiPr)_4$, entries 8-9 and 17-19] did not improve the conversion to the desired product. The attempts using the chiral (cyclopentadienone)iron complexes (**36b-c**) and their nitrile complexes (**36b-ACN** and **36b-PhCN**) did not lead to good enantioselectivity. The obtained enantiomeric excesses were always around 8%, and the use of Lewis acids additives did not allow to improve the stereoselectivity. Only catalyst (*R*)-**36c**, featuring free OH groups at the 3,3'-position of the binaphthyl system, formed the product of reductive amination with amine **97** with a slightly higher enantiomeric excess (20% *ee*). This finding is possibly due to the hydrogen bond donor properties of the OH group.

Table 28. Attempts for the reductive amination of benzyl acetone promoted by Knölker type iron complexes.[a]

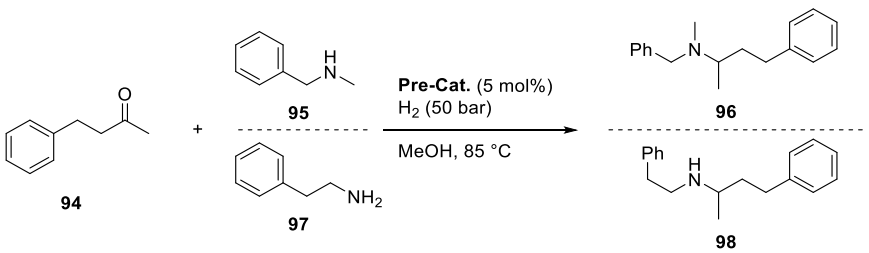

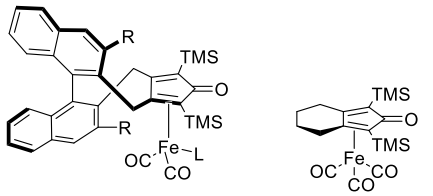

36b: R = OMe; L = CO
36b-ACN:R = OMe; L = ACN
36b-PhCN:R = OMe; L = PhCN
36c: R = OH, L = CO

30 **39** **39-ACN**

#	Cat.	Activation	Amine	Lewis Acid (mol%)	Conv. (%)[b]	*ee* (%)[c]
1	**30**	Me_3NO (10 mol%)	**95**	-	64	-
2	**39-ACN**	-	**95**	-	58	-
3	**39**	-	**95**	-	53	-
4	**36b**	Me_3NO (10 mol%)	**95**	-	83	8
5	**36b-ACN**	-	**95**	-	12	-
6	**36b-PhCN**	-	**95**	-	86	9
7	**36c**	Me_3NO (10 mol%)	**95**	-	62	8
8	**36b**	Me_3NO (10 mol%)	**95**	$Sc(OTf)_3$	83	6
9	**36b**	Me_3NO (10 mol%)	**95**	$Fe(acac)_3$	83	7
10	**30**	Me_3NO (10 mol%)	**97**	-	93	-
11	**39-ACN**	-	**97**	-	97	-
12	**39**	-	**97**	-	78	-
13	**36b**	Me_3NO (10 mol%)	**97**	-	99	8
14	**36b-ACN**	-	**97**	-	68	-
15	**36b-PhCN**	-	**97**	-	86	-
16	**36c**	Me_3NO (10 mol%)	**97**	-	67	20
17	**36b**	Me_3NO (10 mol%)	**97**	$Sc(OTf)_3$	74	8
18	**36b**	Me_3NO (10 mol%)	**97**	$Ti(OiPr)_4$	85	7
19	**36b**	Me_3NO (10 mol%)	**97**	$Fe(acac)_3$	84	8

[a] Reaction conditions: **94**/**Pre-Cat.**/Me_3NO = 100:5:10, solvent: MeOH, p_{H2} = 50 atm, T = 85 °C, 14 h, $C_{s,\mathbf{94}}$ = 0.5 M (1 mmol); [b] Conversion determined by ^1H NMR; [c] *ee* determined by chiral HPLC. In case of amine **97**, the crude product **98** was benzoylated (**28**-**Bz**) for the HPLC analysis.

Although catalyst (*R*)-**36b** and its PhCN derivatives showed a good activity, only very low levels of enantioselectivity were obtained, the use of ketones with more eminent side differentiation might possibly improve the enantiomeric

excess. Indeed, the difference – in terms of steric hinderance – between the methyl and methylene group on the ketone derivative is small. Thus, using pre-catalyst **36b-PhCN** we screened several different ketones featuring substituents with a larger difference in terms of steric bulk. With the exception of product P56 (Table 29, entry 2), no or very low conversion could be obtained, which made the determination of the enantiomeric excess more difficult.

Table 29. Screening of ketones in reductive amination catalyzed by (*R*)-**36b-PhCN.**[a]

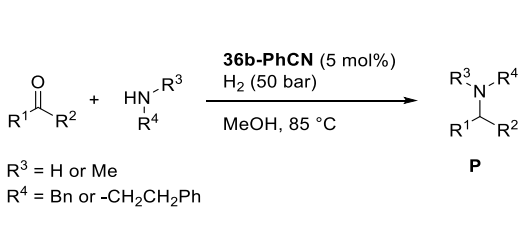

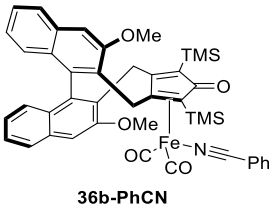

36b-PhCN

#	Product		Yield Amine (%)[b]	*ee* (%)
1	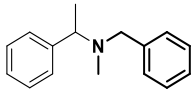	**P55**	12 (78%)[c]	-
2	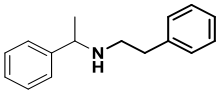	**P56**	85 (6%)[c]	40
3	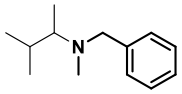	**P57**	-	-
4	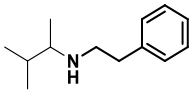	**P58**	-	-
5	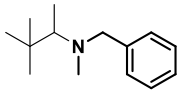	**P59**	-	-
6	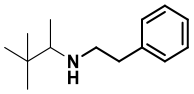	**P60**	-	-
7	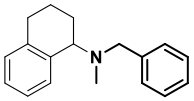	**P61**	15 (16%)[c]	-
8	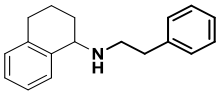	**P62**	Traces	-
9	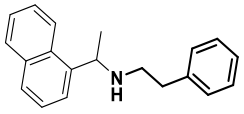	**P63**	Traces	-
10	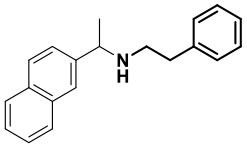	**P64**	Traces	-

[a] Reaction conditions: Ketone/**36b-PhCN** = 100:5, solvent: MeOH, p_{H2} = 50 atm, T = 85 °C, 14 h, C_{ketone} = 0.5 M (1 mmol); [b] Isolated yield; [c] In bracket conversion of corresponding alcohol, bases on ^{1}H NMR spectrum.

Aliphatic ketones underwent degradation under the reaction conditions, since neither the starting material or its reduced form could be recovered. As for aromatic ketones, the bulkier ones were too hindered to form the corresponding Schiff base, so the reaction was too slow compared to the competing reduction of the ketone, giving a prevalence of the corresponding alcohols in the reaction product.[80]

Only the reaction between acetophenone and phenethylamine gave the corresponding α-branched amine in good yield. This was the only reaction whose enantiomeric excess could be determined (by chiral HPLC after derivatization with benzoyl chloride), obtaining an encouraging 40% *ee*. Thus, several *para*-substituted acetophenones were screened in the reductive amination in the presence of phenethylamine (Table 30). Both an achiral and a chiral catalyst were used, because the racemic products were needed to set up the HPLC method for *ee* determination. Unfortunately, some acetophenone derivatives proved unreactive (Table 30, entries 2, 6 and 8) and only two substrates gave appreciable conversion and *ee*.

Table 30. Screening of acetophenone derivatives in reductive amination promoted by **36b-PhCN** and **39-PhCN.**[a]

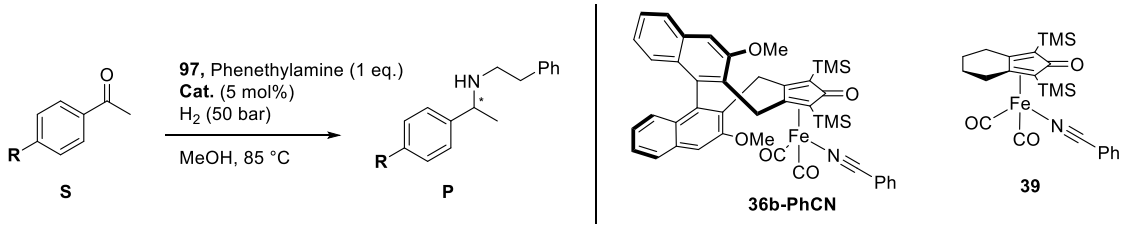

#	R	cat.	Yield[b]	*ee*[c]
1	H	**36b-PhCN**	80%	40%
2	OCH_3	**39**	0%	-
3	CF_3	**39**	13%	-
4	CH_3	**39**	16%	-
5	Cl	**39**	17%	-
6	CF_3	**36b-PhCN**	0%	-
7	Cl	**36b-PhCN**	41%	50%
8	CH_3	**36b-PhCN**	traces	-

[a] Reaction conditions: **S**/Cat. = 100:5, solvent: MeOH, p_{H2} = 50 atm, T = 85 °C, 14 h, C_{ketone} = 0.5 M (1 mmol); [b] Isolated yield; [c] Determined by chiral HPLC.

As seen in the table, the best results were obtained with 4-clorophenylmethyl ketone, which gave 50% *ee*, albeit in lower yield than acetophenone. It should be also noted that the chiral catalyst **36b-PhCN** gave higher amine yields

than complex **39**. A possible reason of this fact is that the sterically hindered complex **36b-PhCN** performs a slow ketone reduction, which does not compete with the desired condensation of the imine.

Summarizing, the family of chiral Knölker catalysts **36** showed activity toward reductive amination. The best conversion and *ee* values were obtained with the aliphatic amine **97**. While the best yields were generally obtained with 4-phenyl-2-butanone, acetophenone derivatives gave the most promising levels of enantioselectivity (up to 50% *ee*). Unfortunately, however, only two acetophenone derivatives gave the desired amine in reasonable yield. To improve these performances several strategies will be investigated in the future, including additional tests with the dihydroxy-substituted complex **36c,** which shows promising results (Table 28, Entry 16), it might be re-synthesized and tested with a wider group of ketones and amines.

5.3 Asymmetric Hydrogenation of Pre-formed Imines

Although in the last years some iron catalysts for asymmetric hydrogenation of imines have been reported (see Chapter 1), still their number is limited. Due to the synthetic efforts which have been spent in the synthesis of the family of chiral catalysts **36**, their reactivity was exploited also towards the asymmetric hydrogenation of pre-formed imines. Using *N*-(4-Methoxy-phenyl)-(1-phenyl-ethylidene)-amine **S21** as a benchmark substrate, catalysts **36a-c** were tested under 50 bar of H_2 at 85 °C.

Table 31. Catalytic attempts for the asymmetric hydrogenation of imine **S21** promoted by chiral (cyclopentadienone)iron complexes **36.**[a]

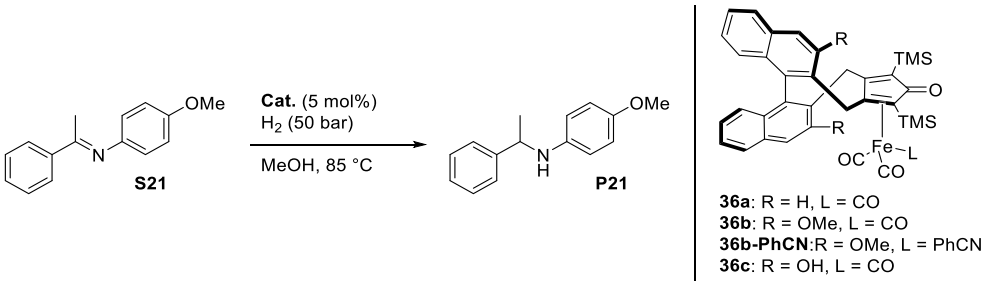

#	Catalyst	Lewis Acid[b]	Conversion[c]	*ee*[d]
1	**36b**[e]	-	34	7
2	**36b**[e]	$Fe(acac)_3$	38	20
3	**36b-PhCN**	-	51	42
4	**36b-PhCN**	$Fe(acac)_3$	81	33
5	**36c**[e]	-	traces	-
6	**36a**[e]	$Fe(acac)_3$	66	13

[a] Reaction conditions: **S21**/Cat. = 100:5, solvent: MeOH, p_{H2} = 50 atm, T = 85 °C, 14 h, C_{S21} = 0.5 M (1 mmol); [b] 20 mol%; [c] Determined by ^{1}H NMR; [d] Determined by chiral HPLC; [e] Reaction conditions: **S21**/Cat./Me_3NO : 100:5:10.

A direct comparison of catalyst **36b** and **36b-PhCN** demonstrated that the nitrile complex **36b-PhCN** affords a better conversion to the desired product than the *in situ* activated pre-catalyst **36b**. The additional Lewis acid $Fe(acac)_3$ improved the conversion up to 81%. Furthermore, the **36b-PhCN** afforded higher enantiomeric excesses than pre-catalyst **36b**. Asymmetric catalytic hydrogenation using **36b-PhCN** gave 42% *ee* without additional Lewis acid. The comparison with catalyst **36a** gave the clue that less steric hindrance in 3,3'-position leads to a lower enantiomeric excess of 13% *ee* (Table 31). To better understand the limitations of **36**, other two imines were tested in asymmetric hydrogenation promoted by **36b-PhCN** and **36a**.

Table 32. Asymmetric Hydrogenation of **S31** and **S34** promoted by (*R*)-**36b-PhCN**.[a]

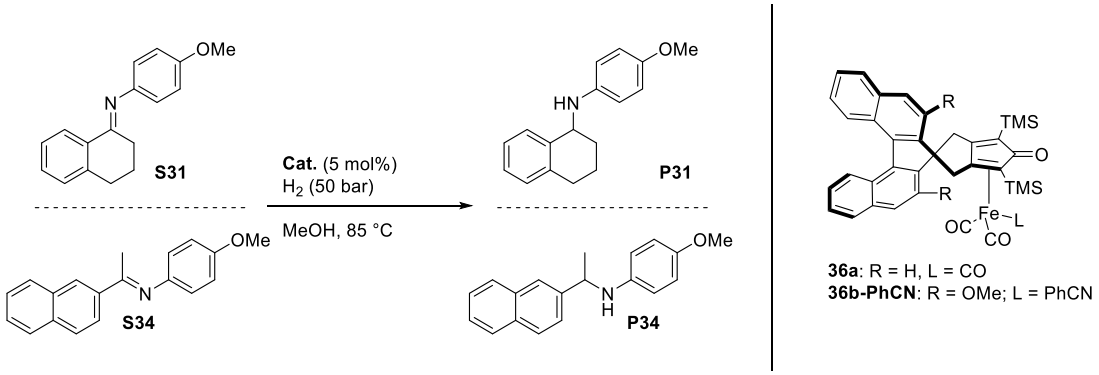

#	Substrate	Catalyst	Lewis acid	Conv. (%)[b]	*ee* (%)[c]
1	**S31**	**36b-PhCN**	-	41	35
2	**S31**	**36b-PhCN**	$Fe(acac)_3$	74	31
3	**S31**	**36a**[d]	$Fe(acac)_3$	53	36
4	**S34**	**36b-PhCN**	-	67	29
5	**S34**	**36b-PhCN**	$Fe(acac)_3$	>99	7
6	**S34**	**36a**[d]	$Fe(acac)_3$	67	8

[a] Reaction conditions: **S**/Cat. = 100:5, solvent: MeOH, p_{H2} = 50 atm, T = 85 °C, 14 h, C_{Sub} = 0.5 M (1 mmol); [b] Determined by ^{1}H NMR; [c] Determined by chiral HPLC; [d] Reaction conditions: **S**/Cat./Me_3NO = 100:5:10.

The reduction of imine **S34** afforded up to quantitative yields using the catalyst **36b-PhCN** and additional $Fe(acac)_3$, even though the best *ee* of 29% was obtained in the absence of $Fe(acac)_3$. A direct comparison between the catalysts **36a** and **36b-PhCN** showed a lower stereoselectivity with **36a** (Table 32, entries 4-6). The asymmetric hydrogenation of imine **S31** afforded conversions up to 74% and consistent enantiomeric excesses of 31-36% *ee*.

The attempts of imines hydrogenation using chiral Knölker-type complexes showed a good activity with the *in situ* activated tricarbonyl pre-catalysts (**36a, 36b, 36c**) and the nitrile complex pre-catalyst **36b-PhCN**. The reduction shows conversions up to 100%. The highest enantiomeric excess obtained was 42%.

5.4 Asymmetric Transfer Hydrogenation of Pre-formed Imines

Compound **36b** and its benzonitrile derivative **36b-PhCN** were tested also in transfer hydrogenation of pre-formed imines. Apparently, the presence of a Lewis acid is needed to gain the reactivity, as previously reported by Zhao *et al.*.[89] However, the role of the Lewis acid is still not totally clear.

N-(4-Methoxyphenyl)-1-phenylethan-1-imine **S21** was chosen as model substrate and the first attempts using the achiral nitrile pre-catalysts **39** and $Fe(acac)_3$ as activating Lewis acid lead to full conversions (Table 33, entries 1-2), whereas silver(I) fluoride allowed to obtain only 56% conversion (entry 3). The chiral complexes **36b** and **36b-PhCN** gave lower conversions (up to 44%), and again $Fe(acac)_3$ was found to be a more effective additive than AgF (entries 5-8 vs. entry 9).

Table 33. Catalytic tests for the asymmetric transfer hydrogenation of imine **S21** promoted by (cyclopentadienone)iron complexes.[a]

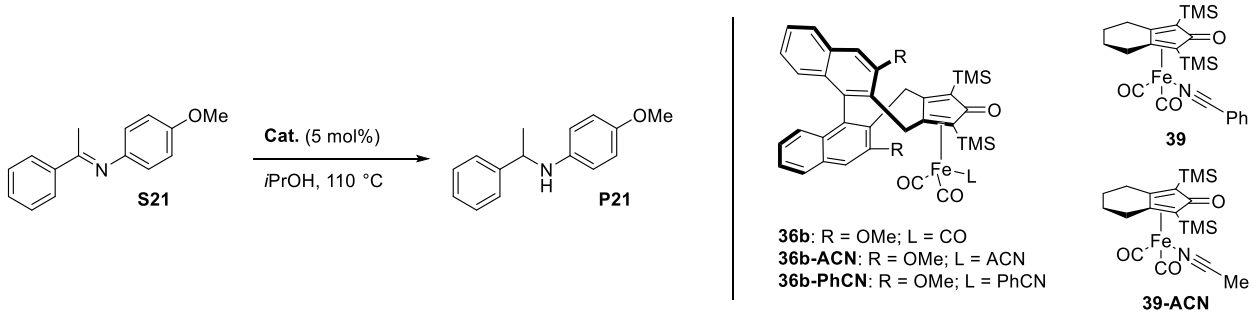

#	Catalyst	Lewis Acid	Lewis Acid Amount (mol%)	Conversion (%)[b]
1	**39-ACN**	$Fe(acac)_3$	20	>99
2	**39**[c]	$Fe(acac)_3$	20	>99
3	**39**[c]	AgF	40	56
4	**36b**[c]	$Fe(acac)_3$	40	-

5	**36b-ACN**	$Fe(acac)_3$	20	13
6	**36b-PhCN**	$Fe(acac)_3$	10	12
7	**36b-PhCN**	$Fe(acac)_3$	20	44
8	**36b-PhCN**	$Fe(acac)_3$	40	36
9	**36b-PhCN**	AgF	40	25

[a] Reaction conditions: **S21**/Cat. = 100:5, solvent: *i*PrOH, T = 110 °C, 48 h, C_{S21} = 0.5 M (1 mmol); [b] Determined by ^{1}H NMR; [c] Reaction conditions: **S21**/Cat./Me_3NO : 100:5:10.

Using **36b-PhCN** as catalyst, several acids were tested in the transfer hydrogenation of **S21**. It turned out that $Fe(acac)_3$ is the most effective activator (Table 34). Even the use of lanthanide salts like ytterbium(III) triflate and indium(III) triflate or scandium(III) triflate did not afford the desired amine **P21**, but only the reduced hydrolysis products of the starting imine **S21** (Table 34).

Table 34. Lewis acid screening in ATH of **S21** promoted by **36b-PhCN**.[a]

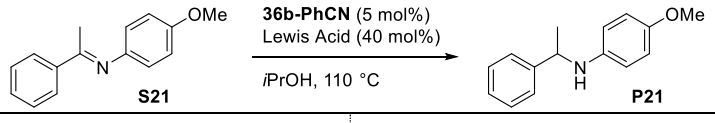

#	Acid	Conversion (%)[b]	#	Acid	Conversion (%)[b]
1	$Fe(acac)_3$	36	10	NH_4PF_6	-
2	AgF	25	11	$Yb(OTf)_3$	-
3	$Fe(OAc)_2$	-	12	$Sc(OTf)_3$	-
4	$Fe(OTf)_2$	21	13	$In(OTf)_3$	-
5	$FeCl_2$	22	14	BF_3OEt_2	traces
6	$Ni(OAc)_2$	13	15	$Zn(OTf)_2$	-
7	$Ti(OiPr)_4$	30	16	TMS-OTf	-
8	$AgBF_4$	33	17	Bu_2SnO	-
9	$AgSbF_6$	8			

[a] Reaction conditions: **S21**/Cat./Lewis acid = 100:5:40, solvent: *i*PrOH, T = 110 °C, 16 h, C_{S21} = 0.5 M (1 mmol); [b] Determined by ^{1}H NMR.

Under optimized conditions, a screening of imine substrates was performed (Table 35). In the case of imine **S34**, the desired product **P34** could not be obtained, the starting material being recovered unreacted (entry 4). With imines **S21** and **S31** (entries 2-3) conversions up to 44% and enantiomeric excesses up to 35% *ee* were achieved.

Table 35. Asymmetric Transfer Hydrogenation of pre-formed imines promoted by **36b-PhCN.**[a]

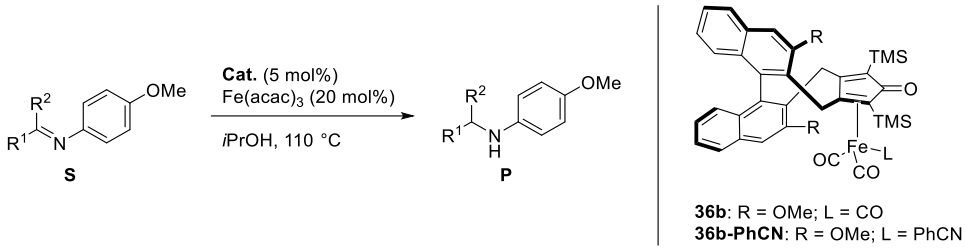

#	Substrate	Catalyst	Conversion (%)[b]	*ee* (%)[c]
1	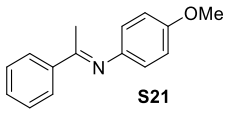 S21	**36b-PhCN**	44	33
2	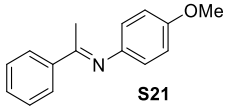 S21	**36b**[d]	34	35
3	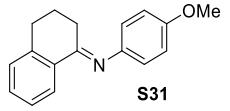 S31	**36b-PhCN**	38	24
4	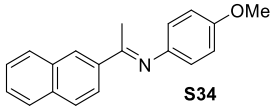 S34	**36b-PhCN**	-	-

[a] Reaction conditions: **S**/Cat./$Fe(acac)_3$ = 100:5:20, solvent: *i*PrOH, T = 110 °C, 48 h, C_{Sub} = 0.5 M (1 mmol); [b] Determined by ^1H NMR; [c] determined by chiral HPLC; [d] Reaction conditions: **S**/**36b**/Me_3NO/$Fe(acac)_3$= 100:5:10:20.

5.5 Summary of Chiral Knölker Catalysts Reactivity

Synthesis of three members of the chiral (cyclopentadienone)iron family **36a**, **36b** and **36c** was carried out. The synthesized catalysts were tested in hydrogenation and transfer hydrogenation of pre-formed imines and in reductive amination. Complexes **36b** and **36b-PhCN** turned out to be the most effective. In particular, the benzonitrile derivative **36b-PhCN** was found especially practical because needs no addition of an activating reagent. Unfortunately, however, the tested cyclopentadienone chiral catalyst displayed lower activity compared to the achiral complex **39**, and the obtained *ee* were always lower than 50%. Addition of a Lewis acid was found very beneficial for obtaining a good conversion. $Fe(acac)_3$ being the most effective additive.

Following the procedure reported by Renaud,[75f] a reductive amination protocol was also investigated. Both benzylic (**95**) and aliphatic amines (**97**) were coupled with an aliphatic ketone (**94**). The highest yields were obtained with phenethylamine **97**. Several other ketones were screened in combination with **97**, but only acetophenone showed a

good reactivity. Therefore, a substrate scope was performed, but only few derivatives gave reasonable yields (albeit with poor *ee* values).

Although complexes **36** were one of the first chiral (cyclopentadienone)iron complexes reported, they have clearly shown some drawbacks. The possible mechanism involved in the (cyclopentadienone)iron hydrogenation is an outer-sphere mechanism (see Scheme 24, page 25) involving a TS in which the distance between the stereogenic unit (binaphthyl residue) and the substrate plays an important role. In complexes **36**, the distance is apparently too long to effectively transfer the stereochemical information and this is the reason why the obtained *ee* are low. Furthermore, increasing the steric hindrance in the 3,3'-position, instead of improving the stereoselectivity, just decreases the reactivity leading the substrate approach difficult. Based on these evidences, a new generation of chiral (cyclopentadienone)iron catalysts are currently under design in our group.

5.6 Experimental Section

Synthetic procedure and NMR data of compounds **44**, **45**, **46**, **47a**, **44**, **48**, **49**, **50**, **51**, **52**, **53**, **54** and **47b** have been already reported in Paragraph 2.6 Experimental section, page 43.

2,2'-Bis(iodomethyl)-1,1'-binaphthalene (92a):

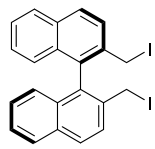

Sodium iodide (4.10 g, 28.0 mmol, 10.0 eq.) was added to a stirred solution of bis-bromide **47a** (1.25 g, 2.8 mmol, 1.0 eq.) in dry acetone (20 mL). The reaction mixture was refluxed in a sealed tube for 16 hours. After cooling down to r.t., the solvent was removed under high vacuum and water (20 mL) was added. The suspension was stirred for 30 minutes and filtered on a frit. The obtained solid was washed with water (20 mL), sodium thiosulfate solution (10 mL, aq., sat.), water (20 mL), an ice-cold mixture of hexane/methanol (2:1) and dried in high vacuum. The product **92a** (1.46 g, 2.74 mmol, 96%) was obtained as fine pale yellow powder.

^{1}H NMR (400 MHz, acetone-d6): δ 8.17 (d, J = 8.4 Hz, 2H), 7.8 (d, J = 8.2 Hz, 2H), 7.88 (d, J = 8.8 Hz, 2H), 7.61 (td, J = 8.2 Hz, J = 1.1 Hz, 2H), 7.38 (td, J = 8.2 Hz, J = 1.1 Hz, 2H), 7.08 (d, J = 8.4 Hz, 2H), 4.45 (d, J = 9.5 Hz, 2H, AB-system), 4.35 (d, 2J = 9.5 Hz, 2H, AB-system). The reported ^{1}H-NMR data fit with the one reported in the literature.[80]

2,2'-Bis(iodomethyl)-3,3'-dimethoxy-1,1'-binaphthalene (92b):

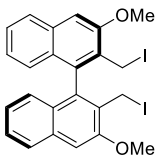

A solution of bis-bromide **47b** (3.57g, 7.14 mmol, 1.0 eq.) and sodium iodide (10.71 g, 71.4 mmol, 10.0 eq.) in acetone (36 mL) was refluxed in absence of light for 16 hours. After removing the solvent *in vacuo*, water (15 mL) was added and the suspension was stirred for 30 minutes at r.t.. After filtering the suspension on a frit, the solid was washed with water (100 mL), sodium thiosulfate solution (50 mL, aq., sat.), water (50 mL), an ice-cold mixture of hexane/ methanol (2:1) and dried in high vacuum. The product **92b** (4.25 g, 7.14 mmol, 100%) was obtained as colorless solid.

^{1}H NMR (400 MHz, acetone-d6): δ 7.95 (d, *J* = 8.2 Hz, 2H), 7.58 (s, 2H), 7.49 (td, *J* = 8.2 , *J* = 6.8, *J* = 1.2 Hz, 2H), 7.15 (td, *J* = 8.2 , *J* = 6.8, *J* = 1.2 Hz, 2H), 6.92 (d, *J* = 8.2 Hz, 2H), 4.31-4.21 (m, 4H, AB system), 4.17 (s, 6H). The reported ^{1}H-NMR data fit with the one reported in the literature.[80]

2,2'-Bis(3-(trimethylsilyl)prop-2-yn-1-yl)-1,1'-binaphthalene (93a):

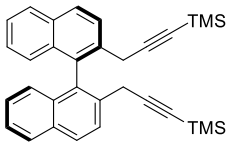

A solution of ethynyltrimethylsilane (0.565 mL, 4.0 mmol, 4 eq.) in THF (5 mL) was added dropwise to a 1M solution of ethylmagnesium bromide in THF (4.0 mL, 4.0 mmol, 4 eq.) kept at 0 °C. The reaction mixture was heated to reflux and stirred for 1 h. After cooling to r.t., CuI (0.095 g, 0.500 mmol, 0.5 eq.) and compound **92a** (0.534 g, 1.0 mmol, 1 eq.) were added. The mixture was heated to reflux and stirred overnight. After cooling down to r.t., the reaction was quenched with sat. aq. NH_4Cl (5 mL), and the obtained aqueous phase was extracted with AcOEt (3 × 25 mL). The organic layer was washed with H_2O (20 mL) and brine (20 mL), dried over Na_2SO_4 and concentrated *in vacuo*. Purification by column chromatography (95:5 hexane/DCM) gave the product **93a** (0.38g, 3.2 mmol, 80%) as a light yellow oil.

^{1}H NMR (400 MHz, CD_2Cl_2): δ 8.03 (d, *J*= 8.5 Hz, 2H), 7.95 (d, *J*= 8.2 Hz, 2H), 7.89 (d, *J* = 8.5 Hz, 2H), 7.45 (td, *J* = 8.2 Hz, *J* = 1.1 Hz, 2H), 7.24 (td, *J* = 8.2 Hz, *J* = 1.3 Hz, 2H), 6.99 (d, *J* = 8.5 Hz, 2H), 3.35 (d, *J* = 19 Hz, 2H, AB system), 3.22 (d, *J* = 19 Hz, 2H, AB system), 0.12 (s, 18H). The reported ^{1}H-NMR data fit with the one reported in the literature.[80]

((3,3'-Dimethoxy-[1,1'-binaphthalene]-2,2'-diyl)bis(prop-1-yne-3,1-diyl))bis(trimethylsilane) (93b):

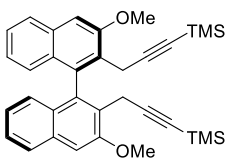

To a stirred solution of TMS-acetylene (3.06 mL, 21.48 mmol, 3.0 eq.) in dry THF (14 mL) at -60 °C under argon atmosphere, *n*-butyl lithium (13.4 mL, 1.6 M, 21.48mmol, 3.0 eq.) was added dropwise from a dropping funnel. After addition, the reaction mixture was allowed to warm up to 0 °C and was stirred for 30 minutes. After recooling to -60 °C, a solution of bis-iodide **47b** (4.25 g, 7.14 mmol, 1.0 eq.) in THF (53 mL) was added dropwise from a dropping funnel. The reaction mixture was allowed to

warm up to r.t. and stirred for 16 hours. The reaction was quenched by addition of ammonium chloride solution (50 mL, aq., sat.) and the aqueous phase was extracted with diethylether (3 × 50 mL). The combined organic layers were dried over sodium sulfate and concentrated under reduced pressure. The product **93b** (3.58 g, 6.69 mmol, 93%) was obtained as a yellow foamy solid and used without purification.

^{1}H NMR (300 MHz, $CDCl_3$): δ 7.79(d, J = 8.2 Hz, 2H), 7.37 (t, J = 8.2 Hz, 2H), 7.30 (s, 2H), 7.07-6.98 (m, 4H), 4.06 (s, 6H), 3.37 (d, J = 16.8 Hz, 2H, AB system), 3.26 (d, J = 16.8 Hz, 2H, AB system), 0.00 (s, 18H). The reported ^{1}H-NMR data fit with the one reported in the literature.[80]

Iron Complex (36a):

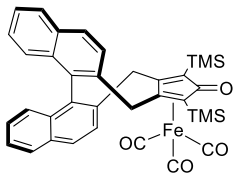

Diyne **93a** (0.510 g, 1.07 mmol, 1 eq.) and $Fe_2(CO)_9$ (0.781 g, 2.14 mmol, 2 eq.) were dissolved in toluene (9 mL) and heated to 90 °C for 4 h. After cooling down to r.t., the reaction mixture was filtered through a pad of Celite® (rinsing with DCM). The filtrate was concentrated *in vacuo*, and the residue was purified by flash column chromatography (8:2 hexane/DCM) to obtain **36a** (0.32 g, 0.49 mmol, 46%) as a pale yellow solid.

^{1}H NMR (400 MHz, CD_2Cl_2): δ 8.04 (d, *J* = 8.5 Hz, 2H), 7.99 (d, *J* = 8.8 Hz, 1H), 7.97 (d, *J* = 8.8 Hz, 1H), 7.68 (d, *J* = 8.5 Hz, 1H), 7.55 (d, *J* = 8.5 Hz, 1H), 7.52-7.45 (m, 2H), 7.30 (td, *J* = 8.5 Hz, *J* = 1.1 Hz, 1H), 7.25 (td, *J* = 8.5 Hz, *J* = 1.1 Hz, 1H), 7.20 (d, *J* = 8.5 Hz, 1H), 7.09 (d, *J* = 8.5 Hz, 1H), 3.76 (d, *J* = 15.7 Hz, 1H), 3.67 (d, *J* = 14.1 Hz, 1H), 3.45 (d, *J* = 15.7 Hz, 1H), 3.38 (d, *J* = 14.1 Hz, 1H), 0.41 (s, 9H), 0.26 (s, 9H). ^{13}C NMR (100 MHz, CD_2Cl_2): δ 209.8, 181.4, 137.0, 135.6, 135.0, 134.6, 133.4, 132.5, 130.0, 129.7, 128.9, 128.7, 127.5, 127.3, 127.1, 127.0, 126.9, 126.5, 113.1, 111.5, 76.0, 74.0, 34.8, 32.8, 0.9, 0.5. The reported ^{1}H-NMR and ^{13}C-NMR data fit with the one reported in the literature.[80]

HRMS (ESI+): Calcd. for $C_{36}H_{35}O_4Si_2Fe$: $[M+H]^+$ *m/z* 643.14294. Experimental: $[M+H]^+$ *m/z* 643.14164.

Iron Complex (36b):

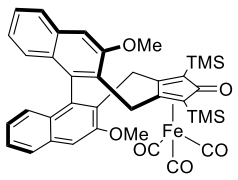

To a stirred solution of diyne **93b** (3.58 g, 6.69 mmol, 1.0 eq.) in dry toluene (50 mL) under argon atmosphere, $Fe_2(CO)_9$ (4.87 g, 13.39 mmol, 2.0 eq.) was added. The reaction was heated to 80 °C and stirred for 5 hours. After cooling down the reaction to r.t., the solvent was evaporated off. Flash chromatography (93:7 hexane:AcOEt) afforded the product **36b** (2.27 g, 3.16 mmol, 48%) as yellow solid.

^{1}H NMR (400 MHz, CD_2Cl_2): δ 7.87-7.83 (m, 2H), 7.43-7.32 (m, 4H), 7.08-7.04 (m, 2H), 6.91-6.85 (m, 2H), 4.38 (d, *J* = 15.5 Hz, 1H), 4.16 (d, *J* = 13.3 Hz, 1H), 4.05 (s, 3H), 3.94 (s, 3H), 3.26 (d, *J* = 13.3 Hz, 1H), 3.15 (d, *J* = 15.5 Hz, 1H), 0.41 (s, 9H), 0.30 (s, 9H).^{13}C NMR (100 MHz, $CDCl_3$): δ 208.7, 181.1, 155.1, 154.8, 138.6, 137.2, 133.9, 133.8, 127.4, 127.2, 127.1, 127.0, 126.9, 126.8, 126.6, 126.5, 126.4, 124.3, 124.1, 115.4, 107.8, 106.3, 105.7, 75.2, 74.9, 55.6, 54.8, 26.3, 26.2, 0.7, 0.2.

HRMS (ESI+): Calcd. for $C_{38}H_{39}O_6Si_2Fe$: $[M+H]^+$ *m/z* 703.16410. Experimental: $[M+H]^+$ *m/z* 703.16264.

Iron Complex (36c):

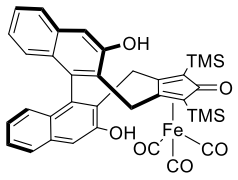

In a Schlenk tube fitted with a Teflon screw cap, BBr_3 (1M DCM solution, 14.0 mL, 14.0 mmol, 10 eq.) was added dropwise to a stirred solution of **36b** (0.99 g, 1.41 mmol, 1 eq.) and Bu_4NI (1.30 g, 3.52 mmol, 2.5 eq.) in DCE (40 mL) kept at 0 °C. The Schlenk was sealed and the mixture was heated to 84 °C and stirred for 3 days. After this time, the reaction was cooled down to 0 °C and ice-cold H_2O (50 mL) was added. The mixture was extracted with DCM (3 × 20 mL), washed with brine (30 mL) and then dried over Na_2SO_4. Filtration of the DCM solution through a short pad of silica allowed to remove the ammonium salts (which eluted before the product), then complex **36c** (0.762g, 1.13 mmol, 80%)– a pale yellow solid – was purified by flash column chromatography (83:17 → 77:23 hexane/AcOEt).

^{1}H NMR (400 MHz, $CDCl_3$): δ 7.71 (d, *J* = 8.2 Hz, 2H), 7.39-7.35 (m, 3H), 7.31 (s, 1H), 7.06 (t, *J* = 7.5 Hz, 2H), 6.98 (dd, *J* = 8.3 Hz, *J* = 2.3 Hz, 2H), 6.32 (br s, 2H), 4.34 (d, *J* = 15.6 Hz, 1H), 4.14 (d, *J* = 13.8 Hz, 1H), 3.24 (d, *J* = 13.8 Hz, 1H), 3.11 (d, *J* = 15.5 Hz, 1H), 0.41 (s, 9H), 0.31 (s, 9H). ^{13}C NMR (100 MHz, $CDCl_3$): δ 208.4, 180.3, 152.3, 152.2, 138.9, 137.7, 134.0, 133.9, 127.3, 127.3, 127.1, 126.4, 126.1, 125.5, 123.8, 123.6, 114.7, 110.4, 109.5, 76.3, 75.4, 29.8, 26.4, 0.9, 0.5. The reported ^{1}H-NMR and ^{13}C-NMR data fit with the one reported in the literature.[80]

HRMS (ESI+): Calcd. for $C_{36}H_{35}O_6Si_2Fe$: $[M+H]^+$ *m/z* 675.13277. Experimental: $[M+H]^+$ *m/z* 675.13152.

Iron Complex (36b-ACN):

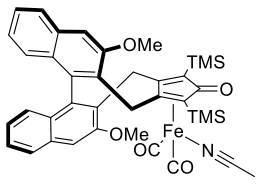

To a stirred solution of **36b** (100 mg, 0.19 mmol, 1.0 eq.) in dry acetone (11.5 mL) under argon atmosphere, trimethylamine *N*-oxide (16 mg, 0.21 mmol, 1.2 eq.) and acetonitrile (19 µl, 0.37 mmol, 2.0 eq.) were added. The reaction was refluxed for 20 hours in a sealed tube. After cooling down the reaction to r.t., the solvent was removed under reduced pressure. Flash chromatography (1:1 hexane/DCM; 8:2 hexane/AcOEt) afforded the product **36b-ACN** (35 mg, 0.06 mmol, 29%) as a yellow solid.

^{1}H NMR (400 MHz, CD_2Cl_2): δ 7.87-7.85 (m, 2H), 7.43-7.34 (m, 5H), 7.08-7.03 (m, 2H), 6.86-6.81 (m, 1H), 4.42 (d, *J* = 14.2 Hz, 1H), 4.16 (d, 2*J* = 14.7 Hz, 1H), 4.08 (s, 3H), 4.01 (s, 3H), 2.84 (d, *J* = 14.8 Hz, 1H), 2.71 (d, *J* = 14.2 Hz, 1H), 2.18 (s, 3H), 0.43 (s, 9H), 0.34 (s, 9H).

Iron Complex (36c-PhCN):

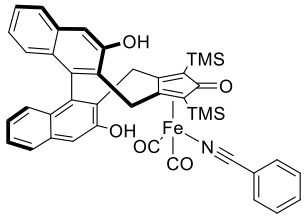

To a stirred solution of **36c** (100 mg, 0.19 mmol, 1.0 eq.) in dry acetone (11.5 mL) under argon atmosphere, trimethylamine N-oxide (16 mg, 0.21 mmol, 1.2 eq.) and benzonitrile (38 µl, 0.37 mmol, 2.0 eq.) were added. The reaction was refluxed for 20 hours in a sealed tube. After cooling down the reaction to r.t., the solvent was removed under reduced pressure. Flash chromatography (1:1 hexane/DCM; 8:2 hexane/AcOEt) afforded the product **36b-PhCN** (77 mg, 0.12 mmol, 58%) as a yellow solid.

^{1}H NMR (400 MHz, CD_2Cl_2): δ 7.91-7.85 (m, 2H), 7.80-7.70 (m, 2H), 7.68-7.62 (m, 1H), 7.56-7.50 (m, 2H), 7.44-7.39 (m, 3H), 7.35 (s, 1H), 7.10-7.01 (m, 2H), 6.89-6.85 (m, 2H), 4.35 (d, *J* = 15.5 Hz, 1H), 4.12 (d, 1H, overlapped with singlet at 4.11), 4.11 (s, 3H), 4.01 (s, 3H), 2.97 (d, *J* = 15.3 Hz, 1H), 2.88 (d, *J* = 13.8 Hz, 1H), 2.18 (s, 3H), 0.40 (s, 9H), 0.30 (s, 9H).

Iron Knölker Complex 30 was synthesized following the procedure reported by Renaud and Co-workers.[75i]

Iron Complex (39):

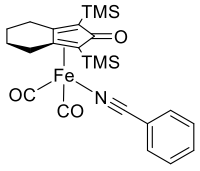

Benzonitrile (99 µl, 0.96 mmol, 2.0 eq.) was added to a solution of **30** (200 mg, 0.48 mmol, 1.0 eq.) and trimethylamine *N*-oxide (43 mg, 0.57 mmol, 1.2 eq.) in dry acetone (20 mL) at r.t.. The reaction mixture was refluxed for 20 hours in a sealed tube. After cooling down to r.t., the solvent was removed under reduced pressure. Flash chromatography (1:1 hexane/DCM; 8:2 hexane/AcOEt) afforded the product **39** (0.39 mmol, 82%) as a yellow solid.

^{1}H NMR (400 MHz, $CDCl_3$): δ 7.83 (d, *J* = 8.2 Hz, 2H), 7.63 (t, *J* = 8.2 Hz, 1H), 7.50 (t, *J* = 8.2 Hz, 2H), 2.45-2.32 (m, 4H), 1.66-1.61 (m, 4H), 0.26 (s, 18H). NMR data fit with the those reported in the literature.[107a]

Iron Complex (39-ACN):

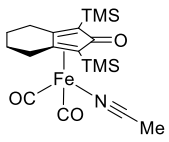

Acetonitrile (50 µl, 0.95 mmol, 2.0 eq.) was added to a solution of **30** (200 mg, 0.48 mmol, 1.0 eq.) and trimethylamine *N*-oxide (43 mg, 0.57 mmol, 1.2 eq.) in dry acetone (20 mL) at r.t.. The reaction mixture was refluxed for 20 hours in a sealed tube. After cooling down to r.t., the solvent

was removed under reduced pressure. Flash chromatography (1:1 hexane/DCM; 1:1 hexane/AcOEt) afforded the product **39-ACN** (1.44 mg, 0.33 mmol, 70%) as an orange solid.

^{1}H NMR (400 MHz, $CDCl_3$): δ 2.21–2.35 (m, 4H), 2.18 (s, 3H), 1.41–1.62 (m, 4H), 0.19 (s, 18H). NMR data fit with the those reported in the literature.[107a]

5.6.1 General Procedure – Catalytic Tests

General procedure a for the Reductive Amination of carbonyl equivalents using iron tricarbonyl pre-catalysts

A 10 mL flame dried autoclave vial containing a stirring bar was charged with carbonyl compound (1.0 eq., 0.5 M), amine (1.2 eq.), Lewis acid (10 mol%) and dry methanol (2/3 of total solvent amount) under argon. The reaction mixture was refluxed in the sealed autoclave vial for 1 hour. In a separate flame dried Schlenk tube, a solution of tricarbonyl catalyst (5 mol%) in dry methanol (1/3 of total solvent amount) was added to solid Me_3NO (5 mol%) and stirred for 30 minutes at r.t. before it was added to the autoclave vial. The autoclave was pressurized to the final pressure of H_2 and stirred at 85 °C for 16 hours. After cooling down to r.t. and careful venting of remaining hydrogen, the reaction mixture was filtered over deactivated neutral alumina (3% of H_2O) and rinsed with AcOEt. After removing the solvent under reduced pressure, the crude was directly used for determination of conversion. The purified product could be obtained by flash chromatography (1:1 hexane/AcOEt + 0.5% TEA).

General procedure for the reductive amination of carbonyl equivalents using iron nitrile complexes

A 10 mL flame dried autoclave vial containing a stirring bar was charged with carbonyl compound (1.0 eq., 0.5 M), amine (1.2 eq.), Lewis acid (10 mol%) and dry methanol (2/3 of total solvent amount) under argon. The reaction mixture was refluxed in the sealed autoclave vial for 1 hour. Subsequently, a solution of nitrile complex catalyst (5 mol%) in dry methanol (1/3 of total solvent amount) was added to the autoclave vial. The autoclave was pressurized to the final pressure of hydrogen and stirred at 85 °C for 16 hours. After cooling down to r.t. and careful venting remaining hydrogen, the reaction mixture was filtered over deactivated neutral alumina (3% of H_2O) and rinsed with AcOEt. After removing the solvent under reduced pressure, the crude was directly used for determination of conversion. The pure product could be obtained by flash chromatography (hexane/AcOEt/0.5% TEA).

General procedure for the benzoylation of crude product

Benzoyl chloride (1.1 eq.) was added to a solution of Crude Amine (1.0 eq.) and triethyl amine (1.5 eq.) in dry DCM and stirred for 12 hours at r.t.. After removing the solvent under reduced pressure, flash chromatography (9:1 hexane/AcOEt) afforded the product in quantitative yields.

General procedure for the hydrogenation of pre-isolated imines using iron tricarbonyl pre-catalysts

A 10 mL flame dried autoclave vial containing a stirring bar was charged with imine (1.0 eq.), $Fe(acac)_3$ (20 mol%) and dry methanol (0.5 M) under argon atmosphere. In a separate flame dried Schlenk tube, a solution of tricarbonyl catalyst (5 mol%) in dry methanol (1 M) of total solvent amount was added to solid Me_3NO (10 mol%) and stirred for 1 hour at r.t. before it was added to the autoclave vial. The autoclave was pressurized to 50 bars of hydrogen and stirred at 85 °C for 16 hours. After cooling down to r.t. and careful venting of remaining hydrogen, the reaction mixture was filtered over deactivated neutral alumina (3% of H_2O) and rinsed with AcOEt. After removing the solvent under reduced pressure, the crude was dissolved in DCM (1 mL/mmol) and hydrochloric acid (1 M, 1ml/mmol) was added. The two-phase mixture was stirred for 3 hours at r.t. before it was basified with sodium hydroxide solution (aq. 1 M). The aqueous layer was extracted with AcOEt (3 × 5 mL) and the combined organic layers dried over sodium sulfate and concentrated under reduced pressure. Flash chromatography (9:1 hexane/AcOEt) afforded the product amine. Ninhydrin staining visualizes the product amine (pale red spot) and the *p*-anisidine (dark red spot).

General procedure for the hydrogenation of pre-isolated imines using iron nitrile complexes

A 10 mL flame dried autoclave vial containing a stirring bar was charged with imine (1.0 eq.), $Fe(acac)_3$ (20 mol%), nitrile complex pre-catalyst (5 mol%) and dry methanol (0.5 M) under argon atmosphere. The autoclave was pressurized to 50 bars of hydrogen and stirred at 85 °C for 16 hours. After cooling down to r.t. and careful venting of remaining hydrogen, the reaction mixture was filtered over deactivated neutral alumina (3% of H_2O) and rinsed with AcOEt. After removing the solvent under reduced pressure, the crude was dissolved in DCM (1 mL/mmol) and hydrochloric acid (1 M, 1mL/mmol) was added. The two-phase mixture was stirred for 3 hours at r.t. before it was basified with sodium hydroxide solution (aq. 1 M). The aqueous layer was extracted with AcOEt (3 × 5 mL) and the combined organic layers were dried over sodium sulfate and concentrated under reduced pressure. Flash chromatography (9:1 hexane/AcOEt) afforded the amine product. Ninhydrin staining allowed to visualize the product amine (pale red spot) and *p*-anisidine (dark red spot).

General procedure for the transfer hydrogenation of pre-isolated imines using iron tricarbonyl pre-catalysts

A flame dried Schlenk tube containing a stirring bar was charged with imine (1.0 eq.), $Fe(acac)_3$ (20 mol%) and dry 2-propanol (0.5 M) under argon atmosphere. In a separate flame dried Schlenk tube, a solution of tricarbonyl catalyst (5 mol%) in dry 2-propanol (1/3 of total solvent amount) was added to solid Me_3NO (10 mol%) and stirred for 1 hour at r.t. before it was added to the imine solution. The reaction mixture was stirred at 110 °C (preheated oil bath) for 48 hours. After cooling down to r.t., the reaction mixture was filtered over deactivated neutral alumina (3% of

H_2O) and rinsed with AcOEt. After removing the solvent under reduced pressure, the crude was dissolved in DCM (1 mL/mmol) and hydrochloric acid (1 M, 1ml/mmol) was added. The two-phase mixture was stirred for 3 hours at r.t. before it was basified with sodium hydroxide solution (aq. 1 M). The aqueous layer was extracted with AcOEt (3 × 5 mL) and the combined organic layers dried over sodium sulfate and concentrated under reduced pressure. Flash chromatography (9:1 hexane/AcOEt) afforded the product amine. Ninhydrin staining visualizes the product amine (pale red spot) and the *p*-anisidine (dark red spot).

General procedure for the transfer hydrogenation of pre-isolated imines using iron nitrile complex pre-catalysts

A flame dried Schlenk tube containing a stirring bar was charged with imine (1.0 eq.), $Fe(acac)_3$ (20 mol%), nitrile complex pre-catalyst (5 mol%) and dry 2-propanol (0.5 M) under argon atmosphere. The reaction mixture was stirred at 110 °C (preheated oil bath) for 48 hours. After cooling down to r.t., the reaction mixture was filtered over deactivated neutral alumina (3% of H_2O) and rinsed with AcOEt. After removing the solvent under reduced pressure, the crude was dissolved in DCM (1 mL/mmol) and hydrochloric acid (1 M, 1mL/mmol) was added. The two-phase mixture was stirred for 3 hours at r.t. before it was basified with sodium hydroxide solution (aq. 1 M). The aqueous layer was extracted with AcOEt (3 × 5 mL) and the combined organic layers dried over sodium sulfate and concentrated under reduced pressure. Flash chromatography (9:1 hexane/AcOEt) afforded the product amine. Ninhydrin staining visualizes the product amine (pale red spot) and the *p*-anisidine (dark red spot).

5.6.2 Imine Conversions

NMR conversions were calculated from the signal integrals (all the substrates and reduction products are known compounds, and our spectra are superimposable to those reported in the literature). The NMR spectra were measured taking d_1 = 20 s.

Amines (name, chemical formula)	^{1}H NMR
***N*-Benzyl-*N*-methyl-4-phenylbutan-2-amine (96):**[75f]	
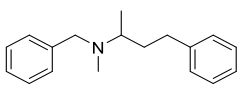	^{1}H NMR (400 MHz, $CDCl_3$): δ 7.30-7.15 (m, 10H), 3.61 (d, *J* = 13.4 Hz, 1H), 3.46 (d, *J* = 13.4 Hz, 1H), 2.81-2.63 (m, 3H), 2.15 (s, 3H), 1.95-1.85 (m, 1H), 1.65-1.57 (m, 1H), 1.03 (d, *J* = 6.6 Hz, 3H).
***N*-Phenethyl-4-phenylbutan-2-amine (98):**[75f]	
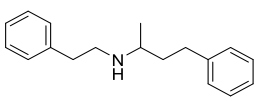	^{1}H NMR (400 MHz, $CDCl_3$): δ 7.41-7.13 (m, 10H), 3.00-3.92 (m, 1H), 2.91-2.77 (m, 3H), 2.76-2.55 (m, 3H), 1.86-1.75 (m, 1H), 1.70-1.60 (m, 1H), 1.52-1.36 (br s, 1H), 1.13 (d, *J* = 6.3 Hz, 1H).

***N*-Benzyl-*N*-methyl-1-phenylethan-1-amine (P55):**[175]

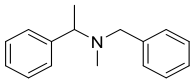

^{1}H NMR (400 MHz, $CDCl_3$): δ 1.42 (d, *J* = 6.8 Hz, 3H), 2.13 (s, 3H), 3.29 (d, *J* = 13.2 Hz, 1H), 3.58 (d, *J* = 13.2 Hz, 1H), 3.64 (q, *J* = 6.8 Hz, 1H), 7.19-7.36 (m, 8H), 7.40 (d, *J* = 7.3 Hz, 2H).

***N*-Phenethyl-1-phenylethan-1-amine (P56):**[176]

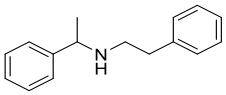

^{1}H NMR (300 MHz, $CDCl_3$): δ 7.31-7.09 (m, 10H), 3.70 (q, *J* = 6.6 Hz, 1H), 2.66-2.42 (m, 2H), 1.47 (br, s, 1H), 1.30 (d, *J* = 6.6 Hz, 3H).

***N*-Benzyl-*N*-methyl-1,2,3,4-tetrahydronaphthalen-1-amine (P61):**[177]

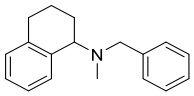

^{1}H NMR (300 MHz, $CDCl_3$): δ 8.06(d, *J* = 7.7 Hz, 1H), 7.59 (d, *J*= 7.5 Hz, 2H), 7.49 (t, *J* = 7.5 Hz, 2H), 7.43 -7.34 (m, 2H),7.30 (t, *J* = 7.3 Hz, 1H), 7.24-7.20 (m, 1H), 4.18-4.09 (m, 1H), 3.91-3.82 (m, 1H), 3.78-3.69 (m, 1H), 3.02-2.83 (m, 2H), 2.37 (s, 3H), 2.24-2.12 (m, 2H), 2.00- 1.82 (m, 2H).

Part B.

Use of the Trost Ligand in the Ruthenium-Catalyzed Asymmetric Hydrogenation of Ketones

The research activity presented in this chapter has been carried out in Leibniz-Institut für Katalyse e.V. (LIKAT) Rostock, Germany under the supervision of Prof. Dr. J.G. de Vries and Dr. Sandra Hinze, during my 5 months of Erasmus + Placement.

The Trost ligand (1*S*,2*S*)-1,2-diaminocyclohexane-*N*,*N*'-bis(2'-diphenylphosphinobenzoyl) **99** has been studied for the first time as ligand in the asymmetric hydrogenation (AH) of ketones. Ligand (*S*,*S*)-**99** was screened in the presence of several metal salts and found to form active catalysts when combined with ruthenium sources in the presence of hydrogen and a base. Reaction optimization was carried out by screening different Ru sources, solvents and bases. Under the optimized conditions, the complex formed by combination of (*S*,*S*)-**99** with $RuCl_3(H_2O)_x$ in the presence of Na_2CO_3, is able to promote the AH of several ketones at r.t. with good yields and up to 96% *ee*. The reaction kinetics measured under the optimized conditions revealed the presence of a long induction period, during which the initially formed Ru species is transformed into the catalytically active complex by reaction with hydrogen. Remarkably, a precursor of the antiemetic drug Aprepitant, was hydrogenated with excellent yield and good *ee*.

CHAPTER 6

TROST LIGAND IN RUTHENIUM-CATALYZED ASYMMETRIC HYDROGENATION OF KETONES

6.1 TROST LIGAND & HYDROGENATION

In spite of the huge advancements in the development of asymmetric catalysis over the past fifty years, its industrial application is still in its early stages.[178] Indeed, at present the resolution of diastereoisomeric salts is still the most widely exploited methodology to obtain enantiomerically pure compounds, despite its intrinsically poor atom economy. Among the enantioselective catalytic methodologies, asymmetric hydrogenation (AH) is probably the most appealing one from the industrial point of view, due to its practicality and to the use of a cheap and clean reducing agent such as H_2.[179] Despite this, the number of industrially implemented AH processes is still fairly limited.[178,179] One of the main reasons for this paradox is the high cost of the catalysts, which often contain expensive metals and/or ligands. For this reason, replacement of the precious metals traditionally used in AH (e.g., Rh, Ir, Ru) with cheap base metals (e.g., Fe, Co, Ni) has recently become an important research goal.[80,180] However, much less attention has been paid to the cost of the chiral ligand, which is often comparable or even higher than that of the metal. For a successful industrial application of AH, the availability on short notice of gram and kilogram amounts of chiral ligands is often a key issue.[181] Actually, noble metals can still be an economically viable option, provided that the chiral ligand is sufficiently cheap, readily available and robust. The "Trost ligand" (1*S*,2*S*)-1,2-diaminocyclohexane-*N*,*N*′-bis(2'-diphenylphosphinobenzoyl) **99** (Figure 30) meets these requirements to a large extent, as it is commercially available at a reasonable price or, alternatively, can be synthesized in one step from *trans*-1,2-diaminocyclohexane, readily available in both the enantiomeric forms. Ligand **99** was developed in 1992 by Trost and Van Vranken for Pd-catalyzed asymmetric allylic alkylations (AAA),[48] and it was soon recognized as one of the most effective ligands for this kind of transformation.[182] Quite surprisingly, despite this success, the use of the Trost ligand has remained mostly restricted to Pd-catalyzed AAA,[183] and – to the best of our knowledge – no successful application in AH has been reported so far.[184] The AH of ketones is a key transformation providing access to chiral alcohols, which are valuable building blocks for the synthesis of fine chemicals and active pharmaceutical ingredients. Over the past decade, the AH of ketones has been predominantly investigated with chiral ruthenium complexes containing various ligand combinations of mono- or bidentate phosphines and diamines, similar to the original Noyori's BINAP–Ru–diamine complexes.[185,186,187] Ruthenium catalysts based on PNNP ligands (in which N = imine or amine) have also been reported in AH and transfer hydrogenation of ketones.[188]

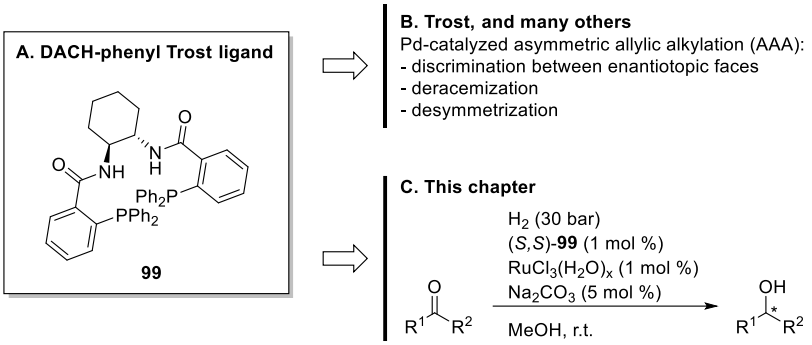

Figure 30. *Trans*-1,2-diaminocyclohexane-*N*,*N*′-bis(2-diphenylphosphino-benzoyl), better known as Trost ligand (A),[48] its best known applications (B),[182] and its new application described in this chapter (C).

6.2 Optimization and Reaction Scope

Thus, we investigated the potential of Trost diphosphine ligand (**99**) for the AH of ketones. Using acetophenone (**S1**) as model substrate and *t*BuOK as base, different metal precursors were screened in the presence of the Trost ligand under 30 bar of H_2 at 80 °C (Table 36, entries 1-12). No or trace conversions were obtained using Ni, Co and Fe salts (Table 36, entries 2-9), with the exception of $NiCl_2$ (Table 36, entry 1, conversion = 98%) which, however, led to racemic product (**P1**). In sharp contrast, several Ru sources led to good activity and promising enantioselectivity (Table 36, entries 10-18). Decreasing the reaction temperature from 80 °C to 60 °C led to a significant improvement of the enantioselectivity without affecting the yield (Table 36, entry 14 *vs.* 11), and for this reason additional Ru sources were screened at 60 °C (Table 36, entries 15-18). As a general trend, the Ru complexes containing PPh_3 gave the product with opposite absolute configuration compared to the others (Table 36, entries 10, 12-13, 16, 18 *vs.* 11, 14-15, 17). In absolute terms, the best *ee* values were obtained with anhydrous or hydrated $RuCl_3$ (Table 36, entries 11, 14 and 15).[189] As $RuCl_3(H_2O)_x$ is remarkably cheaper than anhydrous $RuCl_3$, the hydrated salt was selected as Ru source for further reaction optimization.

A solvent screening was then performed, the results of which are shown in Table 37.

Table 36. Screening of different metal sources in the AH of acetophenone (**S1**) in the presence of the Trost ligand (*S*,*S*)-**99**.[a]

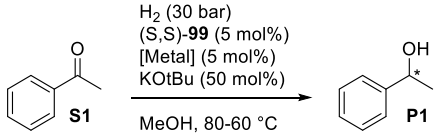

#	Metal source	*T* (°C)	Conv. (%)[b]	*ee* (%),[b] abs. conf.[c]
1	$NiCl_2$	80	98	0

2	$Ni(NO_3)_2{\cdot}6\,H_2O$	80	0	-
3	$Ni(cod)_2$	80	0	-
4	$Ni(CO)_2(PPh_3)_2$	80	0	-
5	$CoCl_2$	80	1	29, *R*
6	$FeBr_2$	80	0	-
7	$FeBr_3$	80	0	-
8	$Fe(CO)_5$	80	0	-
9	$FeCl_2{\cdot}4\,H_2O$	80	1	23, *S*
10	$(PPh_3)_3RuCl_2$	80	96	44, *R*
11	$RuCl_3$	80	98	32, *S*
12	$(PPh_3)_3Ru(CO)H_2$	80	69	29, *R*
13	$(PPh_3)_3RuCl_2$	60	91	43, *R*
14	**$RuCl_3$**	**60**	**97**	**56, *S***
15	**$RuCl_3(H_2O)_x$**	**60**	**99**	**46, *S***
16	$(PPh_3)_4RuCl_2$	60	92	40, *R*
17	$[(C_6H_6)RuCl_2]_2$	60	98	23, *S*
18	$(PPh_3)_3Ru(CO)(Cl)H$	60	4	29, *R*

[a] Reaction conditions: **S1**/[M]/(*S,S*)-**99**/*t*BuOK = 100/5/5/50, P_{H2} = 30 bar, solvent: MeOH, C_0 (**S1**) = 0.2 M, reaction time: 22 h; [b] Determined by GC analysis; [c] Absolute configuration assigned by comparison of the optical rotation sign with literature data.[80]

Table 37. Solvent and temperature screening in the AH of acetophenone (**S1**) with $RuCl_3(H_2O)_x$/Trost ligand (*S,S*)-**99**.[a]

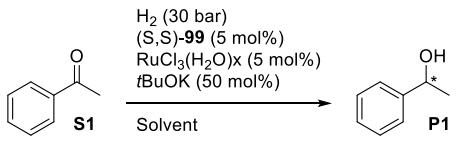

#	Solvent	*T* (°C)	Conv. (%)[b]	*ee* (%),[b] abs. conf.[c]
1	MeOH	60	99	46, *S*
2	MeOH	35	98	67, *S*
3	**MeOH**	**22**	**97**	**69, *S***
4	MeOH	0	63	65, *S*
5	*i*PrOH	60	>99	0
6	DMF	60	>99	35, *S*

7	Benzene	60	74	17, *R*
8	MeCN	60	72	13, *S*
9	Toluene	60	>99	22, *S*
10	THF	60	>99	28, *S*
11	EtOH	60	98	5, *S*
12	1:1 MeOH/H_2O	60	>99	0
13	4:1 MeOH/H_2O	60	81	0
14	1:1 *i*PrOH/H_2O	60	13	6, *R*
15	4:1 *i*PrOH/H_2O	60	>99	0

[a] Reaction conditions: **S1**/$RuCl_3(H_2O)_x$/(*S*,*S*)-**99**/*t*BuOK 100/5/5/50, P_{H2} = 30 bar, C_0 (**S1**) = 0.2 M, reaction time: 22 h; [b] Determined by GC analysis; [c] Absolute configuration assigned by comparison of the optical rotation sign with literature data.[80]

Although full conversion could be achieved with several different solvents (Table 37, entries 1, 5-6 and 9-11), the best *ee* value was obtained in MeOH (entry 1). Decreasing the temperature led to higher *ee* values without substantially affecting the yield (Table 36, entries 2-3), although no improvements could be obtained below r.t. (entry 4). Notably, the presence of water was found to strongly affect the enantioselectivity: when MeOH/H_2O mixtures were used, the *ee* dropped to zero (Table 36, entries 12-13). Furthermore, running the reaction in *i*PrOH yielded racemic **P1** due to the background base-promoted transfer hydrogenation (Table 36, entries 5 and 14-15). On the basis of these results, it was decided to carry out further optimization in MeOH at r.t. (Table 38).

Table 38. Investigation on the role of the base in the AH of acetophenone (**S1**) with $RuCl_3(H_2O)_x$/Trost ligand (S,S)-**99**.[a]

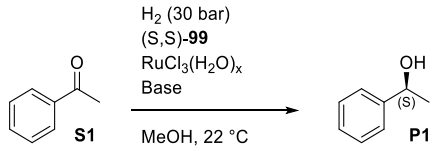

#	Base	Base/cat.	Cat. Loading (mol%)	Conv. (%)[b]	*ee* (%)[b,c]
1	None	-	5	0	0
2	*t*BuOK	10	5	93	70
3	*t*BuOK	5	5	97	76
4	*t*BuOK	1	5	0	0
5	KOH	5	5	>99	71
6	K_2CO_3	5	5	98	53
7	Cs_2CO_3	5	5	98	69

8	LiO*t*Bu	5	5	98	63
9	$LiOH{\cdot}H_2O$	5	5	>99	64
10	NaOMe	5	5	99	70
11	NaO*i*Pr	5	5	31	86
12	NaO*t*Bu	5	5	98	66
13	NaOH	5	5	99	89
14	Na_3PO_4	5	5	99	87
15	Na_2CO_3	5	5	99	89
16	Na_2CO_3	5	2.5	>99	93
17	**Na_2CO_3**	**5**	**1**	**>99 (96%)**[g]	**96**
18	Na_2CO_3	5	0.5	97	94
19[d]	Na_2CO_3	5	0.5	>99	95
20	Na_2CO_3	5	0.1	0	-
21[d]	Na_2CO_3	5	0.1	0	-
22[e]	Na_2CO_3	5	1	42	94
23[f]	Na_2CO_3	5	1	63	95

[a] Reaction conditions: P_{H2} = 30 bar, C_0 (**S1**) = 0.2 M, reaction time: 22 h; [b] Determined by GC analysis; [c] Absolute configuration assigned by comparison of the optical rotation sign with literature data.[80] [d] P_{H2} = 80 bar; [e] Reaction carried out in the presence of 3 Å molecular sieves; [f] Reaction carried out in the presence of Hg^0 (10 mmol/100 eq.). [g] Isolated yield (reaction carried out on a 6 mmol scale).

The role of base was investigated, and it was found that without *t*BuOK the reaction does not proceed (Table 38, entry 1).[185a,190] Varying the base/catalyst ratio (entries 2-4), 5:1 turned out to be the optimum (entry 3). From a base screening (Table 38, entries 5-15), it was found that the base employed has deep influence on the enantioselectivity. Remarkably, simple inorganic bases such as alkaline hydroxides and carbonates did efficiently promote the reaction (Table 38, entries 5-7, 9, 13-15). Among them, those bearing sodium as counter ion led to higher *ee* values than the others. Decreasing the catalyst loading to 1 mol% in the presence of Na_2CO_3 led to a remarkable increase of the enantioselectivity (up to 96% *ee*) leaving the conversion unaffected (Table 38, entries 16-17 *vs.* 15). No further improvement in terms of *ee* could be obtained below 1 mol% catalyst loading (Table 38, entries 18-21). However, full conversion could be still obtained at 0.5 mol% catalyst loading, corresponding to a TON of 200. A similar effect was also observed using NaOH and Na_3PO_4 as base.[191] Increasing P_{H2} had modest or no influence on the enantioselectivity (Table 38, entry 19), while decreasing it to 10 bar led to a drop of conversion and *ee*.[191] Since the presence of H_2O is harmful to the enantioselectivity (see Table 37), a reaction was run in the presence of 3 Å molecular sieves (to scavenge any H_2O traces), but the only observed effect was a drop of conversion (Table 38,

entry 22). Running the hydrogenation in the presence of an excess of Hg^0 led only to a slight decrease of conversion, which leads to the conclusion that the active catalyst is probably homogeneous.[93,52b]

Table 39. Substrate screening in the AH of ketones catalyzed by $RuCl_3(H_2O)_x$/(*S*,*S*)-**99**.[a]

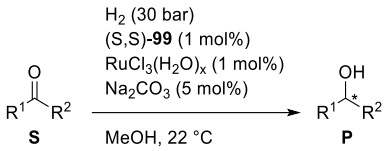

#	Substrate		Conv. (%)[b]	*ee* (%),[c] abs. conf.[d]
1	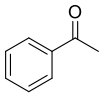	**S1**	>99 (96%)[e]	96, *S*
2	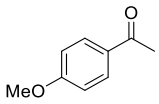	**S3**	>99 (97%)[e]	95, *S*
3	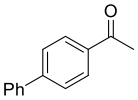	**S65**	98	95, *S*
4	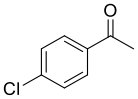	**S66**	>99	93, *S*
5	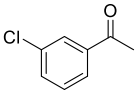	**S67**	>99	95, *S*
6	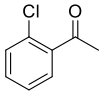	**S6**	32	28, *S*
7	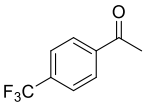	**S68**	>99	92, *S*
8	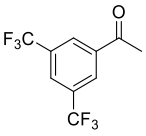	**S69**	>99 (95%)[e]	84, *S*
9	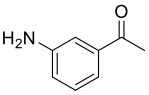	**S70**	31	77, *S*
10	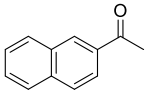	**S71**	>99	94, *S*
11		**S72**	>99	92, *S*
12	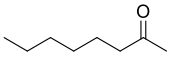	**S73**	40	11, *R*
13	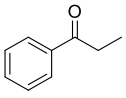	**S74**	64	96, *S*
14	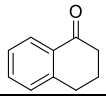	**S8**	>99	0

[a] Reaction conditions: P_{H2} = 30 bar, C_0 (substrate) = 0.2 M, reaction time: 22 h; [b] Determined by GC analysis in the presence of an internal standard (hexadecane). GC traces showed only the presence of the reaction products (secondary alcohols) and, when the reaction is not complete, of the starting ketones. Given the high chemoselectivity, percent conversions and percent isolated yields are practically coincident; [c] Determined by GC or HPLC on a chiral stationary phase (see the Supporting Information); [d] Absolute configuration assigned by comparison of the optical rotation sign with literature data; [e] Isolated yield (reaction carried out on a 6 mmol scale).

The substrate scope of the $RuCl_3(H_2O)_x$/(*S*,*S*)-**99** catalytic system was investigated under the optimized reaction conditions (Table 39). In general, 3- and 4-substituted acetophenones were hydrogenated with good yields and high *ee* (92-95%) irrespective of the electron withdrawing or electron donating properties of the substituent (Table 39, entries 2-5 and 7). The only exception was 1-(3-aminophenyl)ethanone **S70** which – possibly due to catalyst poisoning by coordination of the amino group to ruthenium – gave a low conversion and a diminished *ee* (77%). Remarkably, the 3,5-disubstituted acetophenone **S69**, precursor of the anti-emetic drug Aprepitant,[192] was hydrogenated with excellent yield and good *ee* (Table 39, entry 8). Low conversion and *ee* were obtained with 1-(2-chlorophenyl)ethanone **S6**, most certainly due to the steric bulk created by its *ortho* substituent (entry 6 *vs.* entries 4-5). Other aryl- and heteroaryl-methyl ketones such as **S71** and **S72** were hydrogenated with full conversion and high *ee* (entries 10-11), whereas the fully aliphatic methyl ketone **S73** gave low conversion and *ee* (entry 12). Propiophenone **S74** was reduced with the same *ee* as acetophenone (96%) albeit with lower conversion (Table 39, entry 12 *vs.* 1), thus confirming that the catalyst is rather sensitive to steric factors. Finally, the cyclic ketone **S8** was transformed into the corresponding alcohol with full conversion but no enantioselectivity (Table 39, entry 14).

6.3 Kinetic Studies

To gain information about the $RuCl_3(H_2O)_x$/(*S*,*S*)-**99** catalytic system, the kinetics of the hydrogenation of acetophenone(**S1**) were determined under the optimized catalytic conditions. The conversions were calculated from the hydrogen uptake. The kinetic experiments were carried out using a computer-controlled Parr multireactor which allows to monitor the H_2 uptake.

Table 40. Rate equations used for determination of kinetic parameters.

	Zero Order	First Order
Integrated rate law	$[A]_t=[A]_0-kt$	$[A]_t = [A]_0 e^{-kt}$
Linear Plot	Conv. (%) $=\frac{[A]_0-[A]_t}{[A]_0} = \frac{k}{[A]_0} t = k_{app}t$	$\ln\frac{[A]_t}{[A]_0} = -kt$
Units of k	mol $L^{-1}min^{-1}$	min^{-1}
Half-life	$t_{\frac{1}{2}} = \frac{[A]_0}{2k}$	$t_{\frac{1}{2}} = \frac{\ln(2)}{k}$

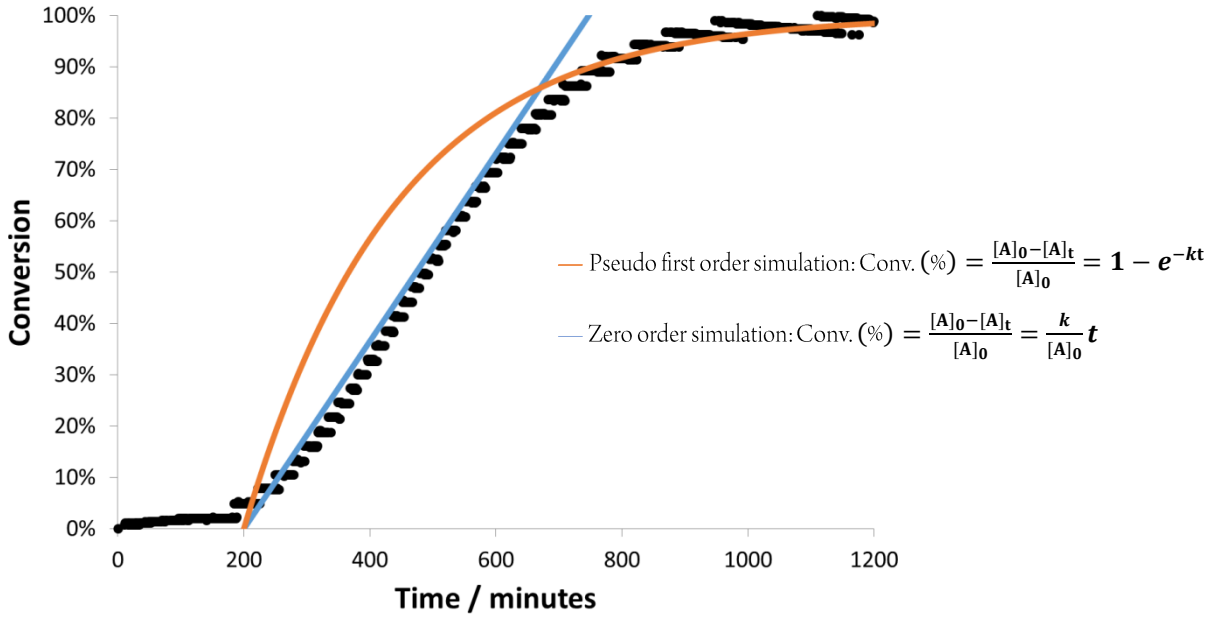

Figure 31. Kinetics of the AH of acetophenone (**S1**) catalyzed by [Ru]/(*S*,*S*)-**99** under the optimized reaction conditions. Hydrogenation conditions: S_1/[Ru]/(*S*,*S*)-**99**/Na_2CO_3 100/1/1/5; solvent: methanol; $C_{0,(S1)}$ = 0.94 M; P_{H2} = 30 bar; T = 19 °C; $C_{cat.}$ = 9.5 mM.

In the plot of conversion *vs.* time shown in Figure 31 (trace •) it can be noted that the reaction has a long induction time (about 3 h). The kinetic parameters (Table 41) and the graphical simulation (Figure 31) appear to fit with the zero order rate law. The calculated half-life time ($t_{1/2}$ = 275 min) fits the experimental value, if the 200 min activation time is taken into account.

Table 41. Kinetics of the AH of acetophenone (**S1**) promoted by $RuCl_3(H_2O)_x$/(*S*,*S*)-**99**/Na_2CO_3.

	Regression Zero Order		Regression Linear Order	
Regression interval =	300-700 min		300-700 min	
	Slope	Intercept	Slope	Intercept
	1.819E-03	-3.964E-01	-4.782E-03	1.614E+00
Standard error =	6.711E-06	3.444E-03	3.430E-05	1.910E-02
R^2 =	0.9946	0.0156	0.9848	0.0517
F index =	73472	399	19436	299
	17.779	0.097	51.965	0.799
	k_{app} (min^{-1}) =	1.82E-03	k_{app} (min^{-1}) =	0.005
	$t_{1/2}$ (min) = $A_0/2k$=	274.87	$t_{1/2}$ (min) = ln(2) / k =	144.95
	k (mol L^{-1} min^{-1}) =	1.72E-03	k (L mol^{-1} min^{-1}) =	0.50

The induction period remained the same independently of the complexation time of (*S*,*S*)-**99** with $RuCl_3(H_2O)_x$ under Ar atmosphere preceding the introduction of H_2 in the reaction vessel. Apparently, this long time is needed for the formation of the active catalyst, which might be a ruthenium complex with an oxidation state lower than III. To prove it, $RuCl_3$ was reduced overnight in *i*PrOH and then used in the hydrogenation of acetophenone **S1**. In the experiments shown in Table 42, ligand and base were added at different stages of this activation process, i.e. before and after the reduction with *i*PrOH.

Table 42. Catalytic tests with $RuCl_3$ pre-treatment followed by hydrogenation of **S1**.[a]

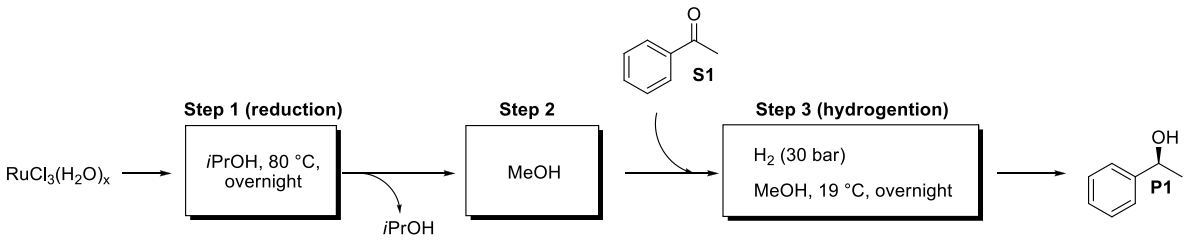

Experiment	Step 1	Step 2	Conv. (%)[b]	*ee* (%)[b]
1, ▲	(*S*,*S*)-**99** (1 mol%) Na_2CO_3 (5 mol%)		>99	7
2, ■	(*S*,*S*)-**99** (1 mol%)	Na_2CO_3 (5 mol%) 30 min, 18 °C	>99	10
3, ◆	-	(*S*,*S*)-**99** (1 mol%) Na_2CO_3 (5 mol%) 30 min, 18 °C	>99	96

4, ●	-	(*S*,*S*)-**99** (1 mol%) Na_2CO_3 (5 mol%) 30 min, 40 °C	>99	92

[a] Hydrogenation conditions: **S1**/[Ru]/(*S*,*S*)-**99**/Na_2CO_3 = 100/1/1/5; solvent: methanol; C_0 (**S1**) = 0.94 M; P_{H2} = 30 bar; *T* = 16 °C; $C_{cat.}$ = 9.5 mM; [b] Determined by GC analysis.

In all the kinetic profiles shown in Figure 32 a strong decrease of the induction time can be observed. However, only experiments **3** (trace ◆) and **4** (trace ●) gave results similar to those obtained under the optimized conditions (i.e., zero order kinetic profile and high *ee*). Experiments **1** (trace ▲) and **2** (trace ■) gave different kinetic profiles and very low *ee* values.

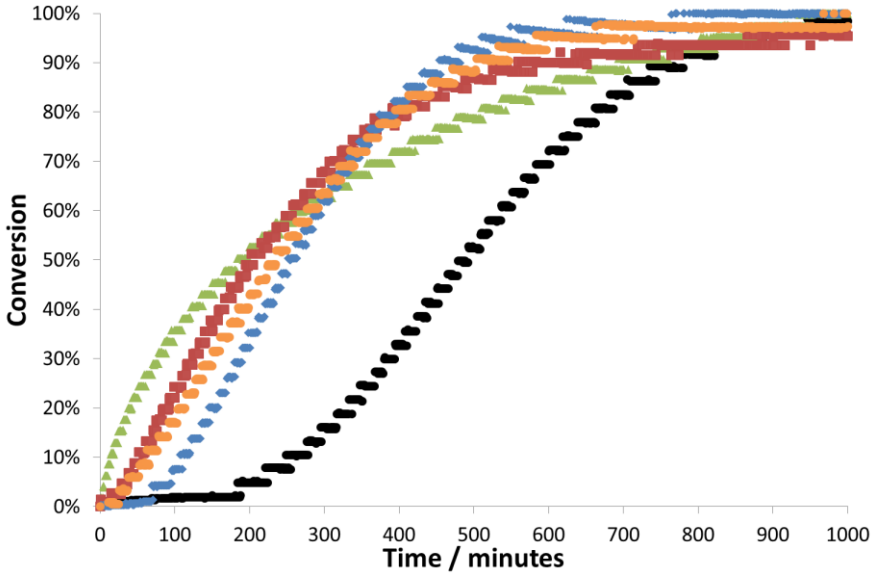

Figure 32. Kinetic experiments run after preliminary reduction of Ru^{III} in *i*PrOH. ▲ Experiment **1** (conv. >99%, 7 *ee*); ■ Experiment **2** (conv. >99%, 10% *ee*); ◆ Experiment **3** (conv. >99%, 96% *ee*); ● Experiment **4** (conv. >99%, 92% *ee*); • Experiment run under the optimized conditions (conv. >99%, 96% *ee*).

Kinetic profile, *ee* value and the kinetic parameters of experiments **3** ◆ and **4** ● (Figure 33) strongly support the hypothesis that the catalyst formed may be the same as the one obtained with the standard protocol (Figure 31).

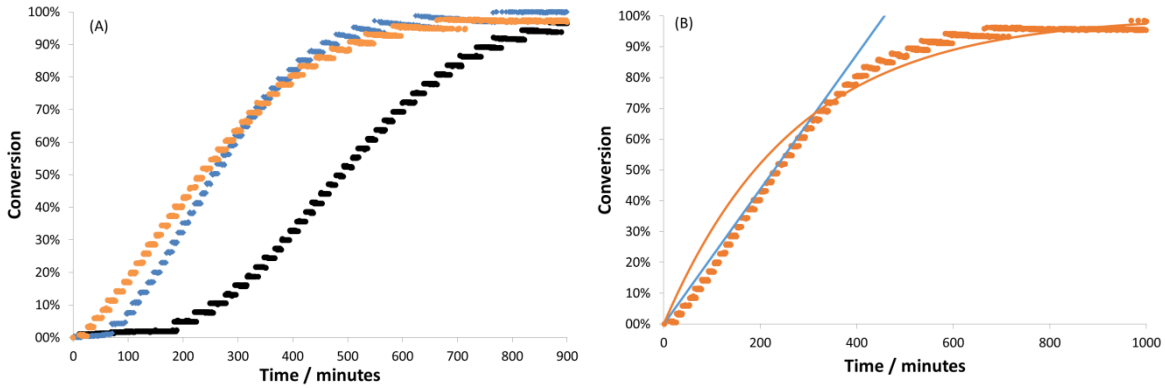

Figure 33. A) Kinetic experiments run after preliminary reduction of Ru^{III} in *i*PrOH; ◆ Experiment **3** (conv. >99%, 96% *ee*); ● Experiment **4** (conv. >99%, 92% *ee*); ● Experiment run under the optimized conditions (conv. >99%, 96% *ee*). Hydrogenation conditions: **S1**/[Ru]/(*S*,*S*)-**99**/Na_2CO_3 = 100/1/1/5; solvent: methanol; C_0 (**S1**) = 0.94 M; P_{H2} = 30 bar; T = 16 °C; $C_{cat.}$ = 9.5 mM. B) ● Experiment B4 (conv. >99%, 92% *ee*). — First order kinetic profile simulation; — Zero order kinetic profile simulation.

Table 43. Kinetics of acetophenone AH catalyzed by [Ru]/(*S*,*S*)-**99** with different pre-treatment procedures.

1, CURVE ▲	Regression First Order	
Regression interval =	200-400 min	
	Slope	Intercept
	-2.89E-03	-1.24E-01
Standard error =	1.36E-05	5.67E-03
R^2 =	0.9912	0.0316
F index =	44928.7326	399.0000
	44.7605	0.3975
	k_{app} (min^{-1}) =	2.89E-03
	$t_{1/2}$ (min) = ln(2)/ k =	240.16
	k ($L\ mol^{-1}\ min^{-1}$) =	3.04E-01

2, CURVE ■	Regression Zero Order		Regression First Order	
Regression interval =	100-300 min		100-300 min	
	Slope	Intercept	Slope	Intercept
	1.90E-03	8.71E-02	-3.89E-03	1.70E-01
Standard error =	1.47E-05	3.91E-03	2.40E-05	5.03E-03
R^2 =	0.9824	0.0222	0.9925	0.0198
F index =	16679.1419	299.0000	26203.6280	199.0000
	8.2249	0.1474	10.2367	0.0777
	k_{app} (min^{-1}) =	1.90E-03	k_{app} (min^{-1}) =	3.89E-03
	$t_{1/2}$ (min) = $A_0/2k$=	262.82	$t_{1/2}$ (min) = ln(2) / k =	178.22
	k (mol L^{-1} min^{-1}) =	1.80E-03	k (L mol^{-1} min^{-1}) =	4.10E-01

3, CURVE ◆	Regression Zero Order		Regression First Order	
Regression interval =	100 - 400 min		100 - 400 min	
	Slope	Intercept	Slope	Intercept
	2.63E-03	-1.94E-01	-5.46E-03	6.38E-01
Standard error =	1.09E-05	2.90E-03	5.08E-05	1.35E-02
R^2 =	0.9949	0.0164	0.9748	0.0765
F index =	58222	299	11584	299
	15.7202	0.0807	67.8474	1.7512
	k_{app} (min^{-1}) =	2.63E-03	k_{app} (min^{-1}) =	5.46E-03
	$t_{1/2}$ (min) = $A_0/2k$=	190.11	$t_{1/2}$ (min) = ln(2) / k =	126.86
	k (mol L^{-1} min^{-1}) =	2.49E-03	k (L mol^{-1} min^{-1}) =	5.76E-01

4, CURVE ◆	Regression Zero Order		Regression First Order	
Regression interval =	48-349 min		48-349 min	
	Slope	Intercept	Slope	Intercept
	-3.03E-04	4.44E-03	-3.68E-03	1.75E-01
Standard error =	1.29E-06	2.84E-04	2.19E-05	4.30E-03
R^2 =	0.9948	0.0019	0.9912	0.0253
F index =	55004	290	28266	250
	0.1910	0.0010	18.0243	0.1594
	k_{app} (min^{-1}) =	3.03E-04	k_{app} (min^{-1}) =	3.68E-03
	$t_{1/2}$ (min) = $A_0/2k$=	228.66	$t_{1/2}$ (min) = ln(2) / k =	188.54
	k (mol L^{-1} min^{-1}) =	2.88E-04	k (L mol^{-1} min^{-1}) =	0.39

6.4 NMR STUDIES

To understand better which were the species present in solution, NMR studies were carried out (Figure 34). In a first experiment, $RuCl_3(H_2O)_x$ was refluxed in *i*PrOH overnight before evaporating the solvent, re-dissolving the crude in MeOH and adding ligand and base (Experiment 1, Figure 34). The ^{31}P NMR spectrum of the obtained mixture was recorded and showed no phosphine oxide or any other signals except that of the free ligand (see Figure 35 A). A second NMR experiment was performed after treating $RuCl_3(H_2O)_x$ according to the optimized reaction protocol, i.e. stirring the metal source with (*S*,*S*)-**99** and Na_2CO_3 for 30 min and then analyzing the mixture: in this case a number of different ^{31}P NMR signals were found, mostly located at chemical shifts typical of phosphine oxides (Experiment 2, Figure 34 and Figure 35 B). A similar result was obtained in a third experiment, in which $RuCl_3(H_2O)_x$ was pre-treated with (*S*,*S*)-**99** in the absence of base (Experiment 3, Figure 34 and Figure 35 B).

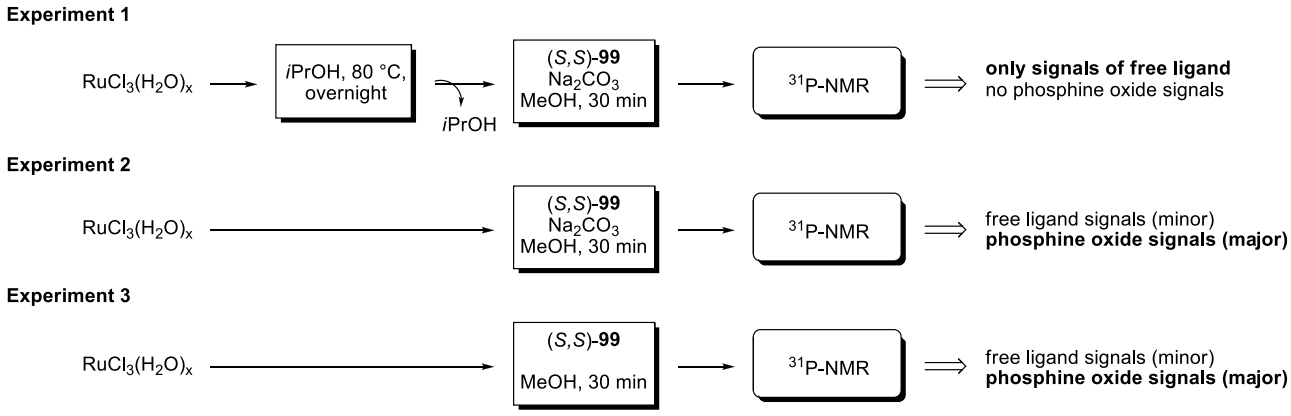

Figure 34. Investigation of the catalyst formation process by NMR.

Altogether, these NMR experiments lead to hypothesize that probably, in the standard optimized protocol, a slow phosphine-catalyzed reduction of Ru^{III} takes place in which the excess H_2 acts as terminal reductant. After this process, the catalytic complex forms rapidly, although it must be only stable under H_2 pressure, as witnessed by the fact that we could never observe it under inert atmosphere.

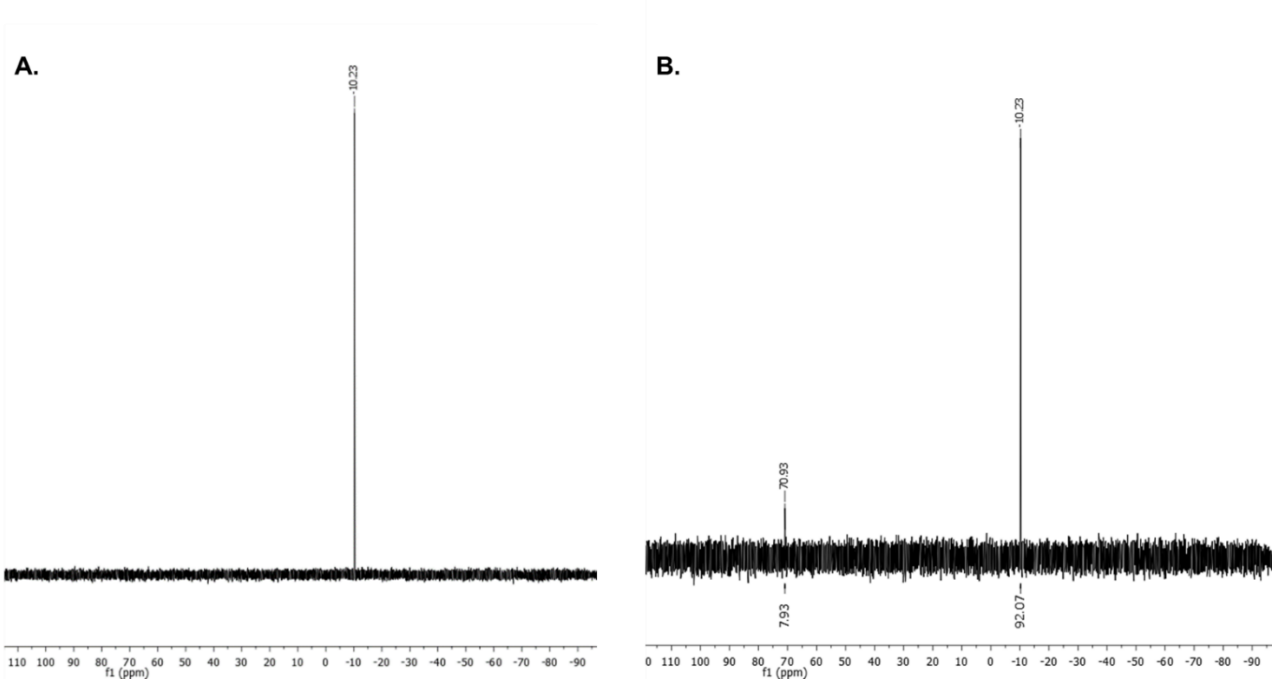

Figure 35. A. ^{31}P-NMR spectrum of the product obtained by boiling $RuCl_3(H_2O)_x$ in *i*PrOH overnight and then adding (*S*,*S*)-**99** and Na_2CO_3 (experiment **N1**). ^{31}P-NMR (162 MHz, CD_3OD): δ -10.23. **B.** ^{31}P-NMR spectrum of the product obtained after treating $RuCl_3(H_2O)_x$ in methanol with (*S*,*S*)-**99**/Na_2CO_3 (experiment **N2**) or (*S*,*S*)-**99** alone (experiment **N3**). ^{31}P-NMR (162 MHz, CD_3OD): δ -70.93, δ -10.23.

Several attempts were made in order to isolate and characterize the catalytic complex but, unfortunately, all of them were unsuccessful due to its high sensitivity.

6.5 Summary of Trost Ligand in Asymmetric Hydrogenation of Ketones

In summary, a new ruthenium-catalyzed AH of ketones based on the use of the Trost ligand (*S*,*S*)-**99** has been reported. To the best of our knowledge, so far the Trost Ligand had never found application in metal-catalyzed reductions. The new $RuCl_3(H_2O)_x$/(*S*,*S*)-**99** catalytic system can be readily prepared *in situ* and provides access to a range of chiral alcohols with good conversions and high enantioselectivity (up to 96% *ee*). Kinetic studies demonstrate that formation of the catalytically active species takes place slowly in the presence of H_2. Compared to numerous other known methodologies for ketone AH,[185] the one described in this paper has the advantage of employing a commercially available chiral ligand (**99**) and a Ru source [$RuCl_3(H_2O)_x$] which is the cheapest available on the market. Therefore, this methodology represents a step forward to address the catalyst cost issues that often discourage the industrial use of asymmetric catalysis.

6.6 Experimental Section

6.6.1 General Remarks

All reactions were carried out in dried glassware with magnetic stirring under argon atmosphere, unless otherwise stated. Reaction solvents were either obtained from a solvent purification system and stored under argon, or distilled over the following drying agents and transferred under nitrogen: CH_2Cl_2 (CaH_2) and THF (Na). Dry toluene, hexane, *i*PrOH and methanol (over molecular sieves in bottles with crown cap) were purchased from Sigma Aldrich and stored under nitrogen. The reactions were monitored by analytical thin-layer chromatography (TLC) using silica gel 60 F254 pre-coated glass plates (0.25 mm thickness). Visualization was accomplished by irradiation with a UV lamp and/or staining with a potassium permanganate alkaline solution. Flash column chromatography was performed using silica gel (60 Å, particle size 40-64 μm) as stationary phase, following the procedure by Still and co-workers.[100] ^{1}H-, ^{13}C- and ^{31}P-NMR spectra were recorded on a Bruker AV 300 or 400 NMR spectrometer. All chemical shifts (δ) are reported in ppm and coupling constants (J) in Hz. All chemical shifts are related to residual solvent peaks [$CDCl_3$: 7.26 ppm (1H), 77.16 ppm (^{13}C)]. All measurements were carried out at r.t. unless otherwise stated. Mass spectra were recorded on a Finnigan MAT 95-XP (Thermo Electron) or on a 6210 Time of- Flight LC/MS (Agilent). Gas chromatography measurements were performed on either a HP 6890 or a 7890B gas chromatograph with a HP5 column (Agilent). Enantiomeric excess values were determined either by chiral gas chromatography on an Agilent 6890 GC equipped with a flame ionization detector, using a Lipodex E chiral capillary column, or by chiral HPLC, measured on a Agilent 1100 system (Chiralcel OD-H, Cellulose or Amylose chiral olumn), connected to a IBZ Chiralyser for determination of the optical rotation. Absolute configurations were determined by comparison of GC retention times or sign of optical rotations with literature values. High resolution mass spectra (HRMS) were measured on a Fourier Transform Ion Cyclotron Resonance (FT-ICR) Mass Spectrometer APEX II & Xmass software (Bruker Daltonics) – 4.7 T Magnet (Magnex) equipped with ESI source. Low resolution mass spectra (MS) were acquired either on a Thermo-Finnigan LCQ Advantage mass spectrometer (ESI ion source) or on a VG Autospec M246 spectrometer (FAB ion source).

6.6.2 Materials

Ketones used in the substrate screening were purchased from commercial suppliers (TCI Chemicals, ACROS, Sigma Aldrich) and distilled over PPh_3 before use. *t*BuOK was purified by sublimation before use. The other commercially available reagents were used as received.

6.6.3 General procedures

6.6.3.1 Screening of metal sources

In oven-dried vials, metal precursors (0.005 mmol, 0.05 eq.) and ligand (S,S)-**99** (3.6 mg, 0.005 mmol, 0.05 eq.), were subjected to 3 vacuum-argon cycles, and dissolved in 0.25 mL of dry methanol. After stirring for 20 min at r.t., 0.27 mL of 0.2 M *t*BuOK solution in methanol (0.05 mmol, 0.5 eq.) were dispensed into each vial and the mixtures were stirred for 1 h. Acetophenone (12 μL, 0.1 mmol, 1 eq.) was added and the vials were transferred into an autoclave, which was purged three times with H_2, pressurized to 30 bar, heated at 80 °C and magnetically stirred for 22 h. After cooling down and venting H_2, hexadecane (0.1 mmol) was added in each vial and GC analysis was performed. The *ee* values were determined by GC with a chiral capillary column (see further section).

6.6.3.2 Solvent screening

In oven-dried vials, $RuCl_3(H_2O)_x$ (1.1 mg, 0.005 mmol, 0.05 eq.), ligand (S,S)-**99** (3.6 mg, 0.005 mmol, 0.05 eq.) and sublimated *t*BuOK (5.8 mg, 0.05 mmol, 0.5 eq.), were subjected to 3 vacuum-argon cycles, and dissolved in 0.52 mL of dry solvent. The mixtures were stirred for 1 h at r.t., and then acetophenone (12 μL, 0.1 mmol, 1 eq.) was dispensed into each vial. The vials were then transferred into an autoclave, which was purged three times with H_2, then pressurized to 30 bar, heated at 60 °C and magnetically stirred for 22 h. After cooling down and venting H_2, hexadecane (0.1 mmol) was added in each vial and GC analysis was performed. The *ee* values determined by GC with a chiral capillary column (see further section).

6.6.3.3 Base screening

In oven-dried vials, $RuCl_3(H_2O)_x$ (1.1 mg, 0.005 mmol, 0.05 eq.), ligand (S,S)-**99** (3.6 mg, 0.005 mmol, 0.05 eq.) and the selected base (0.05 mmol, 0.5 eq.), were subjected to 3 vacuum-argon cycles, and dissolved in 0.52 mL of dry methanol. The mixtures were stirred for 1 h at r.t., and then acetophenone (12 μL, 0.1 mmol, 1 eq.) was dispensed into each vial. The vials were then transferred into an autoclave, which was purged three times with H_2, pressurized to 30 bar and magnetically stirred at r.t. for 22 h. After venting H_2, hexadecane (0.1 mmol) was added in each vial and GC analysis was performed. The *ee* values determined by GC with a chiral capillary column (see further section).

6.6.3.4 General Procedure for Hydrogenation.

In a Schlenk vessel under argon atmosphere, a stock solution of catalyst was prepared dissolving $RuCl_3(H_2O)_x$ (2.7 mg, 0.01 mmol), ligand (*S,S*)-**99** (6.9 mg, 0.01 mmol) and Na_2CO_3 (5.3 mg 0.05 mmol) in 5 mL of dry methanol. The solution was stirred for 45 min at r.t., and then 0.5 mL-aliquots (each corresponding to 0.001 mmol / 0.01 eq. of

[Ru]) were dispensed into vials containing the freshly distilled substrate(s) (0.1 mmol, 1 eq.) placed into an argon-filled vessel. The vials were transferred into an autoclave, which was purged three times with H_2 and then pressurized to 30 bar and magnetically stirred at r.t. for 22 h. After venting H_2, hexadecane (0.1 mmol) was added in each vial and GC analysis was performed. The *ee* values determined by chiral GC or HPLC (see further section).

6.6.3.5 General procedure preparative scale experiments

In a Schlenk vessel under argon atmosphere, $RuCl_3(H_2O)_x$ (17.4 mg, 0.066 mmol, 0.01 eq.), ligand (S,S)-**99** (45.9 mg, 0.066 mmol, 0.01 eq.) and Na_2CO_3 (35.2 mg, 0.33 mmol, 0.05 eq.) were dissolved in 6.2 mL of dry methanol. The solution was stirred for 45 min at r.t. and then the substrate (6.6 mmol, 1 eq.) was added. The mixture was transferred to an autoclave, which was purged three times with H_2 and then pressurized to 30 bar and magnetically stirred at r.t. for 22 h. After venting H_2, the volatiles were evaporated and the residue was purified by flash column chromatography.

6.6.4 Kinetic Experiments

6.6.4.1 Experiment run under the optimized conditions (Label: ●)

In a Schlenk vessel under argon atmosphere, $RuCl_3(H_2O)_x$ (17.4 mg, 0.066 mmol, 0.01 eq.), ligand (*S,S*)-**99** (45.9 mg, 0.066 mmol, 0.01 eq.) and Na_2CO_3 (35.2 mg, 0.33 mmol, 0.05 eq.) were dissolved in 6.2 mL of dry methanol. The solution was stirred for 45 min at r.t.. Acetophenone (0.8 mL, 6.6 mmol, 1 eq.) was added and the solution was moved into an autoclave, which was purged three times with H_2 and then pressurized to 30 bar and mechanically stirred (300 rpm) at r.t.. The reaction was run overnight while monitoring the hydrogen uptake, from which conversion values were calculated. GC analysis of the crude reaction mixture allowed to measure final conversion and *ee*.

Note: time = 0 was marked when the reactor was filled with hydrogen.

6.6.4.2 Experiments run after preliminary reduction of Ru^{III} in *i*PrOH

Experiment 1 (Label ▲)

Under argon atmosphere, $RuCl_3(H_2O)_x$ (17.4 mg, 0.066 mmol, 0.01 eq.), ligand (*S,S*)-**99**(45.9 mg, 0.066 mmol, 0.01 eq.) and Na_2CO_3 (35.2 mg, 0.33 mmol, 0.05 eq.) were dissolved in 2-propanol and heated at 80 °C overnight. After 18 h, 2-propanol was removed under vacuum and dry methanol was added, followed by acetophenone (0.8 mL, 6.6

mmol, 1 eq.). The solution obtained was moved into an autoclave and subjected to hydrogenation under 30 bar or hydrogen measuring the H_2 uptake.

Experiment 2 (Label ■)

Under argon atmosphere, $RuCl_3(H_2O)_x$ (17.4 mg, 0.066 mmol, 0.01 eq.) and ligand (*S*,*S*)-**99**(45.9 mg, 0.066 mmol, 0.01 eq.) were dissolved in 2-propanol and heated at 80 °C overnight. After 18 h, 2-propanol was removed under vacuum. Na_2CO_3 (35.2 mg, 0.33 mmol, 0.05 eq.) and dry methanol were added, followed by acetophenone (0.8 mL, 6.6 mmol, 1 eq.). The solution obtained was moved into an autoclave and subjected to hydrogenation under 30 bar or hydrogen measuring the H_2 uptake.

Experiment 3 (Label ◆)

Under argon atmosphere, $RuCl_3(H_2O)_x$ (17.4 mg, 0.066 mmol, 0.01 eq.) was dissolved in 2-propanol and heated at 80 °C overnight. After 18 h, 2-propanol was removed under vacuum. Ligand (*S*,*S*)-**99**(45.9 mg, 0.066 mmol, 0.01 eq.) and Na_2CO_3 (35.2 mg, 0.33 mmol, 0.05 eq.) were added and dissolved in methanol. After stirring for 30 min at r.t. (18 °C), acetophenone (0.8 mL, 6.6 mmol, 1 eq.) was added and the obtained solution was moved into an autoclave and subjected to hydrogenation under 30 bar of hydrogen measuring the H_2 uptake.

Experiment 4 (Label •)

Under argon atmosphere, $RuCl_3(H_2O)_x$ (17.4 mg, 0.066 mmol, 0.01 eq.) was dissolved in 2-propanol and heated at 80 °C overnight. After 18 h, 2-propanol was removed under vacuum. Ligand (*S*,*S*)-**99**(45.9 mg, 0.066 mmol, 0.01 eq.) and Na_2CO_3 (35.2 mg, 0.33 mmol, 0.05 eq.) were added and dissolved in methanol. After stirring for 30 min at 40 °C, acetophenone (0.8 mL, 6.6 mmol, 1 eq.) was added and the obtained solution was moved into an autoclave and subjected to hydrogenation under 30 bar of hydrogen measuring the H_2 uptake.

6.6.5 NMR Experiments

6.6.5.1 Experiment 1

Under argon atmosphere, $RuCl_3(H_2O)_x$ (1.93 mg, 0.007 mmol, 0.01 eq.) was dissolved in 2-propanol and heated at 80 °C overnight. After 18 h, 2-propanol was removed under vacuum. Ligand (*S*,*S*)-**99**(5.1 mg, 0.007 mmol, 0.01 eq.) and Na_2CO_3 (3.91 mg, 0.036 mmol, 0.05 eq.) were added and dissolved in dry methanol. After stirring for 30 min at r.t. (18 °C), the mixture was analyzed by NMR.

6.6.5.2 Experiment 2

Under argon atmosphere, $RuCl_3(H_2O)_x$ (1.93 mg, 0.007 mmol, 0.01 eq.) ligand (*S,S*)-**99**(5.1 mg, 0.007 mmol, 0.01 eq.) and Na_2CO_3 (3.91 mg, 0.036 mmol, 0.05 eq.)were dissolved in dry methanol. After stirring for 30 min at r.t. (18 °C), the mixture was analyzed by NMR.

6.6.5.3 Experiment 3

Under argon atmosphere, $RuCl_3(H_2O)_x$ (1.93 mg, 0.007 mmol, 0.01 eq.) ligand (*S,S*)-**99**(5.1 mg, 0.007 mmol, 0.01 eq.) were dissolved in dry methanol. After stirring for 30 min at r.t. (18 °C), the mixture was analyzed by NMR.

6.6.6 GC Conversions

The conversions were measured based on GC analysis for all the substrates. Hexadecane was added as internal standard and based on a calibration line, the conversions are given by percentage. Using a chiral column, GC analysis was employed also for determination of enantiomeric excess of product: **P1**, **P69** and **P74**.

(*S*)-1-Phenylethanol (P1):

Capillary column: MEGADEX DACTBSβ, diacetyl-*tert*-butylsilyl-β-cyclodextrin, 0.25 µm; diameter = 0.25 mm; length = 25 m; carrier: hydrogen; inlet pressure: 1 bar; oven temperature: 95 °C for 20 min: $t_{\mathbf{S1}}$ = 6.0 min; $t_{(R)\text{-}\mathbf{P1}}$ = 13.8 min; $t_{(S)\text{-}\mathbf{P1}}$ = 14.8 min.

(*S*)-1-(4-Methoxyphenyl)ethanol (P3):

Capillary column: MEGADEX DACTBSβ, diacetyl-*tert*-butylsilyl-β-cyclodextrin, 0.25 µm; diameter = 0.25 mm; length = 25 m; carrier: hydrogen; inlet pressure: 1 bar; oven temperature: 110 °C for 10 min; 30 °C/min gradient; 120 °C for 10 min; 30 °C/min gradient; 130 °C: $\mathbf{t_{S3}}$ = 20.1 min; $t_{(R)\text{-P2}}$ = 21.1 min; $t_{(S)\text{-}\mathbf{P3}}$ = 22.6 min.

(*S*)-1-([1,1'-Biphenyl]-4-yl)ethan-1-ol (P65):

HP5 column, oven temperature: 100 °C for 5 min; 50 °C/min gradient to 200 °C, 100 °C/min gradient to 325 °C; $t_{\mathbf{S65}}$ = 13.61 min; $t_{\mathbf{P65}}$ = 13.48 min; $t_{\text{hexadecane}}$=7.91 min.

(*S*)-1-(4-Chlorophenyl)ethan-1-ol (P66):

HP5 column, oven temperature: 100 °C for 5 min; 50 °C/min gradient to 200 °C, 100 °C/min gradient to 325 °C; t_{S66} = 8.84 min; t_{P66} = 5.41 min; $t_{hexadecane}$=7.91 min.

(*S*)-1-(3-Chlorophenyl)ethan-1-ol (P67):

HP5 column, 70 °C for 5 min, 15 °C/min to 250 °C, 250 °C for 3 min; t_{S67} = 9.00 min; t_{P67} = 8.82 min; $t_{hexadecane}$=11.95 min.

(*S*)-1-(2-Chlorophenyl)ethan-1-ol (P6):

HP5 column, oven temperature: 100 °C for 5 min; 50 °C/min gradient to 200 °C, 100 °C/min gradient to 325 °C; t_{S6} = 5.78 min; t_{P6} = 6.18 min; $t_{hexadecane}$=7.91 min.

(*S*)-1-(4-(Trifluoromethyl)phenyl)ethan-1-ol (P68):

HP5 column, oven temperature: 100 °C for 5 min; 50 °C/min gradient to 200 °C, 100 °C/min gradient to 325 °C; t_{S68} = 3.68 min; t_{P68} = 4.39 min; $t_{hexadecane}$=7.91 min.

(*S*)-1-(3,5-Bis(trifluoromethyl)phenyl)ethan-1-ol (P69):

Capillary column: MEGADEX DACTBSβ, diacetyl-*tert*-butylsilyl-β-cyclodextrin, 0.25 µm; diameter = 0.25 mm; length = 25 m; carrier: hydrogen; inlet pressure: 1 bar; oven temperature: 95 °C for 30 min: T_{S69} = 4.28 min; $t_{(S)\text{-}P69}$ = 12.48 min, $t_{(R)\text{-}P69}$ = 13.49 min.

(*S*)-1-(3-Aminophenyl)ethan-1-ol (P70):

HP5 column, oven temperature: 100 °C for 5 min; 50 °C/min gradient to 200 °C, 100 °C/min gradient to 325 °C; t_{S70} = 7.27 min; t_{P70} = 7.45 min, $t_{hexadecane}$=7.91 min.

(*S*)-1-(Naphthalen-2-yl)ethan-1-ol (P71):

HP5 column, oven temperature: 100 °C for 5 min; 50 °C/min gradient to 200 °C, 100 °C/min gradient to 325 °C; t_{S71} = 12.14 min; t_{P71} = 11.95 min; $t_{hexadecane}$=7.91 min.

(*S*)-1-(Furan-2-yl)ethan-1-ol (P72):

HP5 column, oven temperature: 35 °C for 10 min; 8 °C/min gradient to 280 °C; t_{S72} = 15 min; t_{P72} =14.3 min.

(*R*)-Octan-2-ol (P73):

Capillary column: MEGADEX DACTBSβ, diacetyl-*tert*-butylsilyl-β-cyclodextrin, 0.25 μm; diameter = 0.25 mm; length = 25 m; carrier: hydrogen; inlet pressure: 1 bar; oven temperature: 95 °C for 20 min: t_{S73} = 3.6 min; $t_{(rac)\text{-}P73}$ = 4.1 min.

(*S*)-1-Phenylpropan-1-ol (P74):

Capillary column: MEGADEX DACTBSβ, diacetyl-*tert*-butylsilyl-β-cyclodextrin, 0.25 μm; diameter = 0.25 mm; length = 25 m; carrier: hydrogen; inlet pressure: 1 bar; oven temperature: 95 °C for 20 min: t_{S74} = 9.4 min; $t_{(R)\text{-}P74}$ = 16.6 min; $t_{(S)\text{-}P74}$ = 18.5 min.

1,2,3,4-Tetrahydronaphthalen-1-ol (P8):

Column: Agilent HP-5; 70 °C for 5 min, 15 °C/min to 250 °C, 250 °C for 3 min; t_{S8} = 10.18 min; t_{P8} = 9.99 min, $t_{hexadecane}$ = 11.95 min.

6.6.7 Isolated Yields

The hydrogenation of substrates **S1**, **S3**, and **S69** were carried out on a 6 mmol scale following the General Procedure.

(*S*)-1-Phenylethanol (P1):

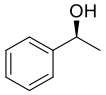

After the hydrogenation, the volatiles were evaporated and the residue was purified by flash column chromatography. The product was isolated as a colorless oil. Yield: 733 mg (96%). Its physical and spectroscopic data fit with those reported in the literature.[107a]

^{1}H-NMR (400 MHz, $CDCl_3$): δ 7.43-7.34 (m, 4H), 7.33-7.28 (m, 1H), 4.92 (q, J = 6.5 Hz, 1H), 1.91 (s, 1H), 1.53 (d, J = 6.5 Hz, 3H).

(*S*)-1-(4-Methoxyphenyl)ethanol (P3):

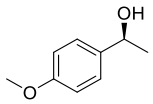

After the hydrogenation, the volatiles were evaporated and the residue was purified by flash column chromatography. The product was isolated as a colorless oil. Yield: 886 mg (97%). Its physical and spectroscopic data are superimposable with those reported in the literature.[193]

^{1}H-NMR (400 MHz, $CDCl_3$): δ 7.32 (d, *J* = 8.7 Hz, 2H), 6.91 (d, *J* = 8.7 Hz, 2H), 4.88 (q, *J* = 6.4 Hz, 1H), 3.83 (s, 3H), 1.82 (br s, 1H), 1.50 (d, *J* = 6.4 Hz, 3H).

(*S*)-1-(3,5-Bis(trifluoromethyl)phenyl)ethan-1-ol (P69):

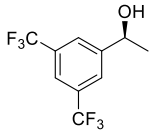

After the hydrogenation, the volatiles were evaporated and the residue was purified by flash column chromatography. The product was isolated as a white solid. Yield: 1.55 g (quantitative). Its physical and spectroscopic data are superimposable with those reported in the literature.[194]

^{1}H-NMR (400 MHz, $CDCl_3$): δ 7.84 (s, 2H), 7.79 (s, 1H), 5.05 (m, 1H), 1.55 (d, *J* = 6.5 Hz, 3H).

6.6.8 Enantiomeric Excess Determination

The *ee* of products **P1**, **P69** and **P74** was determined by GC analysis (already reported). The *ee* of the other substrates was measured by HPLC using a chiral column. All the details are reported in the Supporting Information of the paper.[191]

Summary

In Part A of this thesis the synthesis and reactivity of new iron complexes promoting the reduction of C=O and C=N bonds is reported. The state of the art in homogenous iron catalyzed hydrogenations is introduced in Chapter 1 followed by the results obtained with each class of iron complexes. Chapter 2 shows the synthesis, characterization and reactivity of BINOL-derived tetra isonitrile iron complexes. Two different families were designed differing in the length of the arm bearing the isonitrile group. Those complexes proved to promote ATH and AH of acetophenone under basic conditions. Although the initial results were encouraging, the further attempts to improve the performances were mostly ineffective. Lack of activity, enantioselectivity and reproducibility issues convinced us to not proceed further.

Chapter 3 reports a new class of isonitrile-phosphine ligands called PCCP: a chelating system bearing phosphine and isonitrile groups in the same BINOL-derived scaffold. Design, synthesis and characterization of the PCCP ligand are here reported. Once the corresponding iron complex was obtained, ATH of acetophenone was performed but only racemic 1-phenylethanol was yielded. Synthesis of the second generation of PCCP is still undergoing.

Chapter 4 is mainly dedicated to the synthesis and the catalytic properties of the (cyclopentadienone)iron pre-catalyst [bis(hexamethylene) cyclopentadienone] iron complex **81**. In the first part of the chapter the synthesis of **81** by the reaction of cyclooctyne with $Fe(CO)_5$ and the investigation of its catalytic properties in C=O bond reduction is reported. As a result of the peculiar reactivity of cyclooctyne, **81** was formed in good yield (56%) by intermolecular cyclative carbonylation/complexation with $Fe(CO)_5$. **81** was fully characterized and its crystal structure was determined by using XRD. Catalytic tests revealed that, upon *in situ* activation with Me_3NO, **81** promotes the hydrogenation of ketones, aldehydes, and activated esters as well as the transfer hydrogenation of ketones and shows a higher activity than the classical "Knölker complex" **30**. Studies on the hydrogenation kinetics in the presence of **81** and **30** suggest that this difference in activity is probably caused by the better stability of the **81**-derived complex than that of the *in situ* generated Knölker–Casey catalyst. In the second part of Chapter 4 the first catalytic transfer hydrogenation of non-activated imines promoted by a Fe-catalyst **81** in the absence of Lewis acid co-catalysts is reported. Use of the (cyclopentadienone)iron complex **81** allowed to reduce a number of N-aryl and N-alkyl imines in very good yields using *i*PrOH as hydrogen source. The reaction proceeds with relatively low catalyst loading (0.5-2 mol%) and, remarkably, its scope includes also ketimines, whose reduction with a Fe-complex as the only catalyst has little precedents. Based on this new methodology, we developed a one-pot catalytic transfer hydrogenation protocol for the reductive amination of aldehydes/ketones, which provides access to secondary amines in high yield without the need to isolate imine intermediates.

Chapter 5 is focused on the catalytic performances of BINOL-derived (cyclopentadienone)iron complexes recently synthesized in our group. Those iron complexes showed good activity in asymmetric hydrogenation of ketones and although the *ee* values are clearly inferior to the best literature examples of ketone asymmetric hydrogenation, they still represent the best results obtained so far with chiral (cyclopentadienone)iron complexes. Their reactivity in imine reduction (AH and ATH) was investigated and the results are reported. Both pre- and *in situ* formed imines were screened and promising results were obtained for acetophenone-derived imines.

Part B of this thesis is focused on the use of ruthenium and Trost Ligand as catalyst for asymmetric hydrogenation of ketones. This research was carried out during my Erasmus+ Placement in LIKAT (Leibniz Institute for Catalysis, Rostock, Germany) under the supervision of Prof. Dr. J.G. de Vries and Dr. Sandra Hinze.

In Chapter 6, we described the use of Trost ligand as ligand in the AH of ketones. Trost ligand was screened in the presence of several metal salts and found to form active catalysts when combined with ruthenium sources in the presence of hydrogen and a base. Reaction optimization was carried out by screening different Ru sources, solvents and bases. Under the optimized conditions, the complex formed by combination of Trost ligand with $RuCl_3(H_2O)_x$ in the presence of Na_2CO_3, is able to promote the AH of several ketones at r.t. with good yields and up to 96% *ee*. The reaction kinetics measured under the optimized conditions revealed the presence of a long induction period, during which the initially formed Ru species is transformed into the catalytically active complex by reaction with hydrogen.

List of Abbreviations

Å	1 angstrom (10^{-10} m)
acac	Acetylacetonate
ATH	Asymmetric Transfer Hydrogenation
AH	Asymmetric Hydrogenation
BINOL	1,1'-Bi-2-naphtol
Bn	Benzyl-
Bu	Butyl-
CAN	Ceric ammonium nitrate
cod	Cyclooctadienyl
CH	Catalytic Hydrogenation
CTH	Catalytic Transfer Hydrogenation
Cy	Cyclohexyl-
DCE	1,2-dichloroethane
DCC	*N,N'*-Dicyclohexylcarbodiimide
DCM	Dichloromethane
DIC	*N,N'*-Diisopropylcarbodiimide
DMAP	4-Dimethylaminopyridine
DME	Dimethoxyethane
DMF	*N,N*-dimethylformamide
dppp	1,3-Bis(diphenylphosphino)propane
δ	Chemical shift
EDC	(3-Dimethylaminopropyl)-*N*-ethylcarbodiimide hydrochloride
EPR	Electron paramagnetic resonance
eq.	Equivalents
ESI	Electrospray-ionization
Et	Ethyl-
AcOEt	Ethyl acetate
hex	Hexyl-
HMDS	Hexamethyldisilazane
HMTA	Hexamethylenetetraamine (urotropine)
HOMO	Highest Occupied Molecular Orbital

HRMS	High resolution mass spectrometry
Hz	Hertz
*i*PrOH	2-Propanol
J	Coupling constant
LDA	Lithium diisopropylamide
LUMO	Lowest Unoccupied Molecular Orbital
M	Molar [mol/L]
Me	Methyl-
MOM	Methoxymethyl
MTBE	Methyl-tert-butylether
n	Normal
NHC	*N*-Heterocyclic carbenes
NMR	Nuclear magnetic resonance
NP	Nanoparticles
Ph	Phenyl-
PMP	Para-methoxyphenyl
ppm	Parts per million
Py	Pyridine
rf	Retention factor
r.t.	Room temperature
TBDPS	Tert-Butyldiphenylsilyl
TBDMS	Tert-Butyldimethylsilyl
TBS	Tert-butyldimethylsilyl
TCBC	2,4,6-Trichlorobenzoyl chloride
TEA	Triethylamine
THF	Tetrahydrofuran
TIPS	Triisopropylsilyl
TLC	Thin layer chromatography
TMAO	Trimethylamine oxide
TMDS	1,1,3,3-Tetramethyldisilazane
TMS	Trimethylsilyl
TOF	Turnover Frequency
TON	Turnover Number
TS	Transition State

XRD X-ray Diffraction

List of Publications

- *Use of the Trost Ligand in the Ruthenium-Catalyzed Asymmetric Hydrogenation of Ketones.* M. Cettolin, P. Puylaert, L. Pignataro, S. Hinze, C. Gennari, J.G. de Vries, *ChemCatChem* **2017**, *9*, 3125-3130.

- *Synthesis of [Bis(hexamethylene)cyclopentadienone]iron Tricarbonyl and its Application to the Catalytic Reduction of C=O Bonds.* S. Vailati Facchini, J.-M. Neudörfl, L. Pignataro, M. Cettolin, C. Gennari, A. Berkessel, U. Piarulli, *ChemCatChem* **2017**, *9*, 1461-1468.

- *Highly Efficient Synthesis of Amines by Iron-Catalyzed C=N Transfer Hydrogenation and C=O Reductive Amination.* M. Cettolin, S. Vailati Facchini, X. Bai, G. Casamassima, L. Pignataro, C. Gennari, U. Piarulli, *Adv. Synth. Catal.*, DOI : 10.1002/adsc.201701316, *in press.*

References

1 a) G. Blaschke, H. P. Kraft, K. Fickentscher, F. Köhler, *Arzneimittelforschung* **1979**, *29*, 1640; b) W. Heger, H.-J. Schmahl, S. Klug, A. Felies, H. Nau, H.-J. Merker, D. Neubert, *Teratogenesis, Carcinogenesis, and Mutagenesis* **1994**, *14*, 115.

2 Prices obtained from http://www.infomine.com/investment/metal-prices/ as for 1.12.2015.

3 K. S. Egorova, V. P. Ananikov, *Angew. Chem. Int. Ed.* **2016**, *55*, 12150.

4 A. K. Patra, K. S. Dube, G. C. Papaefthymiou, J. Conradie, A. Ghosh, T. C. Harrop, *Inorg. Chem.* **2010**, *49*, 2032.

5 I. Bauer, H.-J. Knölker, in *Iron Catalysis in Organic Chemistry*, Wiley-VCH Verlag GmbH & Co. KGaA, **2008**, pp. 1-27.

6 J. D. Lee, *Concise Inorganic Chemistry* **1996**, 5th Edition, Chapman & Hall, London.

7 V. Smil, *Nature* **1999**, *400*, 415.

8 K. W. Kolasinski, *Where are Heterogenous Reactions Important. Surface science: foundations of catalysis and nanoscience*, **2002**, John Wiley and Sons. pp. 15–16.

9 L. Mond, F. Quinke, *J. Chem. Soc.* **1891**, *59*, 604.

10 M. Berthelot, C. R. Hebd. *Seances Acad. Sci.* **1891**, *112*, 1343.

11 T. J. Kealy, P. L. Pauson, *Nature* **1951**, *168*, 1039.

12 W. Reppe, H. Vetter, *Justus Liebigs Ann. Chem.* **1953**, *582*, 133.

13 (a) M. Tamura, J. Kochi, *Synthesis* **1971**, 303; (b) M. Tamura, J. Kochi, *J. Am. Chem. Soc.* **1971**, *93*, 1487.

14 P. T. Anastas, J. C. Warner, in *Green chemistry: theory and practice* **1998**, Oxford University Press, Oxford [England].

15 H. U. Blaser, C. Malan, B. Pugin, F. Spindler, H. Steiner, M. Studer, *Adv. Synth. Catal.*, **2003**, *345*, 103.

16 S. Blanchard, E. Derat, M. Desage-El Murr, L. Fensterbank, M. Malacria, V. Mouriès-Mansuy, *Eur. J. Inorg. Chem.* **2012**, *2012*, 376.

17 B. de Bruin, *Eur. J. Inorg. Chem.* **2012**, 340.

18 K. Jørgensen, *Coord. Chem. Rev.* **1966**, *1*, 164.

19 a) P. H. M. Budzelaar, *Eur. J. Inorg. Chem.* **2012**, *2012*, 530; b) K. G. Caulton, *Eur. J. Inorg. Chem.* **2012**, *2012*, 435; c) R. E. Cowley, G. J. Christian, W. W. Brennessel, F. Neese, P. L. Holland, *Eur. J. Inorg. Chem.* **2012**, *2012*, 479; d) W. Kaim, *Eur. J. Inorg. Chem.* **2012**, *2012*, 343; and other paper from the special issue 3 "Coopertive & Redox Non-Innocent Ligands in Directing Organometallic Reactivity".

20 a) H. Grützmacher, *Angew. Chem. Int. Ed.* **2008**, *47*, 1814; b) J. I. van der Vlugt, J. N. H. Reek, *Angew. Chem. Int. Ed.* **2009**, *48*, 8832.

21 a) E. N. Frankel, E. A. Emken, H. M. Peters, V. L. Davison, R. O. Butterfield, *The Journal of Organic Chemistry* **1964**, *29*, 3292; b) E. N. Frankel, E. A. Emken, V. L. Davison, *The Journal of Organic Chemistry* **1965**, *30*, 2739.

22 R. Noyori, I. Umeda, T. Ishigami, *The Journal of Organic Chemistry* **1972**, *37*, 1542.

23 a) B. H. Weiller, M. E. Miller, E. R. Grant, *J. Am. Chem. Soc.* **1987**, *109*, 352; b) B. H. Weiller, E. R. Grant, *J. Am. Chem. Soc.* **1987**, *109*, 1051; c) M. E. Miller, E. R. Grant, *J. Am. Chem. Soc.* **1987**, *109*, 7951.

24 M. Kamitani, Y. Nishiguchi, R. Tada, M. Itazaki, H. Nakazawa, *Organometallics* **2014**, *33*, 1532.

25 V. C. Gibson, C. Redshaw, G. A. Solan, *Chem. Rev.* **2007**, *107*, 1745.

26 J. A. Osborn, F. H. Jardine, J. F. Young, G. Wilkinson, *J. Chem. Soc. A* 1966, 1711.

27 R. Crabtree, *Acc. Chem. Res.* **1979**, *12*, 331.

28 S. C. Bart, K. Chłopek, E. Bill, M. W. Bouwkamp, E. Lobkovsky, F. Neese, K. Wieghardt, P. J. Chirik, *J. Am. Chem. Soc.* **2006**, *128*, 13901.

29 R. J. Trovitch, E. Lobkovsky, E. Bill, P. J. Chirik, *Organometallics* **2008**, *27*, 1470.

30 a) S. C. E. Stieber, C. Milsmann, J. M. Hoyt, Z. R. Turner, K. D. Finkelstein, K. Wieghardt, S. DeBeer, P. J. Chirik, *Inorg. Chem.* **2012**, *51*, 3770; b) A. M. Tondreau, S. C. E. Stieber, C. Milsmann, E. Lobkovsky, T. Weyhermüller, S. P. Semproni, P. J. Chirik, *Inorg. Chem.* **2013**, *52*, 635.

31 S. K. Russell, J. M. Darmon, E. Lobkovsky, P. J. Chirik, *Inorg. Chem.* **2010**, *49*, 2782.

32 R. J. Trovitch, E. Lobkovsky, P. J. Chirik, *Inorg. Chem.* **2006**, *45*, 7252.

33 C. Bianchini, A. Meli, M. Peruzzini, P. Frediani, C. Bohanna, M. A. Esteruelas, L. A. Oro, *Organometallics* **1992**, *11*, 138.

34 G. Wienhofer, F. A. Westerhaus, R. V. Jagadeesh, K. Junge, H. Junge, M. Beller, *Chem. Commun.* **2012**, *48*, 4827.

35 E. J. Daida, J. C. Peters, *Inorg. Chem.* **2004**, *43*, 7474.

36 H. Fong, M.-E. Moret, Y. Lee, J. C. Peters, *Organometallics* **2013**, *32*, 3053.

37 K. Kano, M. Takeuchi, S. Hashimoto, Z.-i. Yoshida, *J. Chem. Soc., Chem. Commun.* **1991**, 1728.

38 a) S. Sakaki, T. Sagara, T. Arai, T. Kojima, T. Ogata, K. Ohkubo, *J. Mol. Catal.* **1992**, *75*, L33; b) S. Sakaki, T. Kojima, T. Arai, *J. Chem. Soc., Dalton Trans.* **1994**, 7.
39 a) H. Inoue, M. Suzuki, *J. Chem. Soc., Chem. Commun.* **1980**, 817; b) H. Inoue, M. Sato, *J. Chem. Soc., Chem. Commun.* **1983**, 983.
40 P.-H. Phua, L. Lefort, J. A. F. Boogers, M. Tristany, J. G. de Vries, *Chem. Commun.* **2009**, 3747.
41 R. B. Bedford, M. Betham, D. W. Bruce, S. A. Davis, R. M. Frost, M. Hird, *Chem. Commun.* **2006**, 1398.
42 M. Stein, J. Wieland, P. Steurer, F. Teolle, R. Moulhaupt, B. Breit, *Adv. Synth. Catal.* **2011**, *353*, 523.
43 T. N. Gieshoff, A. Welther, M. T. Kessler, M. H. G. Prechtl, A. Jacobi von Wangelin, *Chem. Commun.* **2014**, *50*, 2261.
44 V. Kelsen, B. Wendt, S. Werkmeister, K. Junge, M. Beller, B. Chaudret, *Chem. Commun.* **2013**, *49*, 3416.
45 a) L. Markó, M. A. Radhi *J. Organomet. Chem.* **1981**, 218, 369; b) L. Markó, J. Pala, *Transition Met. Chem.* **1983**, *8*, 207.
46 J.-S. Chen, L.-L. Chen, Y. Xing, G. Chen, W.-Y. Shen, Z.-R. Dong, Y.-Y. Li, J.-X. Gao *Acta Chim. Sin.* **2004**, *62*, 1745.
47 J.-X. Gao, T. Ikariya, R. Noyori, *Organometallics* **1996**, *15*, 1087.
48 a) B. M. Trost, D. L. Van Vranken, *Angew. Chem. Int. Ed.* **1992**, *31*, 228; b) B. M. Trost, D. L. Van Vranken, C. Bingel, *J. Am. Chem. Soc.* **1992**, *114*, 9327.
49 J.-X. Gao, H. Zhang, X.-D. Yi, P.-P. Xu, C.-L. Tang, H.-L. Wan, K.-R. Tsai, T. Ikariya, *Chirality* **2000**, *12*, 383.
50 Y.-Y. Li, H. Zhang, J.-S. Chen, X.-L. Liao, Z.-R. Dong, J.-X. Gao, *J. Mol. Catal. A: Chem.* **2004**, *218*, 153.
51 C. Sui-Seng, F. Freutel, A. Lough, R. H. Morris, *Angew. Chem. Int. Ed.* **2008**, *47*, 940.
52 a) J. F. Sonnenberg, R. H. Morris, *ACS Catal.* **2013**, *3*, 1092; b) J. F. Sonnenberg, N. Coombs, P. A. Dube, R. H. Morris, *J. Am. Chem. Soc.* **2012**, *134*, 5893.
53 P. E. Sues, A. J. Lough, R. H. Morris, *Organometallics* **2011**, *30*, 4418.
54 A. A. Mikhailine, M. I. Maishan, R. H. Morris, *Org. Lett.* **2012**, *14*, 4638.
55 A. A. Mikhailine, M. I. Maishan, A. J. Lough, R. H. Morris, *J. Am. Chem. Soc.* **2012**, *134*, 12266.
56 a) C. A. Sandoval, T. Ohkuma, K. Muñiz, R. Noyori, *J. Am. Chem. Soc.* **2003**, *125*, 13490; b) R. Noyori, M. Kitamura, T. Ohkuma, *Proc. Natl. Ac. Sci.* **2004**, *101*, 5356.
57 a) W. Zuo, A. J. Lough, Y. F. Li, R. H. Morris, *Science* **2013**, *342*, 1080; b) P. O. Lagaditis, P. E. Sues, J. F. Sonnenberg, K. Y. Wan, A. J. Lough, R. H. Morris, *J. Am. Chem. Soc.* **2014**, *136*, 1367; c) S. A. M. Smith, R. H. Morris, *Synthesis* **2015**, *47*, 1775.
58 W. Zuo, S. Tauer, D. E. Prokopchuk, R. H. Morris, *Organometallics* **2014**, *33*, 5791.
59 a) M. Ranocchiari, A. Mezzetti, *Organometallics* **2009**, *28*, 1286; b) R. Bigler, E. Otth, A. Mezzetti, *Organometallics* **2014**, *33*, 4086; c) R. Bigler, A. Mezzetti, *Org. Lett.* **2014**, *16*, 6460; d) R. Bigler, R. Huber, A. Mezzetti, *Angew. Chem. Int. Ed.* **2015**, *54*, 5171.
60 S. Yu, W. Shen, Y. Li, Z. Dong, Y. Xu, Q. Li, J. Zhang, J. Gao, *Adv. Synth. Catal.* **2012**, *354*, 818.
61 Y.-Y. Li, S.-L. Yu, W.-Y. Shen, J.-X. Gao, *Acc. Chem. Res.* **2015**, *48*, 2587.
62 Y. Li, S. Yu, X. Wu, J. Xiao, W. Shen, Z. Dong, J. Gao, *J. Am. Chem. Soc.* **2014**, *136*, 4031.
63 D. M.-Morales, C. Jensen, in *The Chemistry of Pincer Compounds* **2007**, Elsevier Science, Amsterdam.
64 a) R. Langer, G. Leitus, Y. Ben-David, D. Milstein, *Angew. Chem. Int. Ed.* **2011**, *50*, 2120; b) R. Langer, M. A. Iron, L. Konstantinovski, Y. Diskin-Posner, G. Leitus, Y. Ben-David, D. Milstein, *Chem. Eur. J.* **2012**, *18*, 7196.
65 S. Enthaler, B. Hagemann, G. Erre, K. Junge, M. Beller, *Chem. – Asian J.* **2006**, *1*, 598.
66 S. Enthaler, G. Erre, M. K. Tse, K. Junge, M. Beller, *Tetrahedron Lett.* **2006**, *47*, 8095.
67 A. Naik, T. Maji, O. Reiser, *Chem. Commun.* **2010**, *46*, 4475.
68 A. Quintard, J. Rodriguez, *Angew. Chem. Int. Ed.* **2014**, *53*, 4044.
69 a) H.-J. Knölker, J. Heber, C. H. Mahler, *Synlett* **1992**, *1992*, 1002; b) H.-J. Knölker, J. Heber, *Synlett* **1993**, *1993*, 924; c) H.-J. Knölker, E. Baum, J. Heber, *Tetrahedron Lett.* **1995**, *36*, 7647.
70 a) A. J. Pearson, R. A. Dubbert, *J. Chem. Soc., Chem. Commun.* **1991**, 202; b) A. J. Pearson, R. J. Shively, R. A. Dubbert, *Organometallics* **1992**, *11*, 4096; b) A. J. Pearson, R. J. Shively, *Organometallics* **1994**, *13*, 578; c) A. J. Pearson, A. Perosa, *Organometallics* **1995**, *14*, 517; d) A. J. Pearson, X. Yao, *Synlett* **1997**, *1997*, 1281.
71 H.-J. Knölker, E. Baum, H. Goesmann, R. Klauss, *Angew. Chem. Int. Ed.* **1999**, *38*, 2064.
72 a) Y. Blum, D. Czarkie, Y. Rahamim, Y. Shvo, *Organometallics* **1985**, *4*, 1459; b) Y. Shvo, D. Czierkie, Y. Rahamin, D. F. Ghodosh, *J. Am. Chem. Soc.* **1986**, *108*, 7400; c) R. Prabhakaran, *Synlett* **2004**, 2048; d) R. Karvembu, R. Prabhakaran, K. Natarajan, *Coord. Chem. Rev.* **2005**, *249*, 911; e) B. L. Conley, M. K. Pennington-Boggio, E. Boz, T. J. Williams, *Chem. Rev.* **2010**, *110*, 2294.
73 a) C. P. Casey, H. Guan, *J. Am. Chem. Soc.* **2007**, *129*, 5816; b) R. M. Bullock, *Angew. Chem. Int. Ed.* **2007**, *46*, 7360.

74 X. Lu, R. Cheng, N. Turner, Q. Liu, M. Zhang, X. Sun *J. Org. Chem.* **2014**, *79*, 9355.
75 a) T.-Y. Luh, Coord. Chem. Rev. **1984**, *60*, 255; b) Reference 70b; c) Reference 69c; d) B. Dasgupta, W. A. Donaldson, *Tetrahedron Lett.* **1998**, *39*, 343; e) A. J. Pearson, Y. Kwak, *Tetrahedron Lett.* **2005**, *46*, 5417; f) A. Pagnoux-Ozherelyeva, N. Pannetier, M. D. Mbaye, S. Gaillard, J.-L. Renaud, *Angew. Chem. Int. Ed.* **2012**, *51*, 4976; g) S. Moulin, H. Dentel, A. Pagnoux-Ozherelyeva, S. Gaillard, A. Poater, L. Cavallo, J.-F. Lohier, J.-L. Renaud, *Chem. Eur. J.* **2013**, *19*, 17881; h) D. S. Mérel, M. Elie, J.-F. Lohier, S. Gaillard, J.-L. Renaud, *ChemCatChem* **2013**, *5*, 2939; i) T.-T. Thai, D. S. Mérel, A. Poater, S. Gaillard, J.-L. Renaud, *Chem. Eur. J.* **2015**, *21*, 7066.
76 H.-J. Knölker, H. Goesmann, R. Klauss, *Angew. Chem. Int. Ed.* **1999**, *38*, 702
77 a) A. Berkessel, S. Reichau, A. von der Höh, N. Leconte, J.-M. Neudörfl, *Organometallics* **2011**, *30*, 3880; b) A. Berkessel, A. Van der Höh, *ChemCatChem*, **2011**, *3*, 861.
78 a) A. Tlili, J. Schranck, H. Neumann, M. Beller, *Chem. Eur. J.* **2012**, *18*, 15935; b) S. Fleischer, S. Zhou, K. Junge, M. Beller, *Angew.Chem. Int. Ed.* **2013**, *52*, 5120.
79 a) R. Hodgkinson, A. Del Grosso, G. Clarkson, M. Wills, *Dalton Trans.* **2016**, *45*, 3992; b) J. P. Hopewell, J. E. D. Martins, T. C. Johnson, J. Godfrey, M. Wills, *Org. Biomol. Chem.* **2012**, *10*, 134.
80 a) P. Gajewski, M. Renom-Carrasco, S. Vailati Facchini, L. Pignataro, L. Lefort, J. G. de Vries, R. Ferraccioli, U. Piarulli, C. Gennari, *Eur. J. Org. Chem.* **2015**, 5526; b) P. Gajewski, M. Renom-Carrasco, S. Vailati Facchini, L. Pignataro, L. Lefort, J. G. de Vries, R. Ferraccioli, A. Forni, U. Piarulli, C. Gennari, *Eur. J. Org. Chem.* **2015**, 1887.
81 For some reviews on ketone AH, see: a) Reference 61; b) J.-H. Xie, D.-H. Bao, Q.-L. Zhou, *Synthesis* **2015**, *47*, 460; c) R. Noyori, *Angew. Chem. Int. Ed.* **2013**, *52*, 79; d) *Handbook of Homogeneous Hydrogenation* (Eds.: J. G. de Vries, C. J. Elsevier), Wiley-VCH, Weinheim, **2007**.
82 S. Fleischer, S. Zhou, S. Werkmeister, K. Junge, M. Beller, *Chem. Eur. J.* **2013**, *19*, 4997.
83 S. Zhou, S. Fleischer, H. Jiao, K. Junge, M. Beller, *Adv. Synth. Catal.* **2014**, *356*, 3451.
84 T. Yan, B. L. Feringa, K. Barta, **2014**, *5*, 5602.
85 M. Mastalir, M. Glatz, N. Gorgas, B. Stöger, E. Pittenauer, G. Allmaier, L. F. Veiros, K. Kirchner, *Chem. Eur. J.* **2016**, *22*, 12316.
86 B. Emayavaramban, M. Roy, B. Sundararaju, *Chem. Eur. J.* **2016**, *22*, 3952.
87 H.-J. Pan, T. W. Ng, Y. Zhao, *Chem. Commun.* **2015**, *51*, 11907.
88 T. Yan, B. L. Feringa, K. Barta, *ACS Catalysis* **2016**, *6*, 381.
89 H.-J. Pan, T. W. Ng, Y. Zhao, *Org. Biomol. Chem.* **2016**, *14*, 5490.
90 T. Zell, Y. Ben-David, D. Milstein, *Angew. Chem. Int. Ed.* **2014**, *53*, 4685.
91 S. Werkmeister, K. Junge, B. Wendt, E. Alberico, H. Jiao, W. Baumann, H. Junge, F. Gallou, M. Beller, *Angew. Chem. Int. Ed.* **2014**, *53*, 8722.
92 S. Chakraborty, H. Dai, P. Bhattacharya, N. T. Fairweather, M. S. Gibson, J. A. Krause, H. Guan, *J. Am. Chem. Soc.* **2014**, *136*, 7869.
93 P. Gajewski, A. Gonzalez-de-Castro, M. Renom-Carrasco, U. Piarulli, C. Gennari, J. G. de Vries, L. Lefort, L. Pignataro, *ChemCatChem* **2016**, *8*, 3431.
94 A. Dömling, I. Ugi, *Angew. Chem. Int. Ed.* **2000**, *39*, 3168.
95 F. E. Hahn, *Angew. Chem. Int. Ed.* **1993**, *32*, 650.
96 T. Ooi, M. Kameda, K. Maruoka, *J. Am. Chem. Soc.* **2003**, 125, 5139.
97 B. Ye, P.A. Donets, N. Cramer, *Angew. Chem. Int. Ed.* **2014**, *53*, 507.
98 S. Sengupta, M. Leite, D. S. Raslan, C. Quesnelle, V. Snieckus, *J. Org. Chem.* **1992**, *57*, 4066.
99 D. Cahard, V. Bizet, X. Dai, S. Gaillard, J.-L. Renaud, *J. Fluorine Chem.* **2013**, *155*, 78.
100 W. C. Still, M. Kahn, A. Mitra, *J. Org. Chem.* **1978**, *43*, 2923
101 A. Vogler, *Isonitrile Chemistry*, **1971**, Academic Pres inc., New York.
102 M.V. Barybin, V.G. Young, J.E. Ellis, *J. Am. Chem. Soc.* **2000**, *122*, 4678.
103 P. Dydio, R. J. Detz, B. de Bruin, J. N. H. Reek, *J. Am. Chem. Soc.* **2014**, *136*, 8418.
104 Y. Li, S. Das, S. Zhou, K. Junge, M. Beller, *J. Am. Chem. Soc.* **2012**, *134*, 9727.
105 Took inspiration from: M. Bauer, U. Kazmaier, *Eur. J. Org. Chem.* **2009**, *2009*, 2360.
106 M. Van Overschelde, E. Vervecken, S. G. Modha, S. Cogen, E. Van der Eycken, J. Van der Eycken, *Tetrahedron* **2009**, *65*, 6410.
107 a) T. N. Plank, J. L. Drake, D. K. Kim, T. W. Funk, *Adv. Synth. Catal.* **2012**, 354, 597; b) Reference **75g**.
108 C. P. Casey, H. Guan, *J. Am. Chem. Soc.* **2009**, *131*, 2499.
109 S. Elangovan, S. Quintero-Duque, V. Dorcet, T. Roisnel, L. Norel, C. Darcel, J.-B. Sortais, *Organometallics* **2015**, *34*, 4521.

110 a) Reference 79a; b) A. Rosas-Hernández, P. G. Alsabeh, E. Barsch, H. Junge, R. Ludwig, M. Beller, *Chem. Commun.* **2016**, *52*, 8393; Ref **77a**.
111 A. J. Rawlings, L. J. Diorazio, M. Wills, *Org. Lett.* **2015**, *17*, 1086; Refs. 75g,i; 80a.
112 S. Vailati Facchini, J.-M. Neudörfl, L. Pignataro, M. Cettolin, C. Gennari, A. Berkessel, U. Piarulli, *ChemCatChem* **2017**, *9*, 1461.
113 a) D. Fornals, M. A. Pericas, F. Serratosa, J. Vinaixa, M. Font-Altaba, X. Solans, *J. Chem. Soc., Perkin Trans. 1* **1987**, 2749; b) C. G. Krespan, *J. Org. Chem.* **1975**, *40*, 261; c) J. L. Boston, D. W. A. Sharp, G. Wilkinson, *J. Chem. Soc.* **1962**, 3488.
114 a) G. N. Schrauzer, *Chem. Ind.* **1958**, 1403; b) G. N. Schrauzer, *Chem. Ind.* **1958**, 1404; c) W. Hübel, E. H. Braye, *J. Inorg. Nucl. Chem.* **1959**, *10*, 250.
115 L. Brandsma, H. D. Verkruijsse, *Synthesis* **1978**, 290.
116 H. Kolshorn, H. Meier, Eu. Müller, *Tetrahedron Lett.* **1971**, *12*, 1469.
117 J.-L. Renaud, S. Gaillard, *Synthesis* **2016**, *48*, 3659.
118 For discussion on a possible decomposition pathway of the Knölker –Casey catalyst, see: M. G. Coleman, A. N. Brown, B. A. Bolton, H. Guan, *Adv. Synth. Catal.* **2010**, *352*, 967.
119 X. Lu, Y. Zhang, P. Yun, M. Zhang, T. Li, *Org. Biomol. Chem.* **2013**, *11*, 5264.
120 *Handbook of Homogeneous Hydrogenation* (Eds.: J. G. de Vries, C. J. Elsevier), Wiley-VCH, Weinheim, **2007**.
121 D. Wang, D. Astruc, *Chem. Rev.* **2015**, *115*, 6621.
122 a) S. A. Lawrence, *Amines: Synthesis, Properties and Applications*, Cambridge University Press, Cambridge, **2006**; b) A. Ricci, *Amino Group Chemistry: From Synthesis to the Life Sciences*, Wiley-VCH, Weinheim, **2008**.
123 For a recent review on iron catalysis, see: I. Bauer, H.-J. Knölker, *Chem. Rev.* **2015**, *115*, 3170.
124 a) D. Brenna, S. Rossi, F. Cozzi, M. Benaglia, *Org. Biomol. Chem.* **2017**, *15*, 5685; b) Reference 75i; c) Reference 83; d) Reference 57b; e) Reference 75g; f) Reference 82; g) Reference 75h; h) Reference 75f; i) Refence 78b.
125 For a tandem nitro group reduction-imine hydrogenation, see: T. Stemmler, A.-E. Surkus, M.-M. Pohl, K. Junge, M. Beller, *ChemSusChem* **2014**, *7*, 3012.
126 a) Refence 89; b) Reference 59d; c) W. Zuo, R. H. Morris, *Nat. Protoc.* **2015**, *10*, 241; d) Reference 57a; e) Reference 54; f) S. Zhou, S. Fleischer, K. Junge, S. Das, D. Addis, M. Beller, *Angew. Chem. Int. Ed.* **2010**, *49*, 8121.
127 See supporting information of: A. Hasegawa, Y. Naganawa, M. Fushimi, K. Ishihara, H. Yamamoto, *Org. Lett.* **2006**, *8*, 3175.
128 F. I. López, F. N. de la Cruz, J. López, J. M. Martínez, Y. Alcaraz, F. Delgado, A. Sánchez-Recillas, S. Estrada-Soto, M. A. Vázquez, *Med. Chem. Res.* **2017**, *26*, 1325.
129 See Supporting Information: F. Schaufelberger, L. Hu, O. Ramström, *Chem. Eur. J.* **2015**, *21*, 9776.
130 See Supporting Information: J. L. Garcia Ruano, J. Aleman, I. Alonso, A. Parra, V. Marcos, J. Aguirre, *Chem. Eur. J.* **2007**, *13*, 6179.
131 See Supporting Information: N. Mršić, A. J. Minnaard, B. L. Feringa, J. G. d. Vries, *J. Am. Chem. Soc.* **2009**, *131*, 8358.
132 See Supporting Informaton: C. Moessner, C. Bolm, *Angew. Int. Ed.* **2005**, *44*, 7564.
133 See Supporting Information: F.-M. Gautier, S. Jones, S. J. Martin, *Org. Biomol. Chem.* **2009**, *7*, 229.
134 T. Kanemitsu, A. Umehara, R. Haneji, K. Nagata, T. Itoh, *Tetrahedron* **2012**, *68*, 3893.
135 See Supporting Information: W. Li, G. Hou, M. Chang, X. Zhang, *Adv. Synth. Catal.* **2009**, *351*, 3123.
136 T. Hartung, B. Trauthwein *J. Org. Chem.* **2001**, *66*, 6339.
137 S. Liu, Y. Yu, L. S. Liebeskind, *Org. Lett.* **2007**, *9*, 1947.
138 See supporting Information: R. Sarma, D. Prajapati, *Chem. Commun.* **2011**, *47*, 9525.
139 K. Revunova, G. I. Nikonov, *Chem. Eur. J.* **2014**, *20*, 839.
140 F. Jiang, K. Yuan, M. Achard, C. Bruneau, *Chem. Eur. J.* **2013**, *19*, 10343.
141 M. L. Kantam, R. Kishore, J Yadav, M. Sudhakar, A. Venugopal, *Adv. Synth. Catal.* **2012**, *354*, 663.
142 D. Xu, S. Wang, Z. Shen, C. Xia, W. Sun, *Org. Biomol. Chem.* **2012**, *10*, 2730.
143 M. Nardi, G. Sindona, P. Costanzo, M. Oliverio, A. Procopio, *Tetrahedron* **2015**, *71*, 1132.
144 I. P. Query, P. A. Squier, E. M. Larson, N. A. Isley, T. B. Clark, *J. Org. Chem.* **2011**, *76*, 6452.
145 P. Canonne, M. Bernatchez, *J. Org. Chem.* **1987**, *52*, 4025.
146 G. Hamasaka, H. Tsuji, Y. Uozumi, *Synlett* **2015**, *26*, 2037.
147 W. Kuriyama, T. Matsumoto, O. Ogata, Y. Ino, K. Aoki, S. Tanaka, K. Ishida, T. Kobayashi, N. Sayo, T. Saito, *Org. Process Res. Dev.* **2012**, *16*, 166.

148 R. Tomita, K. Mantani, A. Hamasaki, T. Ishida, M. Tokunaga, *Chem. Eur. J.* **2014**, *20*, 9914.
149 E. Brenna, F. Cannavale, M. Crotti, F. Parmeggiani, A. Romagnolo, F. Spina, G. C. Varese, *J. Mol. Catal. B: Enzym.* **2015**, *116*, 83.
150 T. Otsuka, A. Ishii, P. A. Dub, T. Ikariya, *J. Am. Chem. Soc.* **2013**, *26*, 135, 9600.
151 a) G. M. Sheldrick, *Acta Cryst.* **2015**, *C71*, 3-8; b) C. B. Hübschle, G. M. Sheldrick, B. Dittrich, *J. Appl. Cryst* **2011**, *44*, 1281; c) G. M. Sheldrick, *Acta Cryst.* **2015**, *A71*, 3; d) PLATON: A. L. Spek, *Acta Cryst.* **2009**, *D65*, 148; e) E. Keller, **1999**, University of Freiburg, Germany http://www.krist.uni-freiburg.de/~kell/
152 See Supporting Information: D. J. Fisher, J. B. Shaum, C. L. Mills, J. Read De Alaniz, *Org. Lett.* **2016**, *18*, 5074.
153 See supportin information: A. Bartoszewicz, R. Marcos, S. Sahoo, A. K. Inge, X. Zou, B. Martin-Matute, Belen *Chem. Eur. J.*, **2012**, *18*, 14510.
154 T. Hizartzidis, M. Gordon, *RSC Advances* **2014**, *4*, 9709.
155 M. Carmona, R. Rodríguez, I. Méndez, V. Passarelli, F. J. Lahoz, P. García-Orduña, D. Carmona, *Dalton Trans.* **2017**, *46*, 7332.
156 See supporting information: L. Li, Z. Niu, S. Cai, Y. Zhi, H. Li, H. Rong, L. Liu, L. Liu, W. He, Y. Li, *Chem. Comm.* **2013**, *49*, 6843.
157 See Supporting Information: C. Wang, A. Pettman, J. Basca, J. Xiao, *Angew. Chem. Int.* **2010**, *49*, 7548.
158 See Supporting Information: X. Zhu, H. Du, *Org. Biomol. Chem.* **2015**, *13*, 1013.
159 See Supporting Information: P. Renzi, J. Hioe, R. M. Gschwind, *J. Am. Chem. Soc.* **2017**, *139*, 6752.
160 See Supporting Information: R. Mamidala, V. Mukundam, K. Dhanunjayarao, K. Venkatasubbaiah, *Tetrahedron* **2017**, *73*, 2225.
161 See Supporting Information: G. Wang, C. Chen, T. Du, W. Zhong, *Adv. Synth. Catal.* **2014**, *356*, 1747.
162 See Supporting Information: B. S. Takale, S. Tao, X. Yu, X. Feng, T. Jin, M. Bao, Y. Yamamoto, *Tetrahedron* **2015**, *71*, 7154.
163 See Supporting Information: J. Li, C. Wang, D. Xue, Y. Wei, J. Xiao, *Green Chem.* **2013**, *15*, 2685.
164 See Supporting Information: W. Muramatsu, K. Nakano, C-J. Li, *Org. Lett.* **2013**, *15*, 3650.
165 See Supporting Information: S. Guizzetti, M. Benaglia, G. Celentano, *Eur. J. Org. Chem.* **2009**, 3683.
166 P. Mokhov, *Russ. J. Gen. Chem.* **2014**, *84*, 1921.
167 See Supporting Information: C. Qin, T. Shen, C. Tang, N. Jiao, *Angew. Chem. Int.* **2012**, *51*, 6971.
168 See Supporting Information: A. K. Shaikh, A. J. Cobb, G. Varvounis, *Org. Lett.* **2012**, *14*, 584.
169 See Supporting Information: D. Gülcemal, S. Gülcemal, C. M. Robertson, J. Xiao, *Organometallics* **2015**, *34*, 4394.
170 See Supporting Information: P. Bachu, C. Zhu, T. Akiyama, *Tetrahedron Lett.* **2013**, *54*, 3977.
171 See Supporting Information: Y.-H. Wang, J.-L. Ye, A.-E. Wang, P.-Q. Huang, *Org. Biomol. Chem.* **2012**, *10*, 6504.
172 See Supporting Information: P. J. Rani, S. Thirumaran, *Eur. J. Med. Chem.* **2013**, *62*, 139.
173 M. J. Tomaszewski, J. Warkentin, N. H. Werstiuk, *Aust. J. Chem.* **1995**, *48*, 291.
174 See Supporting Information: Q. Lei, Y. Wei, D. Talwar, C. Wang, D. Xue, J. Xiao, *Chem. Eur. J.* **2013**, *19*, 4021.
175 Y. Miki, K. Hirano, T. Satoh, M. Miura, *Angew. Int. Ed.* **2013**, *52*, 10830.
176 O. Saidi, A. J. Blacker, M. M. Farah, S. P. Marsden, J. M. Williams, *Chem. Comm.* **2010**, *46*, 1541.
177 M. Robert, H. L. Perez, D. D. Wei, Y. Kim, BRISTOL-MYERS SQUIBB COMPANY; BORZILLERI, WO2014/25759, **2014**, A1.
178 *Asymmetric Catalysis on Industrial Scale*, 2nd ed. ("Challenges, approaches, Solutions") (Eds.: H.-U. Blaser, H.-J. Federsel), Wiley-VCH, Weinheim, **2010**.
179 For a comprehensive review of the topic, see: a) *Handbook of Homogeneous Hydrogenation* (Eds.: J. G. de Vries, C. J. Elsevier), Wiley-VCH, Weinheim, **2007**. b) D. J. Ager, A. H. M. de Vries J. G. de Vries, *Chem. Soc. Rev.*, **2012**, *41*, 3340.
180 For selected examples from the literature, see: a) R. H. Morris, *Acc. Chem. Res.* **2015**, *48*, 1494, and references therein; b) T. Zell, D. Milstein, *Acc. Chem. Res.* **2015**, *48*, 1979, and references therein; c) Reference 61, and references therein; d) Reference 79a and references therein; e) Reference 79b; f) Reference 77a; g) M. Shevlin, M. R. Friedfeld, H. Sheng, N. A. Pierson, J. M. Hoyt, L.-C. Campeau, P. J. Chirik, *J. Am. Chem. Soc.* **2016**, *138*, 3562; h) J. M. Hoyt, M. Shevlin, G. W. Margulieux, S. W. Krska, M. T. Tudge, P. J. Chirik, *Organometallics* **2014**, *33*, 5781; i) Reference 67.
181 a) J.G. de Vries and A.H.M. de Vries, *Eur. J. Org. Chem.*, **2003**, 799; b) H.-U. Blaser, *Chem. Commun.* **2003**, 293.
182 For recent reviews on allylic alkylation reactions, see: a) B. M. Trost, *Tetrahedron* **2015**, *71*, 5708; b) J. Tsuji, *Tetrahedron* **2015**, *71*, 6330.
183 For examples of use of the Trost ligand in reactions different from AAA, see: a) J. M. Longmire, B. Wang, X. Zhang, *J. Am. Chem. Soc.* **2002**, *124*, 13400; b) B. H. Lipshutz, K. Noson, W. Chrisman, A. Lower, *J. Am. Chem. Soc.* **2003**, *125*, 8779; c) T. Ireland, F. Fontanet, G.-G. Tchao, *Tetrahedron Lett.* **2004**, *45*, 4383; d) R. T. Stemmler, C. Bolm, *Adv. Synth. Catal.* **2007**, *349*, 1185; e) M. M. P. Grutters, J. I.

van der Vlugt, Y. Pei, A. M. Mills, M. Lutz, A. L. Spek, C. Müller, C. Moberg, D. Vogt, *Adv. Synth. Catal.* **2009**, *351*, 2199; f) A. Faulkner, J. F. Bower, *Angew. Chem. Int. Ed.* **2012**, *51*, 1675; g) D. Huang, X. Liu, L. Li, Y. Cai, W. Liu, Y. Shi, *J. Am. Chem. Soc.* **2013**, *135*, 8101.

184 For two unsuccessful attempts to use **L** as ligand for hydrogenation, see: a) C. de Bellefon, T. Lamouille, N. Pestre, F. Bornette, H. Pennemann, F. Neumann, V. Hessel, *Catal. Today* **2005**, *110*, 179; b) C.-C. Tai, J. Pitts, J. C. Linehan, A. D. Main, P. Munshi, P. G. Jessop, *Inorg. Chem.* **2002**, *41*, 1606.

185 For recent reviews on the asymmetric hydrogenation of ketones, see: a) R. Noyori, *Angew. Chem. Int. Ed.* **2013**, *52*, 79; b) Reference 81b; c) P.-G. Echeverria, T. Ayad, P. Phansavath, V. Ratovelomanana-Vidal, *Synthesis* **2016**, *48*, 2523; d) Refs. [180a,c].

186 For recent examples of enantioselective ruthenium-catalyzed ketone hydrogenations, see: a) R. J. Hamilton, S. H. Bergens, *J. Am. Chem. Soc.* **2006**, *128*, 13700; b) N. Arai, M. Akashi, S. Sugizaki, H. Ooka, T. Inoue, T. Ohkuma, *Org. Lett.* **2010**, *12*, 3380; c) B. Stegink, L. van Boxtel, L. Lefort, A. J. Minnaard, B. L. Feringa, J. G. de Vries, *Adv. Synth. Catal.* **2010**, *352*, 2621; d) W. Li, G. Hou, C. Wang, Y. Jiang, X. Zhang, *Chem. Commun.* **2010**, *46*, 3979; e) Y. Li, Y. Zhou, Q. Shi, K. Ding, R. Noyori, C. A. Sandoval, *Adv. Synth. Catal.* **2011**, *353*, 495.

187 Several ruthenium-based catalysts have been reported to promote the AH of aromatic ketones with >99% *ee* and low catalyst loadings (S/C 100000), see: a) T. Ohkuma, M. Koizumi, H. Doucet, T. Pham, M. Kozawa, K. Murata, E. Katayama, T. Yokozawa, T. Ikariya, R. Noyori, *J. Am. Chem. Soc.* **1998**, *120*, 13529; b) K. Matsumura, N. Arai, K. Hori, T. Saito, N. Sayo, T. Ohkuma, *J. Am. Chem. Soc.* **2011**, *133*, 10696. Some of them are commercially available by Takasago International Corporation, see: http://www.takasago.com/en/business/finechemicals/ligands_catalysts.html

188 a) J. X. Gao, H. L. Wan, W. K. Wong, M. C. Tse, W. T. Wong, *Polyhedron* **1996**, *15*, 1241; b) Reference 49; c) Reference 59a; d) S.-M. Lu, Q. Gao, J. Li, Y. Liu, C. Li *Tetrahedron Lett.* **2013**, *54*, 7013; e) R. Patchett, I. Magpantay, L. Saudan, C. Schotes, A. Mezzetti, F. Santoro, *Angew. Chem. Int. Ed.* **2013**, *52*, 10352; see in particular pages 15-17 of the Supporting Information.

189 $RuCl_3$ has been rarely used as catalyst precursor in ketone hydrogenation reactions, see: a) O. Labeeuw, C. Roche, P. Phansavath, J.-P. Genet, *Org. Lett.* **2007**, *9*, 105; b) E. V. Starodubtseva, O. V. Turova, M. G. Vinogradov, L. S. Gorshkova, V. A. Ferapontov, M. I. Struchkova, *Tetrahedron* **2008**, *64*, 11713; c) C. Roche, O. Labeeuw, M. Haddad, T. Ayad, J.-P. Genet, V. Ratovelomanana-Vidal, P. Phansavath, *Eur. J. Org. Chem.* **2009**, 3977.

190 Some recent papers on the role of the base in ruthenium-catalyzed hydrogenation reactions: a) P. A. Dub, N. J. Henson, R. L. Martin, J. C. Gordon, *J. Am. Chem. Soc.*, **2014**, *136*, 3505. b) P. A. Dub, B. L. Scott, J. C. Gordon, *J. Am. Chem. Soc.*, **2017**, *139*, 1245.

191 See Supporting Information: M. Cettolin, P. Puylaert, L. Pignataro, S. Hinze, C. Gennari, J. G. de Vries, *ChemCatChem* **2017**, *9*, 3125.

192 Y. Zeng, L. Xu, Y. Li, M. Maca, C. A. Sandoval, patent no. WO 2015172603.

193 J. Margalef, T. Slagbrand, F. Tinnis, H. Adolfsson, M. Diéguez, O. Pàmies, *Adv. Synth. Cat.* **2016**, *358*, 4006.

194 H. Li, J. Moncecchi, M.D. Truppo, *Org. Process Res. Dev.* **2015**, *19*, 695.